

Alma Mater Studiorum – Università di Bologna

**DOTTORATO DI RICERCA IN
SCIENZE CHIMICHE**
Ciclo XXVIII

Settore Concorsuale di afferenza: 03/C2

Settore Scientifico disciplinare: CHIM/04

**ATOM TRANSFER RADICAL POLYMERIZATION OF POLAR
MONOMERS AND SYNTHESIS OF BLOCK COPOLYMERS FOR
INDUSTRIAL AND BIOMEDICAL APPLICATIONS**

Presentata da: Giovanni Mazzotti

Coordinatore Dottorato

Prof. Aldo Roda

Relatore

Prof. Loris Giorgini

Correlatori

Dott.ssa Tiziana Benelli

Dott.ssa Laura Mazzocchetti

Esame finale anno 2016

Table of contents

| | | |
|-----------|--|-----------|
| 1 | CHAPTER 1 - INTRODUCTION | 1 |
| 1.1 | CONTROLLED/LIVING RADICAL POLYMERIZATION..... | 1 |
| 1.1.1 | <i>Atom Transfer Radical Polymerization (ATRP)</i> | 3 |
| 1.1.1.1 | Reaction conditions | 9 |
| 1.1.1.1.1 | Transition metal..... | 10 |
| 1.1.1.1.2 | Monomer..... | 11 |
| 1.1.1.1.3 | Solvent..... | 12 |
| 1.1.1.1.4 | Ligand | 13 |
| 1.1.1.1.1 | Initiator | 14 |
| 1.1.1.1.2 | Leaving Group..... | 15 |
| 1.1.2 | <i>Comparing ATRP with NMP and RAFT</i> | 15 |
| 2 | CHAPTER 2 - ATRP OF POLAR MONOMERS: SYNTHESIS AND CHARACTERIZATION OF HOMO AND COPOLYMERS | 19 |
| 2.1 | INTRODUCTION..... | 19 |
| 2.1.1 | <i>Synthesis of random and gradient copolymers</i> | 19 |
| 2.1.2 | <i>Aim of the project</i> | 22 |
| 2.2 | RESULTS AND DISCUSSION..... | 24 |
| 2.2.1 | <i>Synthesis of homopolymers by ATRP</i> | 24 |
| 2.2.1.1 | Synthesis of PNVP by ATRP..... | 24 |
| 2.2.1.2 | Synthesis of PNVCL by ATRP..... | 29 |
| 2.2.1.3 | Proving the living character of PNVCL | 36 |
| 2.2.1.4 | Optimization of the ATRP of NVCL | 38 |
| 2.2.1.5 | Comparison of the ATRP kinetics of NVP and NVCL | 39 |
| 2.2.2 | <i>Atom Transfer Radical Copolymerization (ATRCP)</i> | 41 |
| 2.2.2.1 | ATRCP of NVP with BMA or BA..... | 42 |
| 2.2.2.2 | ATRCP of NVCL with BA or VAc..... | 46 |
| 2.2.2.2.1 | NVCL and VAc random copolymers | 48 |
| 2.2.2.3 | NVCL and PEGMEA random copolymers | 52 |
| 2.2.3 | <i>Synthesis and characterization of block copolymers</i> | 56 |
| 2.2.3.1 | Synthesis of PNVCL-b-PVAc | 57 |
| 2.2.3.1.1 | DLS measurements of PNVCL-b-PVAc-90 water solution | 62 |
| 2.2.3.2 | Synthesis of PNVCL-b-PDMAEMA..... | 63 |
| 2.2.3.3 | Synthesis of PNVCL-b-PPEGMEA | 66 |
| 2.2.3.4 | Synthesis of NVCL-b-PNVF..... | 70 |
| 2.3 | CONCLUSIONS | 75 |
| 2.4 | EXPERIMENTAL SECTION | 76 |

| | | |
|----------|---|------------|
| 2.4.1 | <i>Physico-chemical characterization</i> | 76 |
| 2.4.2 | <i>Materials</i> | 77 |
| 2.4.3 | <i>Synthesis of allyl 2-chloropropionate (ACP)</i> | 77 |
| 2.4.4 | <i>Synthesis of poly(ethylene glycol) methyl ether methacrylate (PEGMEA): PEGMEA350, PEGMEA750 and PEGMEA2000</i> | 78 |
| 2.4.5 | <i>Polymerization procedures</i> | 78 |
| 2.5 | POLYMER CHARACTERIZATION | 80 |
| 3 | CHAPTER 3 - STRAIGHTFORWARD SYNTHESIS OF WELL-DEFINED POLY(VINYL ACETATE) AND ITS BLOCK COPOLYMERS BY ATOM TRANSFER RADICAL POLYMERIZATION | 84 |
| 3.1 | INTRODUCTION AND SCOPE | 84 |
| 3.2 | RESULTS AND DISCUSSION..... | 87 |
| 3.2.1 | <i>Kinetic polymerization studies</i> | 87 |
| 3.2.2 | <i>Synthesis of block copolymers</i> | 92 |
| 3.2.3 | <i>Thermal characterization</i> | 99 |
| 3.3 | CONCLUSIONS | 105 |
| 3.4 | EXPERIMENTAL SECTION | 106 |
| 3.4.1 | <i>Physico-chemical characterization</i> | 106 |
| 3.4.2 | <i>Materials</i> | 107 |
| 3.4.3 | <i>Synthesis of allyl 2-chloropropionate (ACP)</i> | 107 |
| 3.4.4 | <i>Kinetic studies of the PVAc homopolymerization</i> | 108 |
| 3.4.5 | <i>Synthesis of the optimized PVAc macroinitiator</i> | 108 |
| 3.4.6 | <i>Synthesis of copolymers</i> | 109 |
| 3.4.6.1 | PVAc-b-PHEMA..... | 110 |
| 3.4.6.2 | PVAc-b-PBMA-1..... | 111 |
| 3.4.6.3 | PVAc-b-PBMA-2..... | 111 |
| 3.4.6.4 | PVAc-b-PMMA..... | 111 |
| 3.4.6.5 | Synthesis of PVA-b-PMMA | 112 |
| 4 | CHAPTER 4 - SYNTHESIS AND CHARACTERIZATION OF PH AND TEMPERATURE-SENSITIVE POLYMERS AS CARRIERS FOR DRUG-DELIVERY SYSTEM | 113 |
| 4.1 | INTRODUCTION..... | 113 |
| 4.1.1 | <i>Pluronic block copolymers</i> | 113 |
| 4.1.1.1 | Formation of micelles and gels in Pluronics water solution | 114 |
| 4.1.1.2 | Applications of Pluronics in drug delivery systems..... | 118 |
| 4.2 | AIM OF THE PROJECT | 123 |
| 4.3 | RESULTS AND DISCUSSION..... | 128 |
| 4.3.1 | <i>Synthesis of ATRP macroinitiators</i> | 128 |
| 4.3.2 | <i>Kinetic studies and synthesis of block copolymers</i> | 131 |

| | | |
|---------|---|------------|
| 4.3.3 | <i>NMR characterization</i> | 136 |
| 4.3.4 | <i>Rheological measurements</i> | 140 |
| 4.3.5 | <i>DLS measurements</i> | 145 |
| 4.3.5.1 | PLUR F127 derivatives | 146 |
| 4.3.5.2 | PEG and PEG-bis-OH derivatives | 149 |
| 4.3.6 | <i>Loading measurements</i> | 152 |
| 4.4 | CONCLUSIONS | 158 |
| 4.5 | EXPERIMENTAL SECTION | 160 |
| 4.5.1 | <i>Physico-chemical characterization</i> | 160 |
| 4.5.2 | <i>Materials</i> | 161 |
| 4.5.3 | <i>Preparative procedures</i> | 161 |
| 4.5.4 | <i>DLS and loading measurements samples</i> | 166 |
| 4.5.5 | <i>Study of glucose oxidase kinetic in presence of PLUR-bis-PDEAEMA-L</i> | 166 |
| 5 | REFERENCES | 167 |

1 Chapter 1 - Introduction

1.1 Controlled/living Radical Polymerization

The free radical polymerization (FRP) is one of the most applied systems for the synthesis of commercial polymers. Indeed, almost the 50% of them, with application in many commercial fields, is produced by using radical-chemistry based techniques.

FRP is a versatile technique that is tolerant to various monomers and this allows to synthesize a wide range of homo and copolymers such as poly(styrene) and its copolymers (with acrylonitrile, butadiene, etc.), poly(acrylate)s, poly(ethylene) and poly(vinyl chloride). Furthermore, it can be applied industrially, using several techniques and it does not require complex purification of reactants¹.

Despite to these advantages, by FRP it is not possible to control the molecular weight, the composition and the structure of the synthesized polymer because of termination and transfer reactions that occur during the process^{2,3}.

During the last twenty years much efforts were made to develop polymerization processes that could allow to obtain polymers with pre-determined chain length, structure and PD and this was achieved developing different ‘Controlled-living’ radical polymerizations (CLRPs)⁴⁻¹⁰. Living polymerization is defined as “a chain-growth polymerization that propagates with no irreversible chain-transfer or chain-termination reactions”⁷. For example, anionic and cationic polymerizations are living processes that are well known since the first years of the ninety’s. The living character of polymers synthesized by ionic polymerization techniques offers the possibility to synthesize block copolymers. Unfortunately, this techniques can polymerize a limited range of monomers³. Matyjaszewski and co-authors reported that “free radicals, which are the growing species in radical polymerization, very easily react with another one via coupling and/or disproportionation. Thus, it is inherently impossible to imagine a living radical polymerization. However, by careful adjustment of the reaction conditions, it is possible to prepare well-defined polymers by a radical mechanism”¹¹. In subsequent years, the study of controlled radical polymerizations led to different techniques that allow nowadays to synthesize polymers with well-defined structure by CLRP^{12,13}.

It is important to synthesize polymers with well-defined structure because only if the polymers have uniform length, composition and functionality it is possible to control their assembly in nanostructured materials. Moreover, the properties of materials with defined

structure differ compared to the properties of polymers obtained with classical techniques and no control over the polymer structure¹.

It is worth noting that the development of CLRP also allowed to obtain materials with different polymer architectures (Figure 1) allowing the study of its effect on the final properties of the obtained material¹⁴.

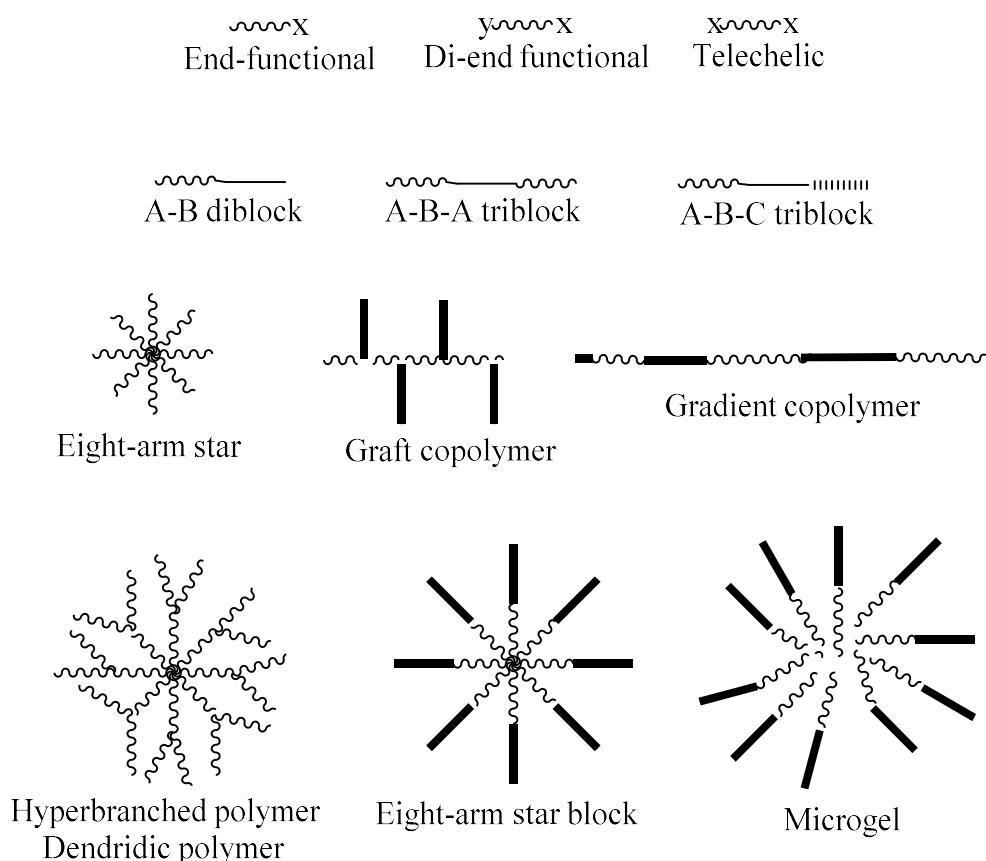


Figure 1: Possible polymer architectures¹⁴.

During a radical polymerization, in order to maximize the control over the reaction and obtain polymers with the desired structure and PD, the reactions of termination by combination and disproportionation need to be negligible but they cannot be completely eliminated, as it is for ionic living polymerization^{2,3}. As stated from Matyjaszewski, “radical polymerizations can become controlled under conditions in which a low, stationary concentration of the active species is maintained and a fast, dynamic equilibrium is established between the active and dormant species”¹¹.

The dormant species mentioned by Matyjaszewski are not able to react with monomers but they are in equilibrium with the active species, in a system in which the propagating radicals are formed intermittently. In a controlled radical polymerization, each time a

dormant specie is converted into an active specie, this latter should react only with few units of monomer and then it returns in the inactive dormant status. There are several type of CLRPs, but all of them show a fast equilibrium between the dormant species and the growing radicals¹. Among CLRPs, the most studied and promising are the Atom Transfer Radical Polymerization (ATRP), the Nitroxide Mediated Radical Polymerization (NMP) and the Reversible Addition-Fragmentation chain Transfer (RAFT).

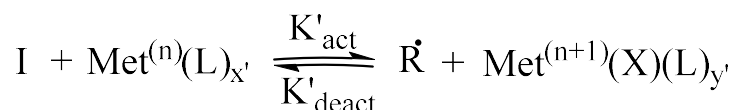
1.1.1 Atom Transfer Radical Polymerization (ATRP)

Among CLRP, ATRP is one of the most convenient, especially if a large scale process has to be developed. Compared to other CLRP, indeed, being more versatile, it can be applied to the polymerization of a wide range of monomers, not requiring any particular purification of commercial reactants. Furthermore it allows the use of several solvent, even water and it leads to the synthesis of macromolecules that can be easily end-functionalized^{1,15}. Thus, during the last years, ATRP has led to the synthesis of polymers with well-defined microstructure, functionality and composition, and some of the developed materials have interesting potential commercial applications.

ATRP is one of the controlled living radical polymerization in which the control over the concentration of the active species is based on the equilibrium between the growing radical and a transition metal complex.

In a typical ATRP reaction four components are needed: monomer, initiator, transition metal with two stable states of oxidation in the reaction conditions and a ligand that allows the solubilization of the transition metal¹⁶.

At the first stage of the process, the initiator and the transition metal give a reversible oxidation reaction which generates radicals (R·) (Scheme 1).



Scheme 1: ATRP initial redox reaction. I=Initiator, Met⁽ⁿ⁾=Reduced catalyst, L=Ligand, R·=Radical, Met⁽ⁿ⁺¹⁾=Oxidized catalyst, X=halogen atom, K'_{act}= Rate constant of activation and, K'_{deact}=Rate constant of deactivation.

Usually, the X (in Scheme 1) is a halogen atom, such as bromine or chlorine, which could be already present in the complex of the transition metal in its lower oxidation state, as Cu(Br)(bpy)¹⁵⁻¹⁷.

Chapter 1: Introduction

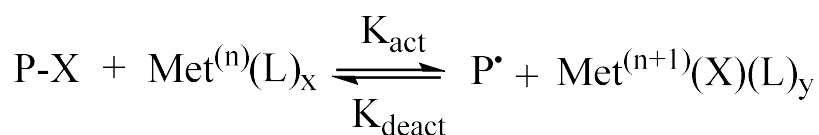
The obtained equilibrium (K'_{act} and K'_{deact}), and thus the rate of this reaction, depends on many factors: e.g. the stability of the complex between the transition metal and the ligand¹⁷, the temperature, the type of initiator, the stability of the two oxidation states of the transition metal and of the generated radical, the solvent etc.

The generated radicals can react with the monomer and the reaction of polymerization starts (Scheme 2).



Scheme 2: First reaction between monomer and radical generated by the initiator. R=Radical, M=Monomer, P=Propagating radical, K_i =Rate constant of initiation.

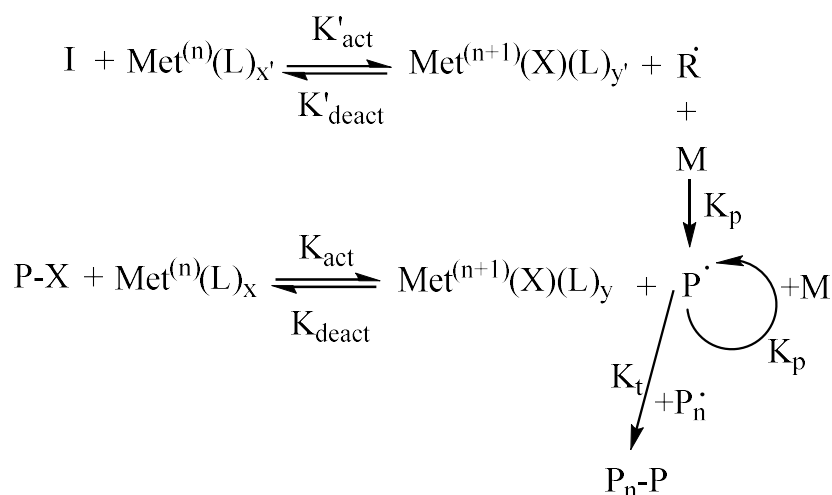
The growing polymer chain is involved in a redox reaction with the oxidized metal that converts the radical chain into a dormant specie (Scheme 3)^{11,18}.



Scheme 3: ATRP equilibrium between dormant and growing chain. P-X= dormant specie, $\text{Met}^{(n)}$ =Reduced catalyst, L=Ligand, P=Propagating radical, $\text{Met}^{(n+1)}$ =Oxidized catalyst, X=halogen atom, K_{act} = Rate constant of activation and, K_{deact} =Rate constant of deactivation.

The ratio between K_{act} and K_{deact} is called K_{ATRP} and it is strictly correlated to other four constants: the constant of oxidation of the metal complex (K_{ox}), the constant of reduction of the halogen into halide ion (K_{ea}), the constant of C-X bond homolysis in the alkyl halide (K_{bh}) and the constant of association of the halide ion to the metal complex (K_{x}). How these constants affect the value of K_{ATRP} will be shown later on¹⁹.

Unfortunately, these are not the only reactions that occur but, for kinetic reasons, some terminations might take place^{20,21}. The overall process is shown in scheme 4^{17,21}.



Scheme 4: ATRP mechanism. I=Initiator, $\text{Met}^{(n)}$ =Reduced catalyst, L=Ligand, R=Radical, $\text{Met}^{(n+1)}$ =Oxidized catalyst, X=halogen atom P-X= dormant specie, P=Propagating radical, M=Monomer, K_{act} = Rate constant of activation, K_{deact} =Rate constant of deactivation, K_p =Rate constant of polymerization and K_t =Rate constant of termination.

It was demonstrated that the absence of one component among ligand, initiator and transition metal leads to a broader PD and a lower control over the molecular weight, showing that these three components are equally important for the control over the process¹⁶.

The transition metal acts as halogen carrier (or pseudo-halogen carrier) while the ligand's task is to solubilize the inorganic salt in the reaction mixture but it also affects the value of the equilibrium constants involved in the process¹⁶.

A good control over the polymerization reaction can be achieved only with: a low concentration of growing radicals, a fast redox reaction compared to those of termination and disproportionation, and a rate of conversion in the dormant species comparable to that of polymerization. In this way the growth of the polymeric chain can be uniform and no more than a few percent of the polymer chains undergoes termination.

Practically, less is the concentration of radical species in the reaction mixture, less is the rate of the termination and disproportionation reactions^{16,22}. Unfortunately, the context is more complicated; indeed, the K_t has the same magnitude order of the diffusion controlled limit and it is higher than the propagation rate constant [$K_t = 10^7 \div 10^9$ l/(mol*s) and K_p $10^2 \div 10^4$ l/(mol*s)]. Furthermore, the value of K'_{act} is in the range of $10^{-4} \div 10^{-6}$ s⁻¹, the average value of decomposition of a classic radical initiator, and these are the reasons why it is impossible to prevent some reactions of termination^{17,20}.

Chapter 1: Introduction

Once the conditions that lead to an overall control over the reaction are reached, several demonstrations can confirm the success of the procedure.

The average molecular weight should follow Equation 1.

$$\text{Equation 1} \quad \overline{M}_{n,th} = \frac{[M_0] - [M]}{[I_0]} * MW_0 \quad 5,6$$

$\overline{M}_{n,th}$ =Average theoretical molecular weight, $[M_0]$ =Initial monomer concentration, $[M]$ =Monomer concentration, $[I_0]$ =Initial initiator concentration and MW_0 =Monomer molecular weight.

A well-controlled reaction means a reaction which leads to polymer with the desired structure, molecular weight and low PD (lower than 1.4-1.5)¹⁶.

Plotting $\ln([M_0]/[M])$ as a function of time, if the reaction is well controlled, a linear plot should be the result, leading to the statement that the concentration of growing radical is constant throughout the reaction^{15,21}. The slope of the fitting line is the K_{app} of the reaction. Indeed, the reaction of polymerization is of the first order for both the concentration of radical species and the concentration of monomer and being the concentration of radical species constant, its value can be included in the K_{app} value as seen in Equation 2²¹.

$$\text{Equation 2} \quad r_p = K_p * [P\cdot] * [M] = K_{app} * [M]$$

r_p =Rate of polymerization, K_p =Rate constant of polymerization, $P\cdot$ =Propagating radical, M =Monomer, K_{app} =Apparent rate constant of polymerization.

A deviation from the linear dependence of $\ln([M_0]/[M])$ with the time means that some reactions have reduced the concentration of radical species and the polymerization is not controlled as desired.

If the conditions of the reaction are such as to allow a fast pre-equilibrium and therefore a low PD, the kinetic laws are the ones stated in Equation 3 and Equation 4²³.

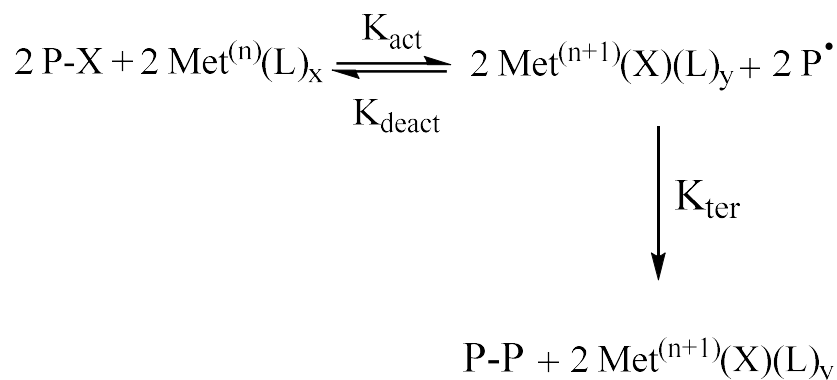
Chapter 1: Introduction

$$\text{Equation 3} \quad K_{ATRP} = \frac{K_{act}}{K_{deact}} = \frac{[P\cdot][Met^{(n+1)}(X)(L)_y]}{[Met^{(n)}(L)_x][P-X]}$$

$$\text{Equation 4} \quad r_p = K_{app}[M] = K_p[P\cdot][M] = K_p[M]K_{ATRP}[I_0] \frac{[Met^{(n)}(L)_x][P-X]}{[Met^{(n+1)}(X)(L)_y]}$$

K_{ATRP} =ATRP rate constant, K_{act} = Rate constant of activation, K_{deact} =Rate constant of deactivation, K_{app} =Apparent rate constant of polymerization, K_p =Rate constant of polymerization, $P\cdot$ =Propagating radical, M =Monomer, $[I_0]$ =Initial initiator concentration, $Met^{(n)}$ =Reduced catalyst, $Met^{(n+1)}$ =Oxidized catalyst, X =Halogen atom, L =Ligand, $P-X$ =Dormant specie.

In these kinetic laws the termination by radical coupling is not considered ($[P\cdot]=[I_0]$), but it is a phenomenon that happens at the beginning of the polymerization and it allows the establishment of the so called “persistent radical effect”. At time ‘0’ the concentrations of oxidized metal end radicals are zero. During the initial stages of the polymerization if the rate of deactivation reaction (that leads the radical to the dormant form) is lower than the rate of termination, and this might happen because they are subject to two different kinetics, the concentration of (propagating) radicals might be high enough to make the rate of termination not negligible compared to the rate of polymerization and coupling reactions may occur (Scheme 5). The fact that the coupling reaction is irreversible, implies that the more coupling reactions occur the more the concentration of oxidized metal increases. As a consequence of the fact that the product $[M^{(n+1)}(X)(L)_y] \cdot [P\cdot]$ (Equation 3) must be constant, the concentration of radicals decreases, thus the rate of coupling reaction becomes gradually lower than the rate of polymerization. This is possible for their different dependence from the concentration of radicals (Equation 4 and Equation 5)¹⁷. This system reaches an equilibrium in which the concentration of oxidized metal is sufficient to make the rate of coupling reaction slow enough for a controlled polymerization to occur²¹.



Scheme 5: Termination reaction between two propagating radical. P and $P_n\cdot$ =Propagating radicals, K_{ter} =Rate constant of termination and $P-P_n$ =Dead chain

Chapter 1: Introduction

Equation 5
$$r_{ter} = K_{ter} * [P\cdot]^2$$

r_{ter} =Rate of termination, K_{ter} =Rate constant of termination and $P\cdot$ =Propagating radical.

If termination reactions are negligible compared to the propagation ones during the polymerization, and the rate of the reaction that leads to the formation of the dormant species is fast, the degree of polymerization (DP) could be predetermined, because it is directly related to the consumed monomer and to the initial concentration of initiator $[M_0]$ as established by Equation 6.

Equation 6
$$DP = \frac{[M_0]-[M]}{[I_0]}$$

DP =Degree of polymerization, $[M_0]$ =Initial monomer concentration, $[M]$ =Monomer concentration and $[I_0]$ =Initial initiator concentration.

Another proof that the conditions in which the reaction has occurred has led to a controlled reaction should be provided by $^1\text{H-NMR}$ analysis. Indeed, the result of such analysis should show the presence of the chain end groups: the initiator residue and the halide (or pseudo halide) at the end of the macromolecules. The presence of these groups indicates that no reactions of termination (or just a negligible amount) occurred¹⁵.

Despite the advantages that ATRP offers, the production on a large scale might be limited, mainly for three reasons:

- All the oxidants should be removed from the reactor in which the polymerization occurs.
- The catalyst should be removed from the final materials and this could be expensive²⁴.
- The transition metal catalysts used in this technique are toxic (i.e. Cu complex...) and the disposal of huge quantity of this toxic material could be dangerous for the environment²⁵.

These disadvantages can increase the cost of the ATRP process applied on a large scale but the higher cost can be balanced by the added value of materials synthesized with this technique.

1.1.1.1 Reaction conditions

Matyjaszewski was one of the first researcher who studied the ATRP process, and he found that a system consisting of 1-phenylethyl chloride as initiator, CuCl complexed by 2,2'-bipyridine as catalyst and monomers allows to synthesize polymers with narrow PD ($\overline{M}_w/\overline{M}_n < 1.5$) and a predetermined molecular weight⁶. The combination of initiator, transition metal and ligand proposed in that article⁶ is not the only possible one: a lot of parameters can be changed to tune the reaction with the aim to obtain the researched goal^{21,22}. The tuning of the reaction should be done because each monomer has its own rate of polymerization, each couple metal/monomer has a different transition state and different value of equilibrium constant and each metal-ligand complex has different solubility in the reaction mixture; all these parameters, together with the concentration of every single specie affect the concentration of growing radicals in solution^{15,17}. Moreover, side reactions must be taken into account during the study of a new reaction mixture.

Once the type of initiator, catalyst combined with the leaving group, ligand and monomer have been chosen, the reactants molar ratios have to be optimized in order to control the polymerization. The correlation between the reaction constant (K_{app}) and the initial concentration of the species is described by Equation 7.

$$\text{Equation 7} \quad K_{app} = \frac{\left\{ \frac{d[M]}{dt} \right\}}{[M]} = K_p [I_0]^x [Met_0^{(n)}]^y [L_0]^z$$

K_{ATRP} =ATRP constant, M =Monomer, t =Time, K_p =Rate constant of polymerization, $[I_0]$ =Initial initiator concentration, $[Met_0^{(n)}]$ =Initial reduced metal concentration and $[L_0]$ =Initial ligand concentration.

The value of x, y and z show how the initial concentration of each component affects the K_{app} and therefore the rate of the reaction. To determine how each initial concentration affects the rate of the reaction, $\ln(K_{app})$ versus the natural logarithm of the concentration of the species under investigation should be plotted. The slopes of the resulting plots represent the values of x, y or z respectively. The initial concentration of the initiator is linearly related to the value of K_{app} because it affects the concentration of growing radicals and its value for x is equal to one, while x and z should be determined for each specific system. On the other hand, as the transition metal acts as a catalyst, only low concentration of the metal in solution is needed to control the reaction¹⁷. The PD is related to the concentration of the oxidized metal as can be seen from Equation 8²⁶.

Chapter 1: Introduction

$$\text{Equation 8} \quad PD = \frac{\overline{M}_w}{\overline{M}_n} = 1 + \frac{1}{DP} + \left(\frac{K_p[I_0]}{K_{deact}[M^{(n+1)}(X)(L)_y]} \right) * \left(\frac{2}{conv} - 1 \right)$$

PD =Polydispersity, \overline{M}_w =Weight average molecular weight, \overline{M}_n =Number average molecular weight, DP =Degree of polymerization, K_p =Constant rate of polymerization, $[I_0]$ =Initial initiator concentration, K_{deact} =Constant rate of deactivation, $Met^{(n+1)}$ =Oxidized metal, L =Ligand, X =Halogen atom and $Conv$ =Conversion.

The concentration of the oxidized metal $[Met^{(n+1)}(X)(L)_y]$ depends on that one of the reduced metal $[Met^{(n)}(L)_x]$ which should be enough to obtain a low PD, even if it has no effect on the rate of polymerization because this latter is correlated to the ratio of the reduced and oxidized species (Equation 4).

1.1.1.1.1 Transition metal

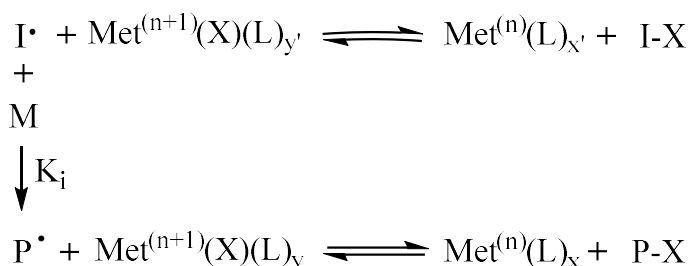
The transition metal should be able to expand its coordination sphere and simultaneously it has to be oxidized during the progress of the reaction²².

The metal in the lower oxidation state has the exclusive role to remove the halogen atoms from the inactive chains, in fact it does not react with the radical species present in solution. The metal in the higher state of oxidation is the specie that control the concentration of radicals in solution and, consequently, its presence is necessary to control the polymerization²¹.

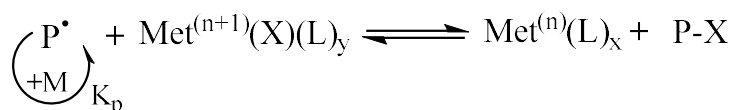
To determine the importance of the oxidized metal, in one experiment, the transition metal in the lower oxidation state was replaced with the same transition metal in its higher oxidation state in presence of classical radical initiator¹⁵. The resulting polymerization was controlled, demonstrating that the oxidized metal has a more important role compared to the metal in its lower oxidation state. The pathway of the reaction results so modified as can be seen in Scheme 6¹⁵.

Chapter 1: Introduction

Initiation:



Propagation:



Scheme 6: ATRP reactions in presence of conventional radical initiator and oxidized catalyst. I=Conventional radical initiator, I·=Radical, Met⁽ⁿ⁾=Reduced metal, X=Halogen atom, L=Ligand, Met⁽ⁿ⁺¹⁾=Oxidized metal, I-X=Dormant initiator, M=Monomer, K_i=Rate constant of initiation, P=Propagating radical, P-X=Dormant specie and K_p=Rate constant of polymerization.

In this case, the control over the reaction, as well as the initiator's efficiency, is enhanced with the concentration of transition metal in the higher oxidation state, proving its central role in ATRP¹⁵.

With the aim to reach an better control over the reaction, it is possible to add a certain amount of oxidized metal, or leave traces of oxygen, in the initial reaction mixture thus decreasing the rate of initial termination reactions¹⁷.

Even if copper is one of the most efficient catalyst for ATRP and it is used to polymerize a broad range of monomers in different media, a variety of transition metals, as Ti, Mo, Re, Fe, Ru, Os, Co, Ni, Pd and Rh was successfully used^{17,27-35}.

1.1.1.1.2 Monomer

ATRP can be applied to the polymerization of vinyl monomers that can react with the radicals generating other radical species still able to react with other monomers, and with substituents that stabilize the radical after its formation. Monomers with complexing properties can compete with the ligand during the solubilization of the catalyst, scavenging it from the ATRP equilibrium and this does not allow to the system to establish a fast and dynamic equilibrium between the dormant specie and the propagating chain. In order to

polymerize monomers that can interact with the metal, it is necessary to use ligands with high complexing efficiency that avoids metal-monomer interactions^{15,21}.

Each monomer has its constant of C-X bond homolysis (K_{bh}), and as said, this influences the value of K_{ATRP} . As each K_{bh} could be significantly different from monomer to monomer, it might happen that, in the same reaction conditions, different monomers have different values of K_{ATRP} , leading to different reaction times to reach the same conversion, or to uncontrolled reactions^{36,37}. So, for each specific monomer it is necessary to find the best experimental conditions to reach the desired conversion in a reasonable time.

1.1.1.1.3 Solvent

The reaction could be carried out with or without solvent; in the first case various solvents and different initial concentrations of the reaction mixture can be used. Being the rate of the polymerization dependent on the concentration of the reactants, the dilution of the system slows down the reaction but it could be useful to better solubilize all the reactants and the resulting polymer⁶. A solvent is needed when the monomer is not a solvent for the corresponding polymer³⁸ or when the monomer is solid³⁹. The choice of the solvent and its quantities should be determined as a function of the system under investigation¹⁶. Common solvents used for ATRP are THF⁴⁰, 1,4-dioxan⁴¹, toluene^{40,42} but many others such as diphenyl ether⁴³ and 1,4-dimethoxybenzene⁴⁴ can be used.

In all the cases, in order to achieve a good control on the process, the reaction of polymerization must be of the first order respect to the monomer and the concentration of radical species should be constant²¹.

The solvent has a strong effect on the value of the constant of reduction of the halogen into halide ion (K_{ea}), and that one of association of the halide ion to the metal complex (K_x). As said, these two constants affect the value K_{ATRP} which becomes itself solvent dependent⁴⁵.

As halide ions are stabilized through solvation, the value of K_{ea} increases in polar solvents⁴⁶. For the same reason K_x decreases with the polar property of the solvent, because of the stabilization of halide ion in the solution⁴⁷. These two considerations are in agreement with the results of experiments in which, using protic polar solvents, the control over the reaction was lost⁴⁸. This happens because the halide is slightly coordinated to the oxidized catalyst and the process of deactivation does not happen with the frequency needed to control the reaction⁴⁸.

1.1.1.1.4 Ligand

During the years several molecules were proved to be good ATRP ligands; in Figure 2 some of the most common ones are shown and arrange in increasing activation rate constant order¹⁴. The complexing properties of a ligand depend on its structure and on the number of atoms with complexing characteristics. As example, cyclic ligands can usually establish stronger interactions with the metal compared to linear ligands¹⁴.

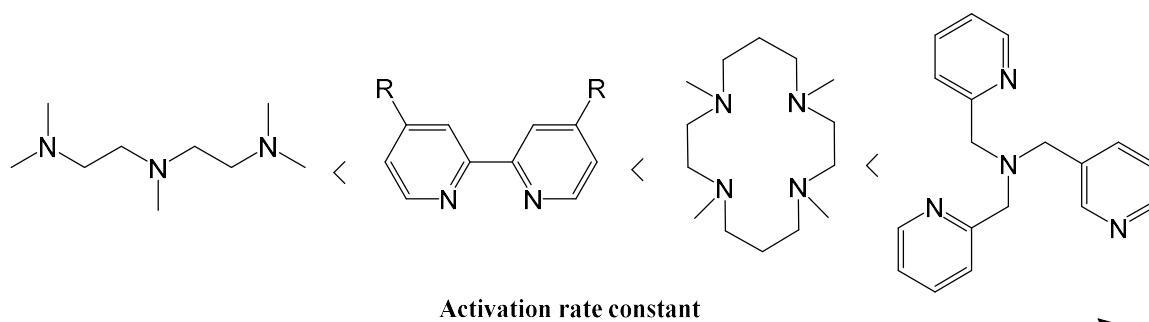


Figure 2: Structure of some ATRP ligands⁴⁹.

Ligands are used to solubilize the transition metal salt in the reaction mixture but they also influence the value of the constants involved in the equilibrium between the dormant specie and the propagating radical. The amount of ligand which is necessary to control the reaction depends on the reaction conditions and on the solubilizing ability of the ligand, and it could be found doing different measures of the K_{app} maintaining constant all the parameters of the reaction except the concentration of ligand. Plotting the value of k_{app} versus the concentration of ligand it could be noted that the constant rises since it reaches a constant value corresponding to the optimum concentration of ligand in the experimental conditions²¹.

The ligand to metal stoichiometry affects also the structure of the complex in solution. The dynamic equilibrium established in solution can involve several metal species whose concentration depends on the relative quantity of ligand and transition metal. As an example, using CuBr and bi-pyridine (byp) in 1:2 molar ratio, the specie which is present in bigger quantity in solution is the monomeric complex $[(byp)_2CuBr]$ (Figure 3). However, if a 1:1 molar ratio is used, the specie with the highest concentration in solution is either the bridged dimer $[LCu(i-X)_2CuL]$, or 2:1 ligand-to-copper cation with a dihalocuprate counteranion $[L_2Cu]^+[CuX_2]^{-50,51}$.

The relative stability of the complexes formed between metal, in both the oxidations states, and ligand, affects the potential of oxidation of the catalyst and the value of K_{ATRP} .

As a consequence, different ligands lead to different potential of oxidation and different K_{ATRP} . The more stable is the higher state of oxidation of the metal-ligand complex, the more the metal in its lower state of oxidation is a strong reducing agent thus catalytically active in ATRP. As already said, also the potential of reduction should lead to a fast reaction of oxidation of the growing chain, carrying it to the dormant species.

In order to minimize the risk of ligand substitution with all the other species present in the reaction mixture (monomers, polymers, solvents), it is convenient to have both the state of oxidation of the metal strongly stabilized from the ligand^{48,52}.

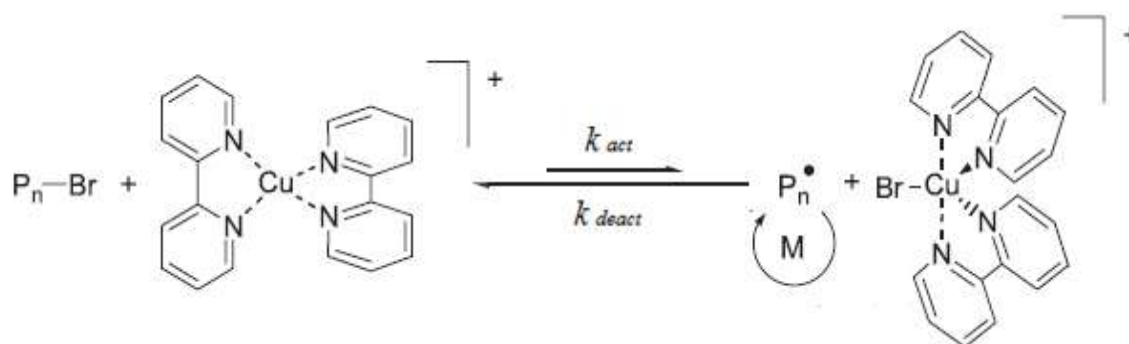


Figure 3: ATRP equilibrium established using bipy.

1.1.1.1.1 Initiator

In order to achieve a good control over the reaction, it is very important to find the conditions that allow the optimum combination of equilibrium constants involved in the reaction pattern. As the equilibrium constant is affected by the stability of the species involved in the reaction, to obtain the proper number of radical species that start the reaction of addition of monomer, the stability of the radical derived from the initiator must be evaluated. The initiators that lead to a proper number of radical species in the reaction mixture are the ones which stabilize the radical product, e.g. initiator with inductive or resonance stabilizing groups. In Figure 4 the structure of possible ATRP initiators is shown. It was demonstrated that initiators like dichloromethane or butyl chloride have poor efficiency at the initial step of the reaction, leading to PD higher than 1.6 because the initial reaction using these initiators is slow and not all the polymer chains start to grow simultaneously. The efficiency could be seen as the ability of the initiator to transfer the halide to the transition metal in the redox reaction; if the C-X bond is strong, the formation of the radical is less favored and the efficiency of the initiator is low¹⁷.

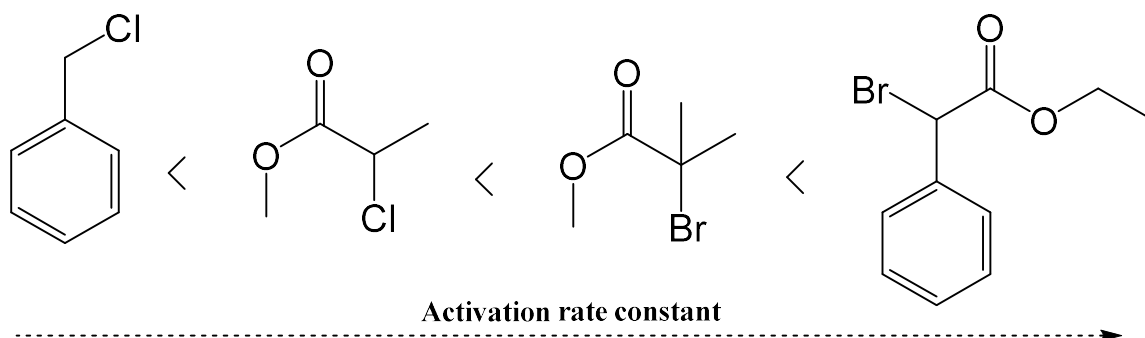


Figure 4: Structure of some ATRP initiators⁵³.

1.1.1.1.2 Leaving Group

As the efficiency of the initiator is related to the bond strength, it is clear that also the leaving group of the initiator plays an important role in determining the efficiency of the process. In its articles Krzysztof Matyjaszewski^{17,53,54}, studied the effect of the leaving group on the control of the ATRP process. In particular by comparing bromine and chlorine derivatives, they show that the first ones lead to a faster reaction and a lower PD, being C-Br bond weaker than C-Cl¹⁷. So the more the leaving group is a good leaving group the more the activation rate constant increases.

The halide ions are the most used leaving group, but also pseudo-halides, carboxylates and non-coordinating triflate and hexafluorophosphate anions could be used⁵⁵.

The k_{ATRP} is influenced by different component present in the ATRP system, and it is not possible to determine which is the best catalyst, solvent, ligand and so on for all the ATRP. Each of them, indeed, has a different influence on the K_{ATRP} . To find the optimal conditions of reaction, and the best species to use to obtain the maximum control over the reaction, a screening should be done, changing one parameter in each experiment. At the end of this screening the best conditions to polymerize a specific monomer should be found¹.

1.1.2 Comparing ATRP with NMP and RAFT

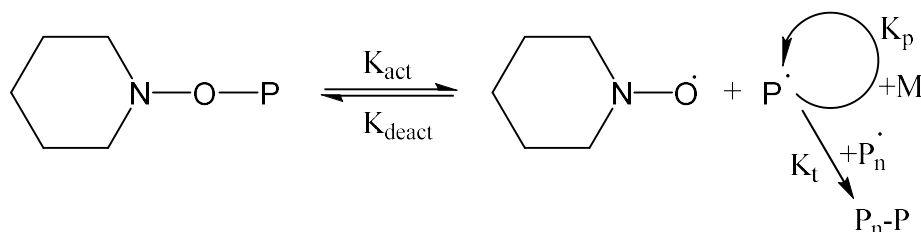
ATRP is not the only CLRP that attracted significant interest. Also nitroxide mediated polymerization (NMP) and reversible addition-fragmentation chain transfer (RAFT) are two types of CLRP which are used to polymerize vinyl monomers.

The principle on which the NMP reactions are based on is the same of ATRP: a low concentration of propagating radicals in solution that reduces bimolecular reaction

between two growing radicals (termination). The two systems are different on how this low concentration is achieved.

In a NMP an equilibrium between a dormant and a growing specie is still present and this is established through a reaction between the growing radicals and a stable nitroxyl radical as shown in Scheme 7^{8,56}.

NMP does not require any specific initiator but common radical initiators are used. Using this latter technique other monomers like methyl methacrylate, methyl acrylate vinyl acetate and so on can be synthesized in presence nitroxide scavenger^{8,9}. Once the radicals have been formed they can react with the nitroxyl radicals, forming the alkoxyamines in situ, and establish the equilibrium that allows to maintain a low concentration of growing species in solution and start the controlled radical polymerization^{8,57}. The dormant species is not directly involved in the polymerization reactions while the radical derived from the dormant specie can undergo two reactions: the polymerization, or the recombination with the nitroxyl radical to form again the dormant specie (Scheme 7).



Scheme 7: Schematic representation of the characteristic NMP reactions¹.

Some example of nitroxides employed in NMP are shown in Figure 5.

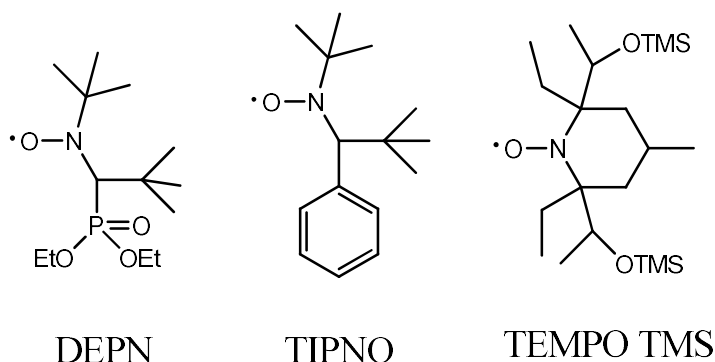
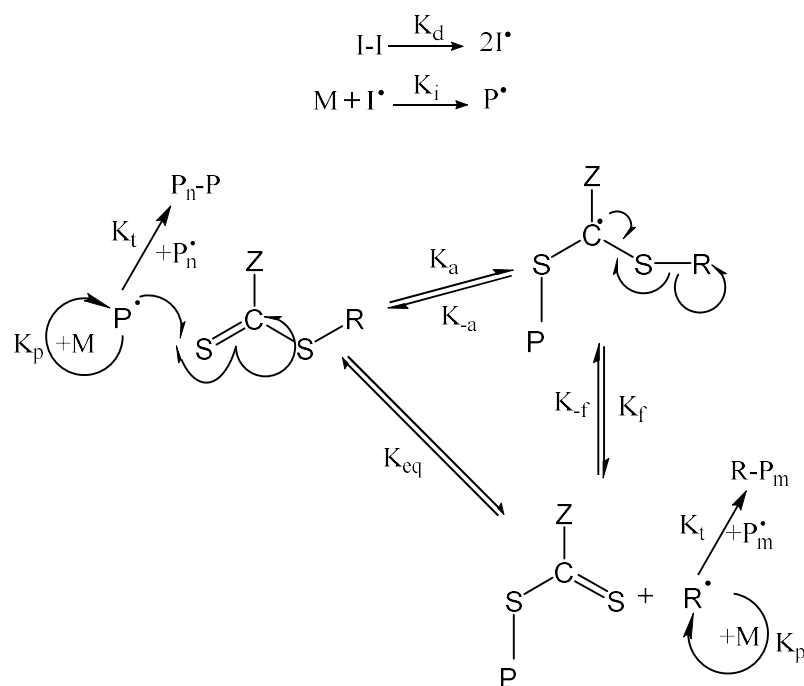


Figure 5: Structures of some NMP scavengers¹.

During RAFT a degenerative transfer process is involved and it allows to obtain polymers with controlled molecular weight and narrow PD (usually < 1.2)⁴. Respect to the other two systems seen, in ATRP and NMP the rate of polymerization is determined by the value of the equilibrium constant of the activation and deactivation reaction and by the persistent radical effect. In RAFT there is no persistent radical effect and the activation and de-activation reactions are chain-transfer reactions¹⁰.

The three fundamental elements for a degenerative transfer process are: monomer, classic radical initiator and a transfer agent. The degenerative transfer process can differ depending on the used transfer agent⁵⁸⁻⁶⁰. In a RAFT process various dithioesters, dithiocarbamates, trithiocarbonates and xanthates could be used as transfer agent^{4,10}.

Common radical initiators are used in order to form radicals in solution that react with the monomers. Once the radicals derived from the monomers are present in solution these can react with the transfer agent and give rise to that equilibrium that characterizes the reversible addition–fragmentation chain transfer (Scheme 8) ⁴.



Scheme 8: Schematic representation of the reactions that occur during RAFT.

If the starting monomer is able to thermal self-initiation, such as styrene, no radical initiator is needed^{10,61}. The growing radicals, obtained by radical initiation, could both react with the monomer or with the RAFT agent that acts as scavengers. Once it reacts with the scavengers it is carried in a dormant form and simultaneously a new radical (R[•]) is formed

and it can react with the monomer continuing the polymerization. To avoid as much as possible termination reactions, the reaction between growing radical and scavenger should be faster respect to coupling reaction, so it should be very high. Only if the exchange between dormant and active species is very high the polymerization has a living character, resulting in polymers with defined and pre-determined structure, molecular weight and low polydispersity⁴. As a consequence of its living character the resulting product still has the RAFT end groups at the ends of the chain⁶².

The reactions conditions used during a RAFT process are the same as those used for a conventional free-radical polymerization, so it can be carried out in bulk, solution, emulsion or suspension, using well known radical initiators and a wide range of molecular weight can be obtained⁴.

ATRP, NMP and RAFT have advantages and limitations. ATRP requires the use of a catalyst that sometimes should be removed from the final product because it is toxic and it colors the material. It should be mentioned that the development of this technique allowed to use very low concentration of catalyst⁴⁰. In NMP and RAFT the mediating species are bonded to the polymer and no metal catalyst are used^{1,4}. At the same time, the presence of functional groups among the repeating units of polymers synthesized by NMP and RAFT can cause some problems if the synthesized materials need to be modified by subsequent reactions. As an example, the ester group which is present in block copolymers synthesized by RAFT can be hydrolyzed and as a consequence of this reaction the polymer chains break⁶³. Usually the purity of block copolymers synthesized by ATRP is higher.

ATRP uses commercially available reactants whilst NMP and RAFT require the use of alkoxyamines and dithioesters that usually should be synthesized on purpose. ATRP is a versatile technique that allows to polymerize a wide range of monomers¹⁴, but the polymerization of acidic monomers is still challenging and it requires protection or neutralization. NMP of methacrylates and less reactive monomer is difficult and RAFT cannot be used for the polymerization of basic monomers¹.

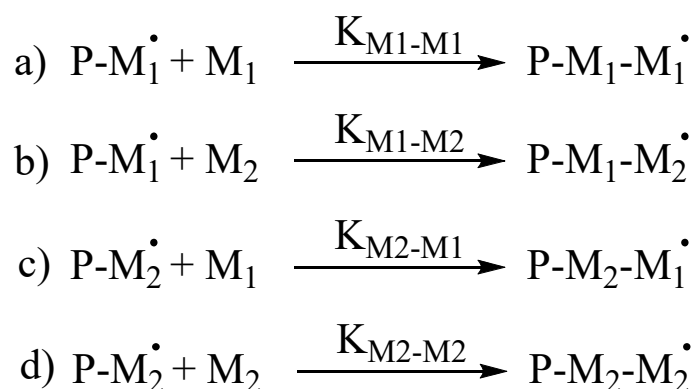
Concluding, the three illustrated CRLP are complementary but ATRP, nowadays, is the easiest to apply on a large scale⁶⁴.

2 Chapter 2 - ATRP of polar monomers: synthesis and characterization of homo and copolymers

2.1 Introduction

2.1.1 Synthesis of random and gradient copolymers

The radical polymerization allows to synthesize random and gradient copolymers if two (or more) monomers (M_1 and M_2) are present simultaneously in the reaction medium⁶⁵⁻⁶⁸. In random copolymers the instantaneous composition (repeating unit sequence) does not change along the polymer chain, while in gradient copolymers it changes passing from the beginning to the end of the chain^{66,69-71}. In order to obtain copolymers with the desired structure and composition, it is necessary to know the rate constants involved. During a radical polymerization the propagation reactions are generally four (Scheme 9).



Scheme 9: Propagation reactions involved during copolymerization⁶⁸.

During a free-radical polymerization also termination reactions occur influencing the copolymer composition⁶⁸. In controlled radical polymerizations, other equilibrium reactions are involved, affecting the resulting copolymer composition and structure, e.g. the ATRP equilibrium that establishes the propagating radical concentration in solution during an ATRP⁶⁹⁻⁷¹.

Once the radicals are formed, the propagating reactions that determine the copolymer composition are the ones shown in Scheme 9. Assuming a constant concentration of propagating radicals, the composition of the copolymer which is formed at any chosen time is described by Equation 9⁷².

Equation 9⁶⁸

$$\frac{\partial[M_1]}{\partial[M_2]} = \frac{[M_1] * \left\{ [M_1] * \left(\frac{K_{M1-M1}}{K_{M1-M2}} \right) + [M_2] \right\}}{[M_2] * \left\{ [M_2] * \left(\frac{K_{M2-M2}}{K_{M2-M1}} \right) + [M_1] \right\}}$$

K_{M1-M1}/K_{M1-M2} corresponds to the reactivity ratio of M_1 (r_1) and K_{M2-M2}/K_{M2-M1} corresponds to the reactivity ratio of M_2 (r_2). Their values allow to determine if the systems tend to form random copolymers or homo/gradient (co)polymers⁷².

Only when r_1 and r_2 are equal to 1 the copolymer composition is equal to the feed composition. Unfortunately, usually the rate constants are not equal and the result is that one of the monomer is preferably incorporated into the polymer. When this happens the feed composition changes during the polymerization and so does the resulting polymer composition. In order to obtain the desired polymer composition, it is possible to act on the temperature, changing the values of the rate constants. It is also possible to act on the monomer feed composition, working in a semi-batch system, feeding the correct amount of monomers with the aim to maintain the feed composition that determine the desired polymer^{68,71}. Depending on the values of the rate constants (K_{M1-M1} , K_{M1-M2} , K_{M2-M1} and K_{M2-M2}) it is possible to obtain gradient copolymers using batch systems^{73,74} but sometimes semi-batch systems are required⁷⁵.

Several models, based on Equation 9, were developed in order to determine the monomer reactivity ratios. These models rely on the determination of the copolymer composition knowing the feed composition. During the polymerization the feed composition changes, so it possible to assume a constant feed composition only when low monomer conversions (5-10% mol/mol) are reached. As a consequence, for each copolymerization study, it is necessary to determine several copolymer composition as a function of different co-monomer feed, carrying out copolymerizations maintaining low conversion values. Results are then interpreted within a specific context^{72,76,77}.

Equation 9 relates the co-monomer feed to the copolymer composition and it can be express in terms of mole fraction (Equation 10).

Chapter 2: ATRP of polar monomers

Equation 10⁷²

$$F_1 = \frac{r_1 * f_1^2 + r_1 * f_2}{r_1 * f_1^2 + 2 * f_1 * f_2 + r_2 * f_2^2}$$

$$\text{where } F_1 = \frac{d[M_1]}{d[M_1] + d[M_2]}; f_1 = \frac{[M_1]}{[M_1] + [M_2]}$$

The limit of Mayo-Lewis equation (Equation 10) is that all the variables should be measured instantaneously. Its integration gives the Meyer-Lewis equation (Equation 11) which allows to determine copolymer composition running experiments until 25-30% of monomer conversion.

Equation 11⁷⁸

$$X_n = 1 - \left[\frac{f_1}{f_{1-0}} \right]^\alpha * \left[\frac{f_2}{f_{2-0}} \right]^\beta * \left[\frac{f_{1-0-\delta}}{f_{1-\delta}} \right]^\gamma$$

Where X_n = conversion; $\alpha = \frac{r_2}{(1-r_2)}$; $\beta = \frac{r_1}{(1-r_1)}$; $\gamma = \frac{1-r_1*r_2}{(1-r_1)*(1-r_2)}$; $\delta = \frac{(1-r_2)}{(1-r_1-r_2)}$; f_{1-0} and f_{2-0} are the initial mole fraction of the monomers.

At higher conversions the basic assumptions done in order to integrate Mayo-Lewis equation are violated. The basic assumptions are three:

- The polymerization is carried out in isothermal conditions.
- The volume of the reaction mixture does not change significantly during the polymerization.
- Reactivity ratios are constant throughout the synthesis.

The last one is the reason why the conversion should be lower than 30%: at higher conversion values, indeed, the diffusion limits can decrease the propagation rate constants⁷⁸.

Mainly, three different approaches were developed to estimate reactivity ratios: linear regression (e.g. Finemann-Ross and Kelen-Tudos model), non-linear least square method and error in variables model. The first one is usually not valid⁷⁹⁻⁸¹. In non-linear least square the error associated to the independent variable should be negligible, so it is necessary to determine exactly the co-monomer feed composition^{73,80,82}. Error in variables models takes into account all the errors that can affect the variables⁸³.

2.1.2 Aim of the project

Poly(*N*-vinylcaprolactam) (PNVCL) and Poly(*N*-vinylpyrrolidone) (PNVP) and their copolymers (or derivatives) found applications in many fields, such as the synthesis of low dosage clathrate inhibitors⁸⁴⁻⁸⁸, biomedical⁸⁹⁻⁹¹, nanoparticle and nano-rod stabilizers^{92,93}, carbon nanotubes dispersants^{94,95}, bioconjugation and surface ligand immobilization⁹⁶.

PNVCL and PNVP are water soluble, amphiphilic, thermo-responsive, low-toxic and biocompatible polymers. Furthermore, they are stable against hydrolysis. These characteristics make them suitable for biomedical applications, indeed, production of hydrogels is the most important field where they are applied. PNVCL and PNVP display a lower critical solution temperature (LCST) which depends on the molecular weight of the polymers (32-45°C)^{89,90,97}. Their amphiphilic character allows them to form micelles that can incorporate drugs^{98,99}. They also form reverse hydrogels upon heating above the LCST of the polymers, offering the possibility to administrate drugs by injection of polymeric solutions that form gels at the body temperature (targeted-administration)^{89,90,97}.

The properties of PNVCL and PNVP depend on the polymer structures. Thus the control of the polymerization will allow to increase the fields of application and the efficiency of PNVCL and PNVP-based systems.

NVCL and NVP can only be polymerized by radical polymerization, but the high reactivity of their radicals makes the controlled radical polymerization of such monomers quite challenging⁹¹.

Being the final properties of a polymer strictly related to its structure and composition, by using controlled radical polymerization (CRP) it is possible to obtain materials with predetermined properties for application in specific fields.

NVCL and NVP, as other vinyl monomers, can be polymerized using a classic radical initiator^{100,101} (e.g. AIBN) but the resulting material has high PD and no living chain-end. As reported in literature, PNVCL or PNVP can be synthesized in a controlled way by xanthate or dithiocarbamate mediated radical polymerization (RAFT/MADIX)¹⁰²⁻¹⁰⁵, by cobalt-mediated radical polymerization (CMRP)^{106,107} or by ATRP^{41,89,108,109}. Being the aim of the project the optimization of PNVCL and PNVP synthesis, different polymerization techniques were evaluated, taking into account the cost of the overall process and the characteristics of the obtained materials.

Among the three cited polymerization technique it was chosen to use ATRP because it offers many advantages:

- It is possible to use reactants that are commercially available¹⁴. RAFT requires to synthesize specific chain transfer agents and by CMRP it is necessary to use a preformed alkylcobalt(III) adduct, increasing in both the case the synthetic steps.
- Copper is less expensive compared to cobalt.
- By ATRP it is possible to polymerize different monomers(methacrylates, acrylates, styrene, etc.)¹⁴, allowing the synthesis of block copolymers without changing the polymerization mechanism or simply by adding a second monomer when the polymerization of the first block reaches high conversions (~90%) (single-step synthesis of block copolymers). Furthermore, being insensitive to many functional groups and tolerant towards impurities present in solvent and reactants, including water¹¹⁰, this technique can be industrially applied.

In this context, we retained of interest to shed some light on the ATRP of polar monomers. In particular, a wide range of monomers, including *N*-vinylcaprolactam (NVCL) and *N*-vinylpyrrolidone (NVP), were polymerized and copolymerized with the aim to synthesize random and block copolymers with well-defined structures, paying particular attention to the achievement of a scalable, safe and cheap synthetic procedure¹⁴.

For this purpose, several kinetic studies were carried out changing the initial molar ratio of monomers and initiator, the concentration, the solvent and the temperature with the aim to set up a process that allows to obtain high monomer conversion. Furthermore, the process was optimized to be carried out at 60-80°C in a solvent with high flash point which can act also as carrier for the final material, thus decreasing the purification costs.

Unfortunately, ATRP requires particular operative conditions^{5,64,111}, such as the absence of oxygen into the polymerization reactor, that increase the cost of the overall synthesis process. At the same time, polymers with well-defined structure can exhibit specific properties that can add value to the final synthesized material¹¹².

2.2 Results and discussion

2.2.1 Synthesis of homopolymers by ATRP

2.2.1.1 Synthesis of PNVP by ATRP

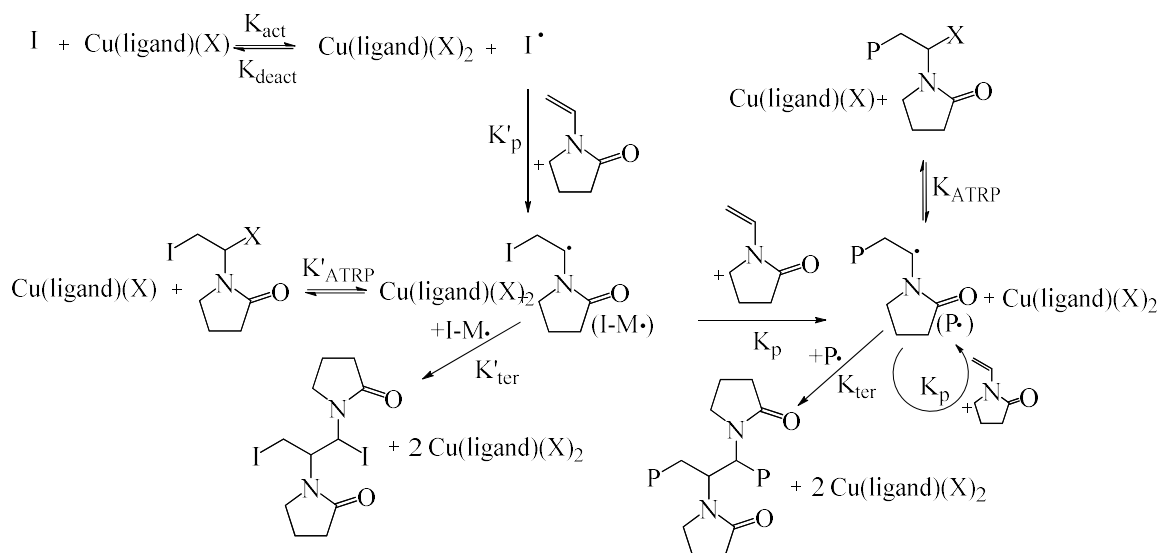
The controlled radical polymerization of NVP is difficult because, despite to other monomers that are easily polymerized in a controlled way, such as styrene^{5,38,113,114}, methacrylates^{5,42,44,115,116}, acrylates^{45,117-119} and so on, it generates an unstable not-conjugated radical.

Several attempts of ATRP of NVP were carried out by using different reactant molar ratio and *N,N,N',N'',N''*-pentamethyldiethylenetriamine (PMDETA) as ligand, CuBr as catalyst, allyl-2-bromo-2-methylpropionate (ABIB) as initiator in anhydrous THF. Unfortunately, no evidences of the occurrence of polymerization were obtained. This could be due to the low activity of PMDETA which is not able to break the CH-Cl bond of the dormant specie formed by the PNVP propagating radicals.

Furthermore, experimentally it was observed that the monomer is able to solubilize the catalyst even in absence of the ligand. Such a behavior suggests that the monomer may interact with the ATRP system stopping the polymerization.

For these reasons we attempted the ATRP of NVP in presence of Me₆Cyclam as ligand. It is reported in the literature, indeed, that such a compound allows to promote the controlled homopolymerization of several polar monomers^{41,89,105,120,121}. The reactions that can occur during the ATRP of NVP are reported in Scheme 10. When the polymerization is controlled, K_{ter} is negligible compared to K_p . Using common ATRP conditions, the initial reaction occurs and the radical generated by the initiator can react with the monomer. Once the propagating radical is converted into the dormant specie the K'_{ATRP} is low and it does not allow the establishment of the ATRP equilibrium.

Chapter 2: ATRP of polar monomers



Scheme 10: Characteristic ATRP equilibrium of NVP with some possible termination that may occur during the polymerization.

Thus, a series of polymerizations of NVP was carried out under ATRP conditions in presence of MCP as initiator, and CuCl complexed by Me₆Cyclam as catalyst in dry 1,4-dioxan/n-propanol 98:2 v/v at room temperature (see procedure 1 in the Experimental section). The initial monomer concentration ([M₀]) was 2.5 M.

The occurrence of polymerization involving the vinylic double bond was confirmed by FT-IR, showing the disappearance of the absorption at 1630 cm⁻¹, ascribed to the stretching vibration of the double bond in the monomer^{122,123}. Accordingly, in the ¹H-NMR spectrum of PNVP, the resonances at 4.44, 4.37 and 7.09 ppm related to the vinyl protons of NVP monomer, are absent. ¹H-NMR analysis of the final reaction mixtures allowed also the determination of the monomer conversion by comparing the signals of the vinylic double bond with those ones of the polymer.

A good control of the polymerization process could be achieved with these experimental conditions, as demonstrated by the linear dependence of ln([M₀]/[M]) as a function of time (Figure 6). The conversion, in fact, shows a logarithmic dependence on the time and the reaction follows a first order kinetics with respect to the monomer concentration reaching a quite high monomer conversion (82%) when a [M₀]/[C]/[L]/[I₀] (M=monomer, C=catalyst, L=ligand and I₀= initiator) = 100/1/1/1 initial molar ratio is used. It is worth noting that, by increasing the concentration of initiator ([M₀]/[C]/[L]/[I₀]=100/2/2/2), the rate of polymerization decreases (Figure 6), suggesting a lower concentration of propagating radicals. Such a behaviour could be ascribed to the occurrence of reactions of termination at the initial step of the process, whose rate increases with the initiator

concentration (see Equation 5) and which lead to the irreversible formation of Cu(II) (persistent radical effect¹²⁴). Thus the ATRP equilibrium shifts towards the dormant species and decreases the rate of polymerization until an equilibrium, with a constant concentration of propagating radical, is reached (see Equation 2)

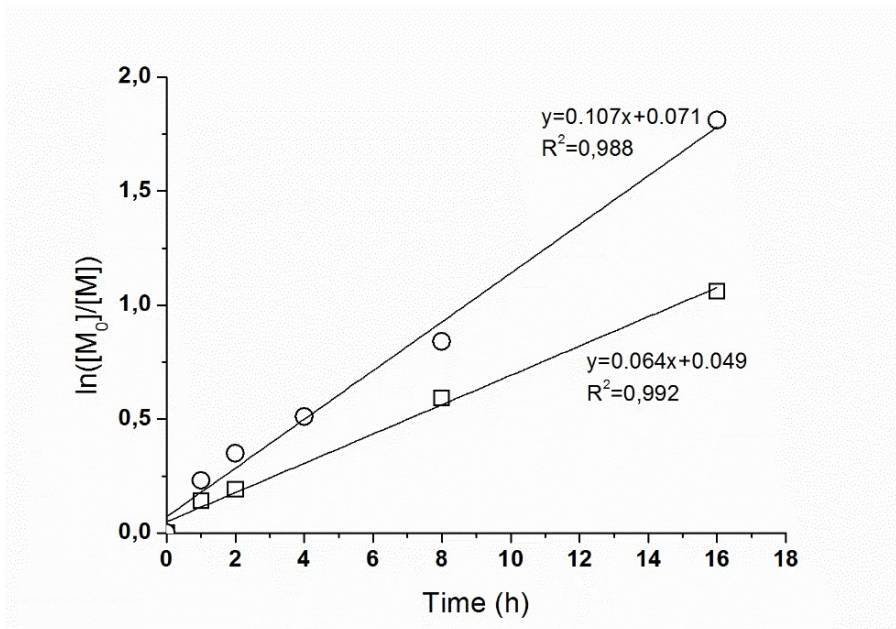


Figure 6: $\ln([M_0]/[M])$ as a function of time for the ATRP of NVP in dry 1,4-dioxan/n-propanol 98:2 v/v ($[M_0]=2.5\text{ M}$) at 25°C. $[NVP]/[CuCl]/[Me_6CyClam]/[MCP] = 100/1/1/1$ (○) and 100/2/2/2 (□).

The occurrence of such terminations is confirmed by the fact that, as shown in Figure 6, the intercepts of the obtained straight lines do not pass through the origin, as expected.

It is worth noting that by replacing MCP with ABIB in presence of Me₆Cyclam as ligand, the polymerization did not occur. Such a behaviour could be ascribed to the more stable tertiary radicals generated by ABIB which react faster with the catalyst leading to a higher concentration of radicals at the initial step of the polymerization and thus to termination reactions.

In order to get an insight into the ATRP polymerization mechanism of NVP, the reactants addition order was modified. In particular, several polymerizations were carried out adding the initiator as last reactant to the reaction mixture before the freeze-thaw cycles (see procedure 2 in the experimental section). The process was studied also upon changing the monomer to initiator ratio and keeping the concentration of all the other reactants unchanged. The conversion after 4 hours of reaction was determined by ¹H-NMR analysis and reported in Table 1.

Table 1: Conversion and PD after 4 hours of PNVP synthesized by ATRP using different initial molar reactants ratio and procedures.

| Polymerization procedure | $[M_0]/[C]/[L]/[I_0]$ | Conv. after 4h (% mol/mol) ^a | PD ^b |
|--------------------------|-----------------------|---|-----------------|
| 1 | 100/1/1/1 | 35 | 1.58 |
| 2 | 100/1/1/1 | 50 | 1.55 |
| 2 | 100/1/1/1.5 | 46 | 1.51 |
| 2 | 100/1/1/2 | 45 | 1.45 |
| 2 | 100/1/1/3 | 40 | 1.42 |

^a Determined by ¹H-NMR.

^b Determined by GPC in DMF.

By comparing the data obtained by the two different procedures (1 and 2) with the same initial molar ratio of reactants ($[M_0]/[C]/[L]/[I_0]=100/1/1/1$) it is clear that the addition of the initiator as the last reactant leads to an increase in the reaction rate (monomer conversion after 4h 35 and 50% respectively). The reason of this behaviour can be found in the lowering of the termination reaction extent with procedure 2, since the addition of initiator marks the actual polymerization beginning and its delay prevents any undesired reactions in the uncontrolled initial preparatory stage. Thus the amount of radicals during the propagation stationary stage of the polymerization increases and so does the polymerization rate.

Moreover, when applying procedure 2, by decreasing the monomer to initiator ratio from 100/1 to 100/3, the conversion after 4 hours drops from 50 to 40% (Table 1) because of the increased rate of termination reactions during the initial step of the polymerization.

All the obtained polymers were analysed by GPC in DMF in order to determine their PD which is in the range 1.4-1.6. Furthermore, the molecular weight distribution is unimodal, confirming that a negligible amount of terminations occurs during the stationary state of the synthesis. Being the average molecular weight determined by GPC affected by error because they depend on the hydrodynamic volume of the polymers, $^{GPC}\overline{M}_n$ values will not be taken into account.

It is known that polymers with amphiphilic character as PNVP^{97,105,107} can form aggregates in solution. The presence of aggregates and the possible interactions between the molecules and the stationary phase during the elution may increase the PD determined by GPC. So the average molecular weight and the PD of some samples were determined

also with MALDI-TOF; the results are summarized in Table 2 and, as an example, in Figure 7 is shown the MALDI-TOF spectrum of PNVP synthesized in 4 hours of reaction, using the polymerization procedure 2 in dry 1,4-dioxan/n-propanol 98:2 v/v ($[M_0]=2.5$ M) at 25°C, $[NVP]/[CuCl]/[Me_6CyClam]/[MCP] = 100/1/1/3$.

Table 2: Conversion, \overline{M}_n and PD of PNVP synthesized with different ATRP conditions.

| Polymerization procedure | $[M_0]/[C]/[L]/[I_0]$ | Reaction time (h) | Conv. (% mol/mol) ^a | Theor. \overline{M}_n (Da) ^c | MALDI \overline{M}_n (Da) ^b | PD ^b | GPC \overline{M}_n (Da) ^d | PD ^d |
|--------------------------|-----------------------|-------------------|--------------------------------|---|--|-----------------|--|-----------------|
| 1 | 100/1/1/1 | 1 | 35 | 4900 | 5000 | 1.22 | 10400 | 1.45 |
| 2 | 100/1/1/3 | 4 | 40 | 170 | 4300 | 1.11 | 9500 | 1.38 |

^a Determined by ¹H-NMR.

^b Determined by MALDI-TOF.

^c Theoretical \overline{M}_n determined considering the monomer conversion and the monomer to initiator ratio.

^d Determined by GPC in DMF.

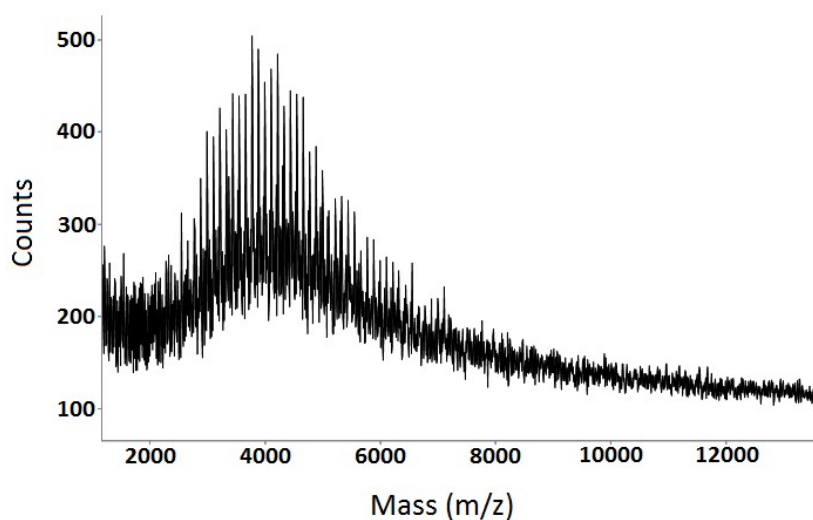


Figure 7: MALDI-TOF spectrum of PNVP synthesized in dry 1,4-dioxan/n-propanol 98:2 v/v ($[M_0]=2.5$ M) at 25°C. $[NVP]/[CuCl]/[Me_6CyClam]/[MCP] = 100/1/1/3$, polymerization procedure 2, reaction time 4h.

The data displayed in Table 2 show that the PD determined by MALDI-TOF is lower than that one determined by GPC, confirming the presence of aggregates and interactions during the elution in the column. Furthermore, procedure 2 allows to obtain materials with lower PD thanks to the better control achieved adding the initiator as last reactant, but also to the reached higher conversion. It is well known, indeed, that during the ATRP the

PD decreases with the conversion reaching a stable and low value⁵. The presence of termination reactions during the initial step of the polymerization is also confirmed from the disagreement between the \overline{M}_n determined by MALDI-TOF and the theoretical one (Table 2), that can be determined considering the monomer to initiator ratio and the conversion (see Equation 1).

2.2.1.2 Synthesis of PNVCL by ATRP

The ATRP of NVCL was carried out by procedure 2 at room temperature in 1,4-dioxan ($[M_0]=2.5$ M) in presence of MCP as initiator, Me₆Cyclam as ligand, CuCl as catalyst and with an initial molar ratio of $[NVCL]/[CuCl]/[Me_6CyClam]/[MCP] = 100/1/1/1$.

The occurrence of polymerization involving the vinylic double bond was confirmed by FT-IR, showing the disappearance of the absorption at 1652 cm^{-1} ascribed to the stretching vibration of the double bond in the monomer¹²². Accordingly, in the ¹H-NMR spectrum of PNVCL, the resonances at 4.40, 4.46 and 7.38 ppm related to the vinyl protons of NVCL, are absent. Although a good control of the polymerization process could be achieved with these experimental conditions, as demonstrated by the linear dependence of $\ln([M_0]/[M])$ as a function of time (Figure 8), the ATRP of NVCL results slower than that of NVP in the same polymerization conditions ($K_{app}=0.022$ and 0.064 h^{-1} respectively). Such a behaviour could be ascribed to the higher hindrance of caprolactam moieties compared to the pyrrolidone ones which makes more difficult the reaction between the double bond and the radical of the propagating chain.

With the aim to study the effect that each component has over the entire polymerization process, the kinetic of the ATRP of NVCL was studied in presence of oxidized catalyst [Cu(II)] using polymerization procedure 3 $\{[M_0]=3.6\text{M}$ $[Cu(I)]/[Cu(II)]=1/0$, $[M_0]=3.6\text{M}$ $[Cu(I)]/[Cu(II)]=1/0.5$ and $[M_0]=1.8\text{M}$, $[Cu(I)]/[Cu(II)]=1/0.5\}$ (Figure 8).

As reported in Figure 8, all the systems show a linear dependence of $\ln([M]_0/[M])$ with time thus indicating a first-order kinetics of the polymerization rate with respect to the monomer concentration and a constant concentration of the growing species throughout the whole process.

In presence of Cu(II) the initial reaction should be more controlled and the ATRP equilibrium should be balanced by the presence of oxidized catalyst. Furthermore, to obtain a good control over the polymerization, the ratio between the rate of polymerization and the rate of termination (see Equation 2 and Equation 5) is very important in order to make negligible the second one compared to the first one. With this aim the ATRP of

NVCL was studied using a monomer concentration of 3.6 M and $[Cu(I)]/[Cu(II)]=1/0.5$. Then, the kinetic study was repeated decreasing the concentration to 1.8 M. It is important to stress that one of the purpose of the project is to use the lowest amount of solvent in order to decrease the cost of the entire process but at the same time it is important to study the effect that each component has over the entire polymerization. Using polymerization procedure 3 the catalyst is not solubilized in the system before to start the polymerization and no termination reactions occur during the preparation of the mixture.

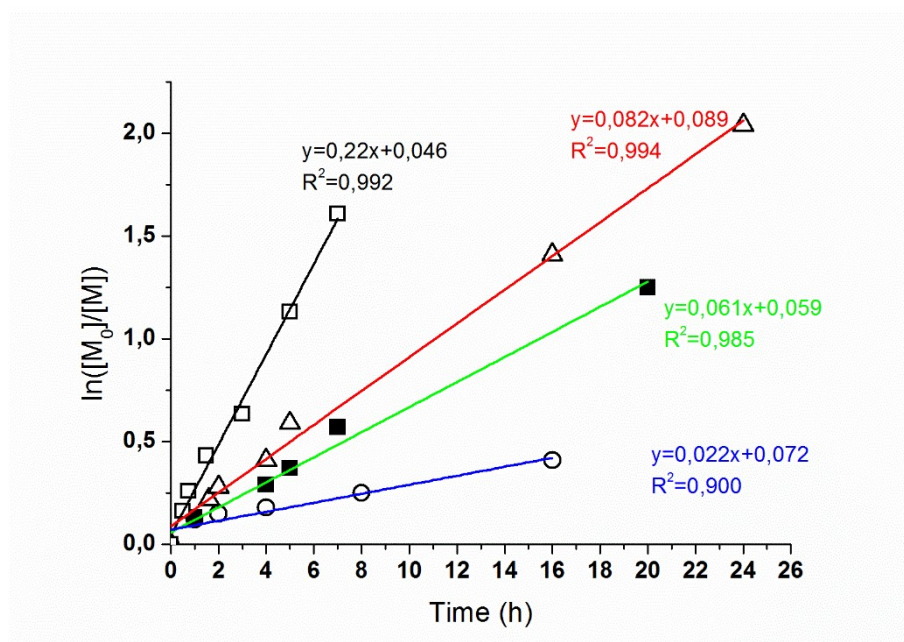


Figure 8: $\ln([M_0]/[M])$ as a function of time for the ATRP of NVCL in 1,4-dioxan at 25°C with $[NVCL]/[CuCl]/[CuCl_2]/[Me6CyClam]/[MCP] = 100/1/0.5/1.5/1$, $[M_0] = 3.6 M$ (■) and $[M_0] = 1.8 M$ (▲), with $[NVCL]/[CuCl]/[CuCl_2]/[Me6CyClam]/[MCP] = 100/1/0/1/1$, $[M_0] = 3.6 M$ (□) and with $[NVCL]/[CuCl]/[CuCl_2]/[Me6CyClam]/[MCP] = 100/1/0/1/1$, $[M_0] = 2.5 M$ (○).

As reported in Figure 8, where the dependence of $\ln([M_0]/[M])$ as a function of time for the ATRP of NVCL using 50% of Cu(II) and different initial monomer concentrations are displayed the polymerization is faster in the more dilute system ($K_{app} = 0.082 \text{ h}^{-1}$ when $[M_0] = 1.8 M$ and $K_{app} = 0.061 \text{ h}^{-1}$ when $[M_0] = 3.6 M$). This effect is mainly due to the lower rate of termination that increases the amount of radicals in the solution and rise up the rate of polymerization making the reaction faster than the one with higher reactants concentration. The increased K_{app} (0.082 h^{-1}) is the demonstration that decreasing the amount of terminations, the polymerization is faster.

The ATRP of NVCL was also attempted in absence of Cu(II) ($[M_0] = 3.6 M$) and the reaction resulted even faster ($K_{app} = 0.22 \text{ h}^{-1}$), reaching 80% of monomer conversion in 7

hours as demonstrated by the $\ln([M_0]/[M])$ as a function of time reported in Figure 8. Such a behavior suggests that the presence of Cu(II) decreases not only the rate of termination, but also that one of polymerization. Indeed, without Cu(II) in a very concentrated system ($[M_0]=3.6M$) it was expected to obtain a faster reaction. Unfortunately, in these conditions the occurrence of termination reactions during the initial step of the polymerization cannot be avoided and the monomer to initiator ratio changes. For this reason, when a precise control over the molecular weight of the polymer is desired, it is necessary to use a suitable amount of Cu(II) in the reaction mixture.

The kinetic studies demonstrate that it is possible to achieve a good control over the process diluting the system and using Cu(II). Changing the initial monomer concentration and the amount of Cu(II) it is possible to set up a controlled process that allows monomer concentrations that are suitable for industrial application.

It is known that PNVCL aggregates^{90,125,126} in solution and this might influence the molecular weight and PD determination by GPC. In order to confirm the formation of aggregates, PNVCL-7800 (PNVCL with $\overline{M}_n=7800$ Da) in water solution with different concentration was analysed by DLS at room temperature. As reported in Table 3, this material self-assembles in water at all the analysed polymer concentration (6,3 and 1 mg/ml).

Table 3: DLS results of PNVCL-7800 water solutions at 25°C.

| Concentration (mg/ml) | Peak 1 | | Peak 2 | | Derived Count Rate | Intercept |
|--------------------------|---------|---------------|---------|---------------|-----------------------|-----------|
| | d. (nm) | Intensity (%) | d. (nm) | Intensity (%) | | |
| 6 | 40 | 66 | 260 | 34 | 10770 | 0.99 |
| 3 | 55 | 76 | 460 | 18 | 5630 | 0.96 |
| 1 | 45 | 71 | 150 | 26 | 2375 | 0.97 |

Being PNVCL a temperature-responsive material^{90,125,126}, increasing the temperature to 37°C the diameter of the aggregates increases (>1000 nm) and DLS is no more suitable for the determination of their size. Thus it is reasonable to assume that PNVCL aggregates also in DMF at 70°C, hence GPC analysis in these conditions cannot be considered reliable.

Unfortunately, the average molecular weight of the synthesized polymers cannot be determined by $^1\text{H-NMR}$ because, the signals of the initiator residue (MCP) are overlaid with those of the backbone.

For this reason, some of the previously reported experiments were repeated by using allyl 2-chloropropionate (ACP) as initiator which has the same reactivity of MCP but contains an allyl group whose related $^1\text{H-NMR}$ signals at 5.93 ppm (1H, $\text{CH}_2=\text{CH}-\text{CH}_2-\text{O}$) and 5.32 ppm (2H, $\text{CH}_2=\text{CH}-\text{CH}_2-\text{O}$) are well identifiable (Figure 9). Thus, the comparison of their integrals with respect to those ones of NVCL residue, allows to assess the number average molecular weight (\overline{M}_n) of the obtained materials (Table 4).

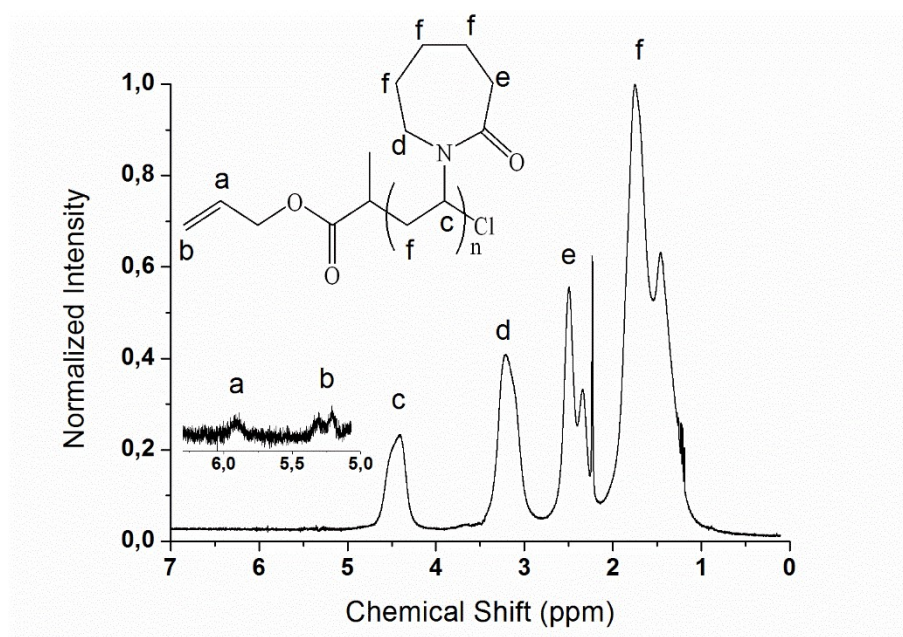


Figure 9: $^1\text{H-NMR}$ of PNVCL synthesized using ACP as initiator.

In order to better understand the mechanism of the initial step of the ATRP of NVCL three polymerizations were carried out without using Cu(II) and changing the concentration of initiator into the initial solution. The results were compared with the ones obtained polymerizing NVCL in presence of Cu(II) and a monomer to initiator ratio of 100 to 1 (a typical molar ratio used during ATRP) (Table 4). The PD index and the shape of the chromatograms determined by GPC in DMF were used as parameter to compare the different systems of polymerization. Even if PD determined by GPC might be higher than the real one it is a good parameter to compare the different polymers.

Chapter 2: ATRP of polar monomers

Table 4: \overline{M}_n determined by $^1\text{H-NMR}$ and PD determined by GPC for the ATRP of NVCL in 1,4-dioxan at 25°C with $[M_0] = 3.6$ using polymerization procedure 3. Reaction time = 30min.

| $[M_0]/[CuCl]/[CuCl_2]/[L]/[I_0]$ | \overline{M}_n (Da) ^a | PD ^b | Polymer repeating units number | Theor. X_n at 100% (mol/mol) of monomer conversion |
|-----------------------------------|------------------------------------|-----------------|--------------------------------|--|
| 100/1/0/1/1 | 15400 | 1.47 | 110 | 100 |
| 100/1/0/1/2 | 8400 | 1.47 | 60 | 50 |
| 100/1/0/1/4 | 4400 | 1.25 | 31 | 25 |
| 100/1/0.5/1.5/1 | 6300 | 1.34 | 45 | 100 |

^a Determined by $^1\text{H-NMR}$.

^b Determined by GPC in DMF at 70°C.

The polymerizations were carried out for 30 minutes with an initial monomer concentration of 3.6 M. As expected, \overline{M}_n (Table 4) decreases linearly by increasing the monomer to initiator ratio thus allowing to predetermine the average molecular weight of the synthesized material. At the same time PD decreases because the rate of termination increases and Cu(I) oxidizes enhancing the concentration of Cu(II) which slows down the rate of polymerization. Thus the amount of radicals in the stationary state becomes lower, a fast and dynamic equilibrium between dormant specie and propagating radicals is established and the reaction results more controlled, as demonstrated by the unimodal distribution of the molecular weights shown in Figure 10.

Comparing the polymer synthesized using Cu(II) with the ones synthesized under the same experimental conditions but no Cu(II) the first one has lower PD and \overline{M}_n (Table 4). The lower PD, even at lower conversion, demonstrates that the use of Cu(II) increase the control over the polymerization. Furthermore, the polymerization with Cu(II) is the only one in which the repeating unit of the material is lower than the ratio between the monomer and initiator moles, showing that increasing the control over the initial step of the polymerization the number of terminations between the radical initiators decreases (Table 4).

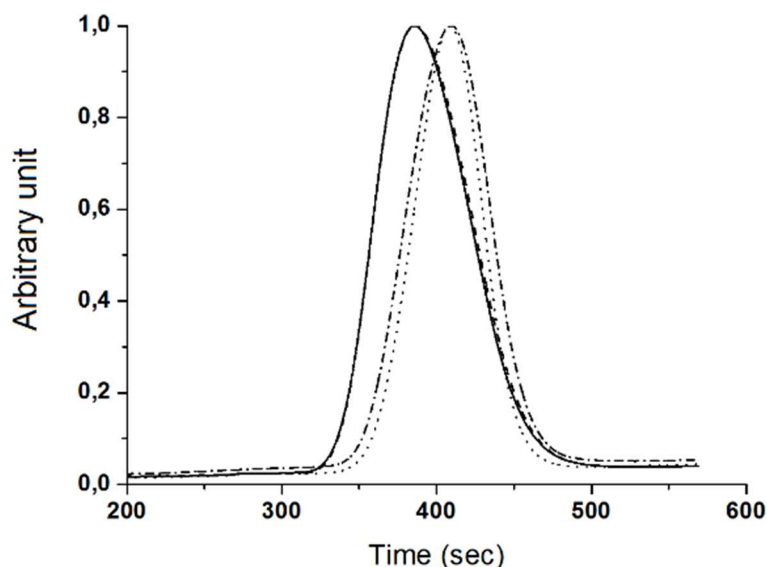


Figure 10: Normalized molecular weight distributions of the synthesized PNVCL determined by SEC in DMF at 70°C. PDI reported in Table 4. $[M_0]/[CuCl]/[CuCl_2]/[L]/[I_0] = 100/1/0/1/1$ (—), $[M_0]/[CuCl]/[CuCl_2]/[L]/[I_0] = 100/1/0/1/2$ (---), $[M_0]/[CuCl]/[CuCl_2]/[L]/[I_0] = 100/1/0/1/4$ (···), $[M_0]/[CuCl]/[CuCl_2]/[L]/[I_0] = 100/1/0.5/1.5/1$ (-·-·).

The reported results highlight that the control of the polymerization is also influenced by the polymerization procedure and by the sequence in which the reactants are added into the reaction mixture.

During the preparation of the reactions, when monomer, initiator, catalyst and solvent are mixed together (polymerization procedure 3), CuCl is partially solubilized in the medium the monomer amide group can interact with Cu(I) while CuCl₂ is solubilized in the mixture only when the ligand is added to the flask. Being the initial reaction very fast, it might happen that when Cu(I) reacts with the initiators forming the radicals, part of Cu(II) does not take part to the reaction and the ATRP equilibrium is more shifted towards the propagating radicals leading to some undesired termination reactions that should not occur if Cu(II) was completely solubilized. With the aim to confirm this assumption two polymerization of NVCL were carried out under the same experimental conditions: one using polymerization procedure 3 and one using polymerization procedure 4. In this latter procedure the monomer, catalysts, ligand and solvent are mixed together and the reaction starts when a degassed initiator solution is added to the reaction mixture. The polymerization were carried out using an initial molar ratio of $[M_0]/[CuCl]/[CuCl_2]/[L]/[I_0] = 100/1/0.3/1.3/1$, $[M_0] = 3.6M$ for 3 hours; in Table 5,

Chapter 2: ATRP of polar monomers

conversion and \overline{M}_n determined by NMR are listed as a function of the polymerization procedure.

Table 5: Theoretical \overline{M}_n and conversion determined by NMR for the ATRP of NVCL in 1,4-dioxan at 25°C with $[M_0] = 3.6$, $[M_0]/[CuCl]/[CuCl_2]/[L]/[I_0] = 100/1/0.3/1.3/1$ using polymerization procedure 3 and 4. Reaction time 3h.

| Procedure | Sample | Conv. % (mol) ^b | \overline{M}_n (Da) ^a | Polymer repeating units ^a | Theoretical polymer repeating unit |
|-----------|--------------|-------------------------------|---------------------------------------|---|---------------------------------------|
| 3 | PNVCL-7800/3 | 35 | 7800 | 56 | 35 |
| 4 | PNVCL-7800/4 | 45 | 7800 | 56 | 45 |

^a Determined by ¹H-NMR.

^b Determined from the monomer conversion.

The data reported in Table 5 demonstrate that the reaction depends on the way it is prepared and not only on the synthesis conditions (concentration, temperature etc...). Comparing the monomer conversion at the end of the polymerizations, the reaction is faster (higher monomer conversion) when the initiator is added as last reactant to the flask. This result confirms the presence of termination reactions that occur when Cu(II) is not completely solubilized and this decreases the rate of polymerization. Using polymerization procedure 3 the molecular weight of the polymer is far from the theoretical one calculated considering the monomer conversion. Also using the polymerization procedure 4 the molecular weight is not equal to the theoretical one but it is closer to it compared to the polymer synthesized with procedure 3. The results demonstrate that solubilizing Cu(I) and Cu(II) before the addition of the initiator the reaction is more controlled. It is so reasonable to suppose that under these conditions the K_{ATRP} does not change during the initial step of the polymerization as it was using procedure 3.

Polymerization procedure 4 is the optimized method for the polymerization of NVCL and it allows the synthesis of polymers with pre-determinable \overline{M}_n .

2.2.1.3 Proving the living character of PNVCL

With the aim to confirm the living character of the synthesized macromolecules, PNVCL-7800/4 (Table 4) (PD 1.73, \overline{M}_n 7800 Da) was used as macroinitiator for the further polymerization of methyl methacrylate (MMA). The polymerization was carried out using the same catalyst (CuCl), ligand (Me₆Cyclam) and solvent (1,4-dioxan, [M₀]=3.3M) used for the synthesis of the PNVCL macroinitiator, and initial reactants molar ratio of [M₀]/[CuCl]/[L]/[I₀]= 200/2/2/1. The occurrence of polymerization involving the methacrylic double bond was confirmed by FT-IR, showing the disappearance of the band at 1634 cm⁻¹, related to the stretching vibration of the double bond in the monomer, and the shift of the ester carbonyl stretching frequency from 1709 cm⁻¹ in the monomer to higher frequencies (1729 cm⁻¹) in the polymer, due to the reduced electron delocalization determined by the reaction of the methacrylic double bond¹²². Accordingly, in the ¹H-NMR spectra (Figure 11) of PNVCL-*b*-PMMA the resonances at 5.60 and 6.10 ppm related to the vinylidenic protons of monomer are absent.

The conversion was determined by ¹H-NMR of the purified block copolymer (Figure 11) by comparing the integral of the signal at 3.6 ppm assigned to O-CH₃ of PMMA and the one at 4.4 ppm assigned to CH-N of PNVCL macroinitiator. In two hours of polymerization 24% of conversion was reached corresponding to a polymer with a second block of PMMA of 4500 Da.

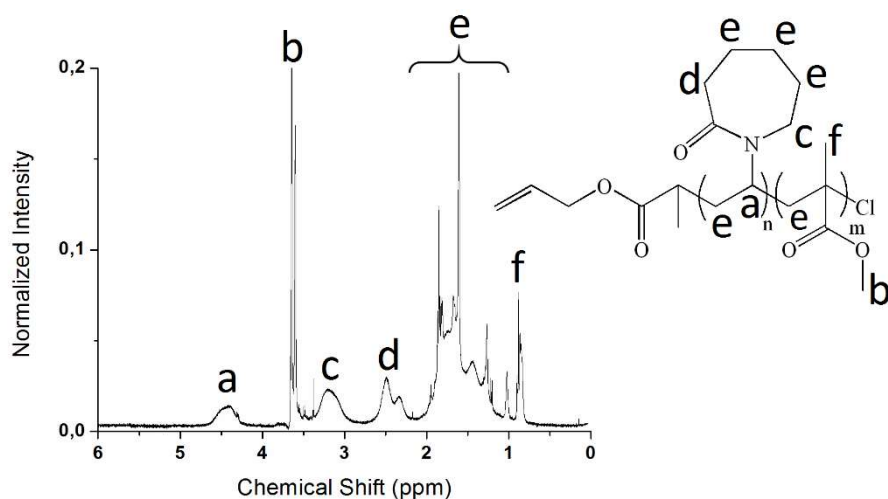


Figure 11: ¹H-NMR of PNVCL-*b*-PMMA.

The conversion obtained in two hours of polymerization is consistent with the conversion reported in the literature¹¹⁶ and confirms the good living character of the previously

synthesized PNVCL. It was so confirmed that with the optimized polymerization system of PNVCL it is possible to synthesize polymers with define structure and living character, that can be used for the synthesis of different block copolymers.

The absence of consistent termination reactions and so the living character of PNVCL can be checked also by $^1\text{H-NMR}$. The ATRP of NVCL was carried out for 48 hours in order to reach the highest possible conversion and termination reactions occurred when the monomer concentration was very low. When coupling reactions occur, the sequence of repeating unit is not head to tail as along all the polymer chain but it should be head to head. The chemical shift of CH-N that underwent coupling reactions is different from the one of the repeating units and it could be clearly seen in the $^1\text{H-NMR}$ spectrum of PNVCL that underwent termination reactions (Figure 12). The signal at 5.3 ppm indicates the presence of many termination reactions. It was so proved that $^1\text{H-NMR}$ is a suitable technique to determine the presence of termination reactions during the ATRP of NVCL.

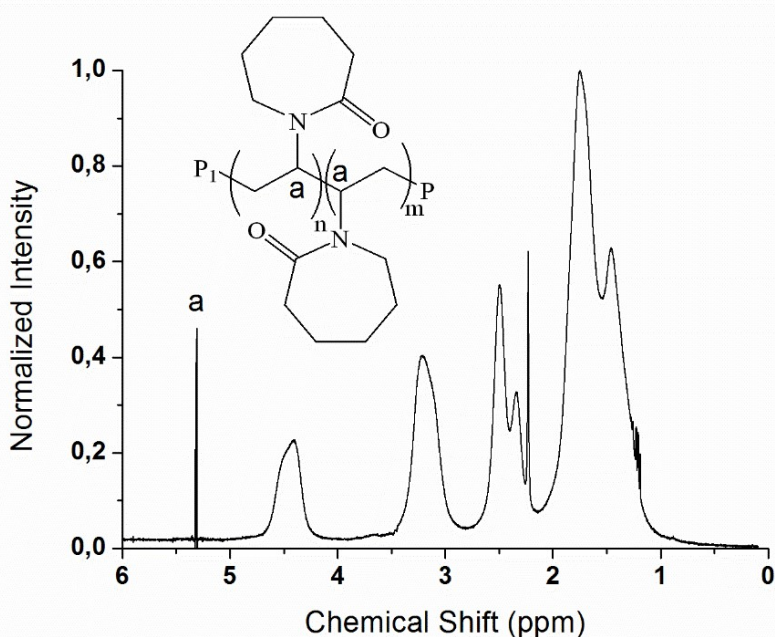


Figure 12: $^1\text{H-NMR}$ of PNVCL that underwent termination reactions.

2.2.1.4 Optimization of the ATRP of NVCL

The ATRP of NVCL was optimized in presence of 1,4-dioxan because it was known to be a good solvent for this polymerization⁹¹. Unfortunately 1,4-dioxan is not suitable for industrial application because of its low flash point value (around 15°C¹²⁷). Indeed, industrially it is cheaper to set up a process which works at 60-80°C and remove the heat of polymerization with water at room temperature, instead of working at 25°C and control the temperature of the reactor with refrigerated liquids.

The polymerization of NVLC was so studied using poly(propylene glycol) (PPG) as solvent which has a hydrophobic main chain but polar hydroxyl chain ends. Thus its polarity depends on its molecular weight.

ATRP of NVCL was attempted using PPG with \overline{M}_n of 425 Da (PPG-425) at 25 and 60°C and in PPG with \overline{M}_n of 1000 Da (PPG-1000) at 60 and 80°C. The kinetics of the polymerizations was studied and $\ln([M_0]/[M])$ as a function of time (Figure 13) was used as parameter to compare the polymerization conditions. Using PPG-425 as solvent and $[Cu(I)]/[Cu(II)]=1/0.3$ at 25°C $\ln([M_0]/[M])$ does not show a linear dependence with the time (\square -Figure 13), indicating that the K_{app} of the polymerization decreases during the process. Such a behaviour could be ascribed to high viscosity of the reaction mixture which leads to the lowering of the diffusion coefficient⁷⁸. By increasing the temperature to 60°C in order to decrease the diffusion limits, $\ln([M_0]/[M])$ does not depend on the time.

The ATRP of NVCL was so attempted at 60°C, in presence of $[Cu(I)]/[Cu(II)]=1/0.6$ (\circ -Figure 13). In these conditions the polymerization results controlled up to 40% of monomer conversion. Then K_{app} of the polymerization slows down because the rate of termination is no more negligible compared to the rate of polymerization and some termination reactions occur forming Cu(II) and shifting the ATRP towards the dormant specie until the system reaches a new stationary state. The fact that increasing the temperature it is not possible to control the process means that the rate of termination increases more than the rate of polymerization. In order to decrease the hydrophilicity of the solvent PPG-425 was replaced with PPG-1000. Indeed, it is known that decreasing the polarity of the solvent the ATRP equilibrium shifts towards the dormant specie thus decreasing the concentration of propagating radicals¹⁴. It is so expected to increase the control over the ATRP of NVCL in presence of PPG-1000. The ATRP of NVCL was studied in PPG-1000 at 60°C with $[Cu(I)]/[Cu(II)]=1/0.3$. A good control of the polymerization process is achieved with these experimental conditions, as demonstrated by the linear dependence of $\ln([M_0]/[M])$ as a function of time (Δ -Figure 13) indicating the

presence of a constant concentration of the growing species throughout the whole process. Increasing the temperature up to 80°C the ATRP of NVCL is still well controlled and the rate of polymerization increases ($K_{app80^{\circ}C} = 0.87 \text{ h}^{-1}$, $K_{app60^{\circ}C} = 0.34 \text{ h}^{-1}$) reaching 90% of monomer conversion in 4 hours (∇-Figure 13).

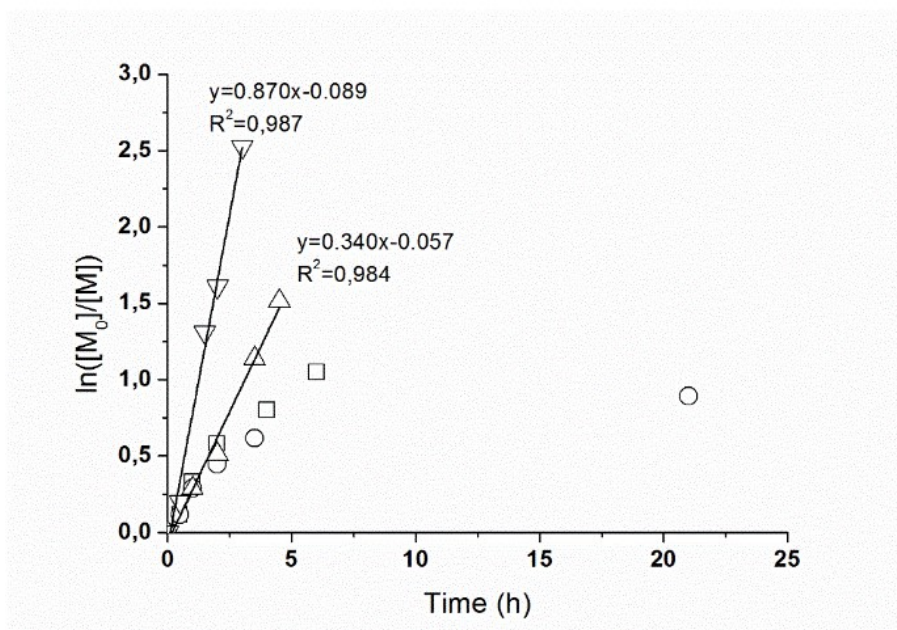


Figure 13: $\ln([M_0]/[M])$ as a function of time for the ATRP of NVCL with $[M_0] = 2.5 \text{ M}$. $[NVCL]/[CuCl]/[CuCl_2]/[Me_6CyClam]/[ACP] = 100/1/0.3/1.3/2$ in PPG-425 at 25°C (□), $[NVCL]/[CuCl]/[CuCl_2]/[Me_6CyClam]/[ACP] = 100/1/0.6/1.6/2$ in PPG-425 at 60°C (○), $[NVCL]/[CuCl]/[CuCl_2]/[Me_6CyClam]/[ACP] = 100/1/0.3/1.3/2$ in PPG-1000 at 60°C (Δ) and 80°C (∇).

2.2.1.5 Comparison of the ATRP kinetics of NVP and NVCL

In Table 6 the K_{app} values of the ATRPs of NVP and NVCL are compared. The kinetic studies on the ATRP of NVP demonstrated that, increasing the concentration of initiator, the polymerization rate decreases, confirming, together with the disagreement between the theoretical and real average molecular weights, the presence of termination reactions before the system reaches its stationary state.

The kinetic studies on the ATRP of NVCL showed that the hindrance of caprolactam compared to the one of pyrrolidone decreases the polymerization rate of the monomer. Decreasing the rate of the initial reaction and decreasing the termination rate by adding Cu(II) into the reaction mixture or by using more dilute system it is possible to increase the control over the reaction and the polymerization rate.

Chapter 2: ATRP of polar monomers

Table 6: K_{app} as function of the monomer polymerized and polymerization conditions. $L=Me_6Cyclam$, $I_0=MCP/ACP$, $Cu(I)=CuCl$ and $Cu(II)=CuCl_2$.

| Monomer | Temp. (°C) | Polymerization procedure | [M ₀] (M) | Solvent ^a | [M ₀]/[Cu(I)]/[Cu(II)]/[L]/[I ₀] | K _{app} (h ⁻¹) |
|---------|------------|--------------------------|-----------------------|----------------------|--|-------------------------------------|
| NVP | 25 | 1 | 2.5 | dioxan/propanol | 100/1/0/1/1 | 0.107 |
| NVP | 25 | 1 | 2.5 | dioxan/propanol | 100/2/0/2/2 | 0.064 |
| NVCL | 25 | 2 | 2.5 | dioxan/propanol | 100/1/0/1/1 | 0.022 |
| NVCL | 25 | 3 | 3.6 | 1,4-dioxan | 100/1/0.5/1.5/1 | 0.061 |
| NVCL | 25 | 3 | 1.8 | 1,4-dioxan | 100/1/0.5/1.5/1 | 0.082 |
| NVCL | 25 | 3 | 3.6 | 1,4-dioxan | 100/1/0/1/1 | 0.221 |
| NVCL | 60 | 4 | 2.5 | PPG-1000 | 100/1/0.3/1.3/2 | 0.340 |
| NVCL | 80 | 4 | 2.5 | PPG-1000 | 100/1/0.3/1.3/2 | 0.870 |

^a dioxan/propanol= 1,4-dioxan/n-propanol 98:2 v/v.

The results of the kinetic studies demonstrated that the most important parameter to control during the ATRP of NVCL and NVP is the rate of termination reactions during the initial polymerization steps. Decreasing them, the rate of polymerization increases and it is possible to reach high conversion without lose the control over the polymerization.

The ATRP of NVCL was optimized also using PPG-1000 at 60 and 80°C, conditions that can be safely applied industrially, obtaining polymers with living character and well-defined structure.

On the basis of the kinetic studies results, it is reasonable to expect that increasing the Cu(II) concentration or diluting the system, the rate of polymerization increases until the effect of the increased amount of radicals is balanced by the shifting of the ATRP equilibrium or by the effect that the dilution has over the reactant concentration (and so on the rate of polymerization).

2.2.2 Atom Transfer Radical Copolymerization (ATRCP)

Having optimized the ATRP of polar monomers that generate reactive and unstable radicals whose polymerization is difficult control, the Atom Transfer Radical Copolymerization (ATRCP) was applied for the synthesis of their corresponding random copolymers. In particular, random copolymers were synthesized with the aim to obtain polymers with tunable and different properties that depend on the copolymer composition.

Thus it was investigated the ATRCP of NVP or NVCL with more hydrophobic monomers with the aim to synthesize defined random copolymers that contain polar NVCL or NVP repeating unit and lipophilic repeating units. Synthesizing polymers with increasing hydrophobicity and changing the hydrophobic/hydrophilic molar ratio of the molecule it is possible to investigate the effect that the composition has on the final properties of the synthesized materials. The reactivity ratios of monomers polymerized by ATRCP are different compared to the ones of monomers polymerized by free-radical polymerization because the radical concentration during a ATRCP is influenced by the monomers K_{ATRP} ¹²⁸. Furthermore, in order to obtain copolymers with high average molecular weight and same monomers repeating units sequence the feed composition should be kept constant throughout the synthesis. The ATRCP of NVP or NVCL with more hydrophobic monomers were studied with the aim to be able to synthesize defined random copolymers that contain polar NVCL or NVP repeating unit together with lipophilic units. Synthesizing polymers with increasing hydrophobicity and changing the hydrophobic/hydrophilic molar ratio of the molecule it is possible to investigate the effect that each component has on the final properties of the synthesized material.

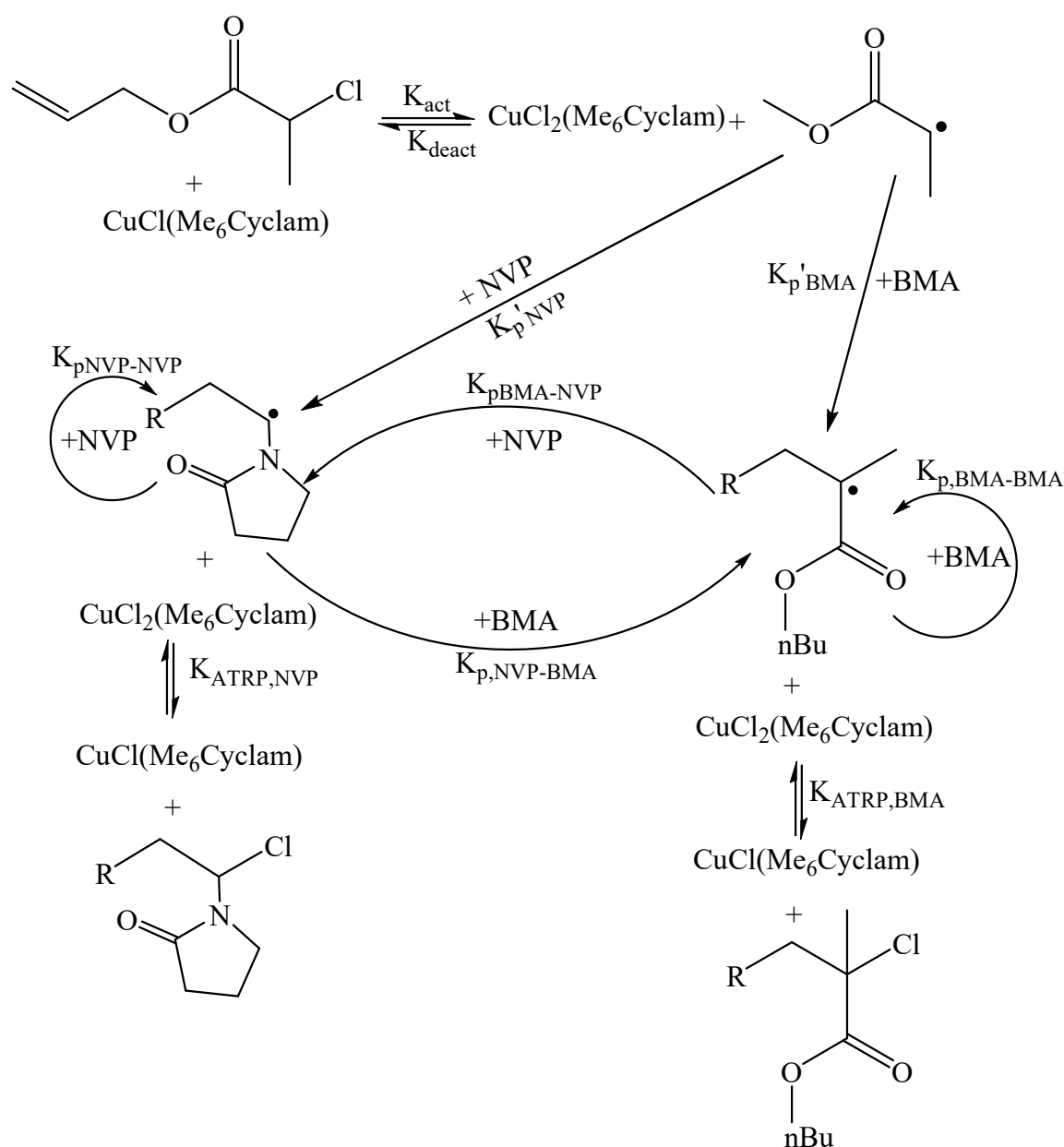
2.2.2.1 Random copolymers

The random copolymerization of NVP with butyl acrylate (BA) or butyl methacrylate (BMA) and of NVCL with BA or vinyl acetate (Vac) were carried out in 1,4-dioxan, at room temperature using the following reactant molar ratio: $[M]/[CuCl]/[CuCl_2]/[Me_6CyClam]/[MCP] = 100/1/0/1/1$. The monomers conversions were kept below 15% in order to assume that the monomer feed was constant throughout all the process and to correlate the copolymer composition to the feed. The occurrence of polymerization involving the vinylic double bond was confirmed by FT-IR and ¹H-NMR. At the end of the polymerization the copolymers were purified and the compositions were determined by ¹H-NMR.

2.2.2.1 ATRCP of NVP with BMA or BA

In Scheme 11 some of the possible reactions that may occur during an ATRCP feeding NVP and BMA as monomers are shown.

As can be seen from the scheme, the number of reactions is high and it is difficult to predict the exact composition of the resulting polymer.



Scheme 11: Example of the possible reactions that occur during an Atom Transfer Radical Copolymerization (ATRCP) of NVP and BMA.

The copolymerization of NVP and BMA with different feed composition was carried out and the data are reported in Table 7. $^1\text{H-NMR}$ analysis confirmed the presence of both *co*-monomers and the different chemical shift of CH-N which overlaps with CH₂-O signal in the copolymer (Figure 14) confirms the presence of the expected random structure.

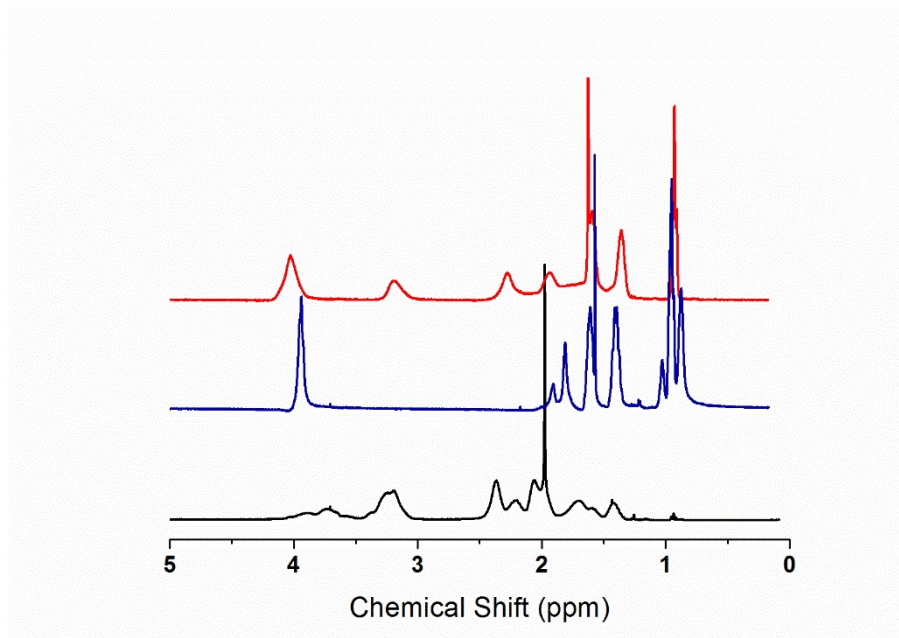


Figure 14: $^1\text{H-NMR}$ spectra of PNVP (black), PBMA (blue) and $P(\text{NVP-co-BMA})$ (red).

The GPC chromatograms of all the synthesized polymers in DMF at 70°C show unimodal molecular weight distributions and low PDs (Table 7), suggesting the occurrence of the copolymerization between NVP and BMA. Average molecular weight are not reported because, as said before, the presence of aggregate does not allow the correct determination of it by GPC. Furthermore, changing the composition of the polymer the hydrodynamic volume changes so it is not possible to compare results of materials with different composition.

Table 7: Characterization data of *P(NVP-co-BMA)* and *P(NVP-co-BA)* copolymers

| Monomer feed composition (%mol/mol) | PD ^a | Copolymer composition (%mol/mol) ^b | |
|--|-----------------|--|-----|
| | | NVP | BMA |
| NVP 90 – BMA 10 | 1.45 | 1 | 99 |
| NVP 75 – BMA 25 | 1.42 | 3 | 97 |
| NVP 50 – BMA 50 | 1.37 | 5 | 95 |
| NVP 25 – BMA 75 | 1.35 | 32 | 68 |
| NVP 10 – BMA 90 | 1.28 | 45 | 55 |
| | | NVP | BA |
| NVP 90 – BA 10 | 1.46 | 16 | 84 |
| NVP 75 – BA 25 | 1.42 | 27 | 73 |
| NVP 50 – BA 50 | 1.46 | 41 | 59 |
| NVP 25 – BA 75 | 1.45 | 47 | 53 |
| NVP 10 – BA 90 | 1.39 | 66 | 34 |

^a Determined by GPC

^b Determined by ¹H-NMR.

The molar final composition of copolymers was assessed by ¹H-NMR (Figure 15 and Table 7) by comparing the integrated signals of C(O)-O-CH₂ of BMA *co*-units located at 4.2-3.6 ppm, to that one related to the N-C(O)-CH₂ of NVP *co*-units at 3.4-2.9 ppm, after subtraction of the contribution given to the integral by the overlapped resonance of CH-N proton in NVP *co*-unit. The results are listed in Table 7.

As reported in Table 7, the molar content of *co*-units in the copolymers does not reflect the feed composition. The copolymerization diagram (Figure 15) clearly indicates an appreciably larger reactivity of BMA with respect to NVP in all the copolymerization runs.

BMA generates a more stable tertiary radical which forms preferably compared to secondary radical generated by NVP. This implies that the propagating radicals react preferably with BMA than with NVP. Furthermore, the $K_{\text{ATRP,BMA}}$ results higher than K_{ATRP} of NVP and consequently its concentration is higher.

With the aim to obtain copolymers with composition which is similar to the *co*-monomer feed molar fraction the copolymerization of NVP and BA was studied.

$^1\text{H-NMR}$ analysis confirmed the presence of both *co*-monomers and the different chemical shift of CH-N which overlaps with CH₂-O signal in the copolymer confirms the presence of the expected random structure.

The different behaviour in the copolymerization of NVP with BMA and BA is mainly due to the different stability of the radical generated by BMA and BA. The $K_{\text{ATRP,BA}}$ is lower than the K_{ATRP} of BMA and it is less incorporated into the final polymer. Results demonstrate that it is possible to synthesize copolymers of NVP and BA with composition which is similar to the *co*-monomer feed molar fraction keeping the NVP molar fraction in the feed below 0.5.

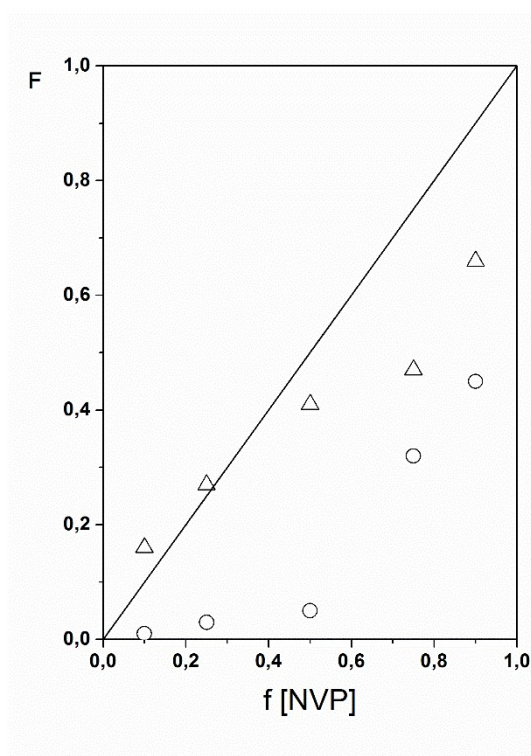


Figure 15: Copolymerization diagrams: molar fraction (F) of NVP co-units in $P(\text{NVP-co-BMA})$ (\circ) and $P(\text{NVP-co-BA})$ (Δ) as a function of molar fraction of NVP in the feed (f).
 $[M]/[\text{CuCl}]/[\text{CuCl}_2]/[\text{Me}_6\text{CyClam}]/[\text{MCP}] = 100/1/0/1/1$ in 1,4-dioxan at 25°C ($[M_0] = 2.5\text{M}$)

2.2.2.2 ATRCP of NVCL with BA or VAc

The copolymerization of NVCL and BA with different feed composition was carried out and the data are reported in Table 8. The GPC chromatograms of all the synthesized polymers show unimodal molecular weight distributions and low PDs (Figure 13), suggesting the occurrence of the copolymerization between NVCL and BA.

$^1\text{H-NMR}$ analysis confirmed the presence of both *co*-monomers and allowed to determine the composition of copolymers (Figure 17 and Table 8) by comparing the integrated signals of C(O)-O-CH₂ of BA *co*-units located at 4.03 ppm, to that one related to the CH-N of NVCL *co*-units at 4.8-4.0 ppm.

As reported in Table 8, the molar content of *co*-units in the copolymers show exactly the same trend seen for the copolymerization of NVP and BA, as expected.

The random copolymerization of NVCL was also studied using VAc as *co*-monomer and the data are reported in Table 8. $^1\text{H-NMR}$ analysis confirmed the presence of both *co*-monomers and the different chemical shift of CH-O which overlaps with CH-N signal in the copolymer confirms the presence of the expected random structure (Figure 16).

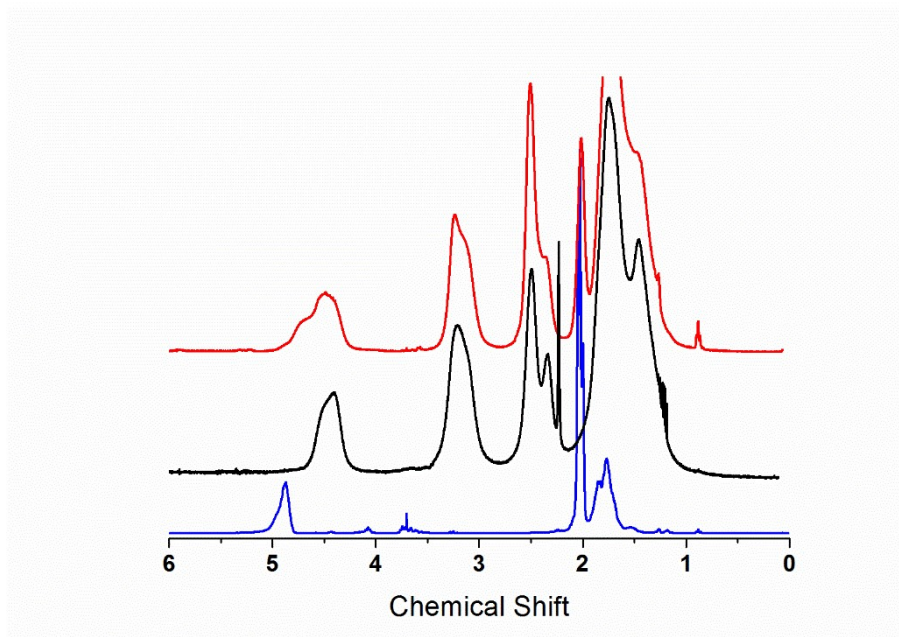


Figure 16: $^1\text{H-NMR}$ spectra of PVAc (blue), PNvCl (black) and P(NvCl-*co*-VAc)-80 (red).

The molar final composition of copolymers was assessed by $^1\text{H-NMR}$ (Figure 17 and Table 8) by comparing the integrated signals of CH-O of VAc *co*-units located at 5.0-4.2 ppm, to that one related to the N-C(O)-CH₂ of NVCL *co*-units at 3.5-2.8 ppm, after

subtraction of the contribution given to the integral by the overlapped resonance of CH-N proton in NVCL *co*-unit.

As reported in Table 8, the molar content of co-units in the copolymers does not reflect the feed composition. The copolymerization diagram (Figure 17) clearly indicates an appreciably larger reactivity of NVCL with respect to VAc in all the copolymerization runs because VAc generates a very unstable radical³⁷, so, as it was seen for the copolymerization of NVP and BMA, during the copolymerization with NVCL this latter reacts faster with the propagating radicals.

Also the random P(NVCL-*co*-VAc) copolymers containing show unimodal molecular weight distribution and low polydispersity (<1.55) (Table 8), thus confirming that it is possible to synthesize random copolymers of NVCL and VAc with different composition by ATRCP.

Table 8: Characterization data of P(NVCL-*co*-BA) and P(NVCL-*co*-VAc) copolymers

| Monomer feed composition (%mol/mol) | PD ^a | Copolymer composition (%mol/mol) ^b | |
|-------------------------------------|-----------------|---|-----|
| | | NVCL | BA |
| NVCL 90 – BA 10 | 1.55 | 14 | 86 |
| NVCL 75 – BA 25 | 1.49 | 25 | 75 |
| NVCL 50 – BA 50 | 1.45 | 43 | 57 |
| NVCL 25 – BA 75 | 1.46 | 50 | 50 |
| NVCL 10 – BA 90 | 1.42 | 68 | 32 |
| | | NVCL | VAc |
| NVCL 90 – VAc 10 | 1.51 | 22 | 78 |
| NVCL 75 – VAc 25 | 1.52 | 46 | 54 |
| NVCL 50 – VAc 50 | 1.35 | 77 | 33 |
| NVCL 25 – VAc 75 | 1.31 | 91 | 8 |
| NVCL 10 – VAc 90 | 1.28 | 99 | 1 |

^a Determined by GPC

^b Determined by ¹H-NMR.

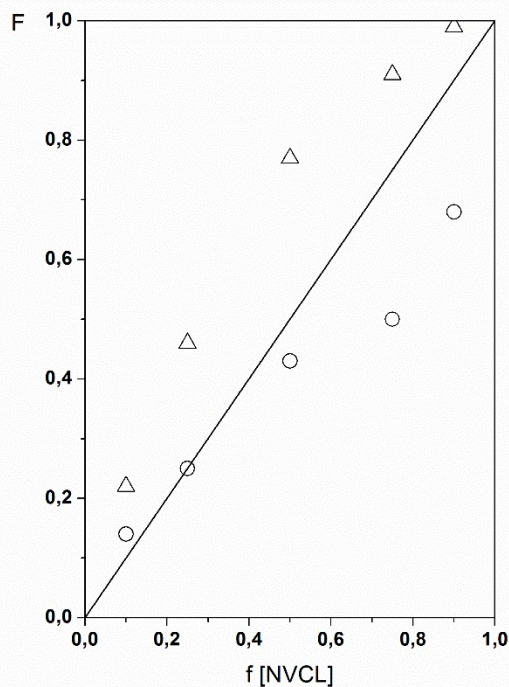


Figure 17: Copolymerization diagrams: molar fraction (F) of NVCL co-units in $P(\text{NVCL-co-BA})$ (○) and $P(\text{NVCL-co-VAc})$ (Δ) as a function of molar fraction of NVCL in the feed (f). $[M]/[\text{CuCl}]/[\text{CuCl}_2]/[\text{Me}_6\text{CyClam}]/[\text{MCP}] = 100/1/0//1/1$ in 1,4-dioxan at 25°C ($[M_0] = 2.5\text{M}$).

The copolymerization studies demonstrate that in order to control the copolymer composition during the ATRCP of NVP or NVCL with more hydrophobic monomers it is easier to use BA and VAc instead of BMA because NVP and NVCL have reactive ratios that are more similar to those ones of VAc and BA. BA and VAc in the copolymerization with NVCL or NVP generates polymer whose composition is similar but not the same as the one of the feed. In order to obtain copolymers with the desired composition with high molecular weight it is necessary to add fresh monomers solution into the reactor during the synthesis.

2.2.2.2.1 NVCL and VAc random copolymers

NVCL was copolymerized by ATRP with VAc (polymerization procedure 4). A fresh and degassed solution of monomers was added to the reactors during the synthesis in order to maintain the desired feed composition. The initial monomer feed composition and the amount of added solution was changed in each polymerization in order to obtain polymers with different composition (Table 9).

The copolymerizations were carried out at room temperature in 1,4-dioxan ($[M_0]=1.4$ M) in presence of ACP as initiator, Me₆Cyclam as ligand, CuCl and CuCl₂ as catalyst and with an initial molar ratio of $[NVCL+VAc]/[CuCl]/[CuCl_2]/[Me_6CyClam]/[ACP] = 100/1/0.5/1.5/1$. The reactions were carried out for 4 hours adding fresh monomer solution at hourly intervals. Feed composition and the amount of added solution were calculated on the basis of the previously studied monomer reactivity. At the end of the synthesis the random copolymers were purified and the occurrence of the polymerization was confirmed by FT-IR and NMR. \overline{M}_n and the molar composition of all the synthesized copolymers were determined by ¹H-NMR by comparing the integrals of the allyl signals (5.9 ppm) to those ones of VAc and NVCL residues at 4-5 ppm (CH VAc and NVCL) and 3.2 ppm (CH₂-C(O) NVCL) respectively.

Polymerization conditions and relevant data concerning the obtained copolymers are summarized in Table 9.

Table 9: Characterization data of P(NVCL-co-VAc) copolymers.

| Sample | Initial NVCL molar fraction (% mol/mol) | Initial VAc molar fraction (% mol/mol) | Amount of added solution (%) ^a | Polymer X _{NVCL} (% mol/mol) ^b | ^{NMR} \overline{M}_n (Da) ^b | T _g (°C) ^c | TheorT _g (°C) ^d | PD ^e |
|-------------------|---|--|---|--|--|----------------------------------|---------------------------------------|-----------------|
| P(NVCL-co-VAc)-82 | 75 | 85 | 9 | 82 | 5500 | 167 | 165 | 1.68 |
| P(NVCL-co-VAc)-75 | 45 | 55 | 4.5 | 75 | 27600 | 150 | 155 | 1.71 |
| P(NVCL-co-VAc)-53 | 25 | 75 | 3.7 | 53 | 41000 | 117 | 123 | 1.53 |
| P(NVCL-co-VAc)-45 | 15 | 85 | 2.2 | 45 | 9400 | 96 | 111 | 1.69 |

^a Volume fraction of fresh solution over initial reaction solution. Monomers concentration= 7.8M, X_{NVCL}=0.987 and X_{VAc}=0.013.

^b Determined by NMR.

^c Determined by DSC.

^d Determined by Fox-Flory equation.

^e Determined by GPC in DMF at 70°C.

In these experimental conditions, NVCL reacts faster than VAc (see chapter 2.2.2.2). As a consequence, in order to keep the correct monomer feed composition, it is necessary to carry out the experiments in excess of NVCL. Adding a fresh and concentrated monomer solution throughout the polymerization increases the monomer to initiator ratio allowing to obtain polymers with high molecular weight (Table 9).

As expected the NVCL molar fraction in the final copolymer decreases with its concentration in the feed. The good agreement between the expected and the obtained composition confirms the reproducibility of the procedure. The GPC traces of the polymers (Figure 18) show unimodal distribution of the molecular weights demonstrating the good control achieved over the process.

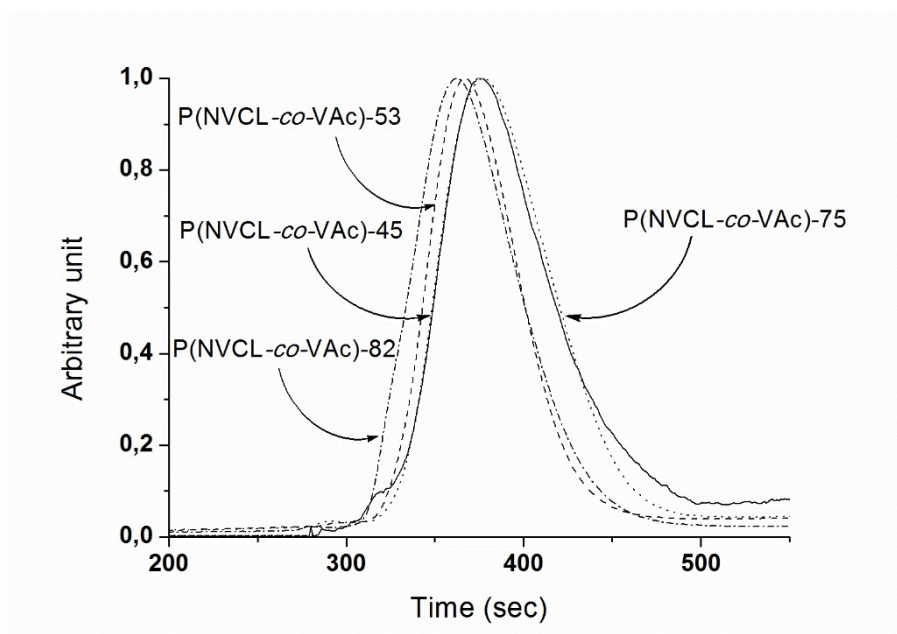


Figure 18: GPC traces of $P(\text{NVCL-co-VAc})$ with different content of VAc.

The thermal transitions of the copolymers were investigated by DSC and the obtained data are summarized in Table 9. All $P(\text{NVCL-co-VAc})$ samples display only one second order transition ascribed to the glass transition as expected for random copolymers. The T_g 's lie in between those of PVAc (30-40°C) and of PNVCL (190-200°C) and they decrease with VAc content into the polymer. The experimental T_g values of the copolymers well compare with the theoretical ones determined using Fox-Flory equation (Equation 12)(Table 9).

Equation 12

$$\frac{1}{T_g} = \frac{v_1}{T_{g1}} + \frac{v_2}{T_{g2}}$$

v = volume fraction in the polymer, T_g = glass transition temperature.

Although the theoretical T_g were calculated using the mass fraction (determined by $^1\text{H-NMR}$) and not the volume fraction, there is a good agreement between theoretical and experimental data, confirming that the composition determined by $^1\text{H-NMR}$ is correct.

The thermal stability of P(NVCL-*co*-VAc) copolymers was studied using TGA under nitrogen atmosphere. TGA traces of the copolymers are displayed in Figure 19 together with that of PVAc and PNVCL homopolymers. PVAc is stable up to roughly 270°C, then shows a double stepwise degradation: the first degradation is consistent with acetic acid elimination (weight loss= 70% w/w) while the second one can be ascribed to the polymer backbone degradation. The solid residue (7%) observed at the end of the run is due to the formation of a char residue, possibly owing to the lack of oxygen in the atmosphere where the measurement is carried out¹²⁹. The degradation pattern of copolymers, instead, depends on their composition. When the content of NVCL is high, such as in P(NVCL-*co*-VAc)-82, the degradation starts at roughly the same decomposition temperature as PNVCL, though the initial degradation is faster than the one in PNVCL because of the formation of acetic acid from VAc that occurs concurrently with PNVCL degradation. Increasing the temperature, the second degradation step practically overlaps PNVCL degradation pattern because of the high fraction of NVCL comonomer in the polymer. In the presence of homopolymeric blocks the degradation pattern should be different, with an initial degradation at 300°C due to the decomposition of PVAc block. Hence, the initial degradation temperature of P(NVCL-*co*-VAc)-82 confirms the expected random structure.

Increasing the content of VAc in the copolymers the initial degradation temperature drops down the one of PVAc (roughly 270°C). Indeed, all these polymers lose acetic acid from VAc units during the first degradation step, and the entity of this weight loss is always smaller than that registered in PVAc homopolymer. In the copolymers the second degradation is tentatively attributed to the degradation of the residual backbone after acetic acid elimination and to the degradation of NVCL.

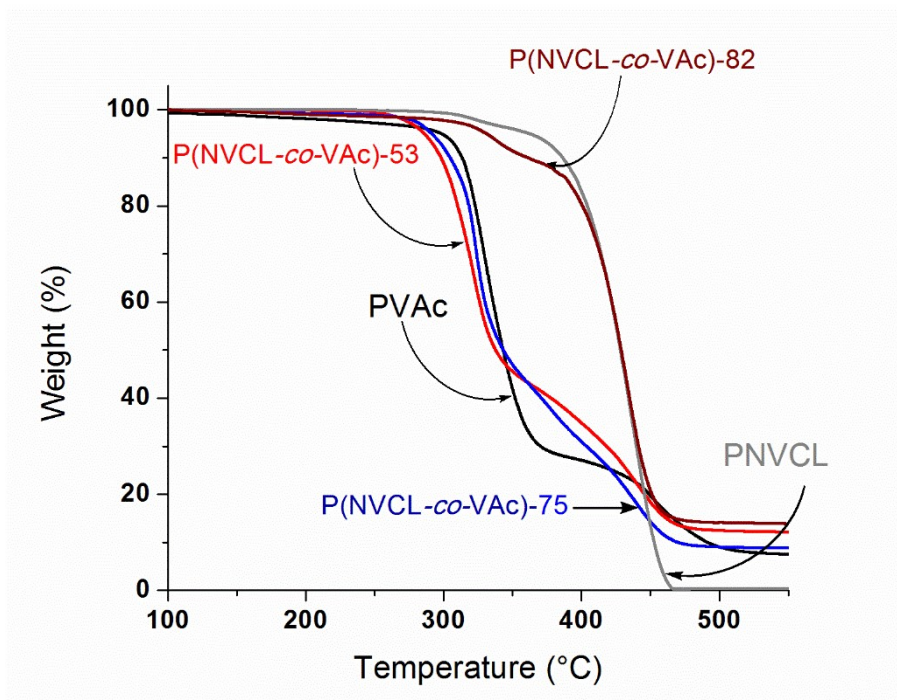


Figure 19: TGA curves of $P(NVCL-co-PVAc)$ copolymers with different composition compared with TGA curves of $PNVCL$ (grey) and $PVAc$ (black) homopolymers.

Hence, the reported experiments demonstrate that we obtained well defined random copolymers with tailored composition that can be defined on the basis of the monomer feed composition.

2.2.2.3 NVCL and PEGMEA random copolymers

Different random copolymers containing NVCL and PEGMEA were synthesized with the aim to obtain polymers with different composition and molecular weight and high PEGMEA content. PEGMEA with different PEG chain length were used in order to understand the effect that the PEG side chain has on the properties of the final copolymer.

All the copolymers were synthesized at room temperature, with an initial monomer concentration of 2.5 M and using polymerization procedure 3. Since the ATRCP of NVCL with BMA demonstrated that the methacrylic *co*-monomer has a higher reactivity with respect to NVCL (see chapter 2.2.1), all the polymerizations were set up with a very high NVCL molar fraction in the feed.

Most of the polymerizations were carried out adding a degassed solution of monomers during the polymerization in order to keep the desired monomer molar ratio during the synthesis. Its concentration was the same as the one in the initial feed (2.5 M). In some cases, in order to have high content of NVCL the starting feed was constituted by 100%

NVCL. The copolymers were synthesized using different monomer to initiator ratio, feed composition and reaction time. At the end of the reactions the polymers were purified and the occurrence of polymerization involving the double bonds was confirmed by FT-IR and NMR.

In Table 10 the characterization data of all the synthesized copolymers are reported.

Table 10: Characterization data of P(NVCL-co-PEGMEA) copolymers.

| Sample | Initial X_{NVCL} (% mol/mol) | $[M_0]/[Cu(I)]/$ $[Cu(II)]/[L]/[I_0]$ | X_{NVCL} in the added solution (% mol/mol) (M/I) | Reaction time (h) | Polymer X_{NVCL} (% mol/mol) | $^{NMR} \overline{M}_n$ (Da) | PD ^a |
|--------------------------|--------------------------------------|--|---|----------------------|--------------------------------------|---------------------------------|-----------------|
| P(NVCL-co-PEGMEA350)-99 | 99.5 | 60/1/0.6/1.6/1 | - | 1.5 | 99 | 5400 | 1.54 |
| P(NVCL-co-PEGMEA350)-93 | 100 | 50/1/0/1/1 | 95 (50/1) ^b | 1 | 93 | 2400 | 1.64 |
| P(NVCL-co-PEGMEA350)-91 | 100 | 50/1/0/1/1 | 65 (50/1) ^c | 1 | 91 | 1200 | 1.36 |
| P(NVCL-co-PEGMEA750)-98 | 99 | 200/2/0/2/1 | 99 (100/1) ^d | 5.5 | 98 | 10700 | 1.68 |
| P(NVCL-co-PEGMEA2000)-95 | 99 | 100/1/0/1/1 | 99 (100/1) ^e | 1 | 95 | 3400 | 1.68 |
| P(NVCL-co-PEGMEA2000)-94 | 100 | 50/1/0/1/1 | 99 (50/1) ^b | 1 | 94 | 16200 | 1.54 |
| P(NVCL-co-PEGMEA2000)-86 | 100 | 100/1/0/1/1 | 99 (100/1) ^e | 1 | 86 | 26000 | 1.36 |

^a Determined by GPC in DMF at 70°C.

^b Two addition every 20 minutes.

^c One addition after 10 minutes and one after 30 minutes.

^d One addition every hour.

^e One addition after 30 minutes.

As an example, in Figure 20 the ¹H-NMR spectrum of P(NVCL-co-PEGMEA350)-91 is shown. In the spectrum the signals of the two repeating units can be clearly detected, confirming the occurred copolymerization.

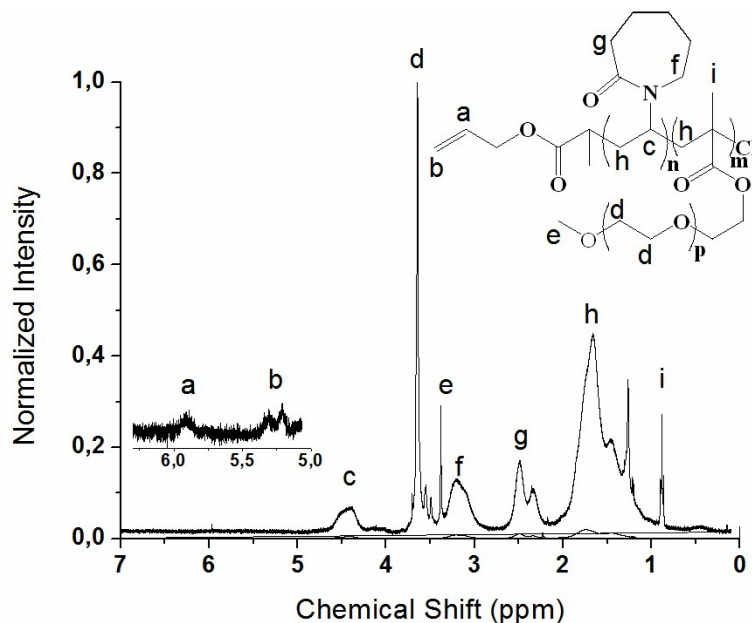


Figure 20: $^1\text{H-NMR}$ of $\text{P}(\text{NVCL-co-PEGMEA350})\text{-91}$.

The composition and the molecular weight of the macromolecules were determined by $^1\text{H-NMR}$ comparing the integrals of the allyl signals (5.9 and 5.3 ppm) with respect to those ones of NVCL and PEGMEA residues at 4.4 ppm (CH-N) and 3.6 ppm ($\text{CH}_2\text{-CH}_2\text{-O}$) respectively.

The data reported in Table 10 show that, as expected, the average molecular weight of the polymers increases with the reaction time and with the monomer to initiator ratio. Furthermore, the copolymer composition is in agreement with the monomer feed and all the polymers have $\text{PD} < 1.7$ (absence of considerable termination reactions). Results indicate that the polymerization conditions allow to achieve a good control over the process.

The good agreement between the copolymer composition and feed and between the \overline{M}_n and the monomer to initiator molar ratio together with the low PD demonstrate that the polymerization system allows to control the composition and the molecular weight of the polymers.

The chain mobility and phase behaviour of the copolymers were investigated by DSC and the obtained data for all the analyzed polymers are summarized in Table 11. All $\text{P}(\text{NVCL-co-PEGMEA350})$ samples display only one second order transition originated by glass transition (T_g), whose position depends on the macromolecule's composition. In particular, the determined T_g are always between the T_g of the two corresponding homopolymers PPEGMEA350 ($< -80^\circ\text{C}$) and PNVCL (190°C) and it decreases with the

amount of PEGMEA350, confirming the composition trend determined by NMR. Such a behavior suggests that these materials are random copolymers.

PEGMEA2000 copolymers show an endotherm transition around 45°C due to the melting of PEG side chains (Table 11) but no T_g can be observed. The melting enthalpy (ΔH_m) of these materials depends on the amount and distribution of PEGMEA2000 incorporated into the polymer chains. Being the PEGMEA2000 repeating units separated by NVCL units, the interactions between PEG is different compared to interactions that occur in PPEGMEA2000 homopolymer.

Table 11: P(NVCL-co-PEGMEA) T_g and ΔH as a function of polymerization conditions.

| Sample | Polymer X _{NVCL} (% mo/mol l) ^a | ^{NMR} \overline{M}_n (Da) ^a | T_g (°C) ^b | T_m (°C) ^b | ΔH_m (J/g) ^b |
|--------------------------|--|--|----------------------------|----------------------------|------------------------------------|
| P(NVCL-co-PEGMEA350)-93 | 93 | 2400 | 169 | - | - |
| P(NVCL-co-PEGMEA350)-91 | 91 | 1200 | 56 | - | - |
| P(NVCL-co-PEGMEA350)-99 | 99 | 5400 | 181 | - | - |
| P(NVCL-co-PEGMEA750)-98 | 98 | 10700 | 169 | - | - |
| P(NVCL-co-PEGMEA2000)-94 | 94 | 16200 | | 42 | 24.6 |
| P(NVCL-co-PEGMEA2000)-95 | 95 | 3400 | | 49 | 117.7 |
| P(NVCL-co-PEGMEA2000)-86 | 86 | 26000 | - | 46 | 77.5 |

^a Determined by ¹H-NMR.

^b Determined by DSC.

The thermal stability of P(NVCL-co-PEGMEA) derivatives was studied by TGA. As reported in Figure 21, PNVCL is stable up to roughly 300°C, then shows a double stepwise degradation pattern with a negligible residue at 500°C. P(NVCL-co-PEGMEA) derivatives show similar degradation behaviour (T_d around 270°C) though the first degradation step is more pronounced and it is greater for copolymers containing PEGMEA2000. It is known from the literature that poly(methacrylate)s depolymerize around 250-300°C¹³⁰. Depolymerization of these materials is promoted by the formation of stable tertiary radicals at the chain end upon heating. In presence of a *co*-monomer that does not generate stable radicals, such as NVCL, the depolymerisation of the methacrylic moieties seems prevented, especially when PEGMEA molar fraction is low. Thus the first weight loss can be ascribed to PNVCL degradation overlapped with that one of PEGMEA

which might be due to depolymerisation and decomposition reactions of the ester side chain. The second degradation step has the same trend as in PNVCL homopolymer so it can be safely ascribed to PNVCL decomposition and degradation of PPEGMEA backbone.

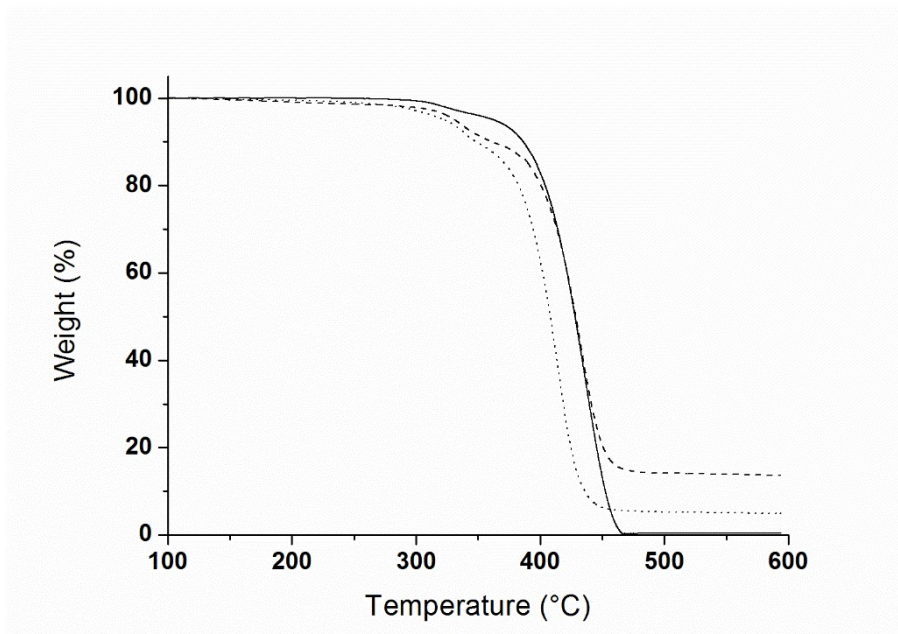


Figure 21: TGA curves of PNVCL (—), $P(NVCL-co-PEGMEA350)-97$ ($\overline{M}_n=10000Da$, $X_{NVCL}=97\%$) (---), $P(NVCL-co-PEGMEA2000)-95$ ($\overline{M}_n=3400Da$, $X_{NVCL}=95\%$) (···).

2.2.3 Synthesis and characterization of block copolymers

In order to synthesize block copolymers with different composition, a series of PNVCL macroinitiators with living character were synthesized (Table 12).

The copolymerizations were carried out at room temperature in 1,4-dioxan in presence of ACP as initiator, Me₆Cyclam as ligand, CuCl and CuCl₂ as catalyst and with different initial molar ratio of [NVCL]/[CuCl]/[CuCl₂]/[Me₆CyClam]/[ACP], using polymerization procedure 4. At the end of the synthesis the polymers were purified and the occurrence of polymerization was confirmed by FT-IR and NMR. The macroinitiators were synthesized using different initial molar ratios and different concentrations. \overline{M}_n was determined by ¹H-NMR by comparing the integrals of the allyl signal (5.9 ppm) to that one of NVCL residue at 4.4 ppm (CH-N). The thermal properties of the different PNVCL were investigated by DSC and TGA. All the polymers show the same glass transition temperature (190-200 °C) and the same degradation pattern (Figure 19).

The synthesis of PNVCL with different molecular weight and living character demonstrate that it is possible to control the ATRP of NVCL, obtaining materials with different \overline{M}_n by changing the operative conditions.

Table 12: Polymerization conditions and \overline{M}_n determined by NMR of PNVCL macroinitiators.

| Sample | [M ₀]/[Cu(I)]/[Cu(II)]/[L]/[I ₀] | [M ₀] | Reaction time (min) | PNVCL ^{NMR} \overline{M}_n (Da) ^a |
|-------------|--|-------------------|---------------------|---|
| PNVCL-14000 | 200/1/0.7/1.7/1 | 2.5 | 18 | 14000 |
| PNVCL-5700 | 40/1/0.5/1.5/1 | 3.6 | 90 | 5700 |
| PNVCL-2800 | 100/1/0/1/1 | 3.6 | 30 | 2800 |
| PNVCL-6400 | 100/1/0/1/1 | 3.6 | 70 | 6400 |
| PNVCL-6800 | 100/1/0/1/1 | 3.6 | 90 | 6800 |
| PNVCL-20600 | 250/1/0.5/1.5/1 | 3.6 | 17 | 20600 |

^a Determined by ¹H-NMR.

The \overline{M}_n of PNVCL shown in Table 12 increases with the monomer to initiator ratio and with the reaction time. As an example, PNVCL-2800, 6400 and 6800 were synthesized using the same conditions and the \overline{M}_n increases with the reaction time. Decreasing the monomer to initiator ratios (sample PNVCL-5700) the \overline{M}_n of the resulting material decreases (reaction time 90 minutes) as expected for a controlled polymerization.

All the polymers were successfully used as macroinitiators for the further polymerization of different monomers. The resulting block copolymers did not show any traces of unreacted macroinitiator demonstrating the living character of the polymers and the good control achieved over the synthesis of PNVCL by ATRP.

2.2.3.1 Synthesis of PNVCL-*b*-PVAc

A series of PNVCL-*b*-PVAc were synthesized using different polymerization conditions. The polymerizations were carried out at 50°C, in 1,4-dioxan in presence of PNVCL as macroinitiator, Me₆Cyclam as ligand, CuCl and CuCl₂ as catalyst and with different initial molar ratio of [VAc]/[CuCl]/[CuCl₂]/[Me₆CyClam]/[PNVCL], using polymerization procedure 3. [M₀], monomer to initiator ratio and reaction time were changed in order to obtain polymers with different composition. At the end of the synthesis the polymers were

purified and the occurrence of polymerization was confirmed by FT-IR and NMR. \overline{M}_n was determined by $^1\text{H-NMR}$ by comparing the integrals of the signal of NVCL residue at 4.4 ppm (CH-N) to that one of VAc residue at 4.85 ppm (CH-O).

Although procedure 4 gave better results when applied for the ATRP of NVCL, it does not allow the addition of the degassed macroinitiator solution which prevents oxygen to enter inside the reactor. The presence of oxygen promotes the oxidation of Cu(I) and the K_{ATRP} changes in an unpredictable and unreproducible way. Furthermore, dissolving the macroinitiator directly into the reaction flask, termination reactions between polymeric radicals are slower than termination reactions between small molecules. It can be so assumed that no termination reactions occur between radical macroinitiator during the initial step of the polymerization when procedure 3 is applied for the synthesis of block copolymers. The different polymerization systems used for the synthesis of PNVCL-*b*-PVAc require to use dilute systems and Cu(II) in order to avoid termination reactions caused by the high reactivity of VAc radical.

From the $^1\text{H-NMR}$ spectra the signals of the two different blocks are clearly detectable (Figure 22) and the molar final composition of the copolymers can be determined by comparing the integrated signals of CH-O of VAc units located at 5.0-4.8 ppm, to that one related to the N-C(O)-CH₂ of NVCL macroinitiator at 4.8-4.0 ppm (Table 13).

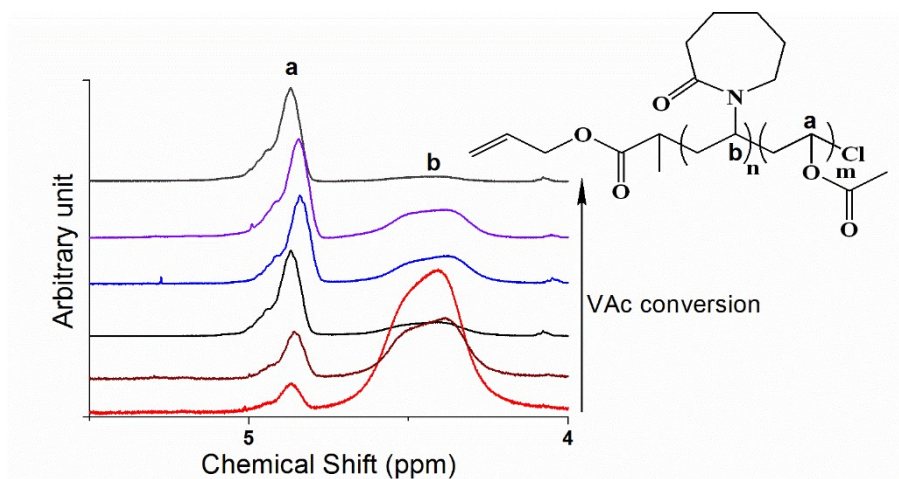


Figure 22: $^1\text{H-NMR}$ spectra between 4 and 5.5 ppm of a series of PNVCL-*b*-PVAc copolymers with increasing PVAc molar fraction.

Table 13: Characterization data of PNVCL-*b*-PVAc block copolymers.

| Sample | [M ₀]/[Cu(I)]/ [Cu(II)]/[L]/[I ₀] | [M ₀] | Reaction time (min) | PNVCL \overline{M}_n (Da) ^a | PVAc \overline{M}_n (Da) ^a | Polymer X _{PNVCL} (%) mol/mol ^a | VAc conv. (% mol/mol) ^a |
|--------------------------|--|-------------------|---------------------------|--|---|---|---------------------------------------|
| PNVCL- <i>b</i> -PVAc-71 | 300/1/0.15/1.15/1 | 2.9 | 20 | 2800 | 700 | 71 | 3 |
| PNVCL- <i>b</i> -PVAc-15 | 300/1/0.15/1.15/1 | 2.9 | 40 | 2800 | 9700 | 15 | 38 |
| PNVCL- <i>b</i> -PVAc-37 | 300/1/0.15/1.15/1 | 2.9 | 40 | 6800 | 7200 | 37 | 28 |
| PNVCL- <i>b</i> -PVAc-80 | 250/1/0.65/1.65/1 | 1.1 | 20 | 20600 | 3100 | 80 | 14 |
| PNVCL- <i>b</i> -PVAc-90 | 250/1/0.65/1.65/2 | 1.1 | 60 | 14000 | 1000 | 90 | 9 |
| PNVCL- <i>b</i> -PVAc-33 | 250/1/0.65/1.65/1 | 1.1 | 120 | 14000 | 17500 | 33 | 81 |
| PNVCL- <i>b</i> -PVAc-44 | 300/1/0.65/1.65/1 | 1.1 | 20 | 5700 | 2200 | 44 | 8 |
| PNVCL- <i>b</i> -PVAc-57 | 300/1/0.65/1.65/1 | 1.1 | 20 | 6400 | 3000 | 57 | 12 |
| PNVCL- <i>b</i> -PVAc-47 | 300/1/0.65/1.65/1 | 1.1 | 40 | 6400 | 4400 | 47 | 17 |

^a Determined by ¹H-NMR.

As reported in Table 13 it can be seen that the monomer conversion increases with the time as so does the PVAc chain length. Conversion also depends on the average molecular weight of the initiator, indeed, the polymerizations carried out for 40 minutes and using two different PNVCL (PNVCL-*b*-PVAc-15, 36) lead to two different PVAc molecular weight. This effect is mainly caused by the molecular weight of the macroinitiator that increases the viscosity and so the diffusion coefficient of the reactant and it reduces the accessibility of the radical at the end of the polymer propagating chain.

Using a dilute system ([M₀]= 1.1 M) the VAc conversion increases with the polymerization time up to 81% in two hours (sample PNVCL-*b*-PVAc-33) showing that it is possible to obtain block copolymers with high conversion of the second block using short reaction time and demonstrating the good efficiency of initiation of the previously synthesized PNVCL.

The thermal properties of PNVCL-*b*-PVAc copolymers were investigated by DSC and TGA (Table 14).

All the PNVCL-*b*-PVAc show an initial degradation temperature (T_d) at 255°C with the exception of PNVCL-*b*-PVAc-90 which, having a very low content of PVAc, shows a higher initial degradation temperature (285°C) though not as high as PNVCL (Figure 23).

Previously it was demonstrated that, in random copolymers, T_d increases with the NVCL content into the polymer. The first weight loss centred at 346°C is consistent with acetic acid elimination¹²⁹, due to the presence of PVAc, and confirms the occurred block copolymerization. The second PVAc characteristic degradation, that occur between 400 and 500°C in the homopolymer and involves the polymer backbone degradation, is partially overlapped by PNVCL degradation that occurs at the same temperature. Being these two events overlapped, the slope of the TGA curve of PNVCL-*b*-PVAc samples is intermediate between the ones of PNVCL and PVAc homopolymers and its value depends on the copolymer composition.

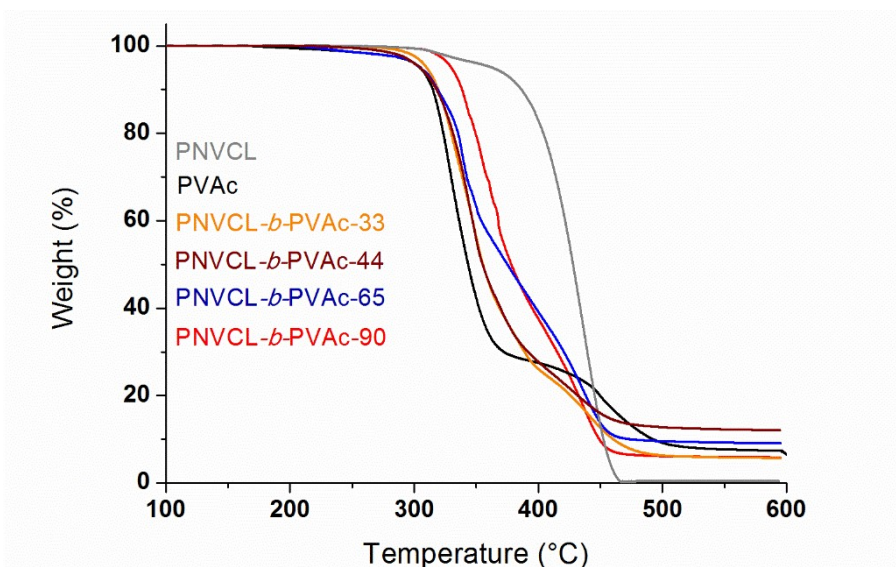


Figure 23: TGA curves of PNVCL-*b*-PVAc copolymers with different composition compared with TGA curves of PNVCL (grey) and PVAc (black) homopolymers

The thermal transitions of the copolymers were investigated by DSC and the obtained data are summarized in Table 14. All PNVCL-*b*-PVAc samples display two second order transition ascribed to glass transitions, as expected for block copolymers. The T_g values are close to the ones of the correspondent homopolymers ($T_{g, \text{PVAc}}=30\text{-}40^\circ\text{C}$ and $T_{g, \text{PNVCL}}=190\text{-}200^\circ\text{C}$) confirming the presence of two homopolymeric blocks.

In Figure 24 the DSC thermograms of some PNVCL-*b*-PVAc samples are shown and compared with the ones of PNVCL and PVAc homopolymers. In Table 14 the T_g and ΔC_p determined by DSC are summarized; the latter were used to determine the composition of the synthesized materials. The intensity of the transitions changes as a function of the composition because the specific heat increment is due to the transition of one of the two

blocks and it is an extensive parameter. The sample PNVCL-*b*-PVAc-90 show only one transition temperature at 195°C, ascribed to PNVCL specific heat increment. The absence of PVAc transition does not mean that there is no PVAc in the copolymer, but just that DSC is not so sensitive to quantify very low specific heat increment such as the one that can be ascribed to PVAc block in copolymers containing only 10% (mol/mol) of PVAc.

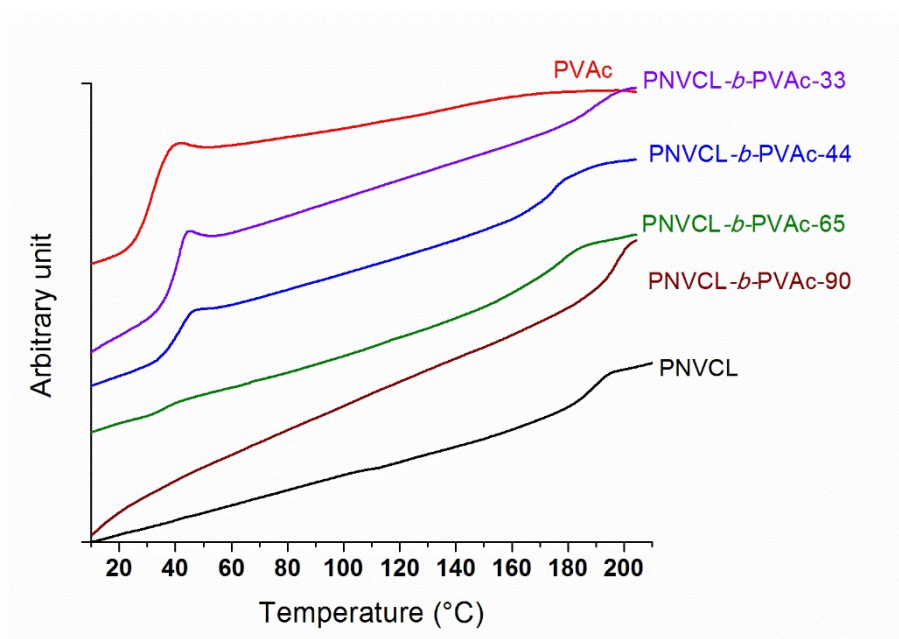


Figure 24: DSC thermograms of PNVCL-*b*-PVAc copolymers with different composition compared with the ones of PNVCL and PVAc.

The mass fraction of the two blocks in the copolymers can be determined by the ratio of the ΔC_p in the copolymer and the one in the homopolymer. ΔC_p changes with the molecular weight but if the \overline{M}_n in the homopolymer is similar to the one in the block copolymer ΔC_p can be considered constant. Being DSC less precise than $^1\text{H-NMR}$ the composition determined with the latter is more reliable but DSC can provide confirmation of the values determined by $^1\text{H-NMR}$. The good agreement between the composition values determined by $^1\text{H-NMR}$ and the ones determined using the ΔC_p (DSC) (Table 14) demonstrates the reliability of the method developed for determining the molecular weight of the polymers by $^1\text{H-NMR}$ analysis.

Table 14: T_g , ΔC_p and T_d values of PNVCL-*b*-PVAc copolymers and comparison between their composition determined by NMR and DSC.

| Sample | X PNVCL (%w/w) ^a | X PVAc (%w/w) ^a | T_{g1} (°C) [ΔC_p (J/g*°C)] ^b | T_{g2} (°C) [ΔC_p (J/g*°C)] ^b | X PNVCL (%w/w) ^c | T_d (°C) |
|--------------------------|--------------------------------|-------------------------------|--|--|--------------------------------|---------------|
| PNVCL | 100 | - | - | 190 [0.27] | - | 300 |
| PVAc | - | 100 | 32 [0.36] | - | - | 270 |
| PNVCL- <i>b</i> -PVAc-44 | 72 | 28 | 40 [0.10] | 176 [0.20] | 74 | 278 |
| PNVCL- <i>b</i> -PVAc-65 | 88 | 12 | 36 [0.06] | 178 [0.21] | 78 | 275 |
| PNVCL- <i>b</i> -PVAc-33 | 45 | 55 | 39 [0.23] | 189 [0.14] | 52 | 267 |
| PNVCL- <i>b</i> -PVAc-90 | 93 | 7 | - | 195 [0.22] | 81 | 277 |

^a Determined by ¹H-NMR^b Determined by DSC^c Determined by DSC as ΔC_p (in the copolymer)/ ΔC_p (homopolymer).2.2.3.1.1 DLS measurements of PNVCL-*b*-PVAc-90 water solution

The PD of PNVCL-*b*-PVAc samples cannot be determined by GPC because of the formation of aggregates during elution. The tendency of aggregation of PNVCL-*b*-PVAc was investigated by DLS measurements of polymeric water solutions at different concentrations. The diameter of the aggregates of the polymer solutions at different concentrations is reported in Table 15.

Table 15: DLS results of PNVCL-*b*-PVAc-90 water solutions at 25°C.

| Concentration (mg/ml) | Peak 1 | | Peak 2 | | Derived | Intercept |
|--------------------------|---------|---------------|---------|---------------|------------|-----------|
| | d. (nm) | Intensity (%) | d. (nm) | Intensity (%) | Count Rate | |
| 6 | 560 | 91 | 30 | 6 | 30020 | 0.95 |
| 3 | 510 | 87 | 60 | 10 | 47010 | 0.97 |
| 1 | 400 | 84 | 60 | 10 | 12040 | 0.98 |

As reported above for PNVCL water solutions, DLS results highlight the presence of aggregates whose size increases with the concentration of the solution. Increasing the temperature to 37°C the diameter of the aggregates increases (>1000 nm) and DLS is not

suitable for the determination of their size. The increased size of the aggregates can be ascribed to the temperature responsiveness of PNVCL as said before.

PNVCL form aggregates but there is not a direct correlation between concentration and size, maybe because the aggregates are not completely stable. The increased amphiphilic character of PNVCL-*b*-PVAc allows the formation of bigger and stable aggregates.

2.2.3.2 Synthesis of PNVCL-*b*-PDMAEMA

A series of PNVCL-*b*-PDMAEMA with different poly[2-(dimethylamino)ethyl methacrylate] (PDMAEMA) chain length were synthesized. The polymerizations were carried out at room temperature, in 1,4-dioxan ($[M_0]= 1.5M$) in presence of PNVCL-5700 as macroinitiator, Byp as ligand, CuCl as catalyst, with an initial molar ratio of $[DMAEMA]/[CuCl]/[Byp]/[PNVCL]=100/1/2/1$ and using polymerization procedure 3. The reactions were stopped after different reaction times in order to synthesize products with different PDMAEMA chain length. The occurrence of the polymerization was confirmed by FT-IR and NMR. \overline{M}_n was determined by 1H -NMR by comparing the integrals of the NVCL residues at 4.4 ppm (CH-N) and the DMAEMA residues at 4.0 ppm (CH₂-O).

In the 1H -NMR spectra (Figure 25) of the synthesized materials, the signals of both blocks, together with those ones of the initiator residue, can be clearly detected and by their integration it is possible to determine the copolymer composition (Table 16).

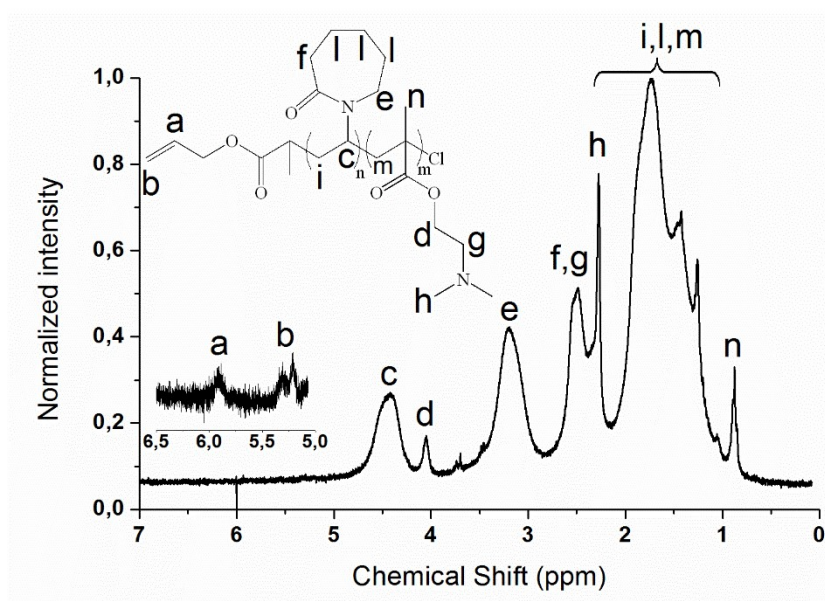


Figure 25: 1H -NMR spectrum of PNVCL-*b*-PDMAEMA-89.

Table 16: Conversion, composition and PDMAEMA \overline{M}_n determined by NMR of PNVCL-*b*-PDMAEMA copolymers. (PNVCL $\overline{M}_n = 5700$ Da)

| Sample | Reaction time (h) | PDMAEMA $^{NMR} \overline{M}_n$ (Da) ^a | Polymer X _{NVCL} (% mol/mol) ^a | DMAEMA conv. (% mol/mol) ^a |
|----------------------------|-------------------|---|--|---------------------------------------|
| PNVCL- <i>b</i> -DMAEMA-95 | 2 | 350 | 95 | 2 |
| PNVCL- <i>b</i> -DMAEMA-89 | 4 | 800 | 89 | 5 |
| PNVCL- <i>b</i> -DMAEMA-81 | 6 | 1500 | 81 | 10 |

^a Determined by ¹H-NMR.

As can be seen from the data shown in Table 16 the reaction is very slow but the conversion increases with the time as expected, allowing to obtain polymers with increasing number of DMAEMA repeating units. The polymerizations were carried out using CuCl/2Byp which is a common catalytic system used for the polymerization of DMAEMA¹³¹. Byp is less active than Me₆Cyclam¹⁴ and this might be reason why the reaction is slow compared to the ones of VAc and MA. Furthermore, Me₆Cyclam is a stronger complexing agent compared to Byp so, PNVCL macroinitiator can compete with the ligand and complex, at least partially, the catalyst which cannot take part in ATRP equilibrium, thus decreasing the rate of polymerization.

The thermal stability of PNVCL-*b*-PDMAEMA derivatives was investigated by TGA (Table 17). In Figure 26 the TGA curves of the block copolymers are displayed and compared with the one of the macroinitiator PNVCL-5700.

PNVCL macroinitiator, as previously described, is stable up to 300°C then degrades in two steps, the first centred at 324°C and the second one at 436°C. During the second step the polymer lose almost 95% of its initial weight. All the block copolymers are stable up to roughly 150°C then they show a sequence of stepwise degradations.

The first step, centred at 150-160°C, can be assigned to a low temperature depolymerisation phenomenon of PDMAEMA, as reported in literature for other polymethacrylates¹³². The degradation that occurs below 350°C cannot be assigned solely to the degradation of the residual PDMAEMA, which did not completely depolymerize, because the weight loss is higher than PDMAEMA weight fraction in the polymers. PDMAEMA degradation can influence and promote PNVCL decomposition, so between 200 and 350°C several degradation processes might be involved, other than the already cited depolymerisation of PDMAEMA and degradation of dimethylamino groups.

Between 350 and 480°C the weight loss is mainly due to PNVCCL decomposition and, eventually, to the degradation of the PDMAEMA polymer backbone.

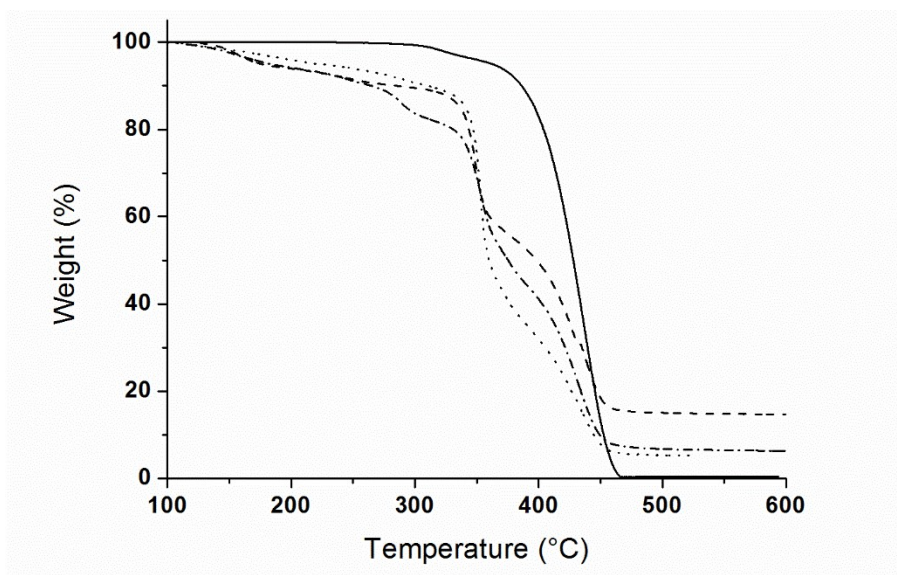


Figure 26: TGA curves of PNVCCL-5700 (—), PNVCCL-*b*-PDMAEMA-95 (---), PNVCCL-*b*-PDMAEMA-89 (···) and PNVCCL-*b*-PDMAEMA-81 (-·-·).

Table 17: Characterization data of PNVC-*b*-DMAEMA copolymers

| Sample | X DMAEMA (% w/w) | T _d (°C) | T _{max} | Weight |
|-----------------------------|---------------------|------------------------|------------------|------------------|------------------|------------------|------------------|------------------|------------------|------------------|
| | | | deg. 1 (°C) | loss 1 (%w/w) | deg. 2 (°C) | loss 2 (%w/w) | deg. 3 (°C) | loss 3 (%w/w) | deg. 4 (°C) | loss 4 (%w/w) |
| PNVCCL-5700 | 0 | 300 | 324 | 4.4 | 436 | 94.5 | - | - | - | - |
| PNVCCL- <i>b</i> -DMAEMA-95 | 6 | 143 | 154 | 5.5 | 349 | 33.5 | 428 | 38.7 | - | - |
| PNVCCL- <i>b</i> -DMAEMA-89 | 12 | 141 | 155 | 5.4 | 291 | 6.4 | 353 | 49.8 | 433 | 33.2 |
| PNVCCL- <i>b</i> -DMAEMA-81 | 21 | 136 | 157 | 7.3 | 289 | 11.2 | 353 | 29.9 | 434 | 44.1 |

The degradation centred at 150-160°C modify the polymer structure and it does not allow to determine correctly the T_g of PNVCCL block by DSC. Adopting a DSC temperature program that heats up to just 100°C (3 heating scans from -20 to 100°C, heating/cooling rate 20°C/min under nitrogen atmosphere), a T_g of 17°C was determined for the sample with higher content of PDMAEMA (PNVCCL-*b*-DMAEMA-81). This stepwise heat capacity increment can be ascribed to PDMAEMA block and it is consistent with data reported in literature¹³³, confirming the presence of PDMAEMA block as determined by

NMR, IR and TGA. In the other copolymers the T_g of PDMAEMA cannot be detected because of the low PDMAEMA chain length.

2.2.3.3 Synthesis of PNVCL-*b*-PPEGMEA

PNVCLs with different average molecular weight were used as macroinitiators for the ATRP of poly(ethylene glycol) methyl ether methacrylate (PEGMEA) monomer with different PEG chain length with the aim to obtain block copolymers with different composition. The polymerizations were carried out at room temperature, in 1,4-dioxan in presence of Me₆Cyclam as ligand, CuCl as catalyst, with different initial molar ratio of [PEGMEA]/[CuCl]/[Me₆Cyclam]/[PNVCL] and using polymerization procedure 3 (Table 18). The reactions were stopped after different reaction times in order to synthesize products with different PPEGMEA chain length. At the end of the synthesis the polymers were purified and the occurrence of polymerization was confirmed by FT-IR and NMR. \overline{M}_n was determined by ¹H-NMR by comparing the integrals of the NVCL residues at 4.4 ppm (CH-N) to that one of PEGMEA residues at 3.6 ppm (CH₂-CH₂-O).

Table 18: Characterization data of PNVCL-*b*-PPEGMEA block copolymers.

| Sample | [M ₀]/[Cu(I)]/ /[L]/[I ₀] | [M ₀] | Reaction time (h) | PNVCL ^{NMR} \overline{M}_n (Da) ^a | PPEGMEA ^{NMR} \overline{M}_n (Da) ^a | Polymer X _{NVCL} (%mol/mol) ^a | PEGMEA conv. (% mol/mol) ^a |
|---------------------------------|--|-------------------|----------------------|---|---|---|---|
| PNVCL- <i>b</i> -PPEGMEA300-91 | 80/1/1/1 | 1.2 | 0.3 | 20600 | 4100 | 91 | 18 |
| PNVCL- <i>b</i> -PPEGMEA300-80 | 80/1/1/1 | 1.2 | 18 | 20600 | 10400 | 80 | 46 |
| PNVCL- <i>b</i> -PPEGMEA300-94 | 80/1/1/1 | 0.5 | 16 | 20600 | 2600 | 94 | 12 |
| PNVCL- <i>b</i> -PPEGMEA300-73 | 100/1/1/1 | 0.4 | 60 | 20600 | 15400 | 73 | 54 |
| PNVCL- <i>b</i> -PPEGMEA350-91 | 40/2/2/1 | 0.6 | 2 | 2800 | 850 | 91 | 5 |
| PNVCL- <i>b</i> -PPEGMEA350-40 | 40/2/2/1 | 0.6 | 7 | 2800 | 12800 | 40 | 75 |
| PNVCL- <i>b</i> -PPEGMEA2000-95 | 20/2/2/1 | 0.15 | 0.5 | 2800 | 2000 | 95 | 5 |
| PNVCL- <i>b</i> -PPEGMEA350-88 | 40/2/2/1 | 0.6 | 3.5 | 6800 | 2800 | 88 | 16 |
| PNVCL- <i>b</i> -PPEGMEA2000-94 | 20/2/2/1 | 0.15 | 2 | 6800 | 6400 | 94 | 16 |

^a Determined by ¹H-NMR.

The data reported in Table 18 show that, as expected, the monomer conversion increases with the reaction time, allowing to obtain copolymers with different PEGMEA chain length. Furthermore, the rate of polymerization is consistent with the initial monomer concentration. The range of composition of the synthesized compounds highlights that we attained a good control over the polymerization.

In order to obtain a copolymer with an higher average molecular weight of PPEGMEA300 block, PEGMEA300 was polymerized at room temperature, in 1,4-dioxan ($[M_0] = 0.9M$), in presence of CuCl as catalyst, Me₆Cyclam ligand, ACP as initiator, with initial molar ratio of $[PEGMEA]/[CuCl]/[Me_6Cyclam]/[ACP] = 100/1/1/1$ and using polymerization procedure 4. After 24 hours of polymerization (PEGMEA300 homopolymerization) a fresh and degassed solution of NVCL was added to the reaction mixture (NVCL polymerization time = 1 hour). NVCL was added to the reaction mixture without purifying the PPEGMEA300 macroinitiator synthesized during the first 24 hours of reaction. The moles of NVCL added into the reactor were high enough to have an initial NVCL to initiator ratio of 200/1. For the sake of comparison, the homopolymerization of PEGMEA300 was carried out in the same conditions and stopped after 24 hours.

The obtained materials were characterized by FT-IR and NMR and the \overline{M}_n were determined by comparing the integrals of the allyl signals (5.9 and 5.3 ppm) to those ones of NVCL and/or PEGMEA residues at 4.4 ppm (CH-N) and 3.6 ppm (CH₂-CH₂-O) respectively.

Reaching PPEGMEA300 homopolymerization a monomer conversion of 90% with an average molecular weight of 34600 Da, it is reasonable to expect that, after the addition of NVCL, the polymer chain of the copolymer (second block) is mainly composed of NVCL. Thus we can assume that we obtained a copolymer named PPEGMEA-*b*-PNVCL-28, constituted by a block of PPEGMEA300 (34600 Da) and a block of PNVCL (4900 Da).

It is worth noting that the ATRP of PEGMEA300 results faster in presence of ACP (90% monomer conversion in 24 hours) than with PNVCL-20600 as initiator (PNVCL-*b*-PPEGMEA300-73 shows a 54% of monomer conversion in 60 hours). It is evident that using a macroinitiator the reaction is slower because of the hindrance of the molecule that makes the radical less available to react with the monomer and because of the higher viscosity (and higher diffusion coefficient) that the solution has when macromolecules are dissolved in the reaction mixture.

The thermal stability of PNVCL-*b*-PPEGMEAs was investigated by TGA. The TGA traces of samples PNVCL-*b*-PPEGMEA300-91 and 80, compared with the ones of PNVCL and PNVCL-*co*-PPEGMEA300-97 are shown in Figure 27.

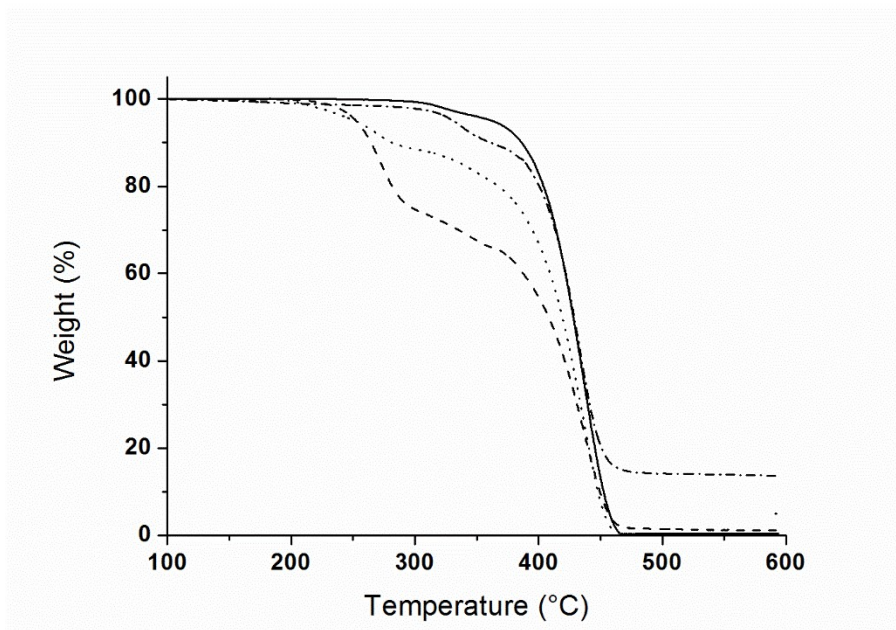


Figure 27: TGA curves of P(NVCL-*co*-PPEGMEA350)-97 (---), PNVCL-*b*-PPEGMEA300-91 (···), PNVCL-*b*-PPEGMEA300-80 (-·-·) copolymers compared with TGA curve of PNVCL-5700(—).

TGA was carried out to highlight the effect the polymer structure has on the thermal behaviour, in particular thermal stability, of the synthesized compounds.

In presence of random copolymers containing NVCL and PEGMEA, the degradation starts at the same temperature of PNVCL homopolymer (see chapter 2.2.2.3). PNVCL-*b*-PPEGMEA300s have a degradation pattern which differs from PNVCL-*co*-PEGMEA300s. Block copolymers show a first degradation around 250°C which is ascribed to PEGMEA300 block because it is consistent with PEGMEA content in the polymer. This degradation do not involve PEG side chains which are known to start degrading at 380-400°C¹³⁴, hence can be ascribed, as seen for PDMAEMA block copolymers, to PPEGMEA depolymerisation and subsequent reactions of the radicals with the functional groups present in the macromolecules. However, if PPEGMEA depolymerizes without further reactions, TGA would not be able to detect this event since the single PEGMEA unit is not volatile. The first weight loss is due to the formation of volatile products that may form after the reactions between radicals (generated after depolymerisation) and PEG chains. The second degradation that can be seen from the TGA curves is very similar to the one of PNVCL and it can be ascribed to the degradation of

PNVCL block and of some non-volatile compounds which formed during the first weight loss.

All the synthesized compounds behave analogously to PNVCL-*b*-PPEGMEA300-91 and 80 with the first weight loss that increases with PPEGMEA content. TGA qualitatively demonstrates the presence of the expected block copolymer structure and upon undertaking a deep study of the degradation mechanism it would be possible to determine the copolymer composition from the weight losses during the two degradation steps.

The chain mobility of PNVCL-*b*-PPEGMEA was studied by DSC. PNVCL-*b*-PPEGMEA2000 copolymers show an endotherm event and a stepwise specific heat increment while the other copolymers show only this latter. In Table 19 the glass transition temperatures, with the specific heat increment, the melting temperature (taken at the maximum of the endotherm), with its enthalpy, are summarized. The copolymer composition was also determined by DSC, comparing the specific heat increment (Table 19). All the synthesized compounds have only one glass transition which can be ascribed to PNVCL block. Its value is usually lower in the copolymers than in the homopolymer; indeed, after the block polymerization, the glass transition of PNVCL can decrease to 168°C. This effect is caused by the presence of PEG side chains, that act as plasticizers for the PNVCL block. The ΔC_p values of this transition is always lower than 0.27 J/g*°C, which is the specific heat increment associated to the glass transition of PNVCL homopolymer. Determining the polymer composition using ΔC_p values, the obtained data are in agreement with the ones determined by NMR and, even if DSC is less precise compared to NMR for determining the composition, the agreement demonstrate the trustworthiness of the data.

The DSC of poly(ethylene glycol) methyl ether 2000 Da (PEG-2000) display a melting event centred at 54°C (167.3 J/g). The block copolymers containing PEGMEA2000 show an analogous transition centred at 51-52°C, with lower enthalpy. This transition is thus ascribed to the melting of the PEG crystal phase, whose crystallinity is influenced by the polymer structure.

Table 19: T_g , ΔC_p , T_m , ΔH of PNVCL-*b*-PPEGMEA copolymer and comparison between composition determined by NMR and DSC.

| Sample | X NVCL (%w/w) ^a | T_g (°C) [ΔC_p (J/g*°C)] ^b | T_m (°C) [ΔH (J/g)] ^b | X NVCL (%w/w) ^c |
|---------------------------------|-------------------------------|---|--|-------------------------------|
| PNVCL | 100 | 190 [0.27] | - | 100 |
| PNVCL- <i>b</i> -PPEGMEA300-91 | 84 | 184 [0.22] | - | 81 |
| PNVCL- <i>b</i> -PPEGMEA300-80 | 66 | 177 [0.18] | - | 67 |
| PNVCL- <i>b</i> -PPEGMEA300-94 | 89 | 195 [0.23] | - | 85 |
| PNVCL- <i>b</i> -PPEGMEA300-73 | 57 | 189 [0.18] | - | 67 |
| PNVCL- <i>b</i> -PPEGMEA350-88 | 71 | 168 [0.18] | - | 67 |
| PNVCL- <i>b</i> -PPEGMEA350-91 | 77 | 185 [0.20] | - | 74 |
| PNVCL- <i>b</i> -PPEGMEA350-40 | 18 | 190 [0.04] | - | 15 |
| PNVCL- <i>b</i> -PPEGMEA2000-95 | 58 | 173 [0.21] | 51 [25.9] | 77 |
| PNVCL- <i>b</i> -PPEGMEA2000-94 | 52 | 180 [0.13] | 52 [28.8] | 48 |

^a Determined by ¹H-NMR^b Determined by DSC^c Determined by DSC as ΔC_p (in the copolymer)/ ΔC_p (homopolymer).

2.2.3.4 Synthesis of NVCL-*b*-PNVF

PNVCL was used as macroinitiator also for the ATRP of N-vinylformamide (NVF) which is a polar monomer with an amide group bonded to the vinyl double bond as NVCL and NVP but it does not have the hydrophobic cycle chain as these latter. The structure of NVF compared with the ones of NVP and NVCL is shown in Figure 28. Furthermore, NVF has a carbonyl group in β to the vinyl double bond as VAc, NVCL and NVP. A series of PNVCL-*b*-PNVF copolymers was so synthesized.

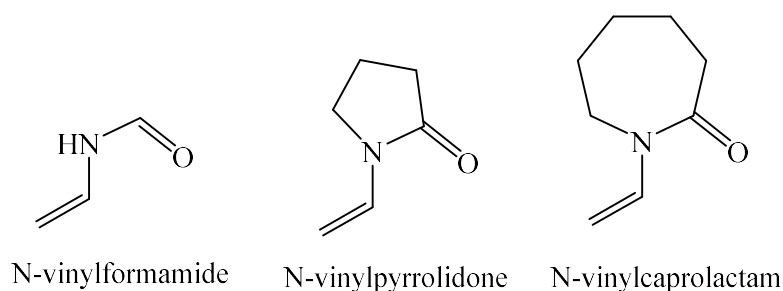


Figure 28: structure of NVF, NVP and NVCL monomers.

The polymerizations were carried out at room temperature, in 1,4-dioxan ($[M_0] = 1.4M$) in presence of PNVCL-14000 as macroinitiator, $Me_6Cyclam$ as ligand, $CuCl$ and $CuCl_2$ as catalyst, with different initial molar ratio of $[NVF]/[CuCl]/[Me_6CyClam]/[PNVCL]$ and using polymerization procedure 3. The reactions were stopped after different reaction times in order to synthesize products with different PPEGMEA chain length. At the end of the synthesis the polymers were purified and the occurrence of polymerization was confirmed by FT-IR and NMR. From the 1H -NMR spectra of the synthesized compounds the signals of the two different blocks are clearly detectable (Figure 29) and their final molar composition can be determined by comparing the integrated signals of $N-C(O)-H$ of NVP units located at 7.9 ppm, to that one related to the $N-C(O)-CH_2$ of NVCL macroinitiator at 4.8-4.0 ppm (Table 20).

PNVF is a polar polymer and even if PNVCL-*b*-PNVF copolymers are soluble in chloroform, the 1H -NMR does not allow to detect and quantify properly the signal of PNVF block. Being both the blocks of the copolymers soluble in water the NMR analysis was carried out in D_2O . As an example, in Figure 29 the 1H -NMR spectrum in D_2O of PNVCL-*b*-PNVF-50 is shown.

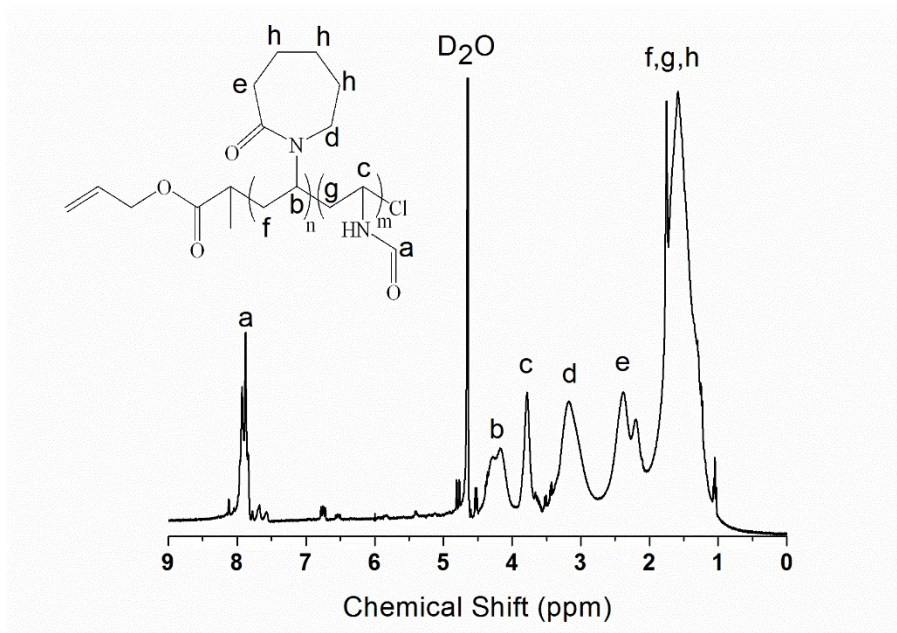


Figure 29: 1H -NMR spectrum in D_2O of PNVCL-*b*-NVF-50.

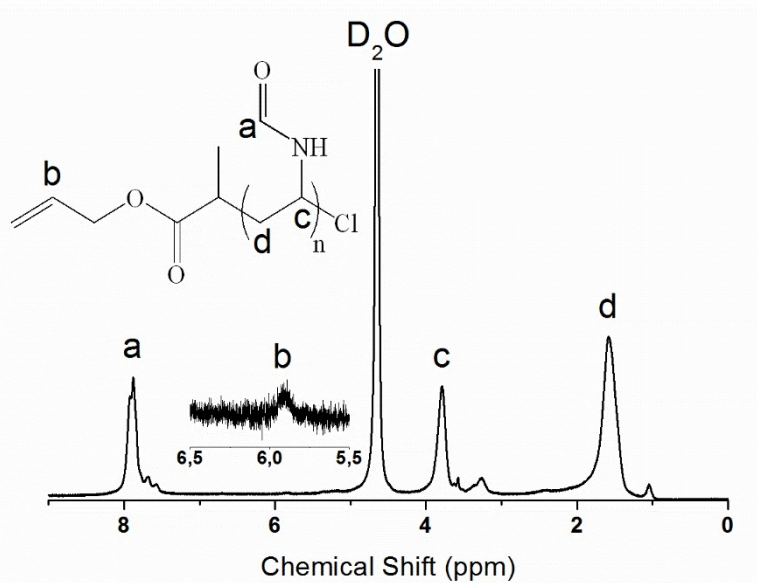
Table 20: \overline{M}_n and composition determined by NMR of PNVCCL-*b*-PNVF copolymers.

| Sample | PNVCCL ^{NMR} | PNVF ^{NMR} | Polymer X _{NVCCL} | NVF conv. | Reaction time (h) |
|---------------------------|------------------------------------|------------------------------------|----------------------------|--------------------------|-------------------|
| | \overline{M}_n (Da) ^a | \overline{M}_n (Da) ^a | (% mol/mol) ^a | (% mol/mol) ^a | |
| PNVCCL- <i>b</i> -PNVF-69 | 14000 | 3200 | 69 | 15 | 0.5 |
| PNVCCL- <i>b</i> -PNVF-55 | 14000 | 5800 | 55 | 27 | 2 |
| PNVCCL- <i>b</i> -PNVF-50 | 14000 | 8100 | 50 | 33 | 3 |

^a Determined by ¹H-NMR

The PNVF chain length increases with the polymerization time as expected, and block copolymers with different PNVF chain length were obtained.

In order to compare the properties of the synthesized compounds, an homopolymer of PNVF was synthesized at room temperature, in 1,4-dioxan ([M₀]= 2.4M) in presence of ACP as initiator, Me₆Cyclam as ligand, CuCl and CuCl₂ as catalyst, with an initial molar ratio of [NVF]/[CuCl]/[CuCl₂]/[Me₆CyClam]/[ACP]=200/1/0.7/1.7/1 and using polymerization procedure 4. The reaction was stopped after 6 hours. At the end of the synthesis the polymer was purified and the occurrence of polymerization was confirmed by FT-IR and NMR. From the ¹H-NMR spectra of the synthesized compound the signal of the ACP residue (5.40-5.27 ppm, CH₂=) is detectable (Figure 30). The comparison of its integral with respect to those ones of NVCL residue, allows to assess the number average molecular weight (\overline{M}_n) of the obtained material which resulted being 2700 Da corresponding to a monomer conversion of 19% in 6 hours.

Figure 30: ¹H-NMR spectrum in D₂O of PNVF-2700.

The thermal behaviour of the PNVF and of the block copolymers was investigated by TGA and DSC under nitrogen atmosphere. In Figure 31 and Table 21, the TGA curves and relevant data about the thermal degradation of the block copolymers and reference homopolymers are displayed. PNVF-2700 degrades in three degradation steps, one centred at 260°C, one at 348°C and the last one at 430°C. The degradation profile of PNVF is different compared to PNVCL, with the latter degrading in two steps and with a higher initial degradation temperature.

For the block copolymers the initial degradation is centred at 251-255°C. This first weight loss, which is not present in PNVCL homopolymers, occurs at the lowest temperature for the copolymer PNVCL-*b*-PNVF-69 while it is comparable for the other two copolymers with similar composition (PNVCL-*b*-PNVF-55 and 50). This is the same pattern that can be detect in PNVF-2700 homopolymer. For these reasons the first weight loss in the copolymers can be ascribed to PNVF block. The second degradation which is centred at 431-436°C, both in PNVCL and in the PNVCL-*b*-PNVF block copolymers, mainly corresponds to PNVCL block degradation.

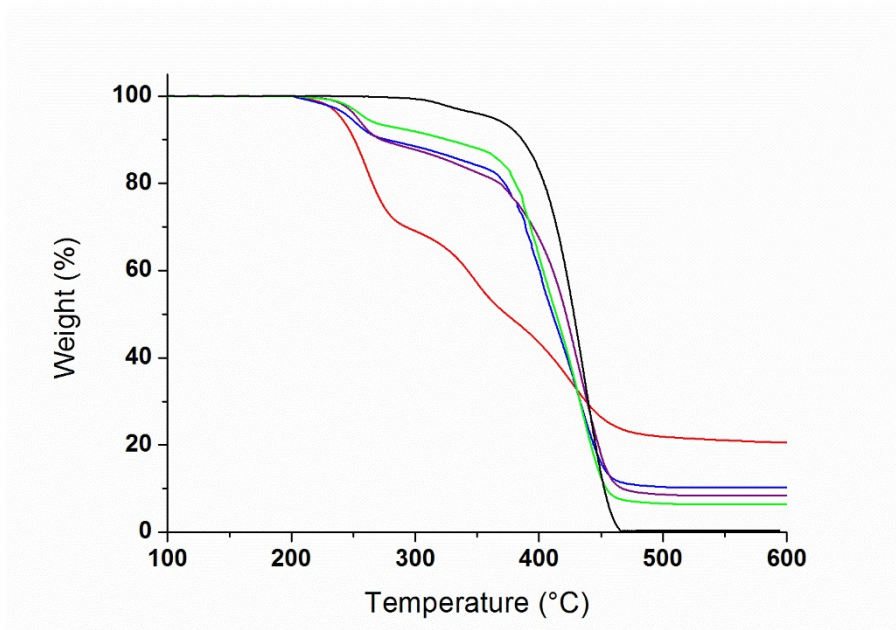


Figure 31: TGA curves of PNVCL-*b*-PNVF-69 (green), PNVCL-*b*-PNVF-55 (violet), PNVCL-*b*-PNVF-50 (blue) copolymers compared with TGA curve of PNVCL (black) and PNVF (red).

Table 21: Composition and TGA weight loss during the thermal degradation of the block copolymers compared with the one of the macroinitiator PNVCL and PNVF (determined by TGA).

| Sample | T _d (°C) | X NVF (% w/w) | T _{max} | Weight | T _{max} | Weight | T _{max} | Weight |
|--------------------------|---------------------|------------------|------------------|------------------|------------------|------------------|------------------|------------------|
| | | | deg. 1 (°C) | loss 1 (%w/w) | deg. 2 (°C) | loss 2 (%w/w) | deg. 3 (°C) | loss 3 (%w/w) |
| PNVCL-14000 | 300 | 0 | 324 | 4.4 | 436 | 94.5 | - | - |
| PNVF-2700 | 231 | 100 | 260 | 31.0 | 348 | 19.4 | 430 | 28.9 |
| PNVCL- <i>b</i> -PNVF-69 | 240 | 19 | 254 | 6.9 | 433 | 86.6 | - | - |
| PNVCL- <i>b</i> -PNVF-55 | 232 | 29 | 255 | 10.7 | 434 | 80.8 | - | - |
| PNVCL- <i>b</i> -PNVF-50 | 228 | 37 | 251 | 10.2 | 431 | 79.5 | - | - |

Results from the chain mobility investigation carried out by DSC are summarized Table 22. DSC of PNVF highlights the presence of a stepwise specific heat increment at 148°C with a ΔC_p of 0.44 J/(g*°C). All the copolymers display two stepwise specific heat increment. The glass transition temperatures are typical of the presence of two polymeric blocks. The T_g at lower temperature (140-150°C) can be ascribed to PNVF block. The T_g of PNVCL block (T_{g2} in Table 22) decreases with PNVF content in the copolymer passing from 188 to 164°C. Actually T_{g2} and T_{g1} of PNVCL-*b*-PNVF are partially overlapped, making trickier the determination of the transition. The decrease of T_g values of PNVCL block is mainly due to the plasticizing effect of PNVF block which has lower T_g.

Table 22: T_g and ΔC_p of PNVCL-*b*-PNVF copolymers

| Sample | T _{g1} (°C) [ΔC_p (J/g*°C)] ^a | T _{g2} (°C) [ΔC_p (J/g*°C)] ^a |
|--------------------------|--|--|
| PNVF-2700 | 148 [0.44] | - |
| PNVCL-14000 | - | 190 [0.27] |
| PNVCL- <i>b</i> -PNVF-69 | 150 [0.13] | 188 [0.20] |
| PNVCL- <i>b</i> -PNVF-55 | 140 [0.27] | 175 [0.11] |
| PNVCL- <i>b</i> -PNVF-50 | 140 [0.25] ^b | 164 [0.19] ^b |

^a Determined by DSC

^b Glass transitions are partially overlapped.

2.3 Conclusions

Optimized ATRP method was successfully employed for the polymerization of polar monomers that generate reactive radicals, such as NVP and NVCL. The influence of the parameters (initial molar ratio, presence of oxidized catalyst and so on) that can affect the result of the synthesis was studied, understanding the mechanism of the polymerization. The polymerizations were optimized in presence of different solvents (e.g. PPG), attaining a good control over the living process up to 90% of monomer conversion, applying conditions for the further development of the possible industrial process.

Several random copolymers containing NVCL or NVP and (meth)acrylate (BMA, BA and PEGMEA) or VAc repeating units were synthesized by ATRP attaining a good control over the composition of the final synthesized material. The results achieved over the random copolymerization show that it is possible to predict the composition and the structure of the polymers on the basis of the reactivity of the monomers. Moreover, the ATRP optimized systems lack in considerable termination reactions that may occur during a radical polymerization.

Furthermore, the synthesized PNVCL was used as macroinitiator for the further ATRP of methacrylic monomers (MMA, DMAEMA and PEGMEA), VAc and NVF, obtaining block copolymers with uni-modal molecular weights distributions and confirming the livingness of the system.

These results were allowed by using a very active catalytic system composed of CuCl, CuCl₂ and Me₆CyClam which allows to maintain a low concentration of propagating species once radicals are formed, hence establishing a fast and dynamic ATRP equilibrium.

The synthetic system paves the way to an industrially scalable process for the production of well-defined block and statistic copolymers containing NVCL and NVP that may find a number of interesting applications.

2.4 Experimental section

2.4.1 Physico-chemical characterization

¹H NMR spectra were obtained at room temperature, on 5-10% w/v CDCl₃, DMSO or D₂O solutions, using a Varian MercuryPlus VX 400 (¹H, 399.9; ¹³C, 100.6 MHz) spectrometer. Chemical shifts are given in ppm from tetramethylsilane (TMS) as the internal reference.

FT-IR spectra were recorded on a Bruker Alpha Platinum-ATR spectrophotometer equipped with ATR Diamond window.

Number average molecular weight of the polymers (\overline{M}_n) and their polydispersity index ($PD = \overline{M}_w/\overline{M}_n$) were determined in THF or DMF solutions at 25 and 70°C respectively by SEC using an HPLC Lab Flow 2000 apparatus equipped with an injector Rheodyne 7725i, a Phenomenex Phenogel 5-micron MXL and MXM columns (THF solutions, monodispersed polystyrene standards 800-35000 and 13300-214000 Da, respectively) or a Tosoh Bioscience TSKgel GMH_{HR}-N 5-micron column (DMF solutions, monodisperse poly(ethylene glycol) standards 400-20000 Da), and a refractive index detector model Knauer RI K-2301.

The glass and melting transition temperature values (T_g and T_m) of polymers and the cyclopentane hydrates formation were determined by differential scanning calorimetry (DSC) on a TA Instrument DSC Q2000 Modulated apparatus adopting a temperature program consisting of three heating and two cooling ramps starting from room temperature (heating/cooling rate 20°C/min under nitrogen atmosphere) on 5-10 mg samples. Thermogravimetric (TGA) measurements were carried out using a TA Instrument SDT Q600 (heating rate 10°C/min) on 10-20 mg samples under nitrogen atmosphere with a 100 ml/min gas flow rate.

X-ray diffraction (XRD) analysis was carried out by means of a PANalytical X'Pert PRO diffractometer equipped with a fast X'Celerator detector. Ni-filtered CuK α radiation was used. For phase identification and structure refinement the 2 θ range was investigated from 15 to 50 2 θ degrees with a step size of 0.033° and time/step of 250 s.

2.4.2 Materials

N-vinylpyrrolidone (NVP) (Sigma-Aldrich, $\geq 99\%$), N-vinylformamide (NVF) (Sigma-Aldrich, 98%), vinyl acetate (VAc) (Sigma-Aldrich, $>99\%$), 2-(dimethylamino)ethyl methacrylate (DMAEMA) (Sigma-Aldrich, 98%), butyl methacrylate (BMA) (Sigma-Aldrich, 99%), butyl acrylate (BA) (Sigma-Aldrich, $\geq 99\%$), methyl methacrylate (MMA) (Sigma-Aldrich, 99%), methyl acrylate (MA) (Sigma-Aldrich, 99%), methacryloyl chloride (Sigma-Aldrich, $\geq 97\%$) and acryloyl chloride (Sigma-Aldrich, 97%) were distilled under reduced pressure in the presence of traces of 2,6-di-*tert*-butyl-*p*-cresol as polymerization inhibitor just before use.

Poly(ethylene glycol) methyl ether methacrylate $\overline{M}_n=300$ Da (PEGMEA300) (Sigma-Aldrich) and 2-chloropropionyl chloride (Sigma-Aldrich, 97%) were eluted through a column filled with neutral alumina to remove the inhibitor.

1,4-Dioxane was distilled over potassium in presence of benzophenone¹³⁵.

CuCl (Sigma-Aldrich, $>99\%$) and CuBr (Sigma-Aldrich, $\geq 98\%$) were washed with glacial acetic acid (three times) and diethyl ether and then dried under vacuum.

5,5,7,12,12,14-Hexamethyl-1,4,8,11-tetraazacyclotetradecane (Me₆CyClam) was synthesized as previously reported¹³⁶.

Dichloromethane (DCM) was distilled over P₂O₅ just before use¹³⁵.

N-vinylcaprolactam (Sigma-Aldrich, 98%) (NVCL), Pentamethyldiethylenetriamine (PMDETA) (Sigma-Aldrich, $\geq 98\%$), CuCl₂ (Sigma-Aldrich, 99%), allyl alcohol (Sigma-Aldrich, $\geq 98.5\%$), 2-chloropropionyl chloride (Sigma-Aldrich, 97%), poly(ethylene glycol) methyl ether $\overline{M}_n=2000$ Da (PEG2000) (Sigma-Aldrich), poly(ethylene glycol) methyl ether $\overline{M}_n=750$ Da (PEG750) (Sigma-Aldrich), poly(ethylene glycol) methyl ether $\overline{M}_n=350$ Da (PEG350) (Sigma-Aldrich), cyclopentane (Sigma-Aldrich, 98%) 2,2'-bipyridyl (byp) (Sigma-Aldrich, $\geq 98\%$), sorbitan sesquioleate (Span83) (Sigma-Aldrich), and others solvents (Aldrich) were used as received without further purification.

2.4.3 Synthesis of allyl 2-chloropropionate (ACP)

A solution of 2-chloropropionyl chloride (9.7 ml, 12.7 g, 0.1 mol) in dry CH₂Cl₂ (50 ml) was added dropwise to an ice-cooled stirred solution of allyl alcohol (6.8 ml, 5.8 g, 0.1 mol) and triethylamine (13.9 ml, 10.1 g, 0.1 mol) in 40 ml of dry CH₂Cl₂. The mixture was stirred for 2 hours, then left at room temperature for 24 hours. At the end of the reaction the triethylammonium chloride by-product was filtered off and the resulting solution was

concentrated under reduced pressure. The organic solution was then washed with 0.1 M HCl, 0.1 M NaOH and finally with water in that order. The organic layer was dried (Na_2SO_4) and the solvent was removed under reduced pressure. The obtained yellow, transparent liquid was purified by distillation under reduced pressure (T_{eb} . 44°C , 7 mmHg). Yield 80%.

^1H NMR (400 MHz, CDCl_3 , δ , ppm): 5.93 (m, $J = 6.8$ Hz, 1H; $\text{CH}=\text{}$), 5.40-5.27 (2m, 2H, $\text{CH}_2=\text{}$) 4.68 (d, $J=5.7$ Hz, 2H; CH_2O), 4.43 (q, $J = 7.0$ Hz, 1H; $\text{CH}(\text{CH}_3)(\text{Cl})$), 1.71 (d, $J = 7.0$ Hz, 3H; CH_3).

2.4.4 Synthesis of poly(ethylene glycol) methyl ether methacrylate (PEGMEA): PEGMEA350, PEGMEA750 and PEGMEA2000.

A solution of methacryloyl chloride (0.01 mol) in dry CH_2Cl_2 (10 ml) was added dropwise to an ice-cooled stirred solution of poly(ethylene glycol) methyl ether (0.01 mol) and triethylamine (0.02 mol) in 250 ml of dry CH_2Cl_2 . The mixture was stirred for 2 hours, then left at room temperature for 24 hours. At the end of the reactions the triethylammonium chloride by-product was filtered off and the resulting solution was concentrated under reduced pressure. The organic solution was then washed with 0.1 M HCl, 0.1 M NaOH and finally with water in that order. The organic layer was dried (Na_2SO_4) and the solvent was removed under reduced pressure. The obtained PEGMEA-2000 was then precipitated into n-hexane (yield 76%) whilst the obtained PEGMEA-350 and PEGMEA-750 were dried under vacuum (yield 86% and 72% respectively).

^1H NMR (400 MHz, CDCl_3 , δ , ppm): 6.13 (s, 1H; $\text{CH}_2=\text{}$), 5.58 (s, 1H; $\text{CH}_2=\text{}$), 4.30 (t, $J=4.9$ Hz, 2H, $\text{C}(\text{O})\text{O}-\text{CH}_2-$), 3.66 (b, 4H, $\text{CH}_2-\text{CH}_2-\text{O}$ PEG main chain), 3.38 (s, 3H; $\text{O}-\text{CH}_3$), 1.95 (s, 3H; methacrylic CH_3).

ATR FT-IR (polymer in powder): 2945 (ν_{as} CH_2), 2882 (ν_{s} CH_2), 1734 (ν_{s} $\text{C}=\text{O}$), 1634 (ν_{s} $\text{CH}_2=\text{C}(\text{CH}_3)$), 1466 (δ_{s} CH_2), 1279, 1240, 1098 (ν_{as} $\text{C}-\text{O}-\text{C}$) cm^{-1} .

2.4.5 Polymerization procedures

The polymerization kinetics were studied preparing several reactions and carrying out the synthesis under the same experimental conditions. Reactions were stopped at different times and the monomer concentration was determined by ^1H -NMR of the final reaction mixtures. The polymers were purified by filtration on basic aluminium oxide followed by

repeated precipitation. The materials were finally dried under vacuum until constant weight. The products were characterized by FT-IR, SEC, DSC, TGA and ^1H NMR.

During the synthesis of random copolymers, fresh solutions of monomers were added to the flask.

For the polymerizations different procedures were followed:

Polymerization procedure 1.

Catalyst, monomer, initiator, solvent and ligand were introduced into the vial under nitrogen atmosphere. The reaction mixture was submitted to several freeze-thaw cycles, heated the desired temperature and stirred.

Polymerization procedure 2.

Catalyst, monomer, solvent, ligand and initiator were introduced into the vial under nitrogen atmosphere, paying attention to add the initiator as last reactant. The reaction mixture was submitted to several freeze-thaw cycles, heated the desired temperature and stirred.

Polymerization procedure 3.

Catalyst, monomer, solvent, and (macro)initiator were introduced into the vial under nitrogen atmosphere, paying attention to add the initiator as last reactant. The reaction mixture was submitted to several freeze-thaw cycles, heated the desired temperature and stirred. A solution of ligand was added using a gastight syringe even under nitrogen atmosphere.

Polymerization procedure 4.

Catalyst, monomer, solvent, and ligand were introduced into the vial under nitrogen atmosphere, paying attention to add the initiator as last reactant. The reaction mixture was submitted to several freeze-thaw cycles, heated the desired temperature and stirred. A solution of initiator was added using a gastight syringe even under nitrogen atmosphere.

2.5 Polymer characterization

PNVP: $^1\text{H NMR}$ (400 MHz, CDCl_3 , δ , ppm): 3.5-4.1 (1H, CH-N), 3.4-3.0 (2H, CH_2 -N), 2.5-2.1 (2H, CH_2 -C(O)), 2.1-1.9 (2H, $-\text{CH}_2-$ side chain), 1.9-1.3 (2H, $-\text{CH}_2-$ polymer backbone).

ATR FT-IR (polymer in powder) (cm^{-1}): 2922-2855 (ν_{CH} aliph.), 1622 ($\nu_{\text{C=O}}$ amide group), 1475 (δ_{CH} polymer backbone), 1194 ($\nu_{\text{C-N}}$ amide group).

PNVCL: $^1\text{H NMR}$ (400 MHz, CDCl_3 , δ , ppm): 5.93 (m, $J = 6.8$ Hz, 1H; CH= ACP residue), 5.40-5.27 (2m, 2H, CH_2 = ACP residue), 4.7-4.1 (1H, CH-N), 3.5-2.8 (2H, CH_2 -N), 2.7-2.1 (2H, CH_2 -C(O)), 2.1-0.8 (8H, CH_2 - CH_2 - CH_2 - side chain and CH_2 - polymer backbone).

ATR FT-IR (polymer in powder) (cm^{-1}): 2924 and 2855 (ν_{CH} aliph.), 1615 ($\nu_{\text{C=O}}$ amide group), 1476, 1440 and 1419 (δ_{CH} polymer backbone), 1194 ($\nu_{\text{C-N}}$ amide group).

PNVF: $^1\text{H NMR}$ (400 MHz, D_2O , δ , ppm): 8.2-7.5 (1H, C(O)H), 5.93 (m, $J = 6.8$ Hz, 1H; CH= ACP residue), 5.40-5.27 (2m, 2H, CH_2 = ACP residue), 3.8 (1H, CH-N), 2.0-1.0 (2H, CH_2 polymer backbone);

ATR FT-IR (cm^{-1}): 2997-2789 (ν_{CH} aliph.), 1652 ($\nu_{\text{C=O}}$ amide group), 1532 (δ_{CH}), 1235 ($\nu_{\text{C-N}}$ amide group).

PVAc: $^1\text{H NMR}$ (400 MHz, CDCl_3 , δ , ppm): 6.41 (1H, CH-Cl end-group), 5.93 (m, $J = 6.8$ Hz, 1H; CH= ACP residue), 5.25-4.75 (1H, CH-O), 4.68 (2H, CH_2 -O ACP residue), 2.15-1.95 (3H, C(O)- CH_3), 1.95-1.40 (2H, CH_2 polymer backbone);

ATR FT-IR (polymer in powder) (cm^{-1}): 2981 and 2925 (asymm ν_{CH} aliph. CH_3 and CH_2), 2850 (symm ν_{CH} aliph. CH_2), 1729 ($\nu_{\text{C=O}}$ ester group), 1433 (δ_{CH} polymer backbone), 1370 (δ_{CH_3} side chain), 1225 ($\nu_{\text{C-O}}$ ester group), 604 ($\nu_{\text{C-Cl}}$ end-group).

PPEGMEA: $^1\text{H NMR}$ (400 MHz, CDCl_3 , δ , ppm): 5.93 (m, $J = 6.8$ Hz, 1H; CH= ACP residue), 5.40-5.27 (2m, 2H, CH_2 = ACP residue), 4.09 (2H, C(O)-O- CH_2), 3.9-3.5 (4H CH_2 - CH_2 -O PEG repeating unit), 3.38 (3H, O- CH_3), 2.2-1.5 (2H, CH_2 polymer backbone), 1.3-0.5 (3H, methacrylic CH_3);

ATR FT-IR (cm^{-1}): 2869 (ν_{CH} aliph.), 2850 (symm ν_{CH} aliph. CH_2), 1725 ($\nu_{\text{C=O}}$ ester group), 1450 (δ_{CH_2}), 1245 and 1101 ($\nu_{\text{C-O}}$ ester group).

Chapter 2: ATRP of polar monomers

PNVCL-*b*-PVAc: ¹H NMR (400 MHz, CDCl₃, δ , ppm): 5.93 (m, J = 6.8 Hz, 1H; CH= ACP residue), 5.25-4.75 (1H, CH-O), 4.7-4.1 (1H, CH-N), 3.5-2.8 (2H, CH₂-N), 2.7-1.9 (CH₂-C(O)-N and C(O)-CH₃), 2.1-0.8 (CH₂ polymer backbone and CH₂-CH₂-CH₂- NVCL side chain);

ATR FT-IR (polymer in powder) (cm⁻¹): 2920 and 2854 (ν_{CH} aliph.), 1737 ($\nu_{\text{C=O}}$ ester group), 1630 ($\nu_{\text{C=N}}$ amide group) 1475, 1439 and 1418 (δ_{CH}), 1366 (δ_{CH_3} VAc side chain), 1230 ($\nu_{\text{C-O}}$ ester group), 1194 ($\nu_{\text{C-N}}$ amide group).

PNVCL-*b*-PNVF: ¹H NMR (400 MHz, D₂O, δ , ppm): 8.2-7.5 (1H, C(O)H), 5.93 (m, J = 6.8 Hz, 1H; CH= ACP residue), 5.40-5.27 (2m, 2H, CH₂= ACP residue), 4.5-3.9 (1H, CH-N NVCL), 3.8 (1H, CH-N NVF), 3.5-2.7 (2H, CH₂-N), 2.7-2.0 (2H, CH₂-C(O)), 2.0-1.0 (CH₂-CH₂-CH₂- NVCL side chain and CH₂- polymer backbone);

ATR FT-IR (polymer in powder) (cm⁻¹): 2921 and 2854 (ν_{CH} aliph.), 1600-1750 ($\nu_{\text{C=O}}$ NVCL and NVF amide group), 1476, 1439 and 1420 (δ_{CH} polymer backbone), 1194 ($\nu_{\text{C-N}}$ NVF and NVCL amide group).

PNVCL-*b*-PDMAEMA: ¹H NMR (400 MHz, CDCl₃, δ , ppm): 5.93 (m, J = 6.8 Hz, 1H; CH= ACP residue), 5.40-5.27 (2m, 2H, CH₂= ACP residue), 4.7-4.1 (1H, CH-N), 4.05 (2H, C(O)-O-CH₂), 3.5-2.8 (2H, CH₂-N NVCL side chain), 2.7-2.0 (CH₂-C(O)-N NVCL side chain, N(CH₃)₂ and CH₂-N DMAEMA), 2.0-1.0 (CH₂-CH₂-CH₂- NVCL side chain and CH₂- polymer backbone), 0.9 (3H, methacrylic CH₃).

ATR FT-IR (polymer in powder) (cm⁻¹): 2923, 2854 and 2769 (ν_{CH} aliph.), 1728 ($\nu_{\text{C=O}}$ DMAEMA ester group), 1631 ($\nu_{\text{C=O}}$ NVCL amide group), 1475, 1440 and 1420 (δ_{CH}), 1194 ($\nu_{\text{C-N}}$ amide group) 1149 ($\nu_{\text{C-O}}$ ester group).

PNVCL-*b*-PPEGMEA: ¹H NMR (400 MHz, CDCl₃, δ , ppm): 5.93 (m, J = 6.8 Hz, 1H; CH= ACP residue), 5.40-5.27 (2m, 2H, CH₂= ACP residue), 4.7-4.0 (1H, CH-N and C(O)-O-CH₂), 3.66 (4H CH₂-CH₂-O PEG repeating unit), 3.5-2.8 (O-CH₃ and CH₂-N), 2.7-1.0 (CH₂-C(O)-N, CH₂-CH₂-CH₂- NVCL side chain and CH₂- polymer backbone), 0.9 (3H, methacrylic CH₃).

ATR FT-IR (polymer in powder) (cm⁻¹): 2882 (ν_{CH} aliph.), 1722 ($\nu_{\text{C=O}}$ ester group), 1631 ($\nu_{\text{C=O}}$ amide group), 1466 (δ_{CH} polymer backbone), 1241 ($\nu_{\text{C-O}}$ ester group), 1146 ($\nu_{\text{C-N}}$ amide group).

Chapter 2: ATRP of polar monomers

P(NVCL-*co*-VAc): $^1\text{H NMR}$ (400 MHz, CDCl_3 , δ , ppm): 5.93 (m, $J = 6.8$ Hz, 1H; CH= ACP residue), 5.25-4.75 (1H, CH-O), 5.0-4.2 (CH-N and CH-O), 3.5-2.8 (2H, $\text{CH}_2\text{-N}$), 2.7-2.1 ($\text{CH}_2\text{-C(O)-N}$ and C(O)-CH_3), 2.1-1.0 ($\text{CH}_2\text{-CH}_2\text{-CH}_2\text{- NVCL}$ side chain and CH_2 polymer backbone);

ATR FT-IR (polymer in powder) (cm^{-1}): 2920 and 2854 (ν_{CH} aliph.), 1733 ($\nu_{\text{C=O}}$ ester group), 1627 ($\nu_{\text{C=N}}$ amide group) 1475, 1440 and 1418 (δ_{CH}), 1368 (δ_{CH_3}), 1232 ($\nu_{\text{C-O}}$ ester group), 1194 ($\nu_{\text{C-N}}$ amide group).

P(NVCL-*co*-PEGMEA): $^1\text{H NMR}$ (400 MHz, CDCl_3 , δ , ppm): 5.93 (m, $J = 6.8$ Hz, 1H; CH= ACP residue), 5.40-5.27 (2m, 2H, $\text{CH}_2\text{= ACP}$ residue), 4.7-4.0 (1H, CH-N and C(O)-O-CH_2), 3.66 (4H $\text{CH}_2\text{-CH}_2\text{-O}$ PEG repeating unit), 3.5-2.8 (O-CH_3 and $\text{CH}_2\text{-N}$), 2.7-1.0 ($\text{CH}_2\text{-C(O)-N}$, $\text{CH}_2\text{-CH}_2\text{-CH}_2\text{- NVCL}$ side chain and $\text{CH}_2\text{- polymer}$ backbone), 0.9 (3H, methacrylic CH_3).

ATR FT-IR (polymer in powder) (cm^{-1}): 2882 (ν_{CH} aliph.), 1722 ($\nu_{\text{C=O}}$ ester group), 1631 ($\nu_{\text{C=O}}$ amide group), 1466 (δ_{CH} polymer backbone), 1241 ($\nu_{\text{C-O}}$ ester group), 1146 ($\nu_{\text{C-N}}$ amide group).

P(NVCL-*co*-BA): $^1\text{H NMR}$ (400 MHz, CDCl_3 , δ , ppm): 4.8-4.2 (1H, CH-N), 4.03 (2H, C(O)-O-CH_2), 3.4-2.9 (2H, $\text{CH}_2\text{-N}$), 2.45 ($\text{CH}_2\text{-C(O)-N}$), 2.3-1.2 ($\text{CH}_2\text{-CH}_2\text{-CH}_2\text{- NVCL}$ side chain, $\text{CH}_2\text{-CH}_2$ BA side chain and $\text{CH}_2\text{- polymer}$ backbone), 1-0.8 (3H, CH_3).

ATR FT-IR (polymer in powder) (cm^{-1}): 2922 and 2852 (ν_{CH} aliph.), 1727 ($\nu_{\text{C=O}}$ ester group), 1652 ($\nu_{\text{C=O}}$ amide group), 1466 (δ_{CH} polymer backbone), 1388 (δ_{CH_3}), 1268 and 1238 ($\nu_{\text{C-O}}$ ester group), 1147 ($\nu_{\text{C-N}}$ amide group).

P(NVP-*co*-BMA): $^1\text{H NMR}$ (400 MHz, CDCl_3 , δ , ppm): 4.2-3.6 (1H, CH-N and C(O)-O-CH_2), 3.4-2.9 (2H, $\text{CH}_2\text{-N}$), 2.45 ($\text{CH}_2\text{-C(O)-N}$), 2.3-1.2 ($\text{CH}_2\text{- NVP}$ side chain, $\text{CH}_2\text{-CH}_2$ BMA side chain and $\text{CH}_2\text{- polymer}$ backbone), 1-0.8 (6H, CH_3 BMA side chain and methacrylic CH_3).

ATR FT-IR (polymer in powder) (cm^{-1}): 2922 and 2852 (ν_{CH} aliph.), 1727 ($\nu_{\text{C=O}}$ ester group), 1652 ($\nu_{\text{C=O}}$ amide group), 1466 (δ_{CH} polymer backbone), 1388 (δ_{CH_3}), 1268 and 1238 ($\nu_{\text{C-O}}$ ester group), 1147 ($\nu_{\text{C-N}}$ amide group).

Chapter 2: ATRP of polar monomers

P(NVP-*co*-BA): $^1\text{H NMR}$ (400 MHz, CDCl_3 , δ , ppm): 4.2-3.6 (CH-N and C(O)-O-CH₂), 3.4-2.9 (2H, CH₂-N), 2.5-1.2 (CH₂-C(O)-N, CH₂ NVP side chain, CH₂-CH₂ BA side chain and CH₂- polymer backbone), 1-0.8 (3H, CH₃).

ATR FT-IR (polymer in powder) (cm^{-1}): 2922 and 2852 (ν_{CH} aliph.), 1727 ($\nu_{\text{C=O}}$ ester group), 1652 ($\nu_{\text{C=O}}$ amide group), 1466 (δ_{CH} polymer backbone), 1388 (δ_{CH_3}), 1268 and 1238 ($\nu_{\text{C-O}}$ ester group), 1147 ($\nu_{\text{C-N}}$ amide group).

3 Chapter 3 - Straightforward synthesis of well-defined poly(vinyl acetate) and its block copolymers by atom transfer radical polymerization

3.1 Introduction and scope

Poly(vinyl acetate) [PVAc] and its hydrolyzed derivative, poly(vinyl alcohol) [PVA], which is biodegradable, biocompatible and water soluble, are used in a number of different fields such as for the production of hydrogels, coating, pharmaceutical, textile, fiber, adhesive and in photographic industries^{137,138}. Whereas PVAc is synthesized, as most of the polymers, by radical polymerization of the corresponding monomer¹³⁹, PVA is commonly produced by hydrolysis of PVAc¹⁴⁰ being vinyl alcohol monomer unstable at room temperature. This compound, indeed, tends to form acetaldehyde by keto-enol tautomerization.

While the free radical polymerization of VAc monomer is a well-established process, in the past few years copious studies were reported attempting a controlled radical polymerization (CRP) approach^{60,63,141-146}, though it is still a challenge to polymerize monomers that generate very reactive radicals³⁷.

CRP would allow to synthesize polymeric materials with low polydispersity and pre-determined molecular weight and structure (such as block, gradient, star, brush, copolymer and so on). Being the final properties of a polymer strictly related to its structure and composition, by using these living techniques it is possible to obtain materials with predetermined properties for application in specific fields.

Among CRP, Atom Transfer Radical Polymerization (ATRP) results one of the most interesting processes because of its versatility, being suitable to polymerize a wide range of monomers (methacrylates, acrylates, styrene, etc.), insensitive to many functional groups and tolerant towards impurities present in solvent and reactants, including water. Thus, this technique, thanks to its robustness, can be industrially applied.

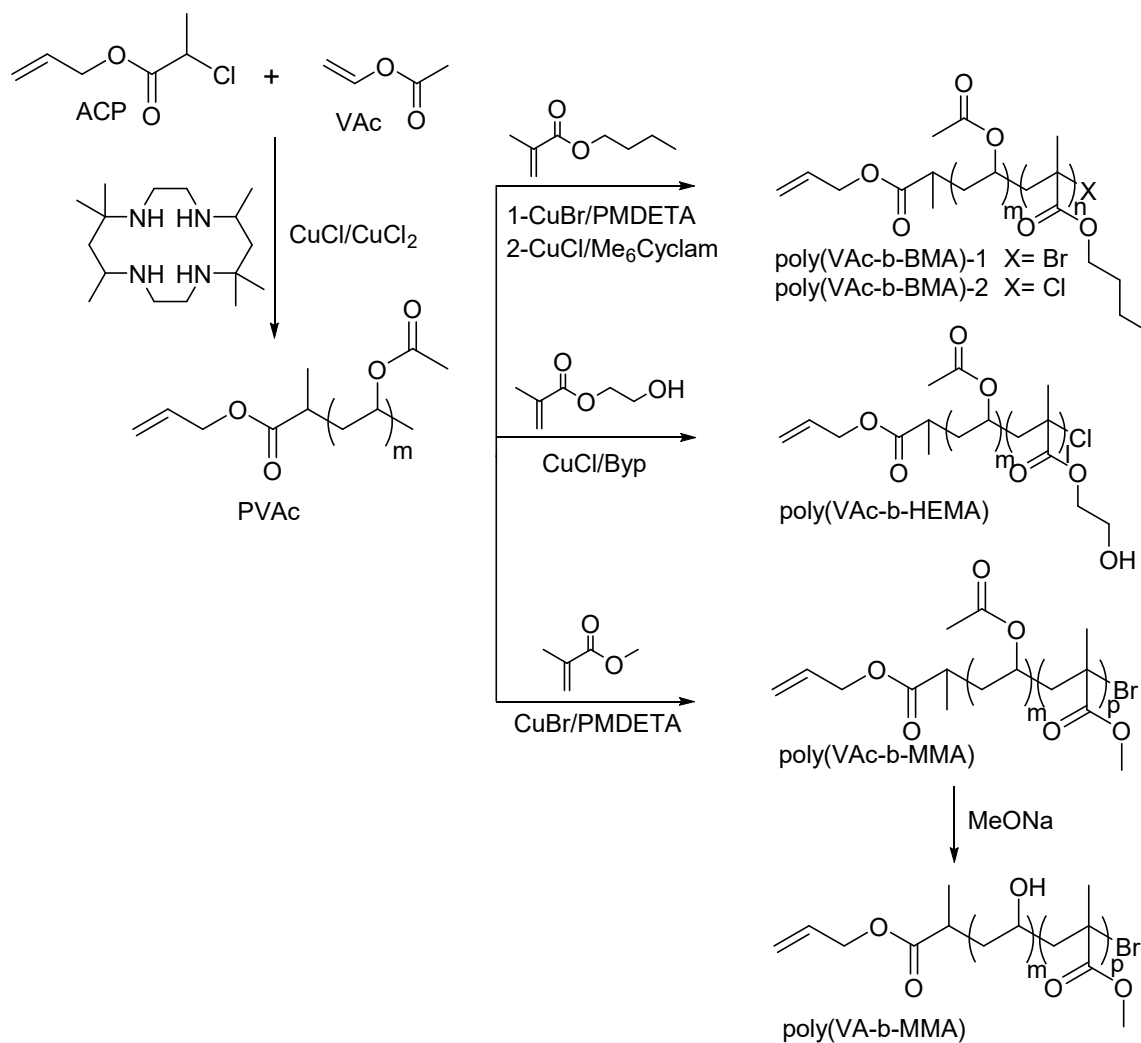
As reported in the literature, PVAc was obtained in a living and controlled way, e.g. by Cobalt-Mediated Radical Polymerization (CMRP)^{145,146} and by Reversible Addition-Fragmentation Chain Transfer (RAFT)⁶³. However, the synthesis of well-defined block copolymers using these PVAc as macroinitiators could only be achieved by an ATRP follow-up for the production of the second block^{63,145,146}. In particular, using the CMRP

method, a modification of the end-living group of PVAc macromolecules was required¹⁴⁵ while, when RAFT is applied, the opportune and specific synthesis of a convenient difunctional initiator suitable for both RAFT and ATRP⁶³ is necessary. Recently it was reported a direct living chain extension from PVAc to PMMA and PS by hybridization of CRMP and ATRP¹⁴⁶. Anyway, all these approaches need additional synthetic processes and purifications and utilize two different consecutive polymerization techniques.

Moreover, by using RAFT, being the PVAc connected to the second part of the copolymers via a hydrolyzable linkage, it cannot be converted by classical hydrolysis into PVA since the process would tear apart the two blocks. All these disadvantages could be overcome using directly ATRP for the synthesis of both copolymer blocks.

To the best of our knowledge, just one paper reports the ATRP synthesis of PVAc¹⁴³ though the process described is still far from optimized and difficult to control as demonstrated by the quite high PD (around 1.6) of the final material. In this context, the optimization of a facile synthetic route, such as ATRP, to obtain PVAc and its relative block copolymers could be of potential interest for several advanced application fields. In fact, it can also pave the way to the industrial production of block copolymers containing PVA, thus increasing applications of PVA derivatives and optimizing their use in biomedical fields, such as for cartilage replacement, in meniscal applications¹³⁸ and for the production of hydrogels¹⁴⁷. Moreover, materials containing a hydrophilic block of PVA and a hydrophobic block of another biocompatible polymer can form micelles to be used for drug delivery systems¹⁴⁸.

Thus, the present paper reports the development of an ATRP system based on the use of a very active catalytic system composed of CuCl, CuCl₂ and the ligand 5,5,7,12,12,14-hexamethyl-1,4,8,11-tetraazacyclotetradecane (Me₆CyClam) that, for the first time, is able to polymerize VAc with a good control over the process. For this aim several kinetic studies at different temperatures were carried out and the process optimized in order to obtain living PVAc with low polydispersity. To confirm the living character of the obtained macromolecules with terminal chlorine, different block copolymers were synthesized using 2-hydroxyethyl methacrylate (HEMA), butyl methacrylate (BMA) and methyl methacrylate (MMA) as *co*-monomers (Scheme 12). Furthermore, being the different blocks connected by a hydrolytically stable linkage, by methanolysis of the PVAc block we obtained amphiphilic block copolymers which can act as nanostructured materials (Scheme 12). Additionally, the thermal properties of the resultant polymers were characterized by DSC and TGA.

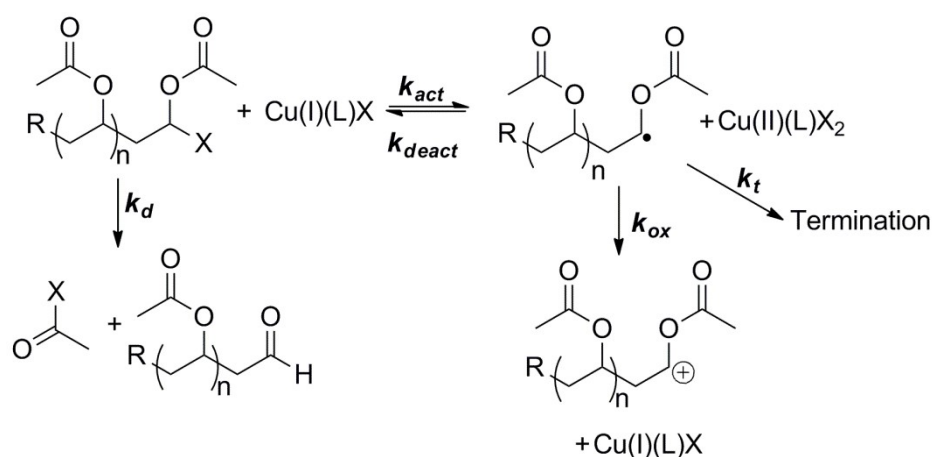


Scheme 12: ATRP synthesis of the investigated polymers.

3.2 Results and discussion

3.2.1 Kinetic polymerization studies

Common ATRP conditions have been proven not to allow the polymerization of VAc in a controlled and living way³⁷. The process, in fact, results hampered because of the high reactivity of the generated radicals that shifts the ATRP equilibrium towards the dormant species hence promoting classical termination (k_t) and side reactions³⁷, such as decomposition (k_d) of the dormant species and radicals oxidation (k_{ox}) (Scheme 13)^{114,149}.



Scheme 13: Characteristic ATRP equilibrium of VAc with some possible termination and side reactions that may occur during the polymerization.

With the aim to minimize termination reactions with respect to propagation, thus improving the control over the ATRP process, it is necessary to establish a fast and dynamic ATRP equilibrium that maintains a low concentration of propagating species once radicals are formed, according to Equation 3 and Equation 5. For this reason, we attempted the polymerization of VAc with a high monomer/initiator ratio [300:1] and in presence of a very active complex composed of $CuCl$, $CuCl_2$ and the ligand $Me_6CyClam$ ¹⁵⁰, which, as previously reported by Huang⁸⁹ allows to polymerize *N*-vinylcaprolactam, despite the presence of very reactive radical species. Huang demonstrated that, in these conditions, the use of an active ligand is able to maintain a particularly low concentration of propagating species, hence establishing a fast and dynamic ATRP equilibrium. Thus, a series of polymerizations of VAc was carried out under ATRP conditions in presence of ACP as initiator (synthesized by a novel procedure) and $CuCl$ complexed by $Me_6CyClam$ as catalyst in 1,4-dioxan/*n*-propanol 98:2 v/v as solvent at 50°C. The initial monomer concentration ($[M_0]$) was 2.70 mol/l. The occurrence of polymerization involving the

vinyl double bond was confirmed by FT-IR, showing the disappearance of the absorption at 1653 cm^{-1} , ascribed to the stretching vibration of the double bond in the monomer, and the shift of the ester-carbonyl stretching frequency from 1790 cm^{-1} in the monomer to 1729 cm^{-1} in the polymer¹²². Accordingly, in the ^1H NMR spectrum of PVAc, the resonances at 4.56, 4.87 and 7.27 ppm related to the vinyl protons of VAc monomer, are absent. Nevertheless, no control of the polymerization process could be achieved with these experimental conditions, as demonstrated by the non-linear dependence of $\ln([M_0]/[M])$ as a function of time (Figure 32). The conversion, in fact, shows no dependence on the time and the reaction does not follow a first order kinetics with respect to the monomer concentration. Such a behaviour could be ascribed to a still too high concentration of the propagating radicals which promotes terminations (see Equation 5).

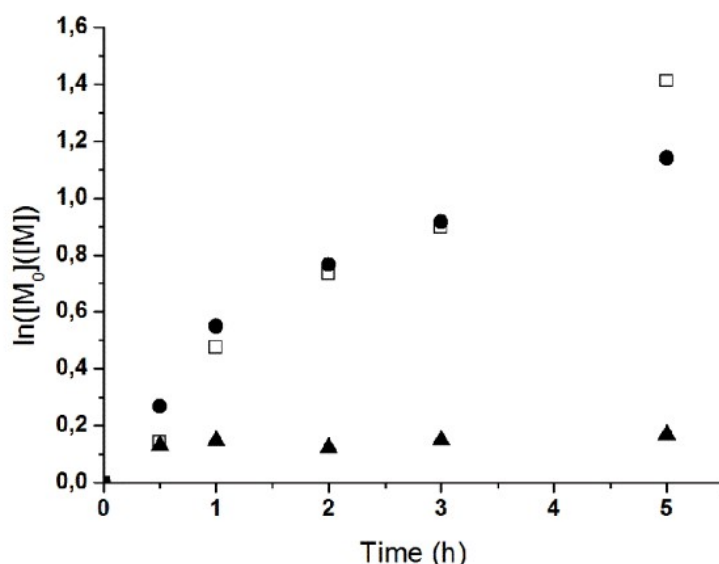


Figure 32: Kinetic plot of $\ln([M_0]/[M])$ vs time for the ATRP of VAc in 1,4-dioxan /n-propanol 98:2 v/v ($[M_0]=2.70\text{ mol/l}$) at 50°C . $[VAc]/[CuCl]/[CuCl_2]/[Me_6CyClam]/[ACP] = 300:1:0:1:1$ (▲), $300:1:0.15:1.15:1$ (□) and $300:1:0.35:1.35:1$ (●).

In order to further shift the ATRP equilibrium towards the dormant species, the polymerization was performed in the presence of different amount of CuCl_2 ($[\text{CuCl}]/[\text{CuCl}_2]=1/0.15$ and $1/0.35\text{ mol:mol}$) which, as previously reported by Matyjaszewski¹¹⁴, allows to decrease the propagating radicals concentration in the process, according to Equation 3.

As reported in Figure 1, in presence of CuCl₂ a linear dependence of ln([M]₀/[M]) with time could be observed during the first hour accounting for a first order kinetics of the polymerization rate with respect to the monomer concentration and a roughly constant concentration of the growing species throughout the process. Despite that, after one hour of reaction the control is lost. Such a behaviour cannot be ascribed to the low concentration of monomer in the solution (the final monomer conversions are just 38 and 42%, respectively), but it might be due to the occurrence of termination reactions which reduce the concentration of propagating radicals, decreasing the K_{app} value (see Table 23) and thus the polymerization rate. It is worth noting that, by increasing the Cu(II) amount, the polymerization results faster during the first hour of reaction (Figure 32 and Table 23), probably due to a lower amount of termination reactions during the initial steps (well known as persistent radical effect)¹²⁴ and thus to the higher concentration of radicals. By proceeding the polymerization (after about 1 hour), the monomer concentration decreases and termination rate becomes relevant, thus losing the process control.

Table 23: Values of K_{app} of the kinetic studies carried out at 50°C, in 1,4-dioxan /n-propanol 98:2 v/v as solvent with different amount of Cu(II). [M₀] = 2.7 mol/l. [VAc]/[CuCl]/[CuCl₂]/[Me₆CyClam]/[ACP] = 300:1:0.15(0.35):1.15(1.35):1.

| [CuCl]/[CuCl ₂] | K _{app} up to 1h (h ⁻¹) ^a | K _{app} after 1h (h ⁻¹) ^b |
|-----------------------------|---|---|
| 1/0.15 | 0.477 | 0.230 |
| 1/0.35 | 0.549 | 0.122 |

^a Determined by linear fitting of the experimental data recorded within the first reaction hour.

^b Determined by linear fitting of the experimental data recorded after the first reaction hour.

By diluting the system [from [M]₀]=2.70 mol/l to 0.98 mol/l] it is possible to maintain the control over the polymerization for a longer time, reaching a conversion of about 65, 77 and 92% using 1/0.1, 1/0.5 and 1/0.65 [CuCl]/[CuCl₂] molar ratio, respectively. As reported in Figure 33 indeed, the latter system shows a linear dependence of ln([M]₀/[M]) with time thus indicating a first-order kinetics of the polymerization rate with respect to the monomer concentration and a constant concentration of the growing species throughout the whole process.

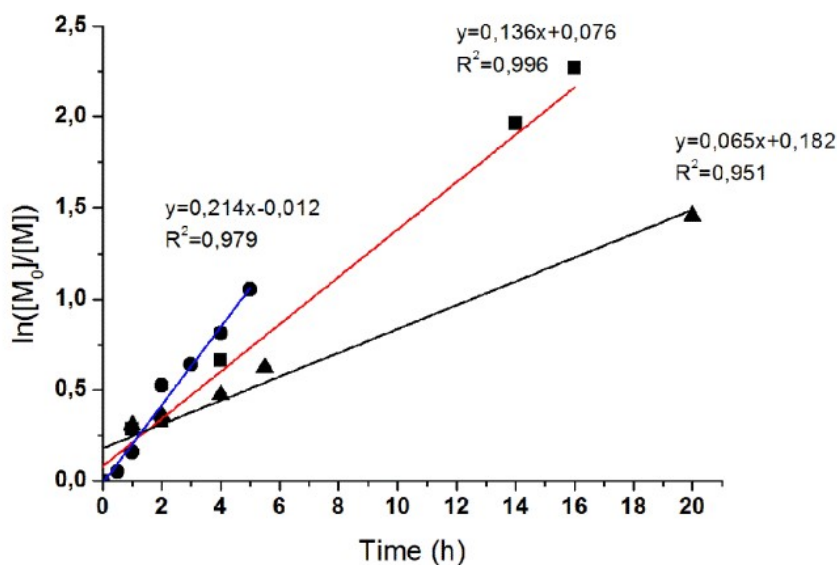


Figure 33: Kinetic plot of $\ln([M]_0/[M])$ vs time for the ATRP of VAc in 1,4-dioxan /n-propanol 98:2 v/v ($[M]_0=0.98$ mol/l), at 50°C. $[VAc]/[CuCl]/[CuCl_2]/[Me_6CyClam]/[ACP]=300:1:0.1:1.1:1$ (●), $300:1:0.5:1.5:1$ (▲) and $300:1:0.65:1.65:1$ (■).

It is worth noting that with $[CuCl]/[CuCl_2]$ molar ratio of 1/0.5, $\ln([M]_0/[M])$ increases linearly with time but, when linearly fitting the experimental data, the intercept of the obtained straight line does not pass through the origin, as expected. Such a behaviour can be explained assuming that, during the initial steps of the reaction, when the concentration of propagating radicals did not yet reach a constant and sufficiently low value to allow the control of the process, termination and propagation occur simultaneously, decreasing the rate of polymerization. Instead, in the presence of a $[CuCl]/[CuCl_2]$ molar ratio of 1/0.65 the amount of termination reactions during the initial step of the polymerization decreases and the polymerization kinetics is faster with a linear dependence of $\ln([M]_0/[M])$ with the time.

Nevertheless, although the high reactivity of the generated radicals, we demonstrated that applying convenient experimental conditions, such as the use of $CuCl_2$ and with a dilute system, it is possible to synthesize PVAc by ATRP with a good process control and high conversion. The amount of Cu(II) compared to Cu(I) is quite high but the experiments demonstrate that it is necessary to compensate the high activity of the ligand that promotes the propagating radical formation and its high reactivity.

In order to demonstrate the reproducibility of the ATRP optimized conditions of VAc polymerization, we repeated this last kinetic study at different polymerization time. The

obtained data well compare with the previously obtained ones (Figure 34), thus confirming the reliability of the process.

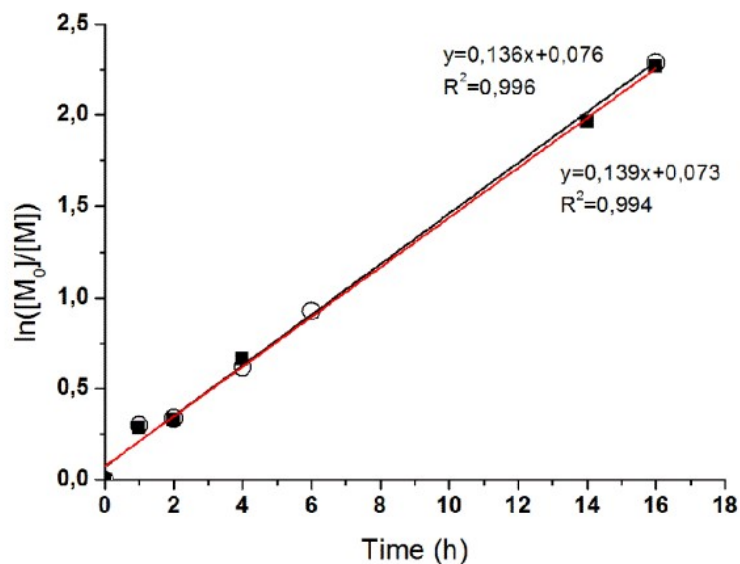


Figure 34: Comparison of two kinetic experiments reported plots of $\ln([M_0]/[M])$ vs time for the ATRP of VAc in 1,4-dioxan /n-propanol 98:2 v/v ($[M_0]=0.98$ mol/l), at 50°C. $[VAc]/[CuCl]/[CuCl_2]/[Me_6CyClam]/[ACP]=300:1:0.65:1.65:1$. Data related to filled symbols (■) are the same appearing also in Figure 33.

In Figure 35 the actual measured \bar{M}_n are compared with the theoretically expected ones, as calculated on the basis of conversion. Within the experimental values they fit nicely with the theoretically expected ones further confirming the attained good process control at least up to 90% of conversion. The polydispersity index is observed to decrease with conversion down to constant and low value (roughly 1.3) as expected on the basis of a controlled/living polymerization.

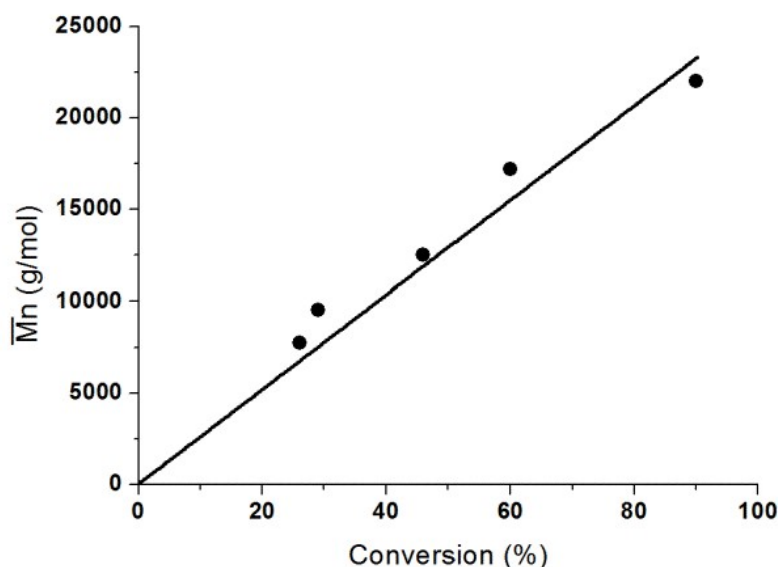


Figure 35: Experimental \bar{M}_n determined by $^1\text{H-NMR}$ vs conversion for the ATRP of VAc in 1,4-dioxan /n-propanol 98:2 v/v ($[M_0]=0.98$ mol/l), at 50°C . $[\text{VAc}]/[\text{CuCl}]/[\text{CuCl}_2]/[\text{Me}_6\text{CyClam}]/[\text{ACP}]=300:1:0.65:1.65:1$. The straight line corresponds to the theoretical expected \bar{M}_n vs conversion.

Upon raising the temperature (from 50 to 70°C), the reaction is faster (25% respect to 41% of monomer conversion reached in 1 hour at 50°C and 70°C , respectively, with all the other parameters unchanged). Unfortunately, the process is no more under control due to the higher concentration of propagating radicals thus increasing the terminating processes. Hence, in order to keep the livingness of the polymerization, a specific tuning of reaction conditions is required for each applied temperature.

3.2.2 Synthesis of block copolymers

In order to confirm the living character of the synthesized PVAc macromolecules with terminal chlorine, they were used as macroinitiators for the further polymerization of several monomers (BMA, HEMA and MMA) (Scheme 12). In particular, PVAc synthesized in conditions which allow the best control of the ATRP process $\{[M]=0.98$ mol/l, $[\text{VAc}]/[\text{CuCl}]/[\text{CuCl}_2]/[\text{Me}_6\text{CyClam}]/[\text{ACP}]=300/1/0.65/1.65/1$, at 50°C in 1,4-dioxan /n-propanol 98:2 v/v}, was fully characterized (Figure 36) in order to allow a further comparison of the starting macroinitiator PVAc properties with those of the resulting block-copolymers. As shown in Figure 36, $^1\text{H-NMR}$ spectrum of PVAc displays the resonances of the allyl protons of the ACP initiator residue at 4.68 ppm (2H, $\text{CH}_2=\text{CH}-$

CH₂-O) and 5.93 ppm (1H, CH₂=CH-CH₂-O) together with the one of the CH-Cl end-group at 6.41 ppm.

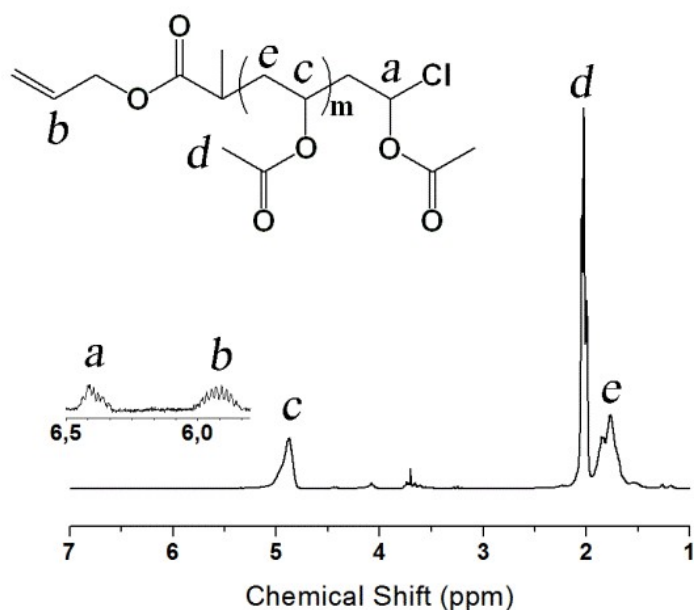


Figure 36: ¹H-NMR of PVAc macroinitiator.

Thus, the identification of both the chain end moieties allowed, by comparing the integral of the allyl NMR signals with respect to those of VAc group, to precisely assess the number average molecular weight \bar{M}_n (Table 26 in the experimental section) which could appear to be in disagreement with those ones determined by SEC. This discrepancy may be attributed to the use of monodispersed polystyrene and PEG standards for SEC calibration, which are both unsuitable for an accurate determination of samples having a very different hydrodynamic volume, though can still provide good comparative data.

Moreover, SEC is able to provide the polydispersity (PD) of the analyzed samples, and the obtained values (Table 26 in the experimental section) are very low considering the high reactivity of the monomer and, to the best of our knowledge, they are among the lowest obtained by ATRP of VAc¹⁴³ thus confirming that a good process control was reached.

The further ATRP copolymerizations of MMA and BMA in presence of PVAc as macroinitiator were performed in mild conditions (CuBr/PMDETA as catalytic system). The polymerization of HEMA was performed with CuCl/Byp as catalytic system in 2-butanone /n-propanol (7:3 v/v) (Scheme 12).

The occurrence of the polymerization was confirmed, in all cases, by $^1\text{H-NMR}$ analysis which displays, besides the already discussed signals of PVAc, the ones of the second block. As an example, the spectrum of PVAc-*b*-PHEMA (Figure 37) shows the resonances at 3.59 and 3.90 ppm related to the O-CH₂-CH₂-O of HEMA.

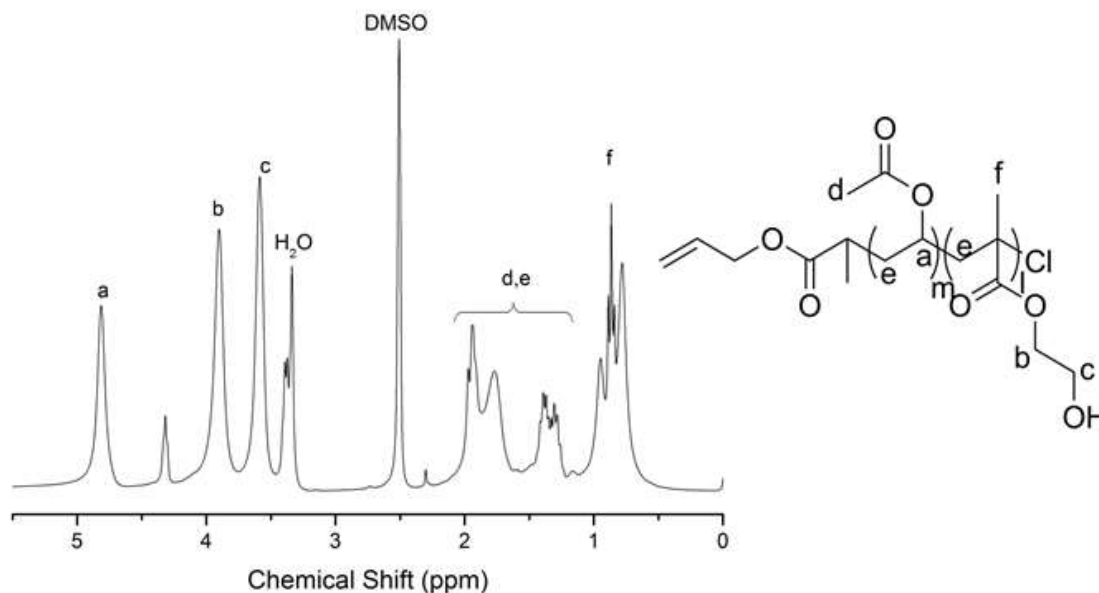


Figure 37: $^1\text{H-NMR}$ of PVAc-*b*-PHEMA.

For the synthesis of block copolymers by ATRP the reactivity of the macroinitiator should be higher than ATRP reactivity of the growing/dormant methacrylate chain ends. Despite the lower reactivity of the CH-Cl living group of PVAc compared to the ones of PBMA, PHEMA and PMMA, we obtained block copolymers with well-defined structure and low polydispersity, thus proving the living character of PVAc macromolecules.

$^1\text{H-NMR}$ analysis allowed also to determine the second monomer conversion and the molar composition for each synthesized copolymers, which are reported in Table 26. The obtained conversion data allowed to compare the polymerization performance of each applied system. In particular, given the same monomer to initiator molar ratio ($[\text{M}]/[\text{I}] = 200/1$), the use of PMDETA/CuCl as catalytic system allows to reach higher monomer conversions with respect to Me₆Cyclam/CuBr within the same timespan (58% and 46% for PVAc-*b*-PBMA-1 and -2, respectively), resulting in a faster reaction. Indeed, despite PMDETA is known to establish an ATRP equilibrium more shifted towards the dormant species with respect to Me₆Cyclam¹⁴, its combination with the very active catalyst CuBr and the higher temperature applied (90°C vs. 25°C) lead to an enhancement of the

polymerization rate. Furthermore, the data reported in Table 26 display a further increasing of the monomer conversion by passing from PVAc-*b*-PBMA-1 to PVAc-*b*-PMMA (whose spectra are shown in Figure 38 and Figure 39 respectively), maintaining all the other parameters unchanged. Such a behaviour could be explained considering the different hindrance of BMA with respect to MMA. The data obtained for PVAc-*b*-PHEMA cannot be compared with the other ones because of the different monomer/initiator ratio used during the synthesis ($[M]/[I] = 400/1$).

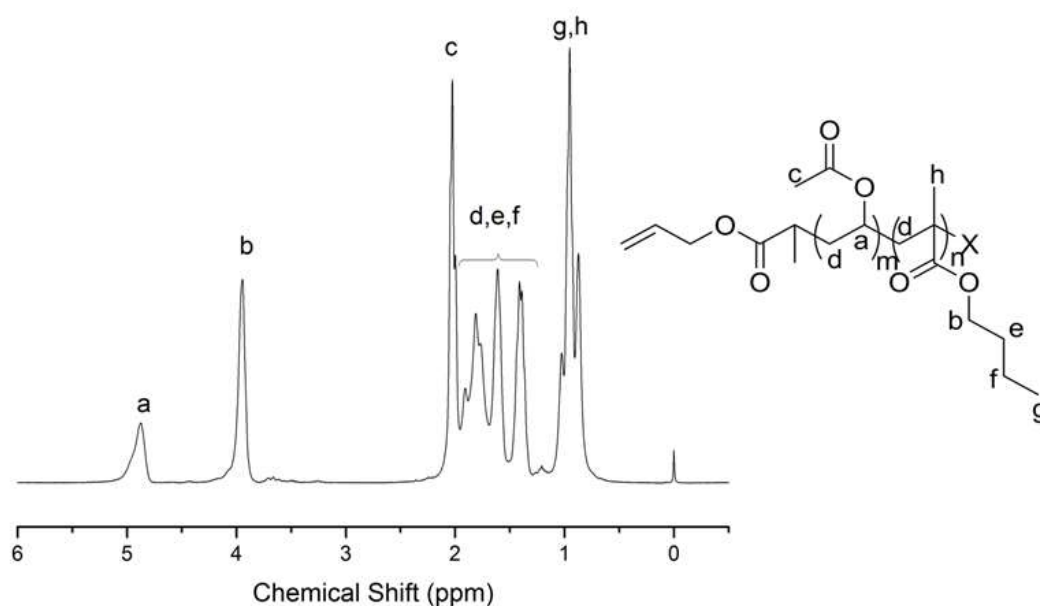


Figure 38: $^1\text{H-NMR}$ of PVAc-*b*-PBMA-1.

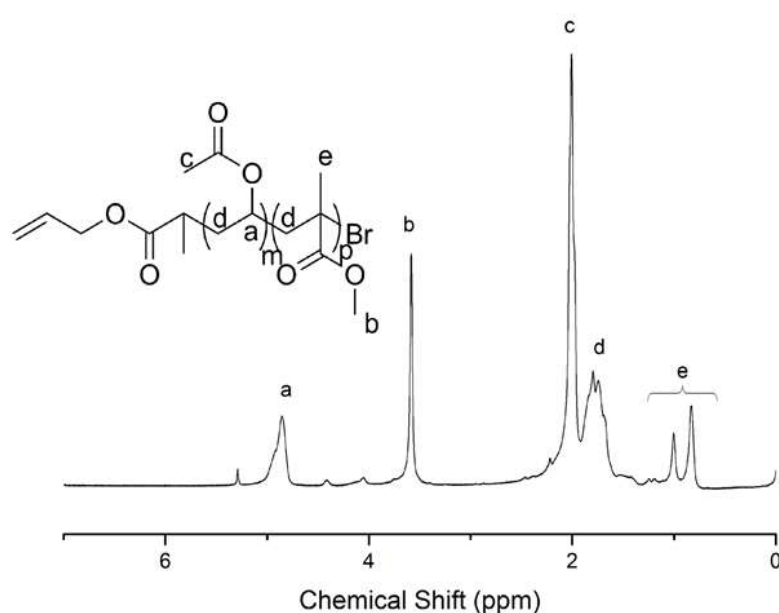


Figure 39: $^1\text{H-NMR}$ of PVAc-*b*-PMMA.

Although the values of average molecular weight obtained by SEC and by $^1\text{H-NMR}$ (Table 26 in the experimental section) do not agree, they show the same trend, confirming the increase of \bar{M}_n when passing from the macroinitiator to the block copolymers. Furthermore, the low polydispersity of all the synthesized copolymers ($\text{PD} < 1.4$) and the absence of shoulders in the chromatograms (Figure 40), confirm the living character of the polymerization and the attained process control that lacks of coupling reactions also during the synthesis of the second block.

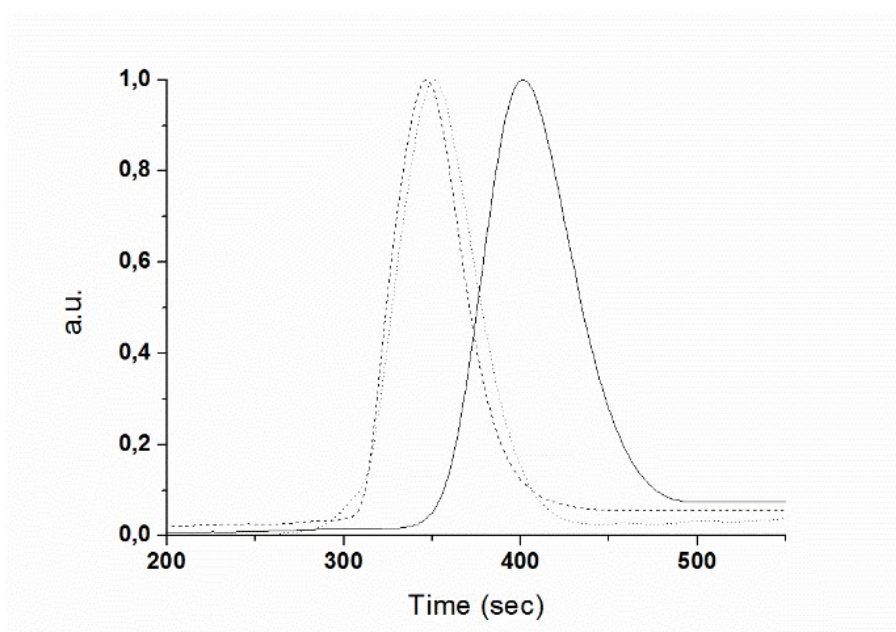


Figure 40: Normalized molecular weight distributions of the synthesized PVAc, PVAc-*b*-PMMA and PVA-*b*-PMMA as determined by SEC in DMF at 70°C.

Hence, the reported experiments demonstrate the possibility to synthesize well defined block copolymers by a two-step pathway by using specific catalytic systems tailored for each of them.

Furthermore, the possibility to use the same catalytic system (CuCl/Me₆Cyclam) and reaction condition both in the synthesis of PVAc macroinitiator and BMA additional block was successfully investigated. This outcome results particularly interesting for industrial applications, because it demonstrates that it is possible to synthesize the PVAc-*b*-PBMA block copolymer simply adding a fresh and degassed solution of BMA at the end of the polymerization of VAc, without any intermediate purification.

Furthermore, with the aim to obtain an amphiphilic block copolymer, PVAc-*b*-PMMA was fully hydrolysed by sodium methoxide as previously described¹⁵¹ obtaining PVA-*b*-

PMMA (Table 26 in the experimental section and Scheme 12). The occurred methanolysis was confirmed by the $^1\text{H-NMR}$ analysis which shows the absence of the signal at 5.25-4.80 and 2.25-1.50 ppm related to the CH-OCO and C-(O)-CH₃ of PVAc respectively, and the presence of the signals at 4.71-4.13 ppm related to the hydroxylic groups of vinyl alcohol repeating units¹⁵² hence reasonably assuming that the hydrolytic cleavage was taken to completion. The $^1\text{H-NMR}$ spectra of PVA-*b*-PMMA is shown in Figure 41.

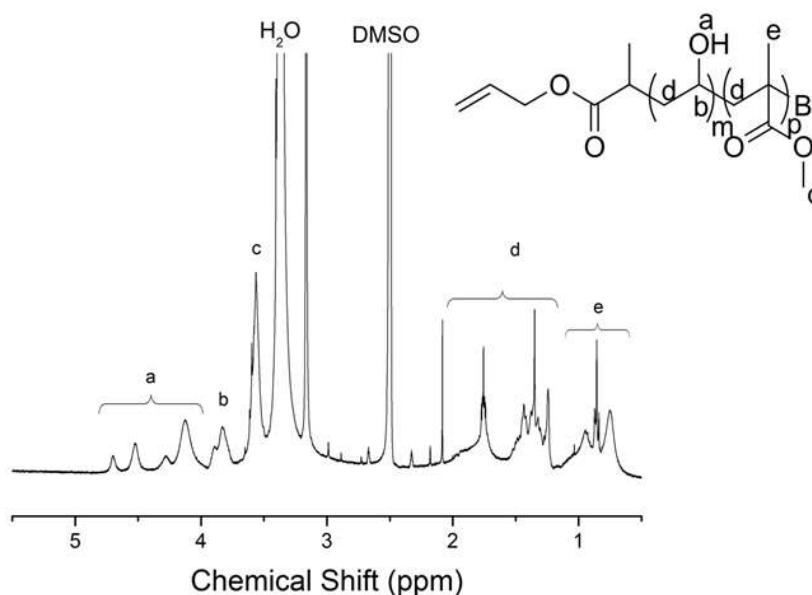


Figure 41: $^1\text{H-NMR}$ of PVA-*b*-PMMA.

The occurred methanolysis was also confirmed by IR. As can be seen from Figure 42, where the IR spectra of PVAc-*b*-PMMA and PVA-*b*-PMMA are compared, after methanolysis the IR spectra show the signal ascribable to OH stretching at 3412 cm^{-1} and the signal at 1725 cm^{-1} has lower intensity compared to the one in PVAc-*b*-PMMA because after hydrolysis only the C=O stretching of PMMA can be detected.

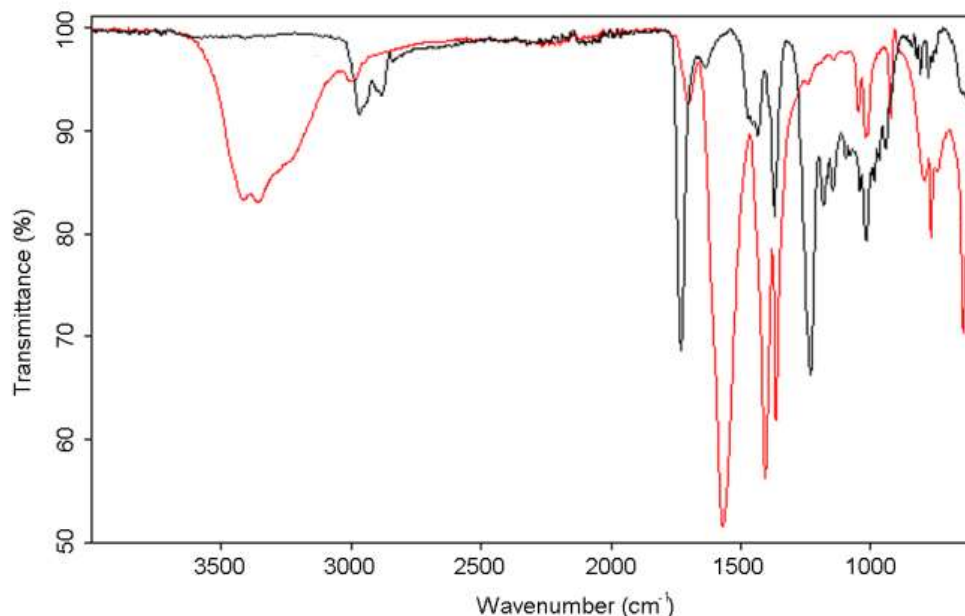


Figure 42: FT-IR spectra of PVAc-*b*-PMMA (—) and PVA-*b*-PMMA (—).

The methanolysis of the PVAc-*co*-PMMA to PVA-*b*-PMMA should lead to macromolecules with an amphiphilic character, hence able to self-organize in micelles in a convenient solvent. With the aim to detect the existence of such self-assembled structures, the behavior of PVA-*b*-PMMA in water was investigated by DLS, displaying the presence of aggregates. The number size distributions of nano-objects forming in PVA-*b*-PMMA water solutions at three different concentrations reported in Figure 43 confirm the formation of polymeric self-assemblies composed of hydrophobic core related to block of PMMA stabilized by a hydrophilic corona related to block of PVA, with a uni-modal distribution and with size increasing from 60 nm to 160 nm with the polymer concentration.

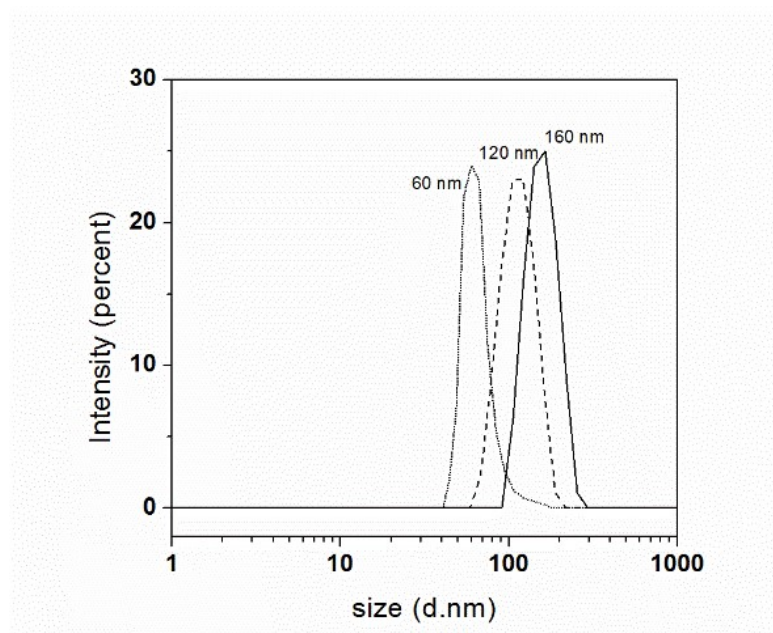


Figure 43: DLS intensity size distribution of PVA-*b*-PMMA in water solutions at different concentrations: 0.312 mg/ml (—), 0.156 mg/ml (---) and 0.078 mg/ml (···).

3.2.3 Thermal characterization

The PVAc macroinitiator and its block copolymers were analysed in order to assess their thermal behaviour.

The thermal stability of the investigated polymers was studied using thermogravimetric analysis (TGA). TGA traces of the copolymers are displayed in Figure 44 together with that of the starting PVAc macroinitiator and the obtained data are reported in Table 24. PVAc macroinitiator is stable up to roughly 300°C, then shows a double stepwise degradation pattern with a first weight loss up to 400°C corresponding to 70.2% wt. of the initial weight (named *Weight loss 2* in Table 24) and the second one centred at 450°C where the sample loses 19.5% of its weight. The first degradation is consistent with acetic acid elimination¹²⁹ and indeed acetic acid's molecular weight makes up 69.8% wt. of the VAc repeating unit in the polymer. The second weight loss corresponds to the polymer backbone degradation¹²⁹. The solid residue observed at the end of the run might be attributed to the formation of a char residue owing to the lack of the stoichiometric oxygen required for the total oxidation and volatilization of the carbon-based polymeric backbone, once the acetic acid has been released.

Table 24: Composition and TGA weight loss during the thermal degradation of the block copolymers compared with the one of the macroinitiator PVAc.

| Sample | VAc block weight fraction ^a (%) | Methacrylic block weight fraction (%) | T _{max deg.1} (°C) | Weight loss 1 (%) | T _{max deg.2} (°C) | Weight loss 2 (%) |
|------------------------|--|---------------------------------------|-----------------------------|-------------------|-----------------------------|-------------------|
| PVAc | 100 (70) | - | | | 329 | 30 |
| PVAc- <i>b</i> -PHEMA | 27 (19) | 73 | 256 | 10 | 318 | 32 |
| PVAc- <i>b</i> -PBMA-1 | 36 (25) | 64 | 198 | 7 | 335 | 46 |
| PVAc- <i>b</i> -PBMA-2 | 42 (29) | 58 | 231 | 4 | 333 | 38 |
| PVAc- <i>b</i> -PMMA | 34 (24) | 66 | 214 | 9 | 318 | 38 |
| PVA- <i>b</i> -PMMA | 18 | 82 | 227 | 3 | 338 | 57 |

^a Determined by ¹H-NMR. The number in brackets represents the actual acetic acid weight fraction in the polymer calculated from the stoichiometry of the VAc repeating unit.

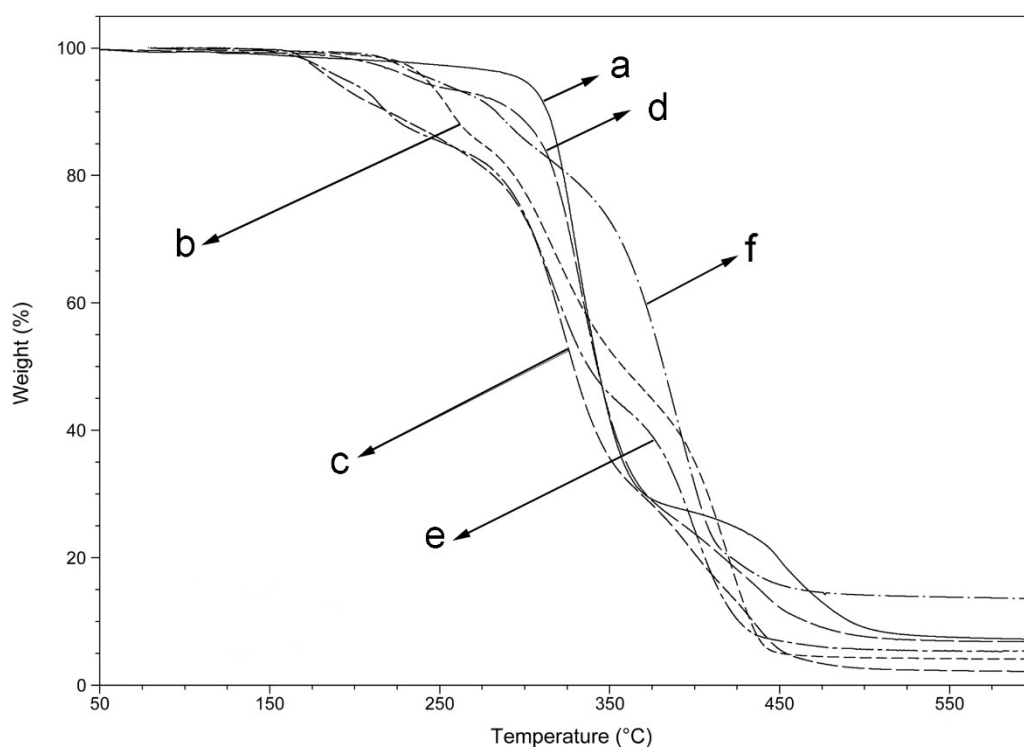


Figure 44: TGA curves of the synthesized samples: a) PVAc; b) PVAc-*b*-PHEMA; c) PVAc-*b*-PBMA-1; d) PVAc-*b*-PBMA-2; e) PVAc-*b*-PMMA; f) PVA-*b*-PMMA.

When the PVAc fragment is used to obtain block copolymers, its degradation pattern is expected to be found in the TGA traces of the corresponding copolymer together with the additional features deriving from the second added block. Indeed, the TGA curve of the copolymer with PHEMA displays, a 6.6% weight loss during a degradation process centred

at 256°C (labelled *Weight loss 1* in Table 24) that is not present in the PVAc thermograms and, according to the literature¹³⁰, is attributed to the depolymerisation of the PHEMA block. During a second degradation centred at 318°C (named *Weight loss 2* in Table 24) the polymer loses 60.0% of its weight: this temperature range well compares with the position of the previously discussed acetic acid elimination though the entity of the loss is greater than expected based solely on the VAc unit content (19% w/w). Worth noting is that the depolymerisation of PHEMA block during the low temperature decomposition is incomplete hence, based on literature reports, the additional mass loss can be safely attributed to the decomposition reactions of the ester side chain in PHEMA that is still present after the initial depolymerisation^{129,130}. The last degradation step, occurring between 400 and 550°C, can be once again ascribed to the degradation of the aliphatic polymer backbone.

All the methacrylic co-units containing copolymers show a degradation pattern similar to that previously discussed for PVAc-*b*-PHEMA and both *Weight loss 1* and *Weight loss 2* registered for all the copolymers are reported in Table 24. The literature reports a low temperature (150-250°C) depolymerisation phenomenon for PBMA¹³² too and, in agreement with the composition determined by NMR, the compound with a higher BMA fraction displays a more intense *Weight loss 1*, because of the higher amount of volatile monomer produced. During *Weight loss 2* the evolution of acetic acid from PVAc and the degradation of the ester side chain moiety of PBMA occur simultaneously^{129,132}, with the loss extent which is now higher, the higher the fraction of VAc. The last degradation step corresponds once again to the degradation of the polymer backbone.

The described mechanism of degradation was confirmed by the FT-IR analysis of the gases evolved during the thermal degradation of the samples. As an example, in Figure 45 FT-IR spectra of the volatile degradation products obtained at different temperatures during the TGA of PVAc-*b*-PBMA-1 are displayed; these spectra are representative of the gas evolved along the whole degradation process and are taken at $T_{\max \text{ deg } 1}$ and $T_{\max \text{ deg } 2}$ respectively, i.e. at 198°C (a) and 335°C (b), in order to maximize the concentration of the evolved species.

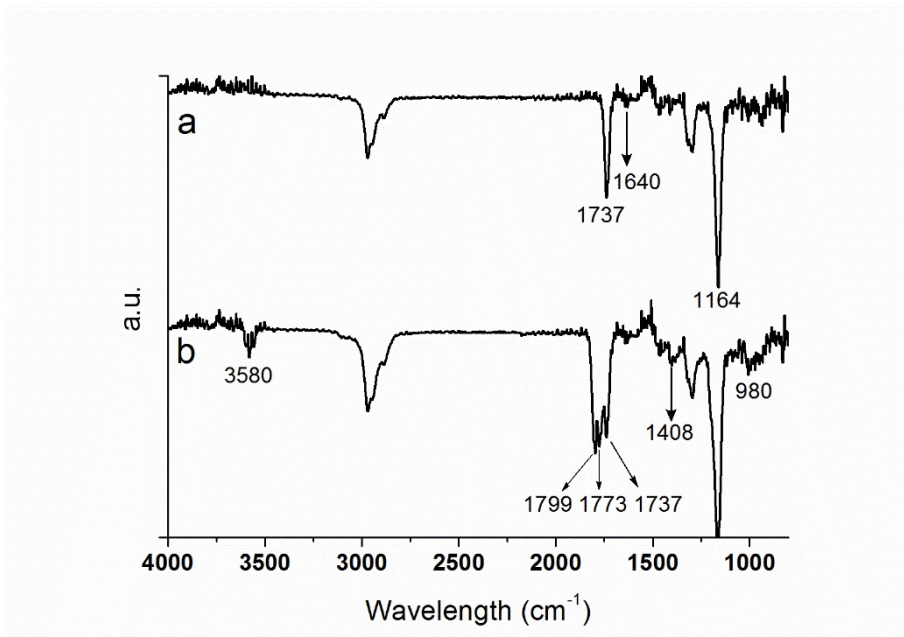


Figure 45: FT-IR spectra of the gases evolved during Weight loss 1 (a) and Weight loss 2 (b) of PVAc-*b*-PBMA-1. Spectra are representative of the gases evolved along the whole degradation process and are taken at $T_{\max \text{ deg } 1}$ and $T_{\max \text{ deg } 2}$, respectively.

During the degradation centred at 198°C (*Weight loss 1*) the previously cited depolymerisation mechanism is confirmed by the presence of C=C stretching signal at 1640 cm^{-1} , ascribed to the methacrylic double bond from the BMA monomer; the other absorptions well compares with the expected butyl methacrylate structure, such as the ones at 1737 and 1164 cm^{-1} related to C=O stretching and C-O bending respectively. During the degradation centred at 335°C (*Weight loss 2*) the evolution of acetic acid in gas phase is confirmed by the presence of O-H stretching and bending (in and out of plane) absorptions centered at 3580, 1408 and 980 cm^{-1} respectively and by the presence of C=O stretching signal in the region 1799-1780 cm^{-1} ¹⁵³. During this high temperature degradation, the signals of C=C and C=O, seen during *Weight loss 1*, are still present, thus confirming that depolymerisation occurs simultaneously with acetic acid formation. The presence of the characteristic asymmetric stretching signal of carbon dioxide at 2350 cm^{-1} and the presence of three C=O stretching around 1700-1800 cm^{-1} highlight the presence of other degradation compounds in the gases evolved during high temperature degradation that can be associated to ester side chain and polymer backbone degradation products. All the spectra (not shown) recorded for the other copolymers along the TGA run well compare with the spectra recorded and discussed for PVAc-*b*-PBMA-1.

As previously stated, the thermal degradation of PVAc-*b*-PMMA behaves analogously to the previously discussed methacrylic copolymers (Figure 44 and Table 24). The

corresponding hydrolyzed copolymers PVA-*b*-PMMA, instead, shows a different degradation pattern: first of all, PVA-*b*-PMMA early initial degradation (*Weight loss 1*) is not only ascribed to depolymerisation of PMMA but also to the dehydration phenomenon that is prone to occur in the PVA block upon heating¹⁵⁴. The process continues with the degradation of the polymer backbone residue, with no trace of the weight loss corresponding to acetic acid elimination, according to a complete hydrolysis of VAc units prior to the TGA run.

The chain mobility and phase behaviour of the (co)polymers were investigated by DSC and the obtained data for all the analyzed polymers are summarized in Table 25.

Table 25: T_g , ΔC_p , T_m and ΔH determined by DSC of the synthesized polymeric derivatives.

| Sample | T_g first block PVAc (°C) [ΔC_p (J/g °C)] | T_g second block (°C) [ΔC_p (J/g °C)] | T_m (°C) [ΔH (J/g)] |
|------------------------|---|---|-----------------------------------|
| PVAc | 27 [0.51] | - | - |
| PVAc- <i>b</i> -PHEMA | 33 [0.26] | 122 [0.39] | - |
| PVAc- <i>b</i> -PBMA-1 | 30 [0.25] | - | - |
| PVAc- <i>b</i> -PBMA-2 | 31 [0.28] | - | - |
| PVAc- <i>b</i> -PMMA | - | 94 [0.31] | - |
| PVA- <i>b</i> -PMMA | - | 122 [0.30] | 209 [0.68] |

All the (co)polymers display at least a stepwise specific heat increment, and the number, position and intensity of the observed transitions vary depending on the macromolecule's composition. More than one stepwise transition, or additional endotherms, can be indeed observed for some samples, as reported in Table 25 and further discussed.

The starting PVAc homopolymer shows a single stepwise transition, ascribed to the glass transition (T_g), located at 26°C. No sign of endotherms can be observed accounting for the lack of any crystal phase.

PVAc-*b*-PHEMA shows two T_g , the first at 33°C and the second at 122°C. The first T_g well compares with the PVAc one previously discussed and is thus ascribed to the PVAc block¹⁵⁵. This attribution is also confirmed by the lowered ΔC_p value that accounts for a

decrease in the overall fraction of material undergoing this transition in the block copolymer. The second one, instead, is consequently assigned to the PHEMA block in agreement with literature data¹⁵⁶. The slight increase in the PVAc block T_g is due to the addition of a second rigid block covalently bound at one side of PVAc macromolecules, that makes the overall macromolecular structure more rigid.

The copolymers PVAc-*b*-PBMA show only one stepwise signal in the DSC thermogram, and the reason may be the closeness of the two blocks independent glass transitions, with the PBMA homopolymer that is known from the literature to have a T_g close to 20°C¹⁵⁷. However, the ΔC_p value observed for the T_g seems to be coherent with the observed transition being attributed to the PVAc block, since the specific heat variation is almost halved with respect to the homopolymer PVAc and ΔC_p value increase with increase the fraction of the PVAc block. The glass transition of PVAc occurs in a temperature range of 9°C whilst in PVAc-*b*-PBMA copolymers, the overlay of PVAc and PBMA glass transition widens slightly the glass transition temperature range (11°C) in both the copolymers. The copolymer PVAc-*b*-PMMA shows only one T_g at 94°C which, according to the literature, is related to PMMA block¹⁵⁸. The DSC scan highlights that hydrolysing PVAc block to PVA the T_g of PMMA increases from 94°C up to 122°C because of the change in the polymer structure, and the PVA block, which is partially crystalline, melts at 209°C. The heat of fusion (0.68 J/g) is lower compared to what expected from the homopolymer of PVA (>10 J/g)¹⁵⁹ since that the presence of a second non-crystalline block interferes with the ability to crystallize of the PVA fraction lowering its ability to crystallize in the block copolymer.

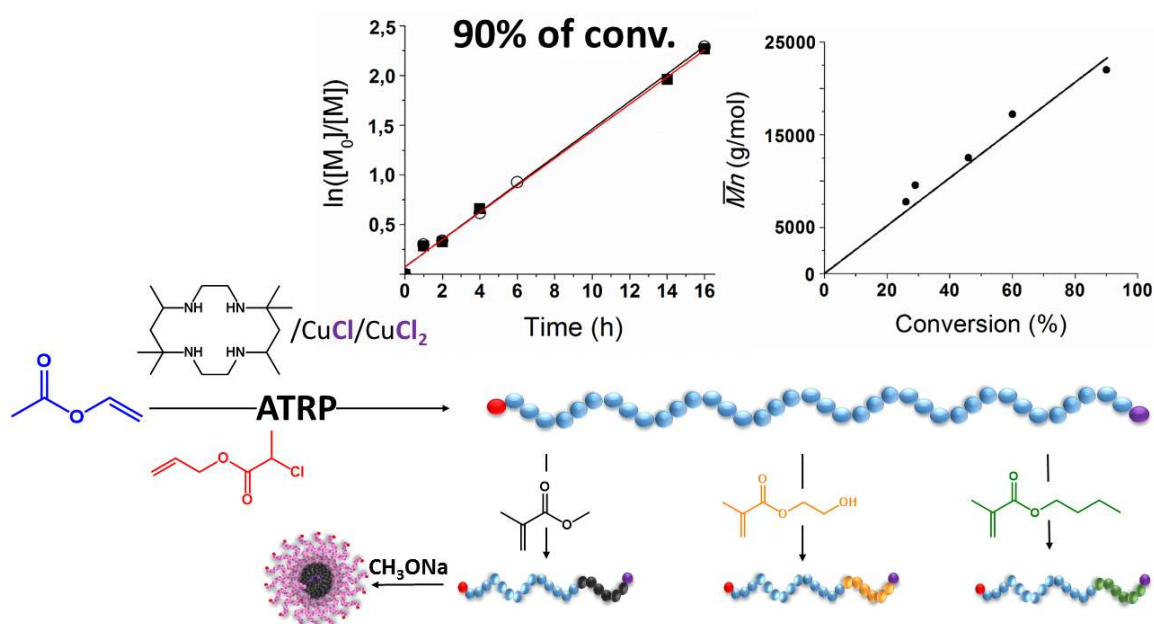
3.3 Conclusions

Optimized and facile ATRP method was successfully employed for the first time to polymerization of VAc attaining a good control over the living process up to 90% of monomer conversion. This result was allowed by using a very active catalytic system composed of CuCl, CuCl₂ and Me₆CyClam which allows to maintain a particularly low concentration of propagating species once radicals are formed, hence establishing a fast and dynamic ATRP equilibrium.

The synthesized narrowly polydispersed PVAc was used as macroinitiator for the further ATRP of several methacrylic monomers (BMA, MMA and HEMA), obtaining block copolymers with uni-modal molecular weights distributions and confirming the livingness of the system. Furthermore, by the methanolysis of PVAc-*b*-PMMA, it was possible to obtain an amphiphilic block copolymer, which, in water solution, arranges in micelles with a volume that depends on the polymer concentration.

In particular, this synthetic system paves the way to an easy industrially scalable process for the production of well-defined PVA based complex structures that may find a number of interesting applications such as in drug delivery systems or in biomedical devices.

A schematic representation of the obtained results is shown in Scheme 14.



Scheme 14.: Schematic representation of the obtained results.

3.4 Experimental section

3.4.1 Physico-chemical characterization

¹H-NMR spectra were obtained at room temperature, on 5-10% w/v CDCl₃ or DMSO solutions, using a Varian MercuryPlus VX 400 (¹H, 399.9; ¹³C, 100.6 MHz) spectrometer. Chemical shifts are given in ppm from tetramethylsilane (TMS) as the internal reference.

FT-IR spectra were recorded on a Bruker Alpha Platinum-ATR spectrophotometer equipped with ATR Diamond window.

Number average molecular weight of the polymers (\overline{M}_n) and their polydispersity index ($PD = \overline{M}_w/\overline{M}_n$) were determined in THF or DMF solutions at 25 and 70°C respectively by SEC using an HPLC Lab Flow 2000 apparatus equipped with an injector Rheodyne 7725i, a Phenomenex Phenogel 5-micron MXL and MXM columns (THF solutions, monodispersed polystyrene standards 800-35000 and 13300-214000 Da, respectively) or a Tosoh Bioscience TSKgel GMH_{HR}-N 5-micron column (DMF solutions, monodisperse poly(ethylene glycol) standards 400-20000 Da), and a refractive index detector model Knauer RI K-2301.

The glass transition temperature values (T_g) of polymers were determined by differential scanning calorimetry (DSC) on a TA Instrument DSC Q2000 Modulated apparatus adopting a temperature program consisting of three heating and two cooling ramps starting from room temperature (heating/cooling rate 20°C/min under nitrogen atmosphere) on 5-10 mg samples. Thermogravimetric (TGA) measurements were carried out using a TA Instrument SDT Q600 (heating rate 20°C/min) on 10-20 mg samples under nitrogen atmosphere with a 100 ml/min gas flow rate. $T_{\max\text{-deg}}$ is the temperature of maximum weight loss rate determined as the peak temperature from the first derivative curve of the weight loss profile. The gases evolved during TGA were guided towards an heated gas cell into a FT-IR spectrophotometer Varian Cary 660 via an heated transfer line for the *in situ* time-resolved analysis of the gas components. Both the transfer line and the gas cell were kept at 280°C and the gas channelled into the spectrophotometer is taken at a flow rate of 70ml/min.

The hydrodynamic radii of micelles were determined by dynamic light scattering (DLS) using a Malvern Zetasizer Nano ZS equipped with a 173° backscatter detector and a He-Ne laser (633nm). The solutions were placed into poly(styrene) 4 optical faces cuvettes with 1 cm optical path. The solutions were prepared by successive dilution of a 0.312

mg/ml starting solution of the polymer in water. The solutions were prepared and filtered (45 μm filter) one day before the DLS analysis in order to allow the micelles formation.

3.4.2 Materials

Vinyl acetate (VAc) (Sigma-Aldrich, >99%), butyl methacrylate (BMA) (Sigma-Aldrich, 99%) and methyl methacrylate (MMA) (Sigma-Aldrich, 99%) were distilled under reduced pressure in the presence of traces of 2,6-di-*tert*-butyl-*p*-cresol as polymerization inhibitor just before use. 2-Hydroxyethyl methacrylate (HEMA) (Sigma-Aldrich, 97%) and 2-chloropropionyl chloride (Sigma-Aldrich, 97%) were eluted through a column filled with neutral alumina to remove the inhibitor. 1,4-Dioxane was distilled over potassium in presence of benzophenone. CuCl (Sigma-Aldrich, >99%) and CuBr (Sigma-Aldrich, $\geq 98\%$) were washed with glacial acetic acid (three times) and diethyl ether and then dried under vacuum. 5,5,7,12,12,14-Hexamethyl-1,4,8,11-tetraazacyclotetradecane (Me₆CyClam) was synthesized as previously reported¹³⁶.

Dichloromethane (DCM) was distilled over P₂O₅ just before use. Pentamethyldiethylenetriamine (PMDETA) (Sigma-Aldrich, $\geq 98\%$), CuCl₂ (Sigma-Aldrich, 99%), allyl alcohol (Sigma-Aldrich, $\geq 98.5\%$), 2,2'-bipyridyl (byp) (Sigma-Aldrich, $\geq 98\%$) and others solvents (Aldrich) were used as received without further purification.

3.4.3 Synthesis of allyl 2-chloropropionate (ACP)

A solution of 2-chloropropionyl chloride (9.7 ml, 12.7 g, 0.1 mol) in dry CH₂Cl₂ (50 ml) was added dropwise to an ice-cooled stirred solution of allyl alcohol (6.8 ml, 5.8 g, 0.1 mol) and triethylamine (13.9 ml, 10.1 g, 0.1 mol) in 40 ml of dry CH₂Cl₂. The mixture was stirred for 2 hours, then left at room temperature for 24 hours. At the end of the reaction the triethylammonium chloride by-product was filtered off and the resulting solution was concentrated under reduced pressure. The organic solution was then washed with 0.1 M HCl, 0.1 M NaOH and finally with water in that order. The organic layer was dried (Na₂SO₄) and the solvent was removed under reduced pressure. The obtained yellow, transparent liquid was purified by distillation under reduced pressure (T_{eb}. 44°C, 7 mmHg). 80% yield.

¹H-NMR (400 MHz, CDCl₃, δ, ppm): 5.93 (m, J = 6.8 Hz, 1H; CH=), 5.40-5.27 (2m, 2H, CH₂=) 4.68 (d, J=5.7 Hz, 2H; CH₂O), 4.43 (q, J = 7.0 Hz, 1H; CH(CH₃)(Cl)), 1.71 (d, J = 7.0 Hz, 3H; CH₃).

3.4.4 Kinetic studies of the PVAc homopolymerization

All polymerization reactions of VAc were carried out in glass vials using ACP as initiator, Me₆Cyclam as ligand and dry 1,4-dioxan/n-propanol 98:2 v/v as solvent at 50°C.

In a general procedure, CuCl, CuCl₂, vinyl acetate and ACP in the desired proportions were added to dry 1,4-dioxan/n-propanol 98:2 ([M₀] = 2.70 or 0.98 mol/l) and the solution was introduced into the vial under nitrogen atmosphere. The reaction mixture was submitted to several freeze-thaw cycles, heated at 50°C and a solution of Me₆Cyclam in 1,4-dioxane was added using a gastight syringe even under nitrogen atmosphere. The reactions were stopped after different times immersing the vials into liquid nitrogen and a sample was withdrawn via gastight syringe for ¹H-NMR analysis with the aim to estimate the monomer conversion vs polymerization time. The obtained polymers were purified by filtration on basic aluminium oxide followed by repeated precipitation in hexane. The materials were finally dried under vacuum until constant weight. All the polymeric products were characterized by FT-IR, SEC and ¹H-NMR.

3.4.5 Synthesis of the optimized PVAc macroinitiator

The ATRP of VAc was carried out in a glass vial using ACP as initiator, Me₆Cyclam as ligand and dry 1,4-dioxan/n-propanol 98:2 v/v as solvent. [M₀] = 0.98 mol/l; initial molar ratios [VAc]/[CuCl]/[CuCl₂]/[Me₆CyClam]/[ACP] = 300/1/0.65/1.65/1.

CuCl, CuCl₂, VAc and ACP were added to dry 1,4-dioxan/n-propanol 98:2 and the solution was introduced into the vial under nitrogen atmosphere. The reaction mixture was submitted to several freeze-thaw cycles, heated at 50°C and a solution of Me₆Cyclam in 1,4-dioxane was added using a gastight syringe even under nitrogen atmosphere. The reaction was stopped after 85 minutes immersing the vial into liquid nitrogen and a sample was withdrawn via gastight syringe for ¹H-NMR analysis. The polymer was purified by filtration on basic aluminium oxide followed by repeated precipitation in hexane. The material was finally dried under vacuum until constant weight. The conversion was determined gravimetrically and the product characterized by FT-IR, SEC, DSC, TGA and

¹H-NMR. Relevant data concerning the obtained PVAc macroinitiator are reported in Table 26.

¹H-NMR (400 MHz, CDCl₃, δ , ppm): 6.41 (1H, CH-Cl end-group), 5.93 (m, J = 6.8 Hz, 1H; CH= ACP), 5.25-4.75 (1H, CH-O polymer backbone), 4.68 (2H, CH₂-O ACP), 2.15-1.95 (3H, C(O)-CH₃ VAc side chain), 1.95-1.40 (2H, CH₂ polymer backbone); IR (cm⁻¹): 2981 and 2925 (asymm ν_{CH} aliph. CH₃ and CH₂), 2850 (symm ν_{CH} aliph. CH₂), 1729 ($\nu_{\text{C=O}}$ VAc ester group), 1433 (δ_{CH} polymer backbone), 1370 (δ_{CH_3} VAc side chain), 1225 ($\nu_{\text{C-O}}$ VAc ester group), 604 ($\nu_{\text{C-Cl}}$ end-group).

3.4.6 Synthesis of copolymers

The copolymerization reactions were carried out in glass vials. Catalyst, monomer, PVAc macroinitiator and dry solvent in the right proportions, were introduced into the vial under nitrogen atmosphere. The reaction mixture was submitted to several freeze-thaw cycles, heated at the desired temperature and a solution of the ligand in 1,4-dioxane was added using a gastight syringe under nitrogen atmosphere. The stirred mixture was allowed to polymerize for 180 minutes and the reaction was stopped immersing the vial into liquid nitrogen. At the end of the reaction a sample was withdrawn via gastight syringe for ¹H-NMR analysis.

The copolymers were purified by filtration on basic aluminium oxide followed by repeated precipitation in hexane. The materials were finally dried under vacuum until constant weight. The conversions were determined gravimetrically and all the products characterized by FT-IR, SEC, DSC, TGA and ¹H-NMR. Specific synthetic conditions are reported below and the relevant data concerning the obtained copolymers are reported in Table 26.

Table 26: Characterization data of polymeric derivatives.

| Sample | Catalytic system | \overline{M}_n (g/mol) | \overline{M}_w (g/mol) | PD | $^{NMR}\overline{M}_n$ (g/mol) | VAc molar fraction | Methacrylic molar fraction | Monomer conv. (%) |
|------------------------|--|-----------------------------|-----------------------------|-------------------|-----------------------------------|--------------------|----------------------------|-------------------|
| PVAc | CuCl/CuCl ₂ / Me ₆ Cyclam | 16000 ^a | 19700 ^a | 1.23 ^a | 9200 ^c | 1 | - | 36 |
| | | 11600 ^b | 14100 ^b | 1.21 ^b | | | | |
| PVAc- <i>b</i> -PHEMA | CuCl/Byp | 16300 ^a | 21700 ^a | 1.33 ^a | 33900 ^d | 0.36 ^d | 0.64 ^d | 48 |
| PVAc- <i>b</i> -PBMA-1 | CuBr/ PMDETA | 67800 ^c | 75200 ^c | 1.11 ^c | 25700 ^c | 0.48 ^c | 0.52 ^c | 58 |
| PVAc- <i>b</i> -PBMA-2 | CuCl/ Me ₆ Cyclam | 62500 ^c | 68900 ^c | 1.10 ^c | 22150 ^c | 0.54 ^c | 0.46 ^c | 46 |
| PVAc- <i>b</i> -PMMA | CuBr/ PMDETA | 26700 ^b | 33900 ^b | 1.31 ^b | 27600 ^c | 0.42 ^c | 0.58 ^c | 85 |
| PVA- <i>b</i> -PMMA | - | 24900 ^b | 33900 ^b | 1.36 ^b | 22400 ^f | 0.42 ^f | 0.58 ^f | - |

^a Determined by GPC in THF at room temperature (MXL column).

^b Determined by GPC in DMF at 70°C.

^c Determined by ¹H-NMR in CDCl₃.

^d Determined by ¹H-NMR in DMSO.

^e Determined by GPC in THF at room temperature (MXM column).

^f Determined by ¹H-NMR in DMSO assuming that all VAc was converted in VA.

3.4.6.1 PVAc-*b*-PHEMA

[M]= 1.07 mol/l. [HEMA]/[CuCl]/[Byp]/[PVAc] = 400/3.3/6.6/1. Temperature: 60°C. Solvent: 2-butanone /n-propanol 7:3 v/v. Reaction time: 180 minutes. Monomer conversion: 48%.

¹H-NMR (400 MHz, DMSO-*d*₆, δ , ppm): 5.10-4.65 (1H, CH-O, polymer backbone VAc block), 4.20-3.75 (2H, CH₂-O-C(O), HEMA side-chain), 3.75-4.45 (2H, CH₂-OH HEMA side-chain), 2.25-1.20 (C(O)-CH₃ VAc side-chain, CH₂, polymer backbone), 0.95-0.78 (3H, CH₃ polymer backbone HEMA block); IR (cm⁻¹): 3367 (ν_{OH} HEMA side chain), 2936 (asymm. ν_{CH} aliph. CH₂), 2873 (symm. ν_{CH} aliph. CH₃), 1724 ($\nu_{C=O}$ VAc and HEMA ester

groups), 1447 (δ_{CH} polymer backbone), 1372 (δ_{CH_3} VAc side chain), 1225 ($\nu_{\text{C-O}}$ VAc ester group), 1152 ($\nu_{\text{C-O}}$ HEMA ester group), 604 ($\nu_{\text{C-Cl}}$ end-group).

3.4.6.2 PVAc-*b*-PBMA-1

[M]= 1.56 mol/l. [BMA]/[CuBr]/[PMDETA]/[PVAc] = 200/1/1/1. Temperature: 90°C. Solvent: 1,4-dioxan. Reaction time: 180 minutes. Monomer conversion: 58%

3.4.6.3 PVAc-*b*-PBMA-2

[M]= 1.56 mol/l. [BMA]/[CuCl]/[Me₆CyClam]/[PVAc] = 200/2/1/1. Temperature: 25°C. Solvent: 1,4-dioxan. Reaction time: 180 minutes. Monomer conversion: 46%.

¹H-NMR (400 MHz, CDCl₃, δ , ppm): 5.25-4.75 (1H, CH-O, polymer backbone VAc block), 4.25-3.80 (2H, CH₂-O, BMA side-chain) 2.15-1.95 (3H, C(O)-CH₃, VAc side-chain), 1.95-1.25 (CH₂, polymer backbone, CH₂, BMA side-chain), 0.95-0.88 (6H, CH₃, BMA backbone and BMA side-chain); IR (cm⁻¹): 2958 (asymm. ν_{CH} aliph. CH₃), 2930 (asymm. ν_{CH} aliph. CH₂), 1725 ($\nu_{\text{C=O}}$ VAc and BMA ester groups), 1447 (δ_{CH} polymer backbone), 1372 (δ_{CH_3} VAc side chain), 1225 ($\nu_{\text{C-O}}$ VAc ester group), 1144 ($\nu_{\text{C-O}}$ BMA ester group), 605 ($\nu_{\text{C-Cl}}$ end-group).

3.4.6.4 PVAc-*b*-PMMA

[M]= 2.08 mol/l. [MMA]/[CuBr]/[PMDETA]/[PVAc] = 200/1//1/1. Temperature: 90°C. Solvent: 1,4-dioxan. Reaction time: 180 minutes. Monomer conversion: 85%.

¹H-NMR (400 MHz, CDCl₃, δ , ppm): 5.25-4.75 (1H, CH-O, polymer backbone VAc block), 3.90-3.30 (3H, C(O)-O-CH₃, MMA) 2.25-1.50 (C(O)-CH₃ VAc side-chain CH₂, polymer backbone), 0.95-0.88 (3H, CH₃, polymer backbone MMA block); IR (cm⁻¹): 2958 (asymm. ν_{CH} aliph. CH₃), 2930 (asymm. ν_{CH} aliph. CH₂), 1725 ($\nu_{\text{C=O}}$ VAc and MMA ester groups), 1447 (δ_{CH} polymer backbone), 1372 (δ_{CH_3} VAc side-chain), 1225 ($\nu_{\text{C-O}}$ VAc ester group), 1143 ($\nu_{\text{C-O}}$ MMA ester group), 605 ($\nu_{\text{C-Cl}}$ end-group).

3.4.6.5 Synthesis of PVA-*b*-PMMA

A 10% methanol solution of sodium methoxide (3.5 mL; 4 M equiv to the VAc structural units) was added dropwise to a solution of PVAc-*b*-PMMA (300 mg) in dry THF (12 ml) and the mixture was stirred for 3 hours at 40°C under nitrogen atmosphere. The reaction was quenched by adding acetic acid (0.7 mL) and methanol (25 mL), and the copolymer was purified by dialysis (Spectrum Laboratories membrane; molecular weight cutoff 3500 Da) in water for 48 hours. The copolymer was recovered by evaporation of water, dissolution of the polymer in THF, precipitation in hexane and subsequently dried under vacuum.

¹H-NMR (400 MHz, DMSO-*d*₆, δ , ppm): 4.8-4.1 (1H, mm, mr, rr OH VA block)¹⁵², 3.90-3.82 (1H, CH-O VA block), 3.70-3.48 (3H, C(O)-O-CH₃, MMA), 1.77-1.24 (2H, CH₂, polymer backbone), 0.95-0.78 (3H, CH₃, polymer backbone MMA block); IR (cm⁻¹): 3416-3358 (ν_{OH} VA); 2958 (asymm. ν_{CH} aliph. CH₃), 2930 (asymm. ν_{CH} aliph. CH₂), 1722 ($\nu_{\text{C=O}}$ MMA ester group), 1435 (δ_{CH} polymer backbone), 1240 ($\nu_{\text{C-O}}$ VA), 1146 ($\nu_{\text{C-O}}$ MMA ester group).

4 Chapter 4 - Synthesis and characterization of pH and temperature-sensitive polymers as carriers for drug-delivery system

4.1 Introduction

4.1.1 Pluronic block copolymers

Pluronic is the commercial name of triblock copolymers, with a central block of poly(propylene glycol) (PPG) and two external blocks of poly(ethylene glycol) (PEG).

Their properties depend on the molecular weight and on the PEG/PPG ratio in the polymeric chain¹⁶⁰. Table 27 provides name, molecular formulas, average molecular weight and other physicochemical properties of some commercially available Pluronics.

Table 27: Characteristics of some commercially available Pluronic polymers¹⁶¹.

| PLURONIC | \overline{M}_n (g/mol) ^a | Average no. of EG units ^b | Average no. of PG unit ^b | Cloud point (°C) ^c | CMC (M) ^d |
|----------|--|---|--|-------------------------------|-------------------------|
| L61 | 2000 | 4.6 | 31.0 | 24 | 1.1 *10 ⁻⁴ |
| L62 | 2500 | 11.4 | 34.5 | 32 | 4.0 *10 ⁻⁴ |
| L64 | 2900 | 26.4 | 30.0 | 58 | 4.8 *10 ⁻⁴ |
| F68 | 8400 | 152.7 | 29.0 | >100 | 4.8 *10 ⁻⁴ |
| L81 | 2750 | 6.2 | 42.7 | 20 | 2.3 *10 ⁻⁴ |
| P84 | 4200 | 38.2 | 43.4 | 74 | 7.1 *10 ⁻⁴ |
| P85 | 4600 | 52.3 | 39.7 | 85 | 6.5 *10 ⁻⁴ |
| F87 | 7700 | 122.5 | 39.8 | >100 | 9.1 *10 ⁻⁴ |
| F88 | 11400 | 207.3 | 39.3 | >100 | 2.5 *10 ⁻⁴ |
| L92 | 3650 | 16.6 | 50.3 | 26 | 8.8 *10 ⁻⁴ |
| F98 | 13000 | 236.4 | 44.8 | >100 | 7.7 *10 ⁻⁴ |
| L101 | 3800 | 8.6 | 59.0 | 15 | 2.1 *10 ⁻⁴ |
| P103 | 4950 | 33.8 | 59.7 | 86 | 6.1 *10 ⁻⁴ |
| P104 | 5900 | 53.6 | 61.0 | 81 | 3.4 *10 ⁻⁴ |
| P105 | 6500 | 73.9 | 56.0 | 91 | 6.2 *10 ⁻⁴ |
| F108 | 14600 | 265.4 | 50.3 | >100 | 2.2 *10 ⁻⁴ |
| L121 | 4400 | 10.0 | 68.3 | 14 | 1.0 *10 ⁻⁴ |
| P123 | 5750 | 39.2 | 69.4 | 90 | 4.4 *10 ⁻⁴ |
| F127 | 12600 | 200.4 | 65.2 | >100 | 2.8 *10 ⁻⁴ |

^a Number average molecular weight provided by the manufacturer (BASF, Wyandotte, MI)

^b Calculated using the average molecular weights

^c Determined in 1% aqueous solution by the manufacturer

^d Critical Micellar Concentration determined using pyrene probe.

4.1.1.1.1 Formation of micelles and gels in Pluronic water solution

The different hydrophilicity of PEG and PPG makes Pluronic behaving as surfactants in water and allows them to form micelles, micro-emulsions and liquid-crystalline phases (gels) (Figure 46), whose properties can be modulated by changing the PEG to PPG molar ratio and the molecular weight of the copolymer^{160,162}.

Figure 46 reports a phase diagram showing the typical transitions that occur in Pluronic solutions as a function of polymer concentration and temperature.

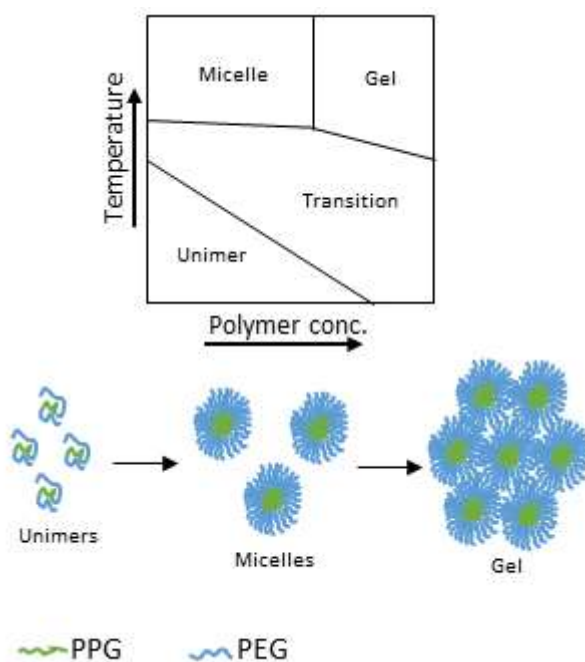


Figure 46: Schematic representation of the characteristic transitions that occur in Pluronic solution^{163,164}.

The critical micellar concentration (CMC) and the critical micelle temperature (CMT) are the most important parameters that characterize the behavior of amphiphilic compounds. The CMC is the concentration above which, at a constant temperature, molecules are forced in a defined structure (micelles). The CMT is the temperature above which, at a constant concentration, the micelles form. Typically, CMT decreases by increasing the Pluronic concentration, and CMC decreases by increasing the temperature. CMC and CMT can be determined by different techniques, e.g. surface tension measurements, chromatography, light scattering, small angle neutron scattering (SANS), small angle X-ray scattering (SAXS), differential scanning calorimetry (DSC),

viscosimetry and others. Different techniques, however, may provide different value of CMC and CMT for the same sample¹⁶¹.

In Pluronics solutions CMC and CMT decrease by increasing the molecular weight of the investigated compound¹⁶⁰.

At low temperature (<15°C) both PEG and PPG blocks are water-soluble and Pluronic macromolecules are present as unimers (Figure 46). Unimers can also be considered as unimolecular micelles because the less hydrophilic PPG adopts a more compact conformation than the more water-soluble PEG. Increasing the temperature above the CMT, PPG becomes insoluble in water producing spherical micelles where a 4-5 nm PPG core is surrounded by a corona of hydrated PEG^{160,163} (Micelle in Figure 46).

The micellization process thermodynamics could be described using the mass-action model which considers that there is an equilibrium between micelles and unimers in solution. The free energy of micellization (ΔG) (Equation 13) is defined as the standard free energy change for the transfer of one mole of unimers from the solution to the micellar phase.

$$\text{Equation 13} \quad \Delta G = RT \ln(X_{CMC})$$

Where R is the gas law constant, T the absolute temperature and X_{CMC} the critical micellization concentration in mole fraction.

The standard enthalpy of micellization can be obtained from Equation 14-a and, assuming that the aggregation number (that is the number of unimers forming a micelle) is not dependent on the temperature, it can be expressed as in Equation 14-b.

$$\text{Equation 14-a} \quad \frac{H}{R*T} = -T * \left[\frac{d(G/R*T)}{dT} \right]_{P,n}$$

$$\text{Equation 14-b} \quad \Delta H = -R * T^2 * \left[\frac{d \ln(X_{CMC})}{dT} \right]_{P,n} = R * \left[\frac{d \ln(X_{CMC})}{d(1/T)} \right]_{P,n}$$

Plotting CMT^{-1} versus the natural logarithm of the copolymer concentration (in mole fraction) a linear plot is obtained confirming the good fitting between experimental and theoretical values derived from Equation 14¹⁶⁰. The entropy change associated to the micellization process can be derived from its dependence by ΔG and ΔH (Equation 15).

Equation 15

$$\Delta S = (\Delta H - \Delta G)/T$$

During micellization, unimers are forced in a defined structure and their entropy decreases ($\Delta S_{\text{unimers}} < 0$). Furthermore, micellization is an endothermic process ($\Delta H > 0$). So, taking into account only the endothermicity of the process and the entropy difference ascribed to unimers during micellization, the process should not be thermodynamically favored (ΔG should be > 0). Micelles formation occurs upon increasing the temperature or the concentration of the polymer in solution and this event is due to the fact that the solubilization of unimers in water causes a significant decrease of the entropy of water molecules, suggesting an increase in the degree of structuring of the water around the polymer. When unimers aggregate in order to form micelles, the release of bound water around the PPG blocks increases the water entropy ($\Delta S_{\text{water}} > 0$), overcoming the entropy loss due to the localization of the hydrophobic chains in the micelles (unimers forced in a defined structure). As a consequence, the difference between the entropy of the overall system before and after micellization results positive ($\Delta S_{\text{unimers}} + \Delta S_{\text{water}} > 0$), making the process thermodynamically favored above a certain temperature which is characteristic of the system under investigation¹⁶⁰.

The temperature affects the Pluronics micellar size (increasing temperature it increases) and its self-assembly in 3D structure, which is generally referred to micellar gels.

Above a critical combination of concentration and temperature (Gel phase in Figure 46), the system reaches a gel state, which often exhibits a long-range order, i.e. a crystalline or para-crystalline organization^{163,165}. There is no specific micellar volume fraction at which the system becomes completely crystalline, whereas there exists a transition interval in which liquid and crystalline domain coexist (Transition in Figure 46). The presence of transition regions is not unexpected: for Pluronics, as much for most amphiphilic polymers, also micellization is not a sharp process and both CMC and CMT should be better described as concentration and temperature “windows”.

The effect of Pluronic concentration on the displayed transitions can be ascribed to the volume fraction occupied by the polymer: the higher is the volume occupied the easier is the organization in ordered structures^{160,166-168}.

The molecular interpretation of the effect that the temperature has on Pluronics transitions is more controversial and may involve several factors. Several studies have been carried out in order to understand the effect of the temperature^{169,170,171}. Studies on Pluronic

F127 cross-linked micelles showed that still exhibit a thermally induced gelation, therefore excluding any significant contribution of PEG chain entanglements¹⁷². Furthermore, Pluronic-based nanoparticles exhibit gelation although they have an overall volumetric contraction¹⁷³. Gelation can be so described by the theory of hard-sphere interaction. When unimers and micelles are present in solution (below the gelation temperature), upon increasing the temperature the equilibrium between unimers and micelles shift towards these latter. As a consequence, the micelles volume fraction increases up to a value (0.53) that forces the micelles to coalesce together forming a long-range ordered gel phase^{174,175}.

It is worth noting that in these micellar assemblies the gelation is reversible, highlighting the purely physical nature of the transition. Compared to a chemical gelation the strength of the interactions involved is weaker¹⁷⁶.

In the gels Pluronic micelles arrange in a cubic geometry which most often is supposed to correspond a body-centered cubic (BCC) lattice. These ordered phases are often associated to shear moduli in the order of 10^4 - 10^5 Pa^{163,176}.

The temperature of the product (gel) can also affect the micellar shape (not only their size, as previously mentioned). At high temperature, the micelles have a core diameter that is almost the size of a fully stretched PPG chain and the system evolves forming micelles with rod-like shape, which arrange in hexagonal structures, decreasing inter-micellar interaction^{160,163} (Figure 47).

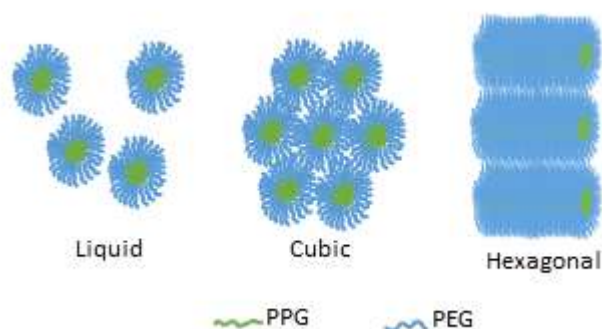


Figure 47: Schematic illustration of micellar phases formed by the Pluronic¹⁶⁴.

4.1.1.2 Applications of Pluronics in drug delivery systems

The ability of Pluronic-based systems to enhance the solubility of hydrophobic compounds in water solution and their reversible thermo-responsiveness make Pluronics very interesting compounds for the development of drug-delivery systems^{161,177-182}.

Using common drug-administration techniques, molecules has to overcome barriers to reach the site into the body where it can perform their biological role, and during their travel through the body they can be absorbed in non-desired sites or they can partially react forming non-active products. Other important problems that should be taken into account during the development of a new drug is its solubility and stability: it might happen that a good drug against a particular disease cannot be used because it is not stable or it is not soluble in the body fluids. Using drug delivery technologies these problems can be overlapped and the current therapies can be improved. A growing number of therapeutic polymers are approved by the regulatory authorities in North America, Europe and Asia for clinical use in treatment of cancer, infectious and genetic diseases¹⁶¹.

Furthermore, Pluronic micelles act as micro-containers for molecules, preventing the degradation of the drug or undesired pharmacokinetics^{160,161}. Another important aspect that differs Pluronic-based drug delivery systems is that they have the ability to enhance drug performance by acting as biological response-modifying agents, which act directly upon the target cells¹⁶¹.

In Pluronic-based drug delivery systems, the drug interacts with the PPG core of the micelles. So, the dimension of these latter must be between 10 and 100 nm (Pluronic micelles are usually within this range). This range is determined by the fact that the particles with diameters larger than 200 nm are sequestered by the spleen and those ones with diameter of 5-10 nm are removed through extravasation and renal clearance.

Because of its interesting properties, among the commercial poloxamers, Pluronic F-127 is one of the most studied copolymer for the development of drug delivery systems to administer drugs through different form of administration¹⁷⁸.

Pluronic-based drug delivery systems can be administrated in two ways:

- administration of a micellar water solution containing the drug
- topical administration of gels
- administration of Pluronic water solution that undergo the gel transition when it reaches the body temperature¹⁷⁸.

The drug incorporation in Pluronic micelles is most often accomplished by exposing a micellar dispersion of Pluronic in water to a solid drug dispersion or to a small volume of drug solution in a water-miscible and volatile organic solvent¹⁶¹.

When a molecule is solubilized in the micelles, an equilibrium between its concentration in water solution and in the PPG core is established (Figure 48).

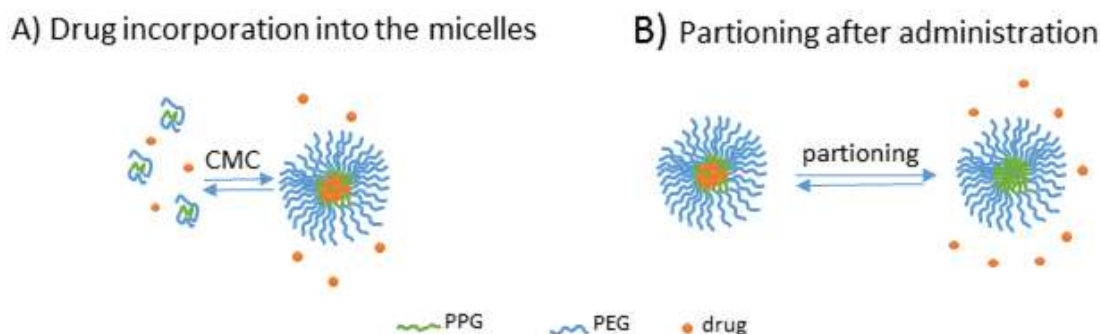


Figure 48: Mechanisms of drug release from micelle: (A) disintegration of the micelles below CMC; (B) release of the drug as a result of partitioning¹⁶¹.

The ratio between the drug concentration in the micelles and in the external water is defined as partition coefficient (P) (Equation 16). It quantifies numerically the dynamic exchange between solubilized molecules into the micelle's core and those dissolved in water when the system has reached the equilibrium.

Equation 16

$$P = \frac{[Dm]}{[Dw]}$$

[Dm] = conc. of drug into the micelle

[Dw] = conc. of drug into the external water

Although the equilibrium is usually not reached in the body, the partitioning value allows to estimate the amount of drug that could be released into the body after dilution in the body fluids¹⁶¹. If the molecule has a low P value, once the drug solubilized in the micelles has been administrated, the drug is released from the micelles before reaching the targeted site. The solubility of a specific molecule in water solutions containing Pluronic micelles can be tuned by acting on the molecular weight and composition of Pluronic¹⁶⁰. Studies made on Pluronic-based systems prove that the concentration of the block copolymers in the plasma is sufficient in order to form micelles¹⁸³. The drug can be released in the external media when the micelles are destroyed as consequence of dilution to a

concentration lower than CMC (A-Figure 48) or as result of partitioning of the drug between the internal core of the micelle and the external media (B-Figure 48)¹⁶¹.

In order to allow the solubilization of drugs into the PPG core of the micelles, the system has to be above its CMC and CMT. Pluronic-based systems are suitable to be used as drug delivery systems because they have a CMT close to 37°C (body temperature).

It should also be taken into account that once the drug has been incorporated into the micelles, the system should not be left at a temperature at which the micelles destroy. If it happens, the drug could not be soluble in the system constituted from solvent and unimers and increase again the temperature might not be sufficient to obtain the previous drug delivery system¹⁶¹.

Before administration it should be taken into account that before the drug (contained into the micelles) reaches the desired site, the system could interact with other sites and it can change the structure as consequence of the fact that pH and temperature can change during the route to the targeted site¹⁶¹. To enhance the recognition mechanism efficiency between the micelles and the site where the pharmacologic action should be carried out, proteins could be attached covalently to Pluronic molecules, using the free hydroxyl groups present in this latter. As an example, the drug delivery system could be built mixing unmodified Pluronic with functionalized Pluronic macromolecules, obtaining micelles that are able to interact selectively with specific sites or receptors as a function of what type of protein is bonded to Pluronic^{161,177}.

The incorporation of the drug into micelles or gels offers several advantages. It can facilitate the overcoming of the drug through the barriers present into the body, as the ones posed by the gastrointestinal tract. Furthermore, the micelles can sensitize specific cells increasing their interactions with the drug, enhancing the activity of the drugs. As example, it has been shown that doxorubicin administrated with Pluronic micelles enhances its cytotoxic activity compared to doxorubicin alone, by two or three order of magnitude against tumors with multidrug-resistant phenotype¹⁸².

When repeated drug administrations are required, it is preferred oral instead of intravenous administration. Pluronic drug formulations have the characteristic to replace intravenous administration for poorly water soluble drugs that cannot overcome the barriers present into the human body. As an example, risperidone is a poorly soluble drug and in order to obtain good level of bioavailability it is administrated by intravenous delivery. Oral delivery of risperidone in formulation with polymeric micelles exhibit similar

delivery properties to intravenous delivery, achieving a bioavailability of 40%, thanks to the overcoming of the intestinal membrane allowed by the presence of the micelles¹⁸⁴.

Topical administration of Pluronic gels can be applied for delivery of analgesic, anti-inflammatory drugs, anti-cancer agents and so on. The possibility to deliver the drug through the skin, exactly where it is needed, allows to use a lower amount of drug compared to other ways of administration (e.g. oral administration). Sometimes topical application requires penetration enhancers in order to allow the drug to pass through the skin. Administration through topical application has been studied for indomethacin, ketoprofen, fenantyl, sodium naproxen, insulin and so on. In topical application, diffusion of Pluronic controls the release rate of the drug, accelerating the process of solute diffusion within lipid bilayers^{179,180,185-187}.

Pluronic gels are also suitable for buccal, rectal, subcutaneous and intramuscular applications. The added value of this type of applications is that gels act as reservoirs of drug and this involves several advantages:

- prolonged pharmacologic action
- reduced side-effects
- gels can be designed in order to interact with specific target and release the drug only in a specific part of the body
- constant drug levels in the desired site throughout all the time the gel performs its action.^{181,188-190}

After administration, the stability of the micelles and gels affects the circulation time and the drug release rate. Indeed, even administering gels, micelles are released after dilution in the body fluids. CMC and P are two parameters that could help during the evaluation of the pharmacokinetic. CMC is related to the thermodynamic of the system but it does not take into account the kinetic stability of the micelles; indeed, micelles with hydrophobic core that have glass transition temperature higher than 37-38°C exhibit long lasting relaxation process that results in slow dissociation kinetic when the system reaches a concentration lower than the CMC. This behavior is due to the fact that if the polymeric chains in the core of the micelles are above the glass transition temperature, they are physically attached to each other and the drug diffuses slowly. The low drug release rate resulting from systems with micelle's core with glass transition temperature near to 37-38°C allows to obtain systems with high blood circulation time and slow release of the drug in the body¹⁶¹.

The possibility to change the composition and the structure of Pluronic-based drug delivery systems by changing the length of hydrophobic and hydrophilic blocks allows to obtain different systems suitable for different type of drug and with different type of pharmacokinetic (different CMC and P) (Figure 49). Once the drug and the site where the pharmacologic action should be carried out are known, the drug delivery system has to be chosen taking into account that:

- the incorporation of the drug into the carrier should lead to an increase in stability and circulation time of the drug into the body
- the release of the drug into the critical site of action should be effective.

These two listed behavior lead to the maximal therapeutic index but obtain them is not so easy. Too high stability of the drug into the micelle's core leads to a high stability of the drug delivery system and high circulation time but the bioavailability of the drug in the desired site could not be sufficient in order to obtain the pharmacologic action. A good ratio between the stability of the drug delivery system and the release of the drug into the desired site should be achieved. This compromise could be achieved by changing the characteristic of the block-copolymer used to build the drug delivery system¹⁶¹.

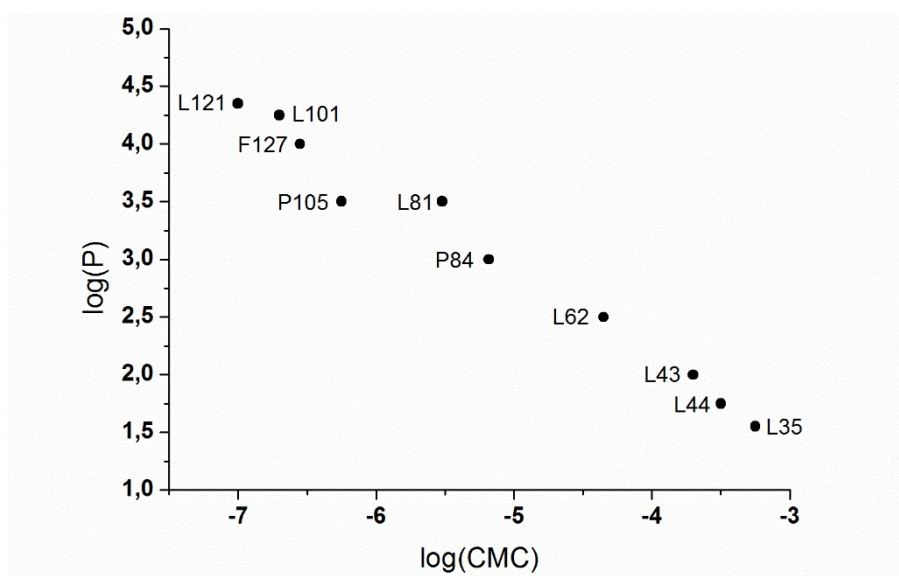


Figure 49: Relationship between the partitioning coefficients of pyrene and CMC in different commercial Pluronic block copolymer systems¹⁹¹.

4.2 Aim of the project

The administration of drugs using common past techniques have some limits. Usually drugs have low solubility in the blood and oral administration implies that the drug is spread throughout the body and not only in the target cells. Inefficient administration requires to increase the amount of administrated drug in order to have the correct drug concentration in the target zone. Furthermore, it results convenient to maintain a constant and controlled drug concentration in the blood throughout the required administration period.

During the last years, several studies were carried out with the aim to increase the drugs administration efficiency; in particular, the application of micelles and gels was studied^{178,192-196}. Gels are three dimensional network consisting of joined polymeric chains swollen in water¹⁹⁶. The incorporation of drug into micelles and gels offers many advantages such as enhanced drug solubility in water systems^{197,198}, possibility to inject the gel in the target zone^{196,199} and targeted-delivery of the drug (especially using responsive micelles)^{131,178,200}. These advantages can be exploited with the aim to decrease the amount of administrated drug, especially when, besides the desired effect, many side effects are present such as in common anti-cancer therapies²⁰¹⁻²⁰³. In the last years, pH-responsive carriers were studied with the aim to release the drug specifically in the target cells^{197,200,204,205}. Indeed, it is known that the extra-cellular pH in a cancer is between 6.5 and 7.2^{206,207} and it decreases again to 5-6.5 and 4.5 in the endosomes and lysosomes respectively^{192,195}; usually, the pH of healthy tissues and blood is around 7.4-7.5²⁰⁶⁻²⁰⁸. Thus, by using a pH sensitive gel as drug carrier, it could be possible to inject it and release the drug directly in the target cells. The possibility to inject the drug into the cancerous cells allows to use a lower amount of drug, decreasing its side effects^{204,205}.

In this context, we retained of interest to synthesize materials that form gels and micelles that can act as drug-carriers and that can exhibit pH-responsiveness. In particular, Pluronic F127 (PLUR F127), which is a tri-block copolymer (poloxamer) that in water is able to self-assemble in gels and micelles, was used as starting material. PLUR F127 and its derivatives are already used in drug delivery systems as carrier for hydrophobic drugs and other purposes^{131,178,193}. Indeed, this material reversibly self-assembles in gels and micelles and the process is favourite increasing the temperature^{163,178}. For example at body temperature (37°C) PLUR F127 in water forms gels when its concentration is between 10 and 20% (w/v)^{209,210}. In order to employ this material as carriers in drug delivery systems,

specifically, in anti-cancer applications, we used it as macroinitiator for the polymerization of different pH-sensitive moieties with the aim to obtain block copolymers which are contemporary temperature and to pH-sensitive.

In particular, the second blocks are characterized by different pK_a : when the pH solution is below their pK_a , this block is protonated and thus hydrophilic; when the pH is above the pK_a the block results hydrophobic. Thus it is reasonable to expect that once the synthesized materials are self-assembled in micelles, by changing the pH they should modify their aggregation structure and release the drug (Figure 50).

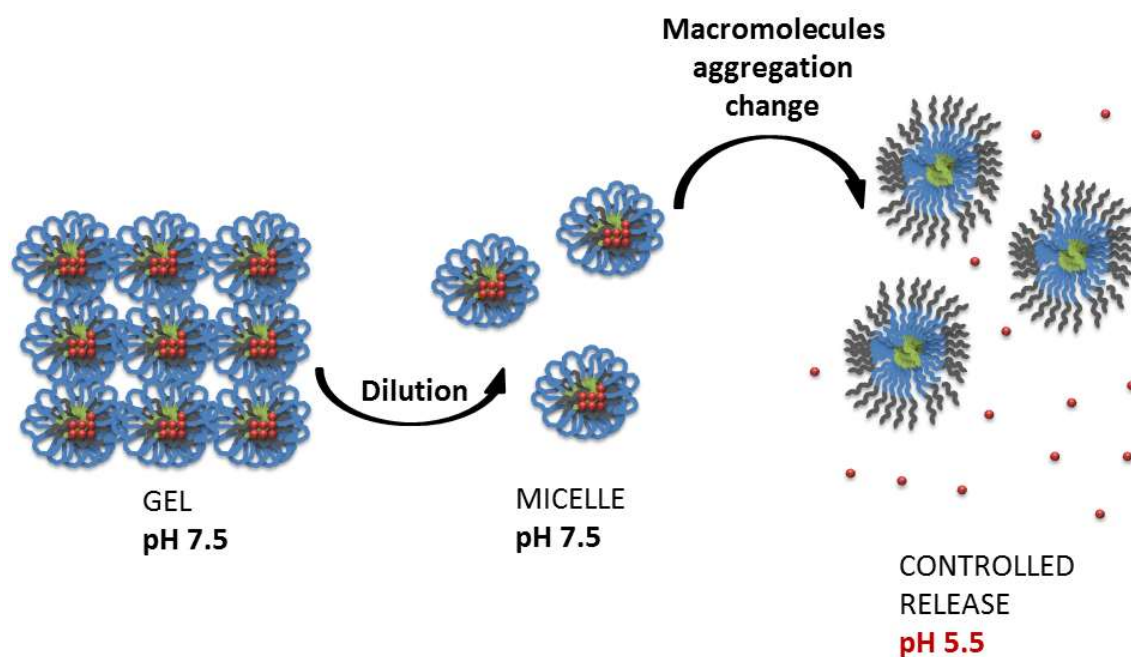


Figure 50: Schematic representation of the controlled drug release in the target zone.

In particular PLUR F127 was used as macroinitiator for the further polymerization of three different pH-sensitive molecules (Figure 51) thus obtaining the polymeric blocks poly[2-(*N,N*-dimethylamino)ethyl methacrylate] (PDMAEMA), poly[2-(*N,N*-diethylamino)ethyl methacrylate] (PDEAEMA) and poly[2-(*N,N*-diisopropylamino)ethyl methacrylate] (PDIAEMA).

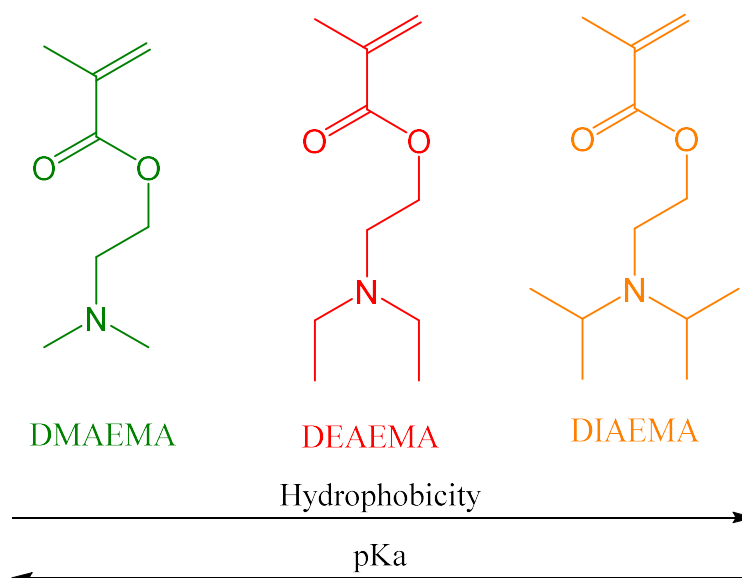
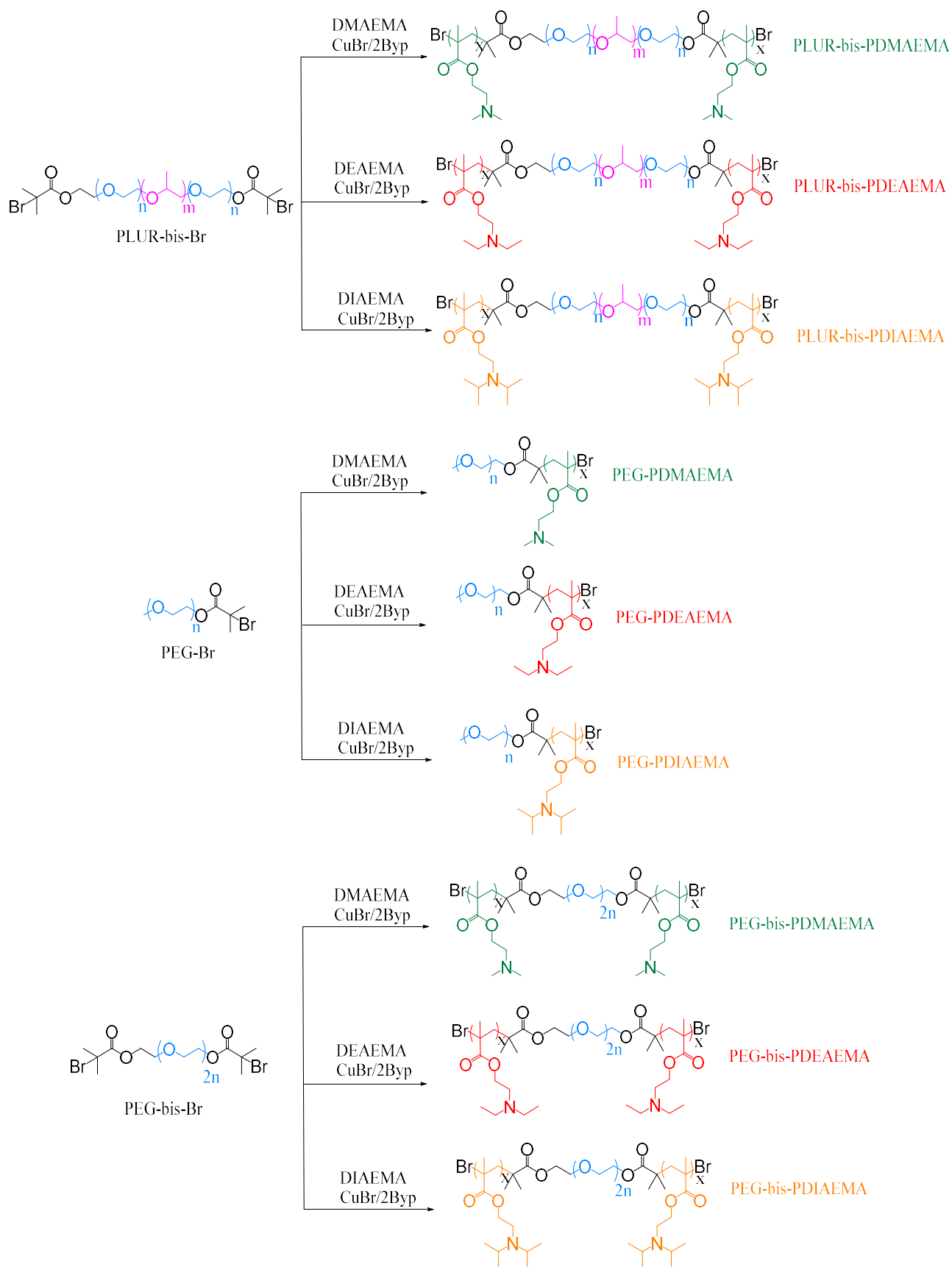


Figure 51: Structure of the monomers used for the synthesis of the pH-sensitive moieties.

As shown in Figure 51, the pK_a of the monomers decreases with the steric hindrance of the substituent bonded to the amine group and the polymeric assemblies will change their structure depending on the pK_a of the methacrylic block. This will allow to understand which is the best pH-sensitive unit for the specific application. In order to understand the effect of PLUR F127 structure on the final properties of the synthesized compounds, poly(ethylene glycol) 8800 Da (PEG-bis-OH), which corresponds to the two hydrophilic block of PLUR F127, and poly(ethylene glycol) methyl ether 5300 Da (PEG), which corresponds to one of the two hydrophilic block of PLUR F127, were extended with the same pH-sensitive moieties used to functionalize PLUR F127. Studying and comparing the properties of the synthesized materials, which have the same pH-sensitive units but different central polymeric block, will allow to understand how PLUR F127 structure affects the behavior of polymeric aggregates and the release properties. In summary, nine different polymeric materials were investigated: PLUR-bis-PDMAEMA, PLUR-bis-PDEMAEMA, PLUR-bis-PDIAEMA, PEG-PDMAEMA, PEG-PDEMAEMA, PEG-PDIAEMA, PEG-bis-PDMAEMA, PEG-bis-PDEMAEMA and PEG-bis-PDIAEMA (Scheme 15).



Scheme 15: Synthesis of PLUR F127, PEG and PEG-bis-OH block copolymers.

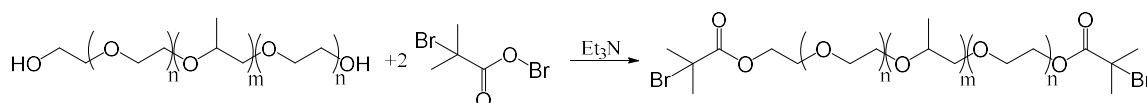
In order to study the effect of the molecular weight of the pH-sensitive units, for each type of compound two molecular weight of the pH-sensitive moieties were synthesized [short (*S*) and long (*L*)].

ATRP was used as polymerization technique because it allows to synthesized polymers with pre-determined molecular weight and low polydispersity (PD). This latter characteristic is important because it is easier to obtain nano-structured materials when the polymeric chains have similar chain length²¹¹.

4.3 Results and discussion

4.3.1 Synthesis of ATRP macroinitiators

In order to use PLUR F127, PEG and PEG-bis-OH as macroinitiators for the further polymerization of pH-sensitive units, the terminal OH groups of the three compounds were converted into the proper ATRP initiator groups through reaction with 2-bromoisobutyryl bromide (Scheme 16) and the final products were analyzed by $^1\text{H-NMR}$, ATR FT-IR, MALDI-TOF and DSC with the aim to confirm the expected functionalization.



Scheme 16: Synthesis of ATRP macroinitiator from PLUR F127.

The FT-IR spectra of the three synthesized compounds highlight the presence of the characteristic C=O stretching signal at 1734 cm^{-1} which can be ascribed to the presence of the ester groups attached to the polymeric chains after the functionalization. The presence of the ester signal and the absence of OH stretching signals in all the IR spectra confirm qualitatively the correct functionalization. It is really important that the functionalization reaches high conversion values because the final application of the synthesized materials is the formation of aggregates which is easier when the macromolecules have the same structure²¹¹. If not all the polymer chains act as ATRP macroinitiator the presence of non-functionalized material can decrease the aggregation of the macromolecules and it would be rather difficult to correlate the properties of the compounds with their structures.

The $^1\text{H-NMR}$ spectra of the macroinitiators show the signals of the 2-bromoisobutyryl bromide residue at the ends of the macromolecules. As an example, in Figure 52 the $^1\text{H-NMR}$ spectrum of PLUR F127 is compared with that one of PLUR-bis-Br. As can be seen from the figure, in the spectra of the macroinitiator the signals resulting from the functionalization (1.86, 3.68 and 4.25 ppm) can be clearly detected and quantified. The OH groups conversion was determined by $^1\text{H-NMR}$, calculating the molecular weight of the starting materials (by end-group analysis) and comparing the integral of the signal ascribable to CH₂-O-C(O) signal with the one that it should have at 100% of conversion. The same results can be obtained using the integrals of the other end groups signals. As can be seen from Table 28, where OH groups conversion is displayed, all the starting

materials show high degree of functionalization (>95% mol/mol) confirming the possibility to use them as proper ATRP macroinitiators.

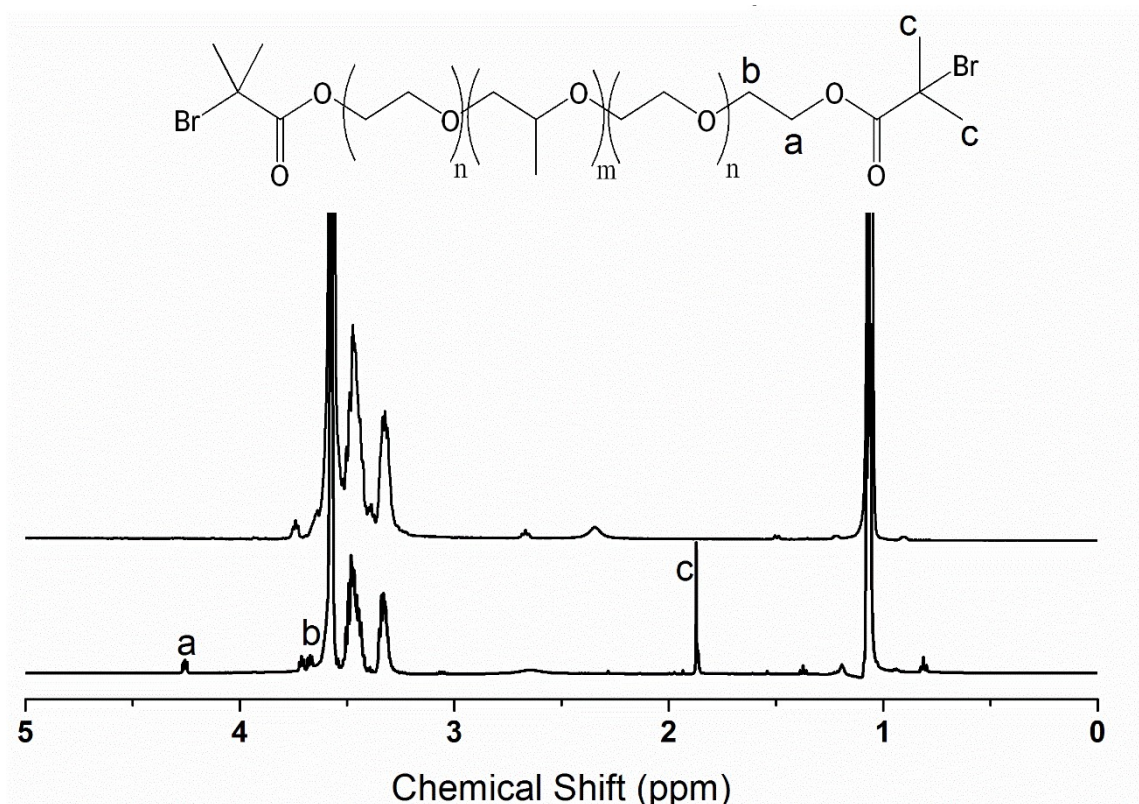


Figure 52: ¹H-NMR of PLUR-bis-Br and PLUR F127.

The average molecular weight of the starting and functionalized macromolecules was determined also by MALDI-TOF analysis and the results are shown in Table 28. Mono-functional PEG (PEG) after functionalization has a \overline{M}_n which is 142 Da higher than the starting material whilst bi-functional PEG (PEG-bis-Br) and PLUR-bis-Br have a \overline{M}_n 316 and 313 Da higher than PEG-bis-OH and PLUR F127 respectively. A mono and di-functionalization should lead products with a \overline{M}_n of 149 and 298 Da higher than the starting product respectively. The good agreement between the expected increase of molecular weight and the ones determined experimentally confirm the high degree of functionalization determined by ¹H-NMR analysis.

PEG is a semi-crystalline material with a melting temperature around 50-60°C. Changing the end-groups of PEG, PEG-bis-OH and PLUR F127 it is reasonable to expect a change in the crystallinity of the samples. PEG-Br, PEG-bis-Br and PLUR-bis-Br were analyzed by DSC in order to determine if the functionalization changes the thermal properties of the materials. In Table 28 the melting temperatures and melting enthalpy of PEG-Br, PEG-

bis-Br and PLUR-bis-Br are compared with the melting temperatures and melting enthalpy of the corresponding starting material and in Figure 53 the DSC thermograms are shown. As can be seen from the reported data determined calculating the maximum of the melting events seen in the DSC thermograms, all the macroinitiators have lower melting temperature and lower melting enthalpy compared to the starting materials. The melting temperature of PLUR F127 is lower than those ones of PEG and PEG-bis-OH because of the presence of PPG block that hampers the crystallization. The crystallization is further disturbed introducing the 2-bromoisobutyryl residue at the ends of the macromolecules, indeed PLUR-bis-Br has the lowest melting temperature and melting enthalpy.

Table 28: Characterization data of the macroinitiators.

| Sample | ^{NMR} \overline{M}_n (g/mol) | ^{MALDI} \overline{M}_n (g/mol) | OH conv. (%mol) ^a | T _m (°C) ^b | ΔH (J/g) ^b |
|-------------|--|--|---------------------------------|-------------------------------------|-----------------------|
| PEG | 5200 | 5292 | - | 62 | 140.8 |
| PEG-Br | 5300 | 5434 | 98 | 61 | 124.8 |
| PEG-bis-OH | 8800 | 8878 | - | 65 | 131.7 |
| PEG-bis-Br | 9000 | 9194 | 95 | 62 | 127.8 |
| PLUR-F127 | 16000 (0.71 PEG weight fraction) | 13322 | - | 58 | 94.8 |
| PLUR-bis-Br | 16200 | 13635 | 100 | 52 | 87.3 |

^a Determined by ¹H-NMR

^b Determined by DSC.

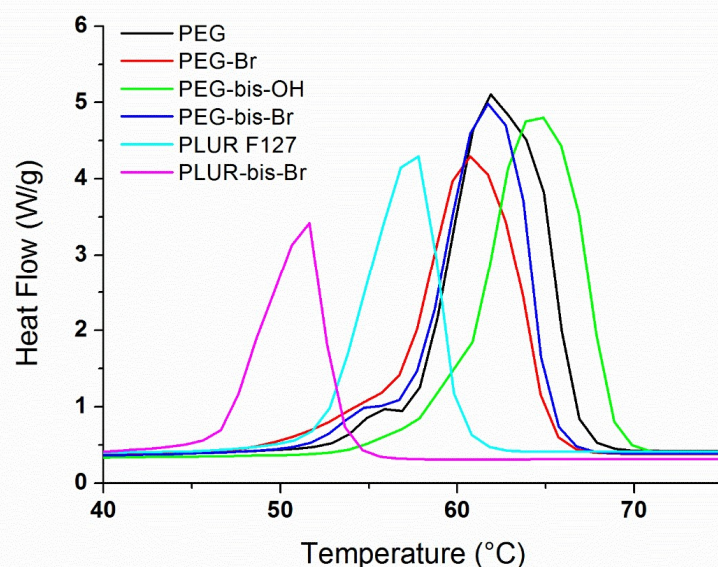


Figure 53: DSC thermograms between 40 and 75°C of the macroinitiators and their corresponding starting materials.

4.3.2 Kinetic studies and synthesis of block copolymers

In order to know the polymerization time needed to obtain polymers with the desired molecular weight, the polymerization kinetics of DMAEMA, DEAEMA and DIAEMA were studied using PEG-Br, PEG-bis-Br and PLUR-bis-Br as macroinitiators. As an example, in Scheme 15 we report the synthesis of PLUR F127, mono and di-functional PEG block copolymers. All the polymerizations were carried out under the same conditions, in presence of the suitable macroinitiator (PLUR-bis-Br, PEG-bis-Br or PEG-Br), CuCl as catalyst, 2,2'-bipyridyl (Byp) as ligand, in dry toluene ($[M_0] = 25\% \text{ v/v}$) at 60°C, and with an initial molar ratio of $[Monomer]/[CuCl]/[Byp]/[macroinitiator] = 70/1/2/1$ (see experimental section). The monomer conversion was determined at different time intervals and $\ln([M_0]/[M])$ was plotted as a function of time (Figure 54). The occurrence of the polymerization was confirmed by $^1\text{H-NMR}$ analysis which displays, besides the signals of the macroinitiators, the ones of the second block (Figure 56). By plotting $\ln([M_0]/[M])$ vs time it is possible to determine the K_{app} of the polymerization (slope of the intercept of the experimental points). The K_{app} values of the different kinetics were determined from the slope of the fitting line of the experimental points. As an example, in Figure 54 the kinetic plots of the polymerization of the three monomers using PLUR-bis-Br as initiator are shown. It is worth noting that all the systems show a linear dependence of $\ln([M_0]/[M])$ with time thus indicating a first-order kinetics of the

polymerization rate with respect to the monomer concentration and a constant concentration of the growing species throughout the whole process. Thus a good process control was achieved up to 80% of monomer conversion; then the system become so viscous that the diffusion limits can decrease the rate of polymerization.

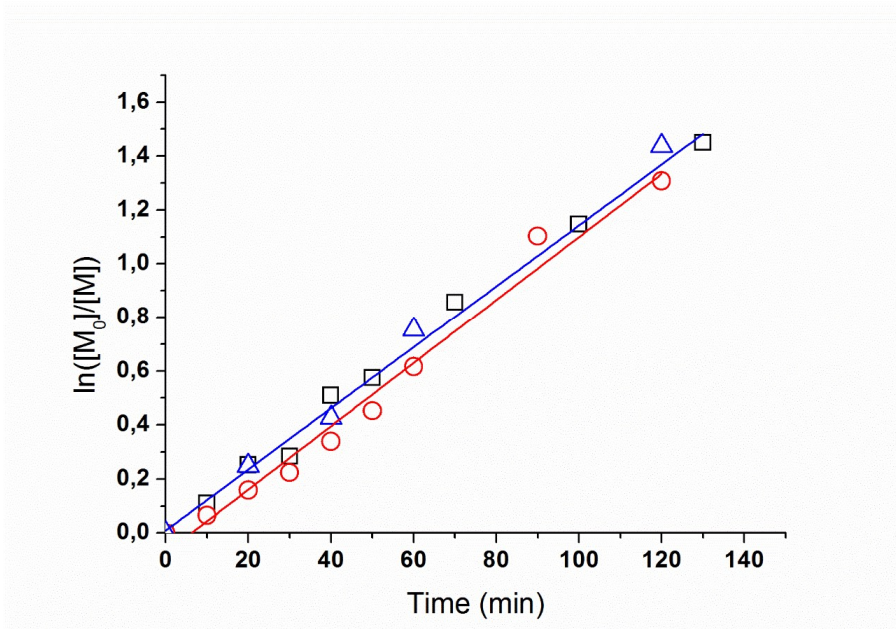


Figure 54: Kinetic plots of the ATRP of DMAEMA (□), DEAEMA (○) and DIAEMA (Δ) using PLUR-bis-Br as macroinitiator.

In Figure 55 the K_{app} values of the ATRP of the three monomers as a function of the macroinitiator are displayed. As shown by the reported data, even if DMAEMA, DEAEMA and DIAEMA have the same reactive methacrylic group, they show different rates of polymerization which depend also on the used macroinitiator. In particular using PEG-Br and PEG-bis-Br as initiators, the polymerization rate decreases on passing from DMAEMA to DEAEMA and DIAEMA. Such a behavior could be ascribed to the increasing hindrance of the substituent of the amine group of the monomer, which prevent the interactions between the monomeric double bond and the propagating radical. It is worth noting that also the molecular weight of the macroinitiator affects the rate of polymerization and this might be mainly caused by two factors: the higher viscosity of systems containing polymers with higher molecular weight and the lower availability of the radical when the macromolecule is in a random coil configuration. Using PLUR-bis-Br as macroinitiator, in fact, the rates of polymerizations are the lowest among the three studied macroinitiators and it does not depend on the monomer structure. PLUR-bis-Br is

the macroinitiator with the highest molecular weight and it is a block copolymer that can self-assemble in aggregates in solutions that might not allow the radical to react with the monomer.

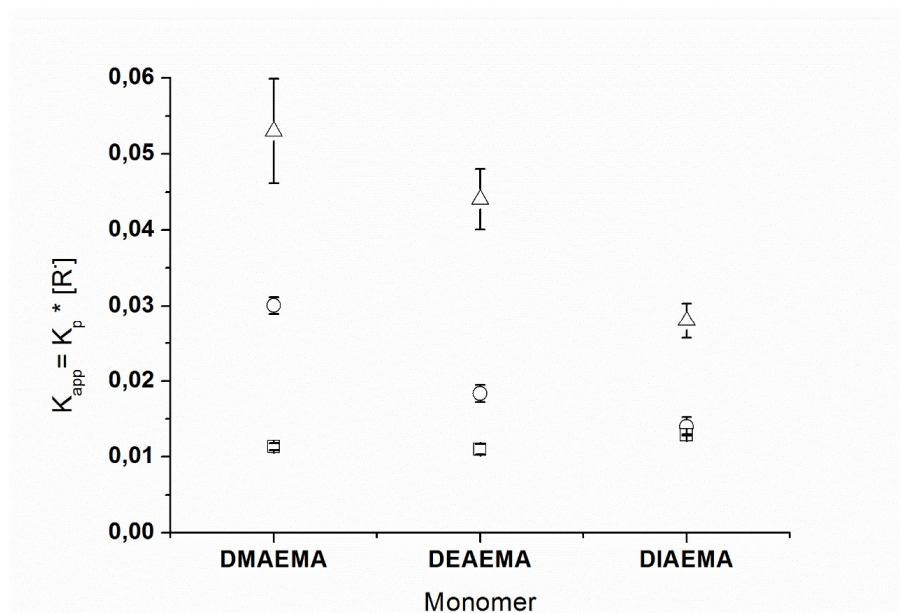


Figure 55: Comparison of the kinetic polymerization apparent constant for each monomer-macroinitiator couple. Macroinitiators: PEG-Br (□), PEG-bis-Br (○), PLUR-bis-Br (Δ).

On the basis of the kinetic studies results, several block copolymers were synthesized in presence of the suitable macroinitiator (PLUR-bis-Br, PEG-bis-Br or PEG-Br), CuCl as catalyst, 2,2'-bipyridyl (Byp) as ligand, in dry toluene ($[M_0] = 25\%$ v/v) at 60°C , and with an initial molar ratio of $[\text{Monomer}]/[\text{CuCl}]/[\text{Byp}]/[\text{macroinitiator}] = 70/1/2/1$. The occurrence of the polymerization was confirmed by $^1\text{H-NMR}$ analysis which displays, besides the signals of the macroinitiators, the ones of the second block. As an example, the spectrum of PEG-PDIAEMA is shown in Figure 56. In the spectrum the resonances at 4.1, 2.9 and 2.7 ppm related to the $\text{O-CH}_2\text{-CH}_2\text{-N}$, $\text{N-(CH(CH}_3)_2)_2$ and $\text{O-CH}_2\text{-CH}_2\text{-N}$ of PDIAEMA respectively, confirms the occurred polymerization.

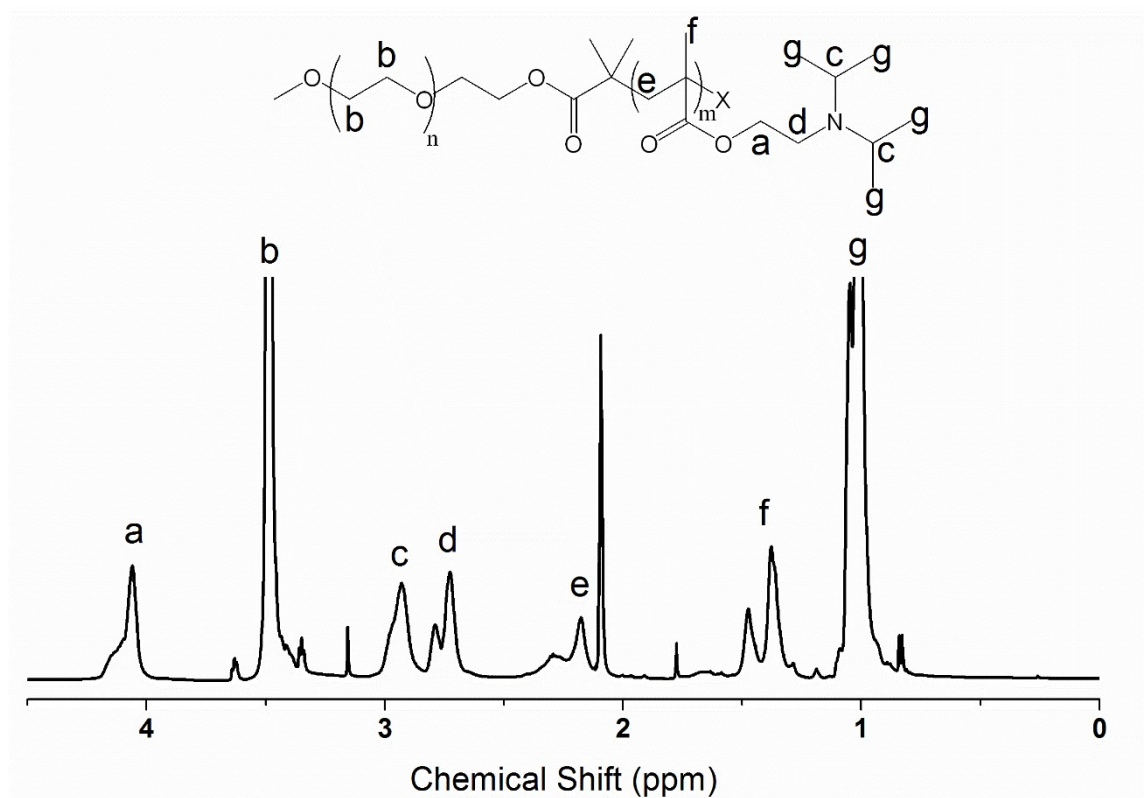


Figure 56: $^1\text{H-NMR}$ in deuterated toluene of PEG-PDIAEMA.

As can be seen from the data reported in Table 29, the average molecular weight of the synthesized copolymers increases, as expected, with the polymerization time, confirming the good control achieved over the process. As desired, for each type of copolymer two methacrylac chain length were obtained. The GPC analysis was carried out in DMF using PEG standards for the calibration. There is a good agreement between the \overline{M}_n determined by NMR and GPC for all the block copolymers synthesized using PEG-Br and PEG-bis-Br as macroinitiators, thus confirming the realability of the data.

Table 29: \overline{M}_n (determined by $^1\text{H-NMR}$) and GPC and polydispersity of the synthesized block copolymers.

| Compound | \overline{M}_n (g/mol) | | PD ^b |
|---------------------------|-------------------------------|------------------|-----------------|
| | $^1\text{H-NMR}$ ^a | GPC ^b | |
| PEG-Br | 5300 | 6100 | 1.12 |
| PEG-PDMAEMA-S | 6100 | 7150 | 1.18 |
| PEG-PDMAEMA -L | 12600 | 8900 | 1.63 |
| PEG-PDEAEMA-S | 5900 | 6500 | 1.10 |
| PEG-PDEAEMA -L | 8100 | 7600 | 1.20 |
| PEG-PDIAEMA-S | 6600 | 8300 | 1.95 |
| PEG-PDIAEMA -L | 9900 | 9400 | 1.30 |
| PEG-bis-Br | 9000 | 10600 | 1.12 |
| PEG-bis-PDMAEMA-S | 10600 | 10500 | 1.30 |
| PEG-bis-PDMAEMA -L | 14100 | 14400 | 1.60 |
| PEG-bis-PDEAEMA-S | 10000 | 8800 | 1.63 |
| PEG-bis-PDEAEMA -L | 14500 | 13800 | 1.26 |
| PEG-bis-PDIAEMA-S | 12200 | 12100 | 1.58 |
| PEG-bis-PDIAEMA -L | 18800 | 18200 | 1.65 |
| PLUR-bis-Br | 16200 | 13600 | 1.20 |
| PLUR-bis-PDMAEMA-S | 18300 | 9600 | 1.90 |
| PLUR-bis-PDMAEMA-L | 31300 | 17900 | 1.83 |
| PLUR-bis-PDEAEMA-S | 21500 | 13400 | 1.63 |
| PLUR-bis-PDEAEMA-L | 26600 | 15400 | 1.65 |
| PLUR-bis-PDIAEMA-S | 21700 | 12050 | 1.58 |
| PLUR-bis-PDIAEMA-L | 31300 | 16600 | 1.36 |

^a Calculated using the \overline{M}_n of the starting material determined by MALDI and the degree of polymerization (DP) calculated by $^1\text{H-NMR}$.

^b Determined by GPC in DMF.

The copolymers of PLUR F127, instead, show a disagreement between these two values. Such a behaviour could be ascribed to the different hydrodynamic volume of block copolymers containing an hydrophobic core of PPG with respect to the PEG standards, which does not allow to a correct determination of the average molecular weight by GPC. Anyway, both the analysis methods underline an increment of \overline{M}_n with the polymerization time.

4.3.3 NMR characterization

All the synthesized copolymers were studied by $^1\text{H-NMR}$ in organic solvents and in D_2O at pH 5.5 and 7.5. As reported in Figure 57, Figure 58 and Figure 59 in organic solvent, when all the polymer chains are solubilized, the NMR signals of all the protons can be detected. In water, instead, some of the signals of the methacrylic chain are absent and other ones decrease in intensity, increasing the pH of the solution. It is worth noting that this phenomenon is more evident for the polymers which are more hydrophobic: signals of PDMAEMA are more intense compared to the ones of PDEAEMA while signals of PDIAEMA cannot be detected at pH 7.5. This behavior is in agreement with the expectation and reflects the pK_a trend of the methacrylic moieties. PDMAEMA indeed is hydrophilic and can be easily protonated while PDIAEMA, which is more hydrophobic, is not well solubilized in water solution. Thus the absence of the methacrylic signals at pH 7.5 is due to the aggregation state of the material in water solution.

These experimental evidences confirm the amphiphilic structure of the synthesized copolymers. The PLUR F127 derivatives are penta-block copolymers with a hydrophobic core of PPG and two hydrophilic or hydrophobic methacrylic external blocks. PLUR F127 self-assembles in micelles and aggregates. When it is extended with hydrophilic chains the external corona is constituted of PEG and methacrylic moieties. Increasing the hydrophobicity of the methacrylic chains it is reasonable to expect that micelles are formed by a core of PPG and methacrylic moieties, while the PEG chains fold on themselves and interact with water (Figure 60).

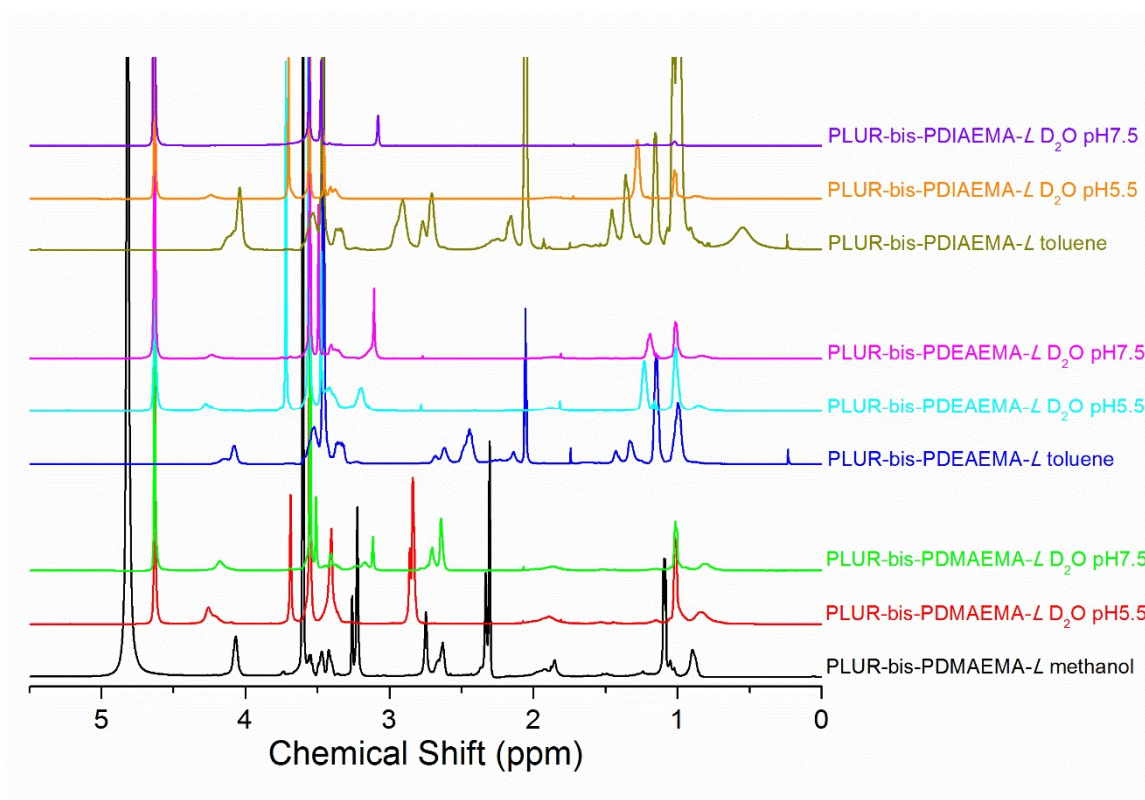


Figure 57: ¹H-NMR of PLUR-bis-PDMAEMA-L, PLUR-bis-PDEAEMA-L and PLUR-bis-PDIAEMA-L in deuterated toluene or methanol and in D₂O at pH 5.5 and 7.5.

PEG and PEG-bis-OH do not form micelles in solution. Extending their chains with the methacrylic moieties they do not aggregate when the pH-sensitive units are hydrophilic. Indeed, at acidic pH in D₂O all the signals of the methacrylic block are detectable. Increasing the pH and the hydrophobicity of the methacrylic chains the signals of these latter decrease until they are not detectable, confirming that PEG-Br and PEG-bis-Br derivatives can aggregate when the pH-sensitive units are hydrophobic.

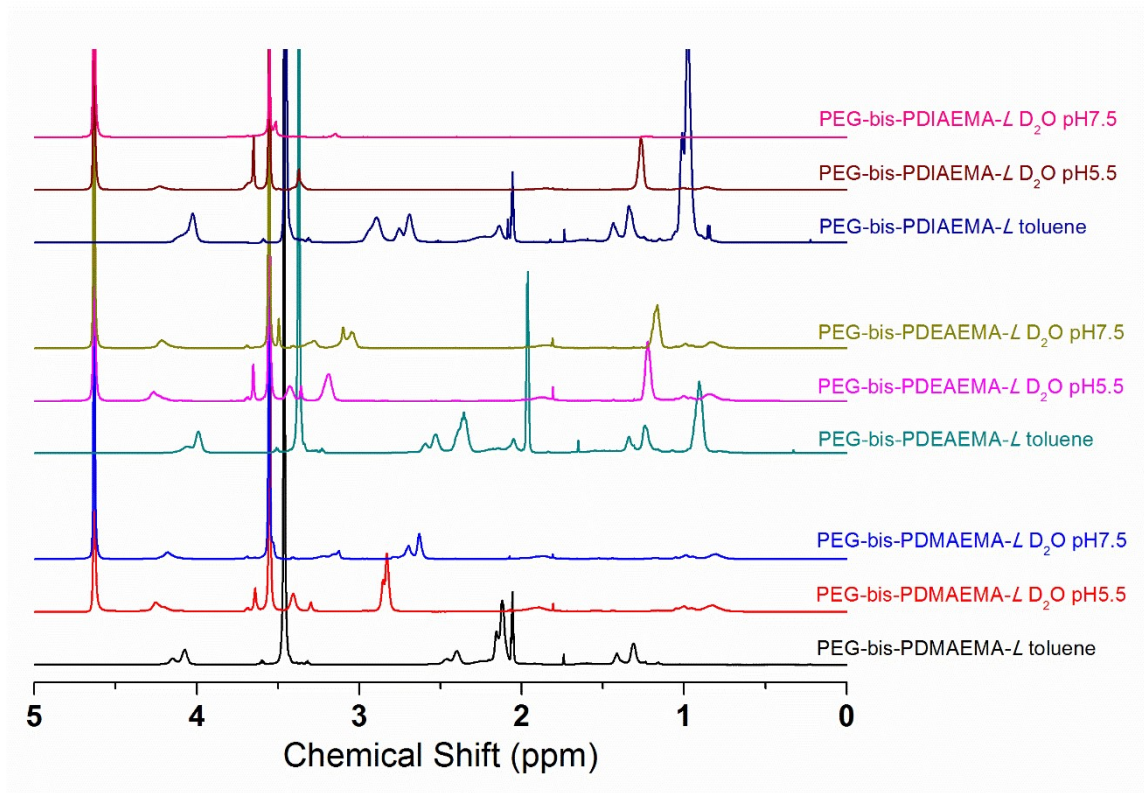


Figure 58 $^1\text{H-NMR}$ of PEG-bis-PDMAEMA-L, PEG-bis-PDEAEMA-L and PEG-bis-PDIAEMA-L in deuterated toluene and in D_2O at pH 5.5 and 7.5.

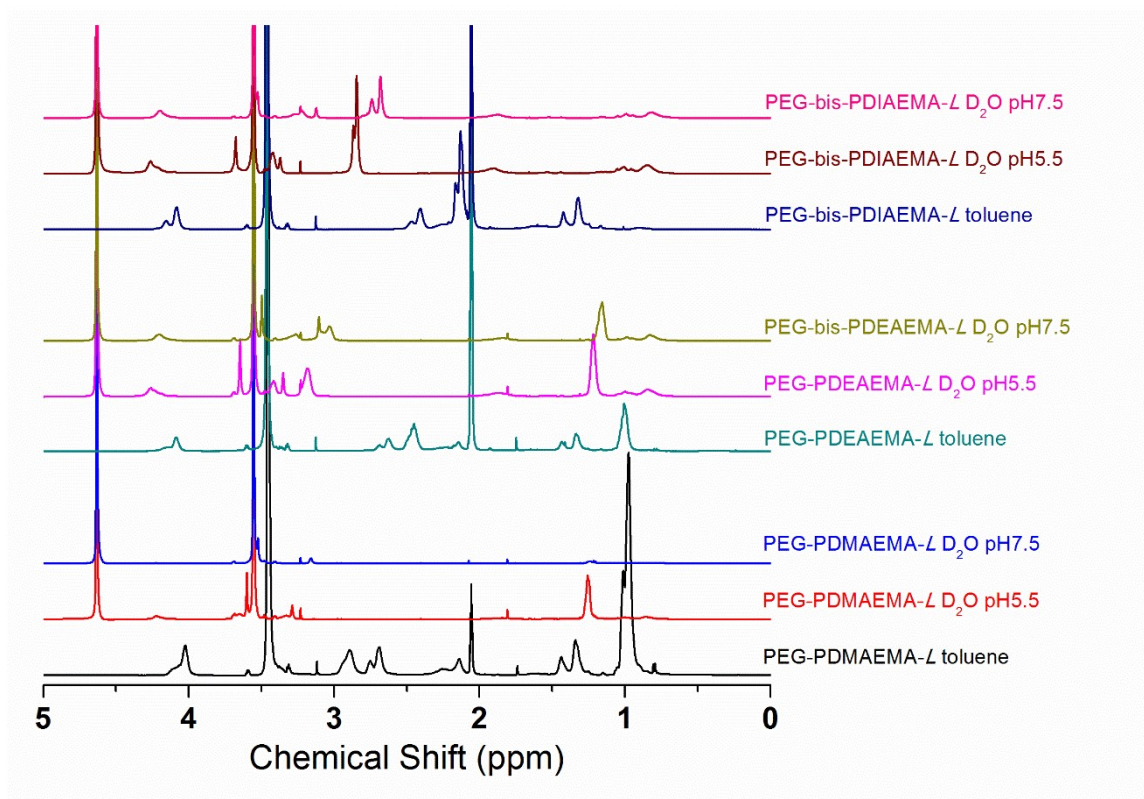


Figure 59: $^1\text{H-NMR}$ of PEG-PDMAEMA-L, PEG-PDEAEMA-L and PEG-PDIAEMA-L in deuterated toluene and in D_2O at pH 5.5 and 7.5.

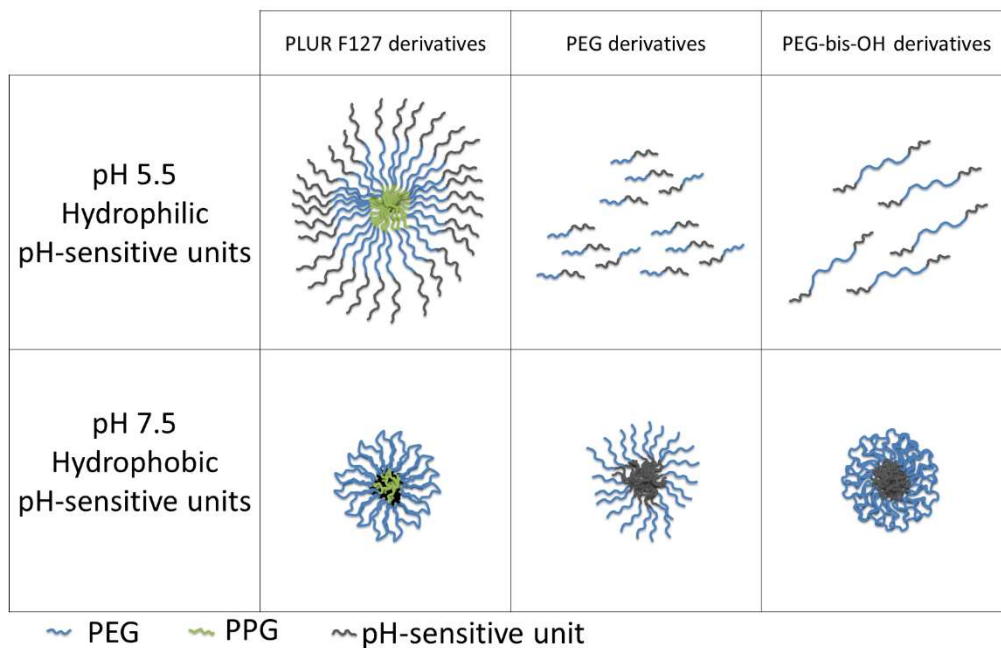


Figure 60: Schematic representation of the structures of polymeric derivatives at different pH in water solution

4.3.4 Rheological measurements

The values of storage and loss modulus (G' and G'') and viscosity (μ) of all the synthesized copolymers were determined by rheological measurements on their water solutions (polymer concentration 16.7% w/w) at different pH (5.5, 6.5 and 7.5) as a function of the temperature (in the range 5-70°C) in order to determine if and when the compounds self-assemble in gels (Figure 61). The collected data are reported in Table 30, Table 31 and Table 32. The rheological behavior of compounds not soluble at pH 6.5 and 7.5 was not studied.

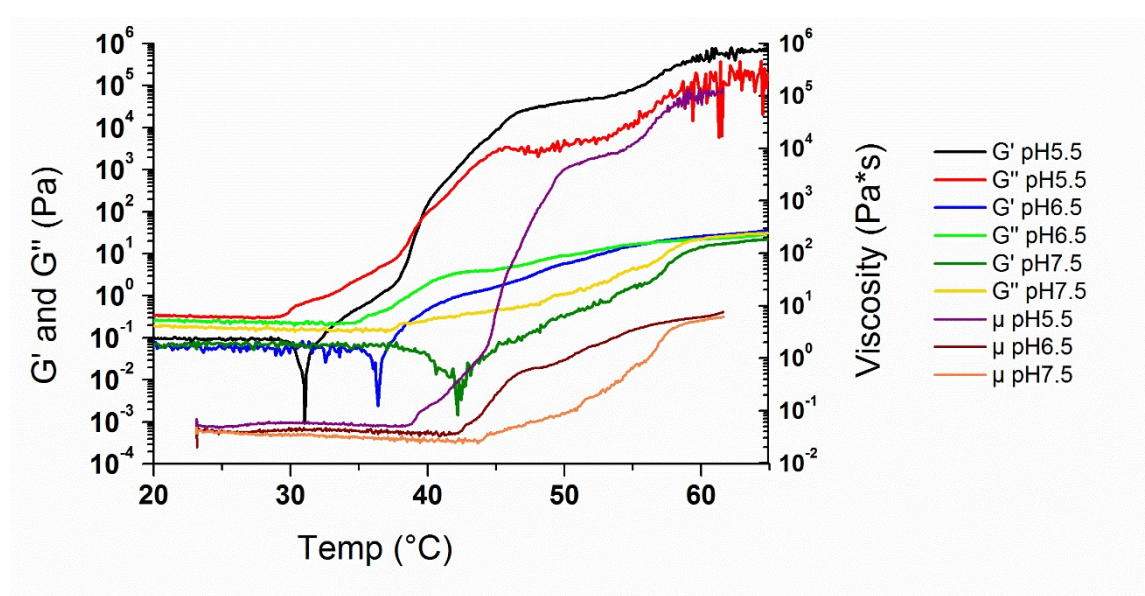


Figure 61: Rheological measurements (G' , G'' and viscosity) as a function of temperature of water solution containing 16.7 % (w/w) of PLUR-bis-PDEAEMA-S at different pH.

In Figure 62 the Gelation Temperature (GT, identified by G' - G'' crossing) of PLUR F127 and of its copolymeric derivatives are displayed as a function of pH. It is worth noting that the GT of PLUR F127 (23°C) does not change with the pH thus confirming that this material is not pH responsive. All PLUR F127 derivatives which can self-assemble in gels, instead, show GT higher than 23°C and with GT that increases with the pH (Table 30 and Figure 62). Furthermore, at lower pH, when gel forms, G' and G'' increase suddenly while the transition becomes less intense increasing the pH. This behavior suggests that compounds synthesized using PLUR-bis-Br tend to form gels when the methacrylic units are hydrophilic.

Such a behavior can be ascribed to the change in the polymeric structure at the different pH that can hamper the aggregation of the material in solution. Gelation transitions in PLUR compounds can be described as hard-sphere crystallization and their GT decreases with the dimension of the aggregates in solution. The increased GT with the pH of the synthesized PLUR F127 derivatives can be explained assuming that when the methacrylic chains are hydrophobic, they aggregate to constitute the small micelle core in solution (Figure 60). Thus, a higher temperature is required in order to form gel because of the lower dimension of the aggregates. When the methacrylic blocks are hydrophilic, instead, they constitute the aggregate shell with the PEG block, thus leading to the formation of big aggregates which do not need a higher temperature for gelation.

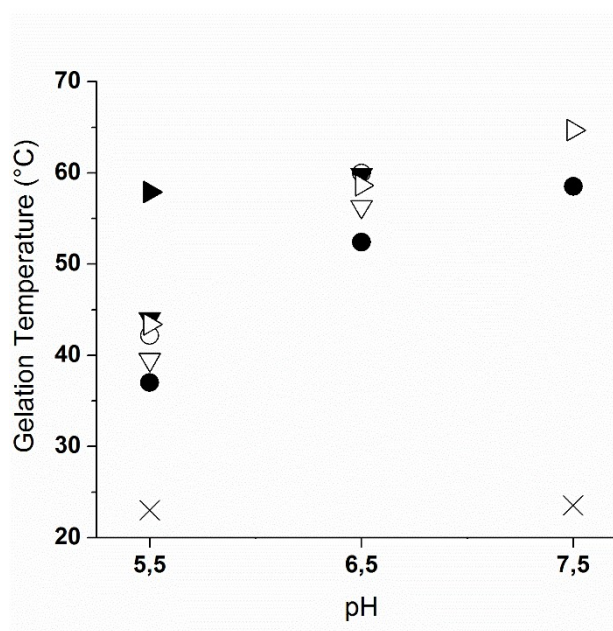


Figure 62: Gelation Temperature vs pH of PLUR F127 derivatives. PLUR F127 (X), PLUR-bis-PDMAEMA-S (○), PLUR-bis-PDMAEMA-L (●), PLUR-bis-PDEAEMA-S (∇), PLUR-bis-PDEAEMA-L (▼), PLUR-bis-PDIAEMA-S (▷) and PLUR-bis-PDIAEMA-L (▶).

In Table 30 the values of GT, G', G'' and μ before and after the gel formation of PLUR F127 derivatives are reported.

The suggested aggregation mechanism can be confirmed evaluating the values of viscosity before and after the gelation as a function of pH (Table 30). The viscosity of PLUR F127 gels does not change with the pH (~ 2000 Pa*s). PLUR F127 derivatives show stepwise increment of G' and G'' at low pH, forming gels with a higher viscosity than PLUR F127 (at least 10 times higher values). Such a behavior might be due to the presence of harder and bigger aggregates because of the longer external hydrophilic corona (PEG and

pH-sensitive unit) (Figure 60). At higher pH (6.5-7.5), the slope of G' and G'' around the gel transition is not as steep as at low pH and the viscosities of the gels are lower (e.g. PLUR-bis-PDMAEMA-S at pH 6.5). Owing to the presence of smaller aggregates, in these conditions the connection between these polymeric aggregates on which the gel is based might be weak and, as a result, the obtained gel is 'soft'. Being the gelation dependent on the concentration it might be possible to obtain hard gels even at high pH increasing the fraction of polymer in water. The supposed mechanism of aggregates and gels formation is represented in Figure 63.

The rheological measurements highlight that the synthesized materials change their aggregation as a function of the temperature and the pH as desired.

Table 30: Rheological properties of PLUR F127 and its derivatives.

| Sample | pH | GT ^a (°C) | G'/G'' at 20°C (Pa) | | G'/G'' at 65°C (Pa) | | μ at 20°C (Pa*s) | μ at 64°C (Pa*s) |
|--------------------|-----|-------------------------|------------------------|-------|---------------------|--------|----------------------------|----------------------------|
| | | | G' | G'' | G' | G'' | | |
| PLUR F127 | 5.5 | 23.0 | 0.0809 | 0.723 | 13300 | 1340 | 0.116 | 2120 |
| | 7.5 | 23.6 | 0.0968 | 0.611 | 12100 | 1500 | 0.0984 | 1940 |
| PLUR-bis-PDMAEMA-S | 5.5 | 42.2 | 0.0666 | 0.191 | 341000 | 111000 | 0.0322 | 54900 |
| | 6.5 | 60.0 | 0.0873 | 0.188 | 1180 | 788 | 0.0331 | 245 |
| PLUR-bis-PDMAEMA-L | 5.5 | 37.0 | 0.0010 | 0.200 | 1170000 | 941000 | 0.0310 | 239000 |
| | 6.5 | 52.4 | 0.0400 | 0.200 | 889000 | 206000 | 0.0310 | 145000 |
| | 7.5 | 58.5 | 0.0610 | 0.202 | 208000 | 38900 | 0.0335 | 36300 |
| PLUR-bis-PDEAEMA-S | 5.5 | 39.6 | 0.0969 | 0.336 | 707900 | 193000 | 0.0555 | 122000 |
| | 6.5 | 56.3 | 0.0631 | 0.262 | 35.2 | 29.0 | 0.0430 | 7.25 |
| PLUR-bis-PDEAEMA-L | 5.5 | 44.0 | 0.0243 | 0.264 | 513000 | 109000 | 0.0420 | 72400 |
| | 6.5 | 59.8 | 0.0388 | 0.216 | 2370 | 1190 | 0.0349 | 422 |
| PLUR-bis-PDIAEMA-S | 5.5 | 43.4 | 0.0514 | 0.325 | 1390000 | 321000 | 0.0529 | 232000 |
| | 6.5 | 58.6 | 0.0770 | 0.214 | 318000 | 110000 | 0.0361 | 53500 |
| | 7.5 | 64.7 | 0.0753 | 0.166 | 223 | 209 | 0.0289 | 48.7 |
| PLUR-bis-PDIAEMA-L | 5.5 | 57.9 | 0.112 | 0.182 | 23900 | 5850 | 0.0339 | 4090 |

^a Gelation Temperature (GT).

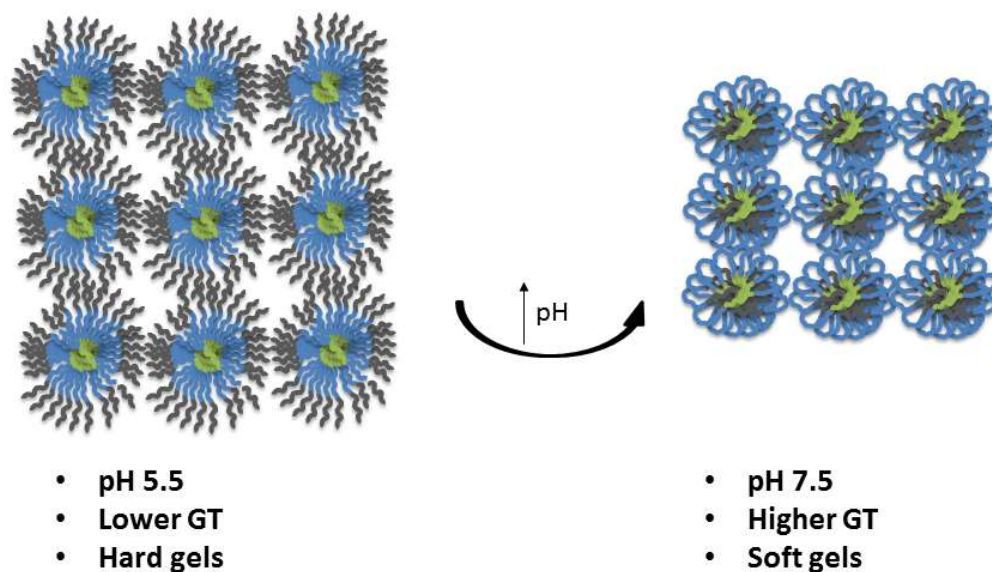


Figure 63: Schematic representation of PLUR F127 derivatives behavior in water (16.7% w/w).

As shown by the data reported in Table 31, PEG-bis-PDMAEMA does not self-assemble in gel at pH 5.5 because of the hydrophilic character of DMAEMA blocks. At pH 6.5, instead, a quite soft gel is formed but the transition is very broad. Increasing the hydrophobicity of the methacrylic moieties (PDEAMA and PDIAEMA) the materials aggregate in gels and the GT decreases with the pH, differently from the case of PLUR F127 derivatives. As seen before the viscosity of the gels is higher at lower pH. It is worth noting that PEG-bis-DEAEMA-*L* and PEG-bis-DIAEMA-*L* form gels even at lower pH (5.5). It can be supposed that even at pH 5.5 not all the methacrylic repeating units are protonated and some of the polymer chains contain hydrophobic block which lead to the aggregation. When the methacrylic chains are shorter most of the methacrylic repeating units are protonated and the material does not aggregate.

Thus these measurements highlight that in order to force the compounds to form aggregates a long hydrophobic methacrylic block is required. Furthermore, increasing the pH the hydrophobicity of the pH-sensitive units increases and so does the tendency of aggregation and the result of this behavior is a lower GT. Results from PEG-bis-OH derivatives confirm the mechanism of aggregation which was supposed for PLUR F127 derivatives: at lower pH the methacrylic chains are more hydrophilic; increasing their hydrophobicity the polymer aggregation changes in order to avoid interactions between water and hydrophobic pH-sensitive units.

Table 31: Rheological properties of PEG-bis-OH derivatives.

| Compound | pH | GT ^a (°C) | G'/G'' at 20°C (Pa) | | G'/G'' at 65°C (Pa) | | μ at 20°C (Pa*s) | μ at 64°C (Pa*s) |
|-------------------|-----|----------------------|---------------------|-------|---------------------|-------|----------------------|----------------------|
| | | | G' | G'' | G' | G'' | | |
| PEG-bis-PDMAEMA-L | 6.5 | 54.4 | 0.0862 | 0.206 | 19300 | 5430 | 0.0355 | 3190 |
| PEG-bis-PDEAEMA-L | 5.5 | 55.4 | 0.0893 | 0.186 | 97300 | 16200 | 0.0329 | 15700 |
| | 6.5 | 52.6 | 0.0854 | 0.189 | 11800 | 3090 | 0.0330 | 1940 |
| | 7.5 | 49.8 | 0.105 | 0.183 | 22400 | 3650 | 0.0336 | 3610 |
| PEG-bis-PDIAEMA-L | 5.5 | 57.0 | 0.0195 | 0.188 | 94000 | 23500 | 0.0300 | 15400 |
| | 6.5 | 55.3 | 0.0427 | 0.178 | 79700 | 12500 | 0.0291 | 12900 |

^a Gelation Temperature

As reported in Table 32, just few PEG derivatives self-assemble in gels, at least in the investigated range of temperature. It is worth noting that the gel formation is evidenced only at pH 5.5 and the resulting gels have viscosities that are comparable to those ones of PLUR F127 and PEG-bis-OH derivatives. Unfortunately, the fact that the GT is high at low pH and no gelation occurs below 55°C make these materials not suitable for the desired application. By increasing the pH, the gelation does not occur or, more likely, it happens at temperatures higher than 70°C. Even if it is not possible to determine a trend in the behavior of these polymers, rheological results are in agreement with the results previously obtained with PEG-bis-OH derivatives.

Table 32: Rheological properties of PEG derivatives.

| Compound | pH | GT ^a (°C) | G'/G'' at 20°C (Pa) | | G'/G'' at 65°C (Pa) | | μ at 20°C (Pa*s) | μ at 64°C (Pa*s) |
|---------------|-----|----------------------|---------------------|--------|---------------------|--------|----------------------|----------------------|
| | | | G' | G'' | G' | G'' | | |
| PEG-PDMAEMA-L | 5.5 | 60.6 | 0.0713 | 0.181 | 378000 | 214000 | 0.0309 | 72000 |
| PEG-PDEAEMA-S | 5.5 | 56.4 | 0.0078 | 0.174 | 602000 | 232000 | 0.0277 | 106000 |
| PEG-PDIAEMA-S | 5.5 | 64.0 | 0.0550 | 0.170 | 85900 | 25400 | 0.0284 | 14300 |
| PEG-PDIAEMA-L | 5.5 | 62.7 | 0.0086 | 0.1564 | 46100 | 11900 | 0.0250 | 7600 |

^a Gelation Temperature

4.3.5 DLS measurements

All the synthesized copolymers in water solutions (1mg/ml) in different pH buffers were analysed by DLS. In Figure 64 the phase diagram realized analysing the DLS results shows an overview of the products solubility in water at pH 5,6,7 and 8 at 25 and 37°C (body temperature). In these conditions some of the compounds are completely solubilized, other self-assemble in micelles and aggregates while the more hydrophobic result insoluble.

As shown by the phase diagram, all PLUR F127 derivatives, when soluble, self-assemble in aggregates or micelles. In PEG and PEG-bis-OH derivatives, instead, the aggregation is promoted by the increment of temperature, indeed only few compounds, those ones that contain hydrophobic chains, tend to aggregate at 25°C. In PEG and PEG-bis-OH derivatives aggregation is favourite when the methacrylic chains are hydrophobic. Furthermore, PEG-bis-OH derivatives contain a PEG hydrophilic block which is longer than in PEG derivatives. As a consequence, PEG-bis-OH derivatives require long hydrophobic pH-sensitive units in order to aggregate. At pH 7 and 8 some of the compounds containing PDIAEMA as pH-sensitive unit are not soluble in water because of the high hydrophobic character of the methacrylic block.

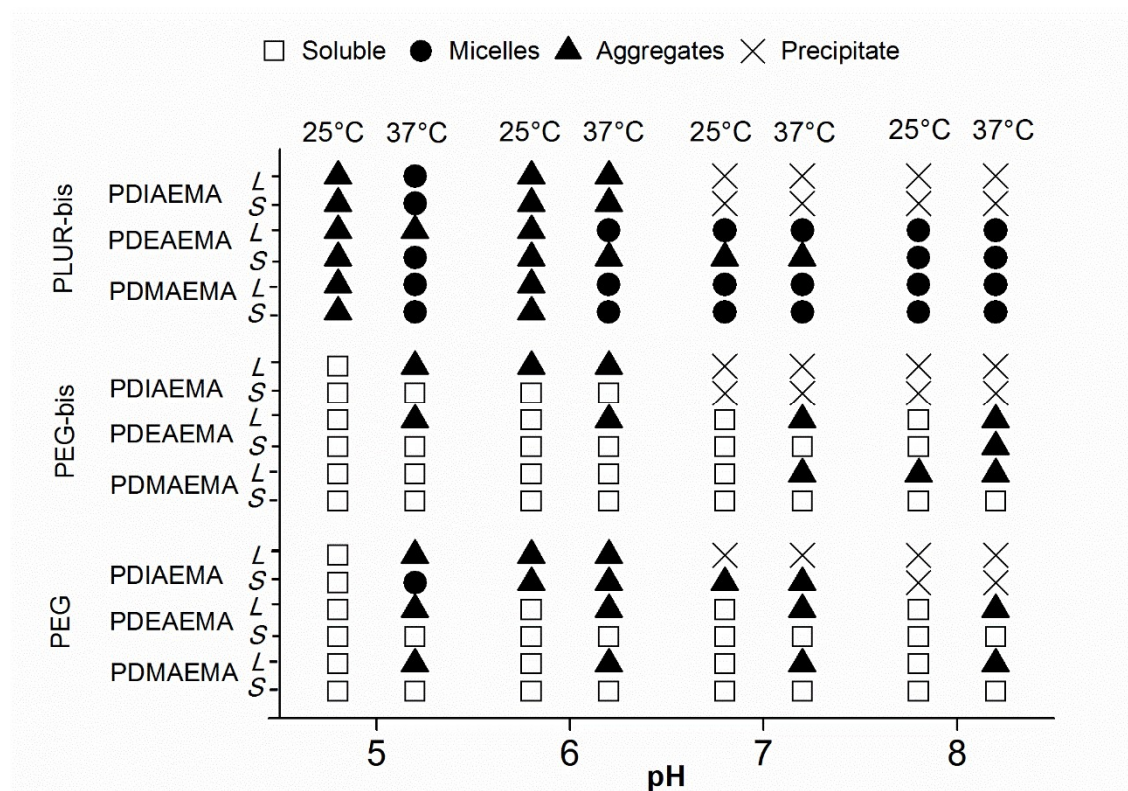


Figure 64: Phase diagram of the synthesized copolymers at 25 and 37°C (conc. 1mg/ml).

4.3.5.1 PLUR F127 derivatives

In Figure 66 the aggregate diameters of PLUR F127 and its derivatives determined by DLS at 25°C are displayed as a function of pH. PLUR F127 micelles have the same diameter at pH 5,6,7 and 8, further confirming its lacking in pH responsiveness.

Its derivatives, instead, self-assemble in micelles and aggregates whose diameter decreases with the pH reaching values comparable to PLUR F127 micelles at pH 8. No direct correlation between the size of the micelles and the methacrylic chain length can be detected because the degree of protonation and the hydrophilicity of the material depends not only on the pK_a of the amine group, but also on the polymeric chain length. Consequently, longer methacrylic chains can be hydrophobic because of the poor protonation, forming smaller aggregates compared to polymers with shorter methacrylic chains that can be completely protonated. The DLS results further confirm the supposed mechanism of aggregation discussed analyzing NMR spectra in organic and water solution at different pH and the rheological results (Figure 57): when the pH-sensitive units are hydrophilic, the aggregates are constituted by an external corona of PEG and methacrylic block; increasing the pH and thus the hydrophobicity of the methacrylic blocks, the polymer chains fold on themselves forming aggregates with a core of PPG and pH-sensitive units and allowing the PEG units to interact with water (Figure 60).

It is worth noting that at 25°C some compounds, e.g. PLUR-bis-PDIAEMA-L, arrange assuming a bi-modal size distribution (Figure 65), suggesting the presence of aggregates with different diameters (130-140 nm and 12-15nm). This result is reproducible and it was confirmed preparing new polymeric solutions. such a behavior could be ascribed to the presence of the methacrylic chain which hampers the aggregation that usually occurs in PLUR F127.

Increasing the temperature to 37°C, all the compounds that displayed a bi-modal size distribution at 25°C show a uni-modal size distribution which is generally centered at lower diameters values (Figure 65). This phenomenon can be ascribed to the higher tendency of aggregation of these compounds at higher temperature and to the decrease of the pK_a with the temperature. Decreasing the pK_a , the hydrophilicity of the pH-sensitive units decreases and the methacrylic chains tend to fold in order to form, together with PPG, the micelles' core, decreasing the size of the aggregates (Figure 60).

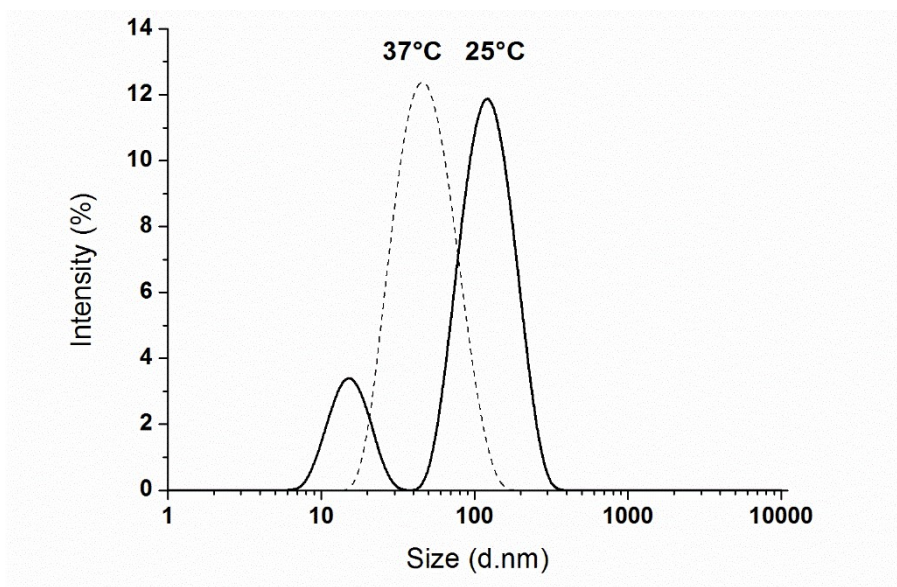


Figure 65: Size distribution by intensity of PLUR-bis-PDIAEMA-L measured by DLS at 25 and 37°C and pH 5 (conc. 1mg/ml).

As reported in Figure 66, the size of PLUR F127 aggregates in water solution at 37°C does not change significantly increasing the pH, at least in 16.7% (w/w) water solutions. Aggregates of PLUR F127 derivatives are generally smaller at 37°C than at 25°C. The major difference can be seen at pH 5: increasing the temperature, indeed, the size of the aggregates drops down (e.g. PLUR-bis-PDIAEMA-L passes from 130 to 40 nm at 25 and 37°C respectively). At pH 6,7 and 8 the sizes at 37°C are comparable to the ones at 25°C.

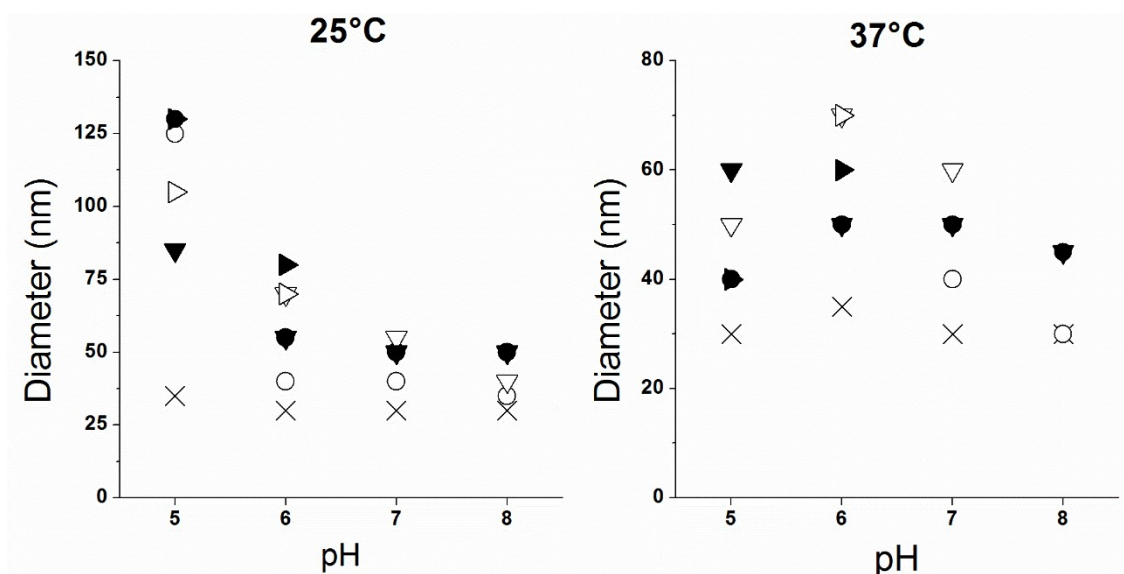


Figure 66: Aggregates diameter of the PLUR F127 derivatives as a function of pH at 25 and 37°C (conc. 1mg/ml). PLUR F127 (X), PLUR-bis-PDMAEMA-S (○), PLUR-bis-PDMAEMA-L (●), PLUR-bis-PDEAEMA-S (∇), PLUR-bis-PDEAEMA-L (▼), PLUR-bis-PDIAEMA-S (▷) and PLUR-bis-PDIAEMA-L (▶).

The lower diameter of the aggregates can be ascribed to the lowering of the pK_a with the temperature and to the enhanced aggregation described previously.

The Z potential of the solutions containing PLUR F127 derivatives was determined at 37°C and it is reported in Figure 67 as a function of pH. It is worth noting that the Z potential of PLUR F127 is close to zero and it does not change with the pH as expected for compounds with no ionizable groups. Those ones of PLUR F127 derivatives is positive at pH 5 (4-15 mV) and it decreases progressively with the pH reaching values close to zero at pH 8. The positive Z potential confirms that, when methacrylic chains are below their pK_a , they are partially protonated, making the aggregates positively charged. Increasing the pH, the degree of protonation decreases and so the Z potential.

Furthermore, by comparing the materials at a specific pH, we can see that, as expected, compounds with longer pH-sensitive blocks, which can be more protonated, are characterized by higher Z potential compared to the corresponding copolymers with shorter methacrylic chains.

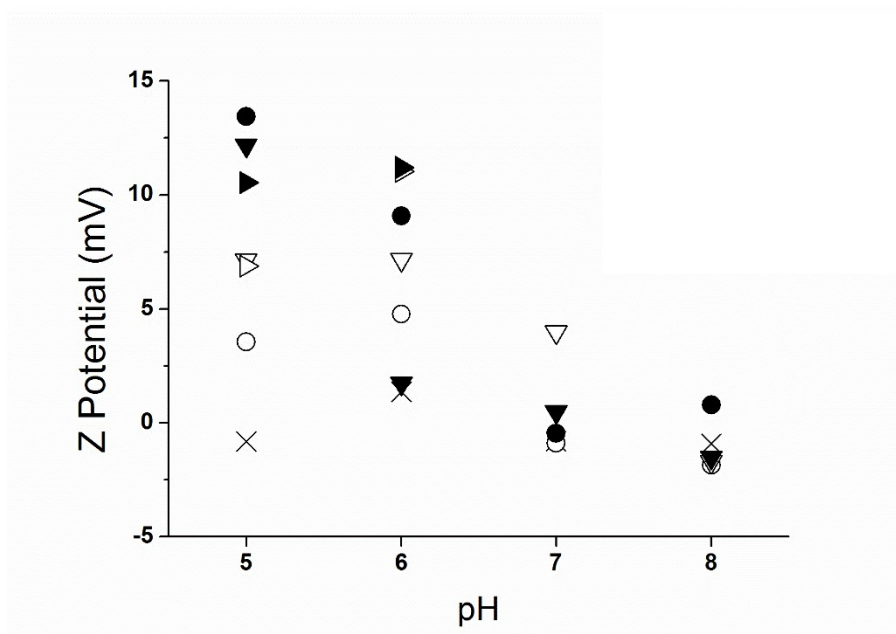


Figure 67: Zeta potentials of PLUR F127 derivatives as a function of pH at 37°C (conc. 1mg/ml). PLUR F127 (X), PLUR-bis-PDMAEMA-S (○), PLUR-bis-PDMAEMA-L (●), PLUR-bis-PDEAEMA-S (∇), PLUR-bis-PDEAEMA-L (▼), PLUR-bis-PDIAEMA-S (▷) and PLUR-bis-PDIAEMA-L (▶).

4.3.5.2 PEG and PEG-bis-OH derivatives

The aggregates diameters of PEG and PEG-bis-OH derivatives measured by DLS at 25 and 37°C as a function of pH are displayed in Figure 68 and Figure 69 and compared with those ones of PLUR F127 micelles.

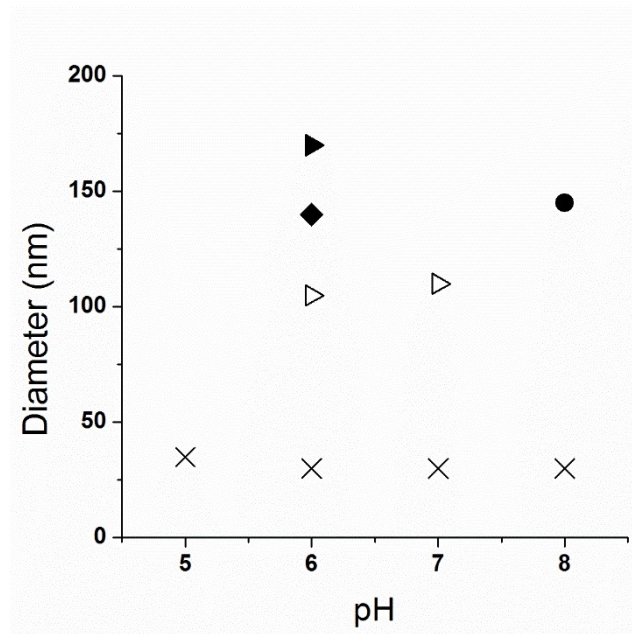


Figure 68: Aggregates diameter of PEG and PEG-bis derivatives as a function of pH at 25°C (conc. 1mg/ml). PLUR F127 (X), PEG-PDIAEMA-S (▷), PEG-PDIAEMA-L (▶), PEG-bis-PDMAEMA-L (●) and PEG-bis-PDIAEMA-L (◆).

It is worth noting that at 25°C only few compounds form aggregates (PEG-PDIAEMA-S, PEG-PDIAEMA-L, PEG-bis-PDMAEMA-L and PEG-bis-PDIAEMA-L) and all of them have a higher diameter than that one of PLUR F127 micelles (Figure 68). In particular, at pH 5, when most of the methacrylic chains are hydrophilic, no aggregation can be detected in all the samples. At higher pH, within the PEG derivatives, only those ones containing a strong hydrophobic block (PEG-PDIAEMA-S, PEG-PDIAEMA-L) self-assemble in micelles whose diameter depends on the molecular weight of this block.

Furthermore, the data reported in Figure 68 show that PEG-bis-OH derivatives can aggregate at 25°C only when their chains are extended with long methacrylic chains. In particular PEG-bis-PDIAEMA-L, thanks to the hydrophobicity of DIAEMA moieties, self-assembles only at pH 6: at higher pH it results not soluble. On the other side, PEG-PDMAEMA-L, because of the less hydrophobicity of DMAEMA units, results more soluble, but requires a higher pH (pH = 8) in order to allow the aggregation of the material.

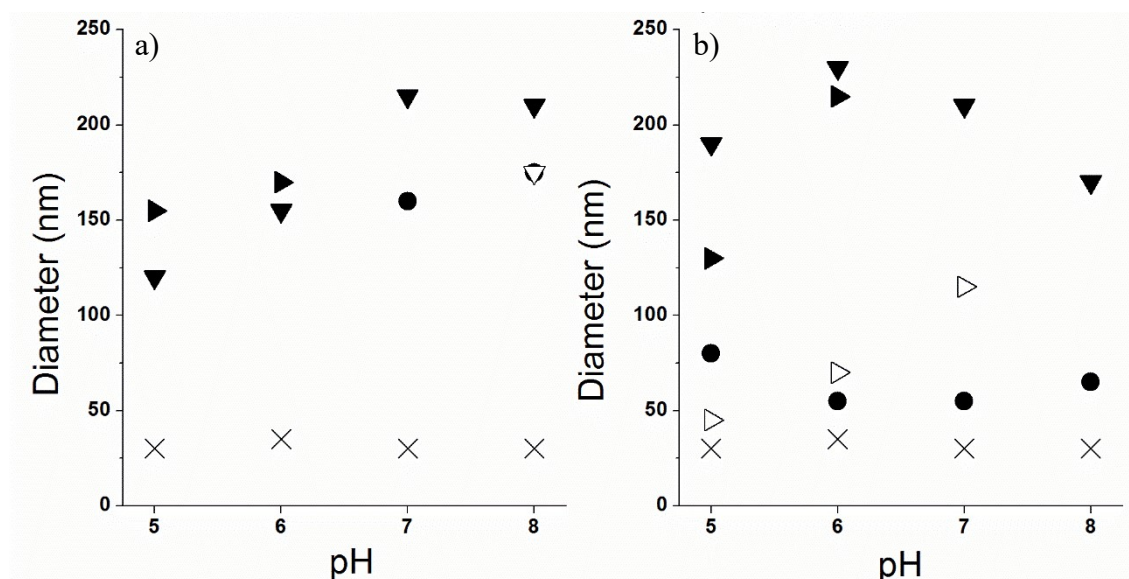


Figure 69: Aggregates diameter of PEG and PEG-bis derivatives as a function of pH at 37°C (conc. 1mg/ml). a) PLUR F127 (X), PEG-bis-PDMAEMA-L (●), PEG-bis-PDEAEMA-S (∇), PEG-bis-PDEAEMA-L (▼) and PEG-bis-PDIAEMA-L (▶). b) PLUR F127 (X), PEG-PDMAEMA-L (●), PEG-PDEAEMA-L (▼), PEG-PDIAEMA-S (▷) and PEG-PDIAEMA-L (▶).

At 37°C (Figure 69), the number of compounds that forms aggregates increases. PEG-PDMAEMA-L form aggregates with size around 50-100 nm at all the investigated pH. By increasing the hydrophobicity of the methacrylic chain (PEG-PDEAEMA-L, PEG-PDIAEMA-S and -L), the aggregates become bigger, but the materials result less soluble by increasing the pH. PEG-PDIAEMA-S and PEG-PDIAEMA-L, indeed, aggregate easily at lower pH, but they are not soluble at pH 8 and 7 respectively.

Similar trends are displayed by PEG-bis derivatives. Also in this case, by increasing the hydrophobicity of the methacrylic chains and their average molecular weight, the materials can self-assemble easily also at lower pH, but they become less soluble.

PEG-bis-PDMAEMA-L and PEG-bis-PDEAEMA-S, indeed, form aggregates only at high pH. PEG-PDIAEMA-L, instead, aggregates at low pH (5-6) but it is insoluble at pH 7 and 8.

In conclusion the aggregation of PEG and PEG-bis-OH derivatives results promoted by the increasing of the temperature and by the presence of a hydrophobic block. Furthermore, it depends also on the molecular weight of this block. It is reasonable to expect that when the material self-assembles, the hydrophobic moieties form the core of the aggregates while the PEG chains constitute the shell.

The Z potential of the PEG and PEG-bis-OH derivatives' aggregates was evaluated at 37°C and reported in Figure 70. The Z potentials of PEG and PEG-bis-OH derivatives is not stable changing the pH and it is not possible to see a trend as seen for PLUR F127 derivatives. These latter have a stable hydrophobic core that allows to form stable aggregates. PEG and PEG-bis-OH derivatives form aggregates that are not stable, at least at pH 5,6 and 7. So it is reasonable to expect that there is an equilibrium in solution between unimers and aggregates and the result is a Z potential value which is not stable. Comparing the Z potentials of PEG derivatives with the values of PLUR F127 derivatives it can be seen that with PEG derivatives the Z potential is much lower when the pH is acidic. Indeed, the Z potentials of PLUR F127 derivatives at pH 5 and 6 are among 4 and 15 mV.

Z potentials values of PEG derivatives demonstrate that some of the methacrylic chains are protonated but the degree of protonation is lower than in PLUR F127 derivatives. The lower degree of protonation makes the methacrylic chains more hydrophobic allowing the aggregation of the compounds in solution.

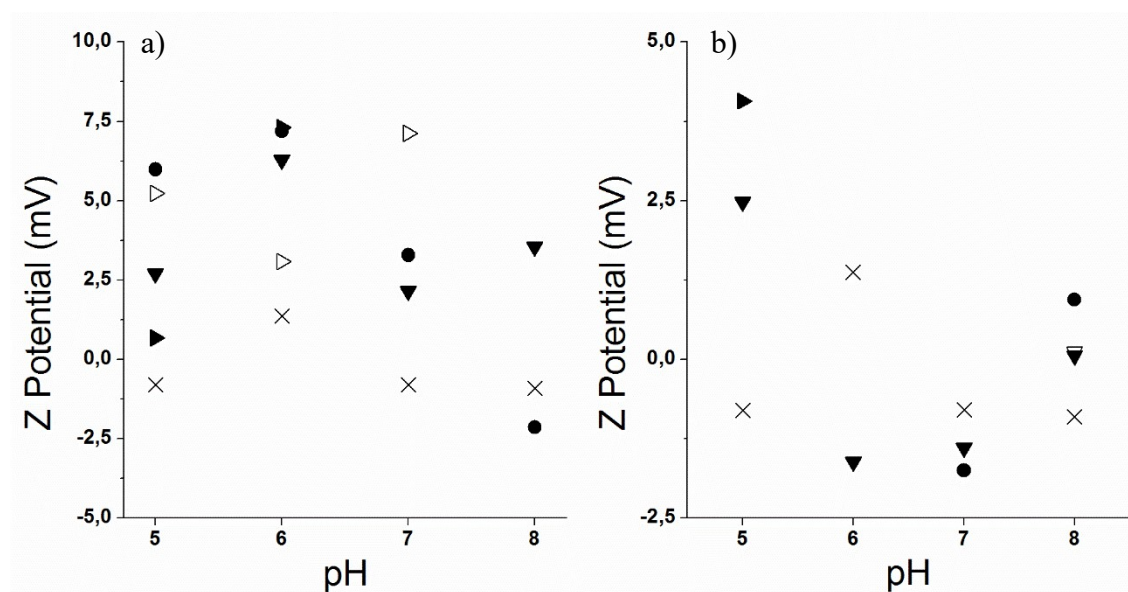


Figure 70: Zeta potentials of PEG and PEG-bis derivatives as a function of pH at 37°C (conc. 1mg/ml). a) PLUR F127 (X), PEG-PDMAEMA-L (●), PEG-PDEAEMA-L (▼), PEG-PDIAEMA-S (▷) and PEG-PDIAEMA-L (▶). b) PLUR F127 (X), PEG-bis-PDMAEMA-L (●), PEG-bis-PDEAEMA-S (▽), PEG-bis-PDEAEMA-L (▼) and PEG-bis-PDIAEMA-L (▶).

4.3.6 Loading measurements

Three selected materials, e.g. PEG-PDEAEMA-*L*, PEG-bis-PDEAEMA-*L* and PLUR-bis-PDEAEMA-*L*, were loaded with Nile Red, and the size of the aggregates and the fluorescence intensities of the solutions were determined.

Nile Red is a fluorescent molecule that in water solution quenches, determining a very low fluorescence intensity. Loading Nile Red into a water dispersion of polymeric aggregates, however, prevents its quenching and its fluorescence increases. As a consequence, the measurement of the fluorescence intensity of a mixture of Nile and self-assembled polymers can be directly correlated to the amount of Nile Red inside the polymeric aggregates.

The size of the loaded aggregates was determined by DLS at 25 and 37°C at pH 8 and the results are shown in Figure 71. The size of PLUR F127 micelles containing Nile Red is strongly influenced by the temperature and it decreases passing from 25 to 37°C reaching 40 nm which is comparable to the size of PLUR F127 micelles without Nile Red. For the three synthesized samples the size does not change significantly changing the temperature. The biggest aggregates are obtained with PEG-PDEAEMA-*L* and their size is comparable to unloaded aggregates. The size of PEG-bis-PDEAEMA-*L* and PLUR-bis-PDEAEMA-*L* loaded aggregates is lower compared to the size of unloaded micelles at the same temperature. Furthermore, PEG-PDEAEMA-*L* and PEG-bis-PDEAEMA-*L* form aggregate at 25°C in presence of Nile Red, while no aggregation occurs when no ‘drug’ is present in solution. The presence of Nile Red increase the aggregation by interacting the methacrylic chains.

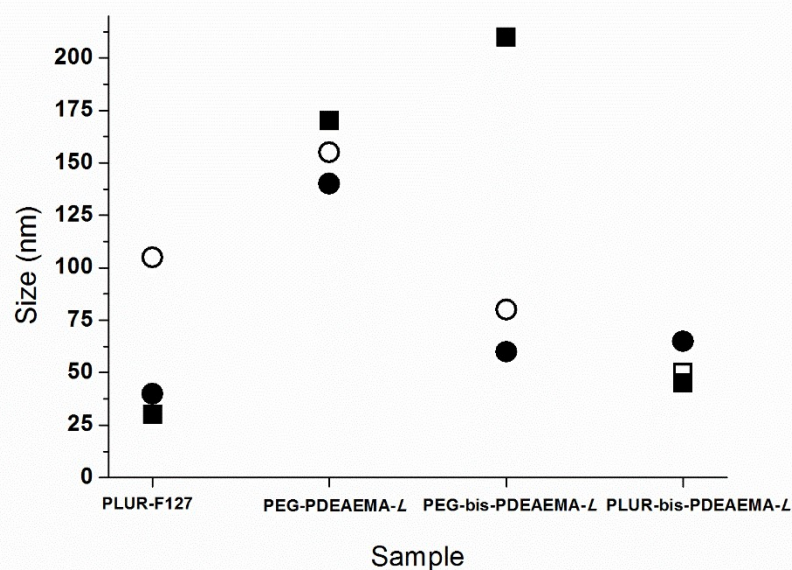


Figure 71: Aggregates diameter of PEG-PDEAEMA-L, PEG-bis-PDEAEMA-L, PLUR-bis-PDEAEMA-L and PLUR F127 loaded with Nile Red at pH 8 at 25°C (○) and 37°C (●) and without Nile Red at pH 8 at 25°C (□) and 37°C (■).

In Figure 72 the fluorescence intensity of solutions containing loaded aggregates with PLUR F127, PEG-PDEAEMA-L, PEG-bis-PDEAEMA-L and PLUR-bis-PDEAEMA-L at different pH is reported. The solutions were prepared and left overnight to reach equilibrium before measurements. As shown in Figure 72, PLUR F127 micelles display the highest fluorescence intensity and, as expected, no pH responsiveness is observed. PEG-PDEAEMA-L and PEG-bis-PDEAEMA-L aggregates show very low fluorescence intensity at pH 5-7 which increases at pH 8. These results demonstrate that, in order to obtain stable aggregates containing Nile Red in the core, a basic pH is required. At pH 8, indeed, all the methacrylic chains are hydrophobic, allowing the product to form stable aggregates that can solubilize Nile Red.

As seen for PLUR F127 micelles, with PLUR-bis-PDEAEMA-L the fluorescence intensities do not change with the pH, though it is lower than the one of PLUR F127 micelles. PLUR-bis-PDEAEMA-L can incorporate Nile Red at the investigated pH because of the presence of the hydrophobic PPG core and the change in the hydrophobicity of the methacrylic chains does not affect the incorporation.

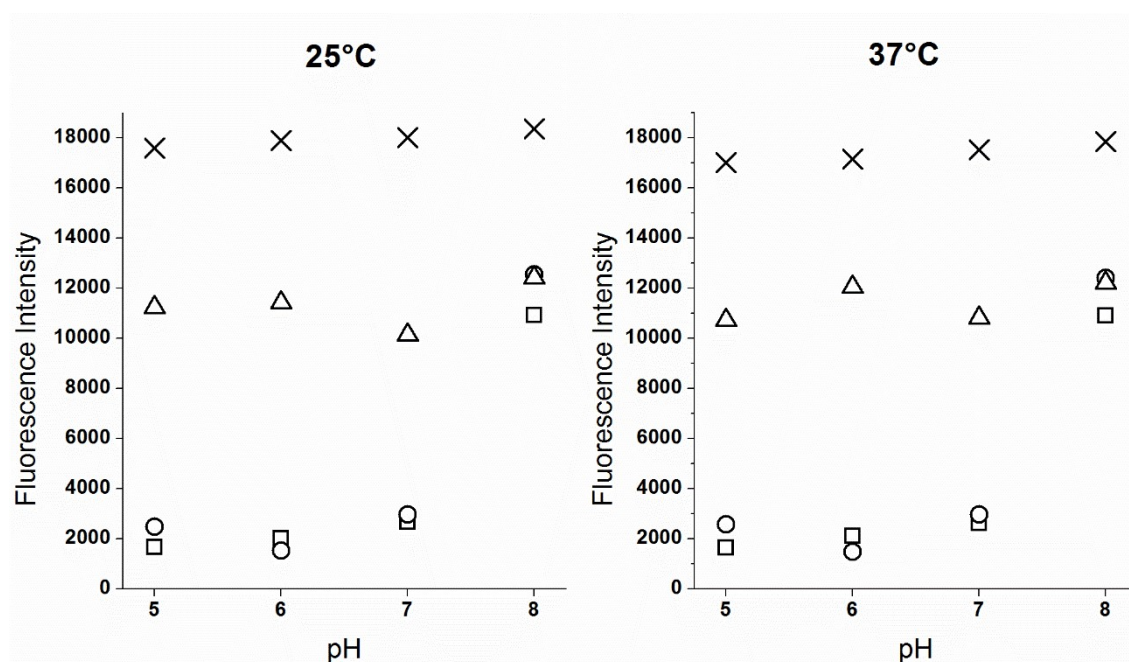
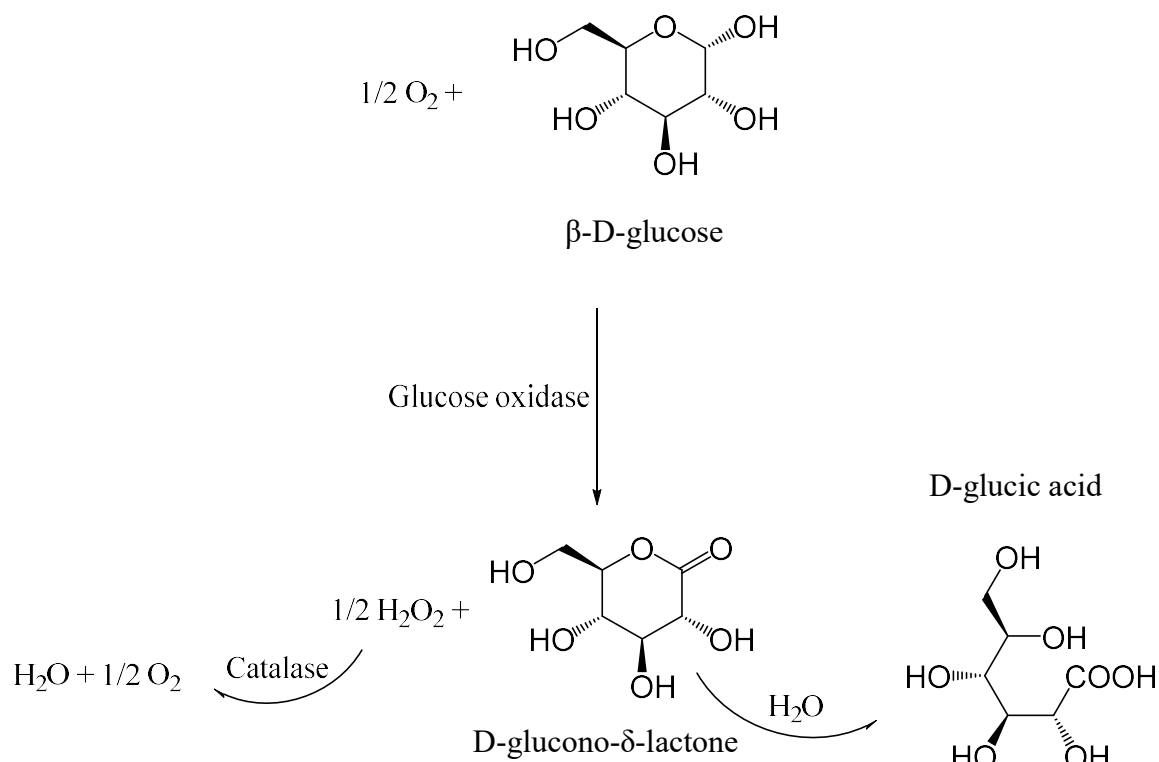


Figure 72: Fluorescence intensity of PEG-PDEAEMA-L, PEG-bis-PDEAEMA-L, PLUR-bis-PDEAEMA-L and PLUR-F127 aggregates loaded with Nile Red at 25 and 37°C at different pH. PLUR F127 (X), PEG-PDEAEMA-L (□), PEG-bis-PDEAEMA-L (○) and PLUR-bis-PDEAEMA-L (△).

DLS measurements showed that the size of PLUR-bis-PDEAEMA-L micelles changes with the pH as a consequence of the changing in the hydrophilicity of the pH-sensitive moieties. In order to understand whether the change in the polymer aggregation affects the release, the pH of PLUR-bis-PDEAEMA-L loaded with Nile Red solutions was changed progressively and the fluorescence intensity was continuously recorded. In order to change the pH in a controlled way, a solution of glucose oxidase in presence of PLUR-bis-PDEAEMA-L, glucose and catalase was used. The reactions involved are shown in Scheme 17. A solution containing PLUR-bis-PDEAEMA-L, loaded with Nile Red, glucose, catalase and glucose oxidase was prepared and the pH was determined as a function of time.



Scheme 17: Reaction scheme of glucose oxidase reaction in presence of catalase.

The kinetic was studied at 25 and 37°C and the results reported in Figure 73 show that the pH of the solution decreases progressively passing from 8 to stable values around 3.5-4 in 30 minutes. The kinetic is faster at 37°C.

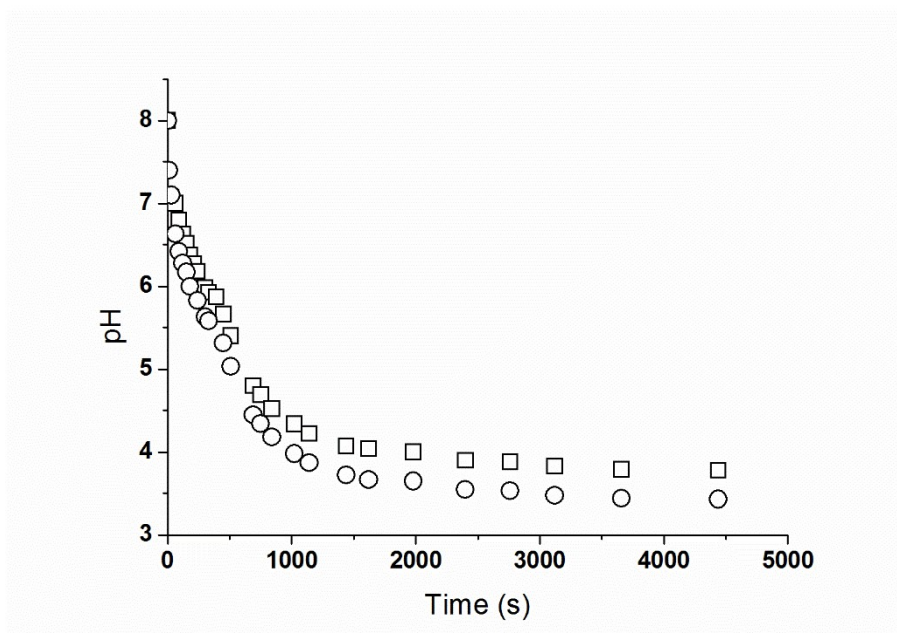


Figure 73: pH as a function of time of 1mg/ml water solution of PLUR-bis-PDEAEMA-L loaded with Nile Red in presence of Glucose oxidase at 25°C (□) and 37°C (○).

A fresh solution of PLUR-bis-PDEAEMA-L loaded with Nile Red containing catalase, glucose and glucose oxidase was prepared and its fluorescence intensity was determined as a function of time. Knowing the dependence of the pH with the time it was possible to correlate the values of fluorescence intensities to the pH of the solution (Figure 74). The fluorescence intensity decreases significantly when the pH starts to decrease. Then, at pH lower than 5.5 it increases again. This behavior well agrees with the expectation: when the methacrylic chains start to be protonated becoming hydrophilic, the aggregates change structure and the drug is released in the media. The fluorescence intensity increases again because when the system is stable and the pH changes slowly, the drug can be solubilized again in the polymeric aggregates reaching the equilibrium condition seen in Figure 72. During the application of the synthesized materials, when the anti-cancer drug is released in the target zone it interacts with the cells and thus should not be solubilized again in the polymeric aggregates.

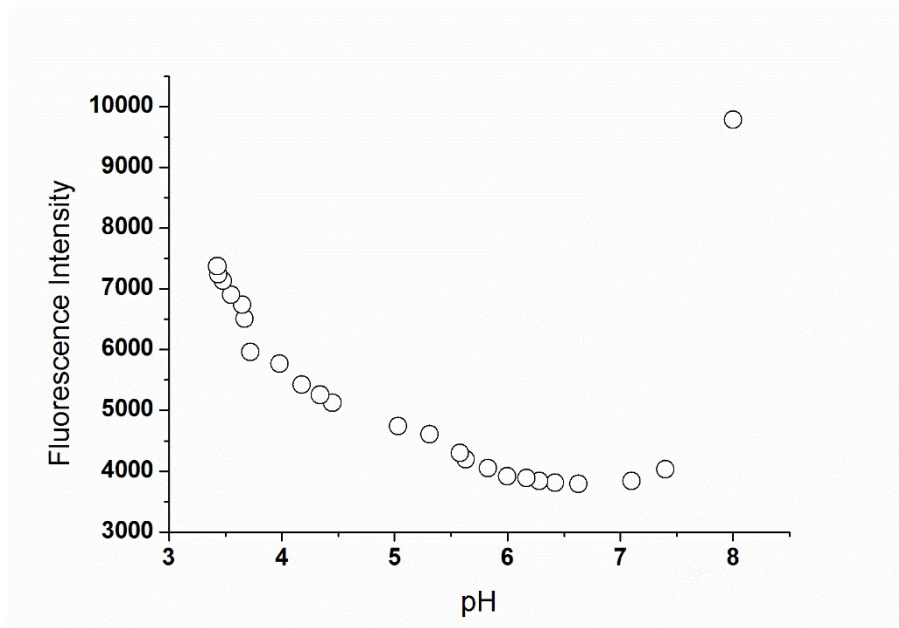


Figure 74: Fluorescence intensity of PLUR-bis-PDEAEMA-L decreasing progressively the pH in presence of glucose oxidase.

In conclusion, PEG and PEG-bis-OH derivatives are not suitable for the desired application because their aggregate are not stable enough to obtain good loading and release of the drugs. Furthermore, their GT are too high to be applied at the body temperature. The study of their behavior, anyway, allowed to explain and further understand the behavior of PLUR F127 derivatives.

PLUR F127 derivatives self-assemble in gels at a temperature which can be suitable for biomedical applications and it can be tuned changing the methacrylic moieties. Furthermore, they shown pH and temperature responsiveness and the possibility to change their structure changing pH of the environment make them suitable for controlled targeted drug release.

4.4 Conclusions

ATRP method was successfully employed for the polymerization of DMAEMA, DEAEMA and DIEAMA in presence of mono and di-functional PEGylated and Pluronic-based macroinitiators.

Proper ATRP macroinitiator were synthesized starting from PLUR F127, PEG-bis-OH and PEG in presence of 2-bromoisobutyryl bromide. Block copolymers with different methacrylic (and pH-sensitive) chain length (18 different final materials) were synthesized on the basis of the polymerizations kinetics studied previously.

DLS measurements highlight that the synthesized compounds can self-organize in water solutions (1mg/mL), and the dimension of the aggregates is pH-dependent. ¹H-NMR in D₂O solution (pH= 5.5 and 7.5) confirm, by the decreasing of the methacrylic signal intensities with increasing the pH, the presence of aggregates as determined by DLS. Loading measurements, carried out in presence of Nile Red and at different pH (5, 6, 7, 8) show that the aggregates can incorporate hydrophobic molecules, and this characteristic can be exploited to enhance the solubility of hydrophobic drugs, such as doxorubicin (a common anti-cancer drug). The loading of the drug depends on the macromolecular structure and composition and on the pH of the environment. The loading measurements show that, in order to obtain a suitable incorporation of the drug inside stable aggregates, the presence of an hydrophobic block is required.

Fluorescence measurements demonstrate that once the drug is inside the hydrophobic core of the aggregates made by PLUR-bis-PDEAEMA-L, the drug is released as a consequence of the change in the macromolecular configuration in solution (when the pH is changed progressively from 8 to 3.5), making this compound suitable for the development of drug-delivery systems. Indeed, this characteristic can be exploited when, in the body fluids, the pH decreases in presence of cancer cells, allowing the controlled release of the drug directly in the target zone.

Some of the synthesized materials (such as PLUR-bis-PDEAEMA-L), in presence of water [16.7% (wt)], display gelation transitions which depend on the macromolecular structure and on the pH of the solutions. Rheological measurements results show that it is possible to modulate the GT changing the molecular structure and the pH-sensitive units length, in order to obtain materials with GT close to the body temperature, as desired.

PLUR-bis-PDEAEMA-L aggregates can be loaded with hydrophobic drugs, with the aim to inject water solutions that form gels when they reach the body temperature. The gel

phase will release loaded micelles that, when close to the target zone (cancer cells), will release the drug, maintaining a constant concentration of pharmaceutical throughout the entire period of administration.

The developed system, applied in the field of drug-delivery, can decrease the amount of administrated drug, the number of administration the patient should be submitted to and the many side effect that the use of common anti-cancer techniques implies.

4.5 Experimental section

4.5.1 Physico-chemical characterization

¹H-NMR spectra were recorded on 1% wt. solutions in deuterated solvents using a DRX 500 Avance, Bruker Biospin GmbH spectrometer (Rheinstetten Germany). FT-IR spectra were recorded in ATR mode on a Shimadzu FTIR-8400S spectrometer (Duisburg, Germany).

MALDI spectra were recorded on 1 mg/mL polymer solutions in *N,N*-dimethylformamide using a Bruker ultrafleXtreme mass spectrometer.

Molecular weight distributions were obtained via Gel Permeation Chromatography (GPC) using a Tosoh Bioscience TSKgel GMH_{HR}-N 5-micron column operating at 70°C. DMF was used as eluent at a flow rate of 1.0 mL min⁻¹. A series of near-mono-dispersed linear poly(ethylene glycol) standards (Fluka; Gillingham, UK) was used for calibration with a refractive index detector for the analysis of the polymers.

Rheological measurements were performed on a Haake Mars Rotational Rheometer in parallel plate configuration (20 mm upper plate diameter; gap: 300 μm; volume applied: 200 μL). The solutions were prepared as follows: 0.30 g of solid were dispersed in 1.5 mL of deionized water [16.7% (w/w)] adjusted at pH = 4 with concentrated HCl and left overnight at 3°C. The solution was finally split in three 0.5 mL aliquots and their pH adjusted to 5.5, 6.5, 7.5 using concentrated NaOH (addition of less than 25 μL, i.e. insignificant variations in the polymer concentration). Loss (G'') and storage (G') moduli were recorded on the solutions as a function of temperature (5 to 70°C homogeneously increased within 45 minutes at a rate of about 1.2°C/min) applying a shear stress of 10 Pa with a frequency of 1 Hz.

The hydrodynamic radii of micelles were determined by dynamic light scattering (DLS) using a Malvern Zetasizer Nano ZS equipped with a 173° backscatter detector and a He-Ne laser (633nm). The solutions were placed into poly(styrene) 4 optical faces cuvettes with 1 cm optical pathlength.

4.5.2 Materials

All chemicals were used as received from suppliers unless otherwise stated.

Poly(ethylene glycol) monomethyl ether (PEG), poly(ethylene glycol) diol (PEG-bis-OH), Pluronic F127 (PLUR-F127), with \overline{M}_n = 5,292 g/mol, 8,878 g/mol and 13,322 g/mol respectively (from MALDI measurements), triethylamine, toluene, n-hexane, 2-bromoisobutyryl bromide, dichloromethane (DCM), dimethylformamide (DMF), copper (I) chloride (CuCl), 2,2'-bipyridyl (Byp), ethylenediaminetetraacetic acid (EDTA) and Nile Red were purchased from Sigma-Aldrich (Gillingham, UK). 2-(*N,N*-dimethylamino)ethyl methacrylate (DMAEMA), 2-(*N,N*-diethylamino)ethyl methacrylate (DEAEMA) and 2-(*N,N*-diisopropylamino)ethyl methacrylate (DIAEMA) were all purchased from Sigma-Aldrich (Gillingham, UK) and passed through a column filled with neutral alumina, just before use. All other chemicals were of analytical grade and used without further purification.

4.5.3 Preparative procedures

Synthesis of ATRP macroinitiators: Poly(ethylene glycol) (2-bromoisobutyrate) monomethyl ether (PEG-Br), poly(ethylene glycol) bis(2-bromoisobutyrate) (PEG-bis-Br), Pluronic F127 bis(2-bromoisobutyrate) (PLUR-bis-Br).

In a typical procedure, 11 g of precursor (corresponding to 2.1 mmol OH groups for PEG, 2.5 mmol for PEG-bis-OH and 0.8 mmol for PLUR-F127) and 300 mL of toluene were introduced under inert Ar atmosphere into a 500 mL three-necked flask connected to Soxhlet apparatus filled with activated molecular sieves and a cooling tower. The solution was azeotropically dried for two hours, cooled at room temperature and further cooled to 5°C into an ice bath. 6.7 equivalents of triethylamine and 5 equivalents of 2-bromoisobutyryl bromide dissolved in 20 mL of DCM were then added dropwise, stirring the heterogeneous mixture for one hour. At the end of the reaction 0.3 mL of water and sodium carbonate were added to the stirred reaction mixture and the solid removed by filtration; the solvents were almost completely removed under vacuum. 40 mL of DCM were added to the residual solution and this latter was washed with 5x10 mL of acetic acid solution (5% wt in water), with 10x10 mL of sodium bicarbonate solution (5%wt in water) and the collected organic phases finally dried over sodium sulfate. The solvent was removed until the solution reached a volume of 20 mL, and the mixture was precipitated twice in excess of hexane (10:1 v:v hexane:DCM) and a white powder was obtained.

PEG-Br: Yields: 87 %wt., conversion (by $^1\text{H-NMR}$): 98 %mol

$^1\text{H-NMR}$ (CDCl_3): $\delta = 1.87$ (s, 6H, $-\text{C}(\text{Br})(\text{CH}_3)_2$), 3.31 (s, 3H, $-\text{CH}_2\text{CH}_2\text{OCH}_3$), 3.43 and 3.72 (side bands of the peak at 3.58 ppm), 3.48 (t, 2H, $-\text{CH}_2\text{OCH}_3$), 3.58 (b, PEG mainchain, $-\text{CH}_2\text{CH}_2\text{O}-$), 3.68 (t, 2H, $-\text{OCH}_2\text{CH}_2\text{OC}(\text{O})\text{C}(\text{Br})(\text{CH}_3)_2$), 4.25 (t, 2H, $-\text{CH}_2\text{CH}_2\text{OC}(\text{O})\text{C}(\text{Br})(\text{CH}_3)_2$) ppm.

ATR FT-IR: shoulder at 2945 ($\nu_{\text{as}} \text{CH}_2$), 2882 ($\nu_{\text{s}} \text{CH}_2$), 1734 ($\nu_{\text{s}} \text{C}=\text{O}$), 1466 ($\delta_{\text{s}} \text{CH}_2$), 1279, 1240, 1098 ($\nu_{\text{as}} \text{C-O-C}$) cm^{-1} .

PEG-bis-Br: Yields: 98 %wt., conversion (by $^1\text{H-NMR}$): 95 %mol

$^1\text{H-NMR}$ (CDCl_3): $\delta = 1.87$ (s, 12H, $-\text{C}(\text{Br})(\text{CH}_3)_2$), 3.43 and 3.71 (side bands of the peak at 3.57 ppm), 3.57 (b, PEG mainchain, $-\text{CH}_2\text{CH}_2\text{O}-$), 3.67 (t, 4H, $-\text{OCH}_2\text{CH}_2\text{OC}(\text{O})\text{C}(\text{Br})(\text{CH}_3)_2$), 4.25 (t, 4H, $\text{OCH}_2\text{CH}_2\text{OC}(\text{O})\text{C}(\text{Br})(\text{CH}_3)_2$) ppm.

ATR FT-IR: shoulder at 2945 ($\nu_{\text{as}} \text{CH}_2$), 2880 ($\nu_{\text{s}} \text{CH}_2$), 1734 ($\nu_{\text{s}} \text{C}=\text{O}$), 1466 ($\delta_{\text{s}} \text{CH}_2$), 1279, 1242, 1098 ($\nu_{\text{as}} \text{C-O-C}$) cm^{-1} .

PLUR-bis-Br: Yields: 95 %wt., conversion (by $^1\text{H-NMR}$): 100 %mol

$^1\text{H-NMR}$ (CDCl_3): $\delta = 1.07$ (b, PPG main chain, $-\text{CH}_2\text{CH}(\text{CH}_3)\text{O}-$), 1.87 (s, 12H, $\text{C}(\text{Br})(\text{CH}_3)_2$), 3.32 (b, PPG mainchain, $-\text{CH}_2\text{CH}(\text{CH}_3)\text{O}-$), 3.48 (b, PPG mainchain, $-\text{CH}_2\text{CH}(\text{CH}_3)\text{O}-$), 3.57 (b, PEG main chain, $-\text{CH}_2\text{CH}_2\text{O}-$), 3.67 (t, 4H, $-\text{OCH}_2\text{CH}_2\text{OC}(\text{O})\text{C}(\text{Br})(\text{CH}_3)_2$), 3.71 (side bands of the peak at 3.65 ppm), 4.25 (t, 4H, $\text{OCH}_2\text{CH}_2\text{OC}(\text{O})\text{C}(\text{Br})(\text{CH}_3)_2$) ppm.

ATR FT-IR: shoulder at 2968 ($\nu_{\text{as}} \text{CH}_2$), 2880 ($\nu_{\text{s}} \text{CH}_2$), 1734 ($\nu_{\text{s}} \text{C}=\text{O}$), 1466 ($\delta_{\text{s}} \text{CH}_2$), 1279, 1242, 1101 ($\nu_{\text{as}} \text{C-O-C}$) cm^{-1} .

Synthesis of block copolymers: Poly(ethylene glycol) monomethyl ether-block-poly[2-(*N,N*-dimethylamino)ethyl methacrylate] (PEG-PDMAEMA), poly(ethylene glycol) monomethyl ether-block-poly[2-(*N,N*-diethylamino)ethyl methacrylate] (PEG-PDEAEMA), poly(ethylene glycol) monomethyl ether-block-poly[2-(*N,N*-diisopropylamino)ethyl methacrylate] (PEG-PDIAEMA), poly(ethylene glycol) bis-block-poly[2-(*N,N*-dimethylamino)ethyl methacrylate] (PEG-bis-PDMAEMA), poly(ethylene glycol) bis-block-poly[2-(*N,N*-diethylamino)ethyl methacrylate] (PEG-bis-PDEAEMA), poly(ethylene glycol) bis-block-poly[2-(*N,N*-diisopropylamino)ethyl methacrylate] (PEG-bis-PDIAEMA), Pluronic F127 bis-block-poly[2-(*N,N*-dimethylamino)ethyl methacrylate] (PLUR-bis-PDMAEMA), Pluronic F127 bis-block-

poly[2-(*N,N*-diethylamino)ethyl methacrylate] (PLUR-bis-PDEAEMA), Pluronic F127 bis-block-poly[2-(*N,N*-diisopropylamino)ethyl methacrylate] (PLUR-bis-PDIAEMA).

In a typical procedure, the ATRP were carried out using a 70:2:1:1 monomer: ligand: catalyst: initiator groups molar ratio. The appropriate macroinitiator, CuCl and 2,2'-Bpy were introduced into a Schlenk tube equipped with a stirring bar and the tube was placed under argon atmosphere by three vacuum/argon cycle. Monomer and toluene were degassed with argon purge for at least 30 min at room temperature into two calibrated Schlenk tubes. Then toluene was added to the monomer in order to have an initial monomer concentration of 25% (vol.) and the flask was placed in a thermostated oil bath at 60°C and stirred until all the solid was solubilized. Finally, the obtained solution was added to the reaction Schlenk containing the macroinitiator and the mixture was stirred at 60°C. To terminate the polymerization reaction, after given reaction times the solution was exposed to air and the catalyst oxidized from the atmospheric oxygen. The obtained polymers were purified by extraction with acidic water (pH=5) followed by dialysis (molecular weight cut off (MWCO) = 3 KDa) in diluted HCl solution (pH=5) with EDTA 10 mM then in bicarbonate water solution (pH 8) with EDTA 10mM and finally in deionized water until constant conductivity (equal to the one of the starting deionized water). At the end of the dialysis the water was removed by sublimation and a white powder was obtained.

Each polymerization was repeated twice; the initial monomer concentration and copolymers compositions were determined by ¹H-NMR after removing the catalyst by filtration on basic alumina. For kinetic studies, 0.15 mL samples were collected at different intervals.

PEG-PDMAEMA: ¹H-NMR (Toluene-d₈): δ = 0.65-1.53 (-CH₂C(CH₃)- methacrylic CH₃), 1.78 (-PEG-O-C(O)C(CH₃)₂-CH₂-), 2.16 (-N(CH₃)₂), 2.22 (-CH₂C(CH₃)- of methacrylic backbone), 2.73 (O-CH₂-CH₂-N-), 3.16 (-O-CH₃ at the end of the macroinitiator chain), 3.50, (CH₂-CH₂-O PEG backbone), 4.10 (O-CH₂-CH₂-N-) ppm.

¹H-NMR (D₂O, pH adjusted to 5.5 with NaOD and HCl): δ = 0.72-1.38 (-CH₂C(CH₃)- methacrylic CH₃), 2.02 (-CH₂C(CH₃)- of methacrylic backbone), 2.93 (-N(CH₃)₂), 3.35 (-CH₃ at the end of the macroinitiator chain), 3.67 (CH₂-CH₂-O PEG backbone), 4.38 (O-CH₂-CH₂-N-) ppm.

PEG-PDEAEMA: $^1\text{H-NMR}$ (Toluene- d_8): $\delta = 1.03$ (-N(CH₂-CH₃)₂), 1.28-1.55 (-CH₂C(CH₃)- methacrylic CH₃), 1.78 (-PEG-O-C(O)C(CH₃)₂-CH₂-), 2.13-2.37 (-CH₂C(CH₃)- of methacrylic backbone), 2.39-2.81 (O-CH₂-CH₂-N- and -N(CH₂-CH₃)₂), 3.13 (-O-CH₃), 3.47, CH₂-CH₂-O PEG backbone), 4.12 (O-CH₂-CH₂-N-) ppm.

$^1\text{H-NMR}$ (D₂O, pH adjusted to 5.5 with NaOD and HCl 5): $\delta = 0.70$ -1.50 (-N(CH₂-CH₃)₂ and (-CH₂C(CH₃)- methacrylic CH₃), 1.76 (-PEG-O-C(O)C(CH₃)₂-CH₂-), 2.02 (-CH₂C(CH₃)- of methacrylic backbone), 3.31 (-N(CH₂-CH₃)₂), 3.66 (CH₂-CH₂-O PEG backbone), 4.39 (O-CH₂-CH₂-N-) ppm.

PEG-PDIAEMA: $^1\text{H-NMR}$ (Toluene- d_8): $\delta = 1.01$ ((-N((CH-(CH₃)₂)₂), 1.26-1.53 (-CH₂C(CH₃)- methacrylic CH₃), 1.78 -PEG-O-C(O)C(CH₃)₂-CH₂-), 2.12-2.43 (-CH₂C(CH₃)- of methacrylic backbone), 2.73 (O-CH₂-CH₂-N-), 2.93 (-N((CH-(CH₃)₂)₂), 3.16 (-O-CH₃), 3.49 (CH₂-CH₂-O PEG backbone), 4.06 (O-CH₂-CH₂-N-) ppm.

$^1\text{H-NMR}$ (D₂O, pH adjusted to 5.5 with NaOD and HCl): $\delta = 0.70$ -1.50 (-N((CH-(CH₃)₂)₂ and CH₂C(CH₃)- methacrylic CH₃), 1.81 (-PEG-O-C(O)C(CH₃)₂-CH₂-), 2.95 (-N((CH-(CH₃)₂)₂), 3.38 (-O-CH₃ at the end of the macroinitiator chain), 3.67 (CH₂-CH₂-O PEG backbone), 4.35 (O-CH₂-CH₂-N-) ppm.

PEG-bis-PDMAEMA: $^1\text{H-NMR}$ (Toluene- d_8): $\delta = 0.65$ -1.53 (-CH₂C(CH₃)- methacrylic CH₃), 1.78 -PEG-O-C(O)C(CH₃)₂-CH₂-), 2.12 (-N(CH₃)₂), 2.22 (-CH₂C(CH₃)- of methacrylic backbone), 2.73 (O-CH₂-CH₂-N-), 3.46, (CH₂-CH₂-O PEG backbone), 4.07 (O-CH₂-CH₂-N-) ppm.

$^1\text{H-NMR}$ (D₂O, pH adjusted to 5.5 with NaOD and HCl): $\delta = 0.72$ -1.38 (-CH₂C(CH₃)- methacrylic CH₃), 2.02 (-CH₂C(CH₃)- of methacrylic backbone), 2.93 (-N(CH₃)₂), 3.67 (CH₂-CH₂-O PEG backbone), 4.38 (O-CH₂-CH₂-N-) ppm.

PEG-bis-PDEAEMA: $^1\text{H-NMR}$ (Toluene- d_8): $\delta = 1.03$ (-N(CH₂-CH₃)₂), 1.28-1.55 (-CH₂C(CH₃)- methacrylic CH₃), 1.78 -PEG-O-C(O)C(CH₃)₂-CH₂-), 2.13-2.37 (-CH₂C(CH₃)- of methacrylic backbone), 2.39-2.81 (O-CH₂-CH₂-N- and -N(CH₂-CH₃)₂), 3.47, (CH₂-CH₂-O PEG backbone), 4.12 (O-CH₂-CH₂-N-) ppm.

$^1\text{H-NMR}$ (D₂O, pH adjusted to 5.5 with NaOD and HCl): $\delta = 0.70$ -1.50 (-N(CH₂-CH₃)₂ and (-CH₂C(CH₃)- methacrylic CH₃), 1.76 (-PEG-O-C(O)C(CH₃)₂-CH₂-), 2.02 (-CH₂C(CH₃)- of methacrylic backbone), 3.31 (-N(CH₂-CH₃)₂), 3.66 (CH₂-CH₂-O PEG backbone), 4.39 (O-CH₂-CH₂-N-) ppm.

PEG-bis-PDIAEMA: $^1\text{H-NMR}$ (Toluene- d_8): $\delta = 0.97$ ($-\text{N}((\text{CH}-(\text{CH}_3)_2)_2)$), 1.26-1.53 ($-\text{CH}_2\text{C}(\text{CH}_3)-$ methacrylic CH_3), 1.74 ($-\text{PEG-O-C(O)C}(\text{CH}_3)_2-\text{CH}_2-$), 2.12-2.43 ($-\text{CH}_2\text{C}(\text{CH}_3)-$ of methacrylic backbone), 2.73 ($\text{O-CH}_2-\text{CH}_2-\text{N-}$), 2.95 ($-\text{N}((\text{CH}-(\text{CH}_3)_2)_2)$), 3.52 ($\text{CH}_2-\text{CH}_2-\text{O}$ PEG backbone), 4.06 ($\text{O-CH}_2-\text{CH}_2-\text{N-}$) ppm.

$^1\text{H-NMR}$ (D_2O pH adjusted to 5.5 with NaOD and HCl): $\delta = 0.70$ -1.50 ($-\text{N}((\text{CH}-(\text{CH}_3)_2)_2)$ and $\text{CH}_2\text{C}(\text{CH}_3)-$ methacrylic CH_3), 1.81 ($-\text{PEG-O-C(O)C}(\text{CH}_3)_2-\text{CH}_2-$), 2.95 ($-\text{N}((\text{CH}-(\text{CH}_3)_2)_2)$), 3.67 ($\text{CH}_2-\text{CH}_2-\text{O}$ PEG backbone), 4.35 ($\text{O-CH}_2-\text{CH}_2-\text{N-}$) ppm.

PLUR-bis-PDMAEMA: $^1\text{H-NMR}$ (Toluene- d_8): $\delta = 0.65$ -1.60 ($\text{CH}_2-\text{CH}(\text{CH}_3)-\text{O}$ of PPG chain, $-\text{CH}_2\text{C}(\text{CH}_3)-$ methacrylic CH_3), 1.74 ($-\text{PEG-O-C(O)C}(\text{CH}_3)_2-\text{CH}_2-$), 2.11 ($-\text{N}(\text{CH}_3)_2$), 2.25 ($-\text{CH}_2\text{C}(\text{CH}_3)-$ of methacrylic backbone), 2.71 ($\text{O-CH}_2-\text{CH}_2-\text{N-}$), 3.35, 3.46, 3.52 ($\text{CH}_2-\text{CH}(\text{CH}_3)-\text{O}$ and $\text{CH}_2-\text{CH}(\text{CH}_3)-\text{O}$ in the PPG chain, $\text{CH}_2-\text{CH}_2-\text{O}$ PEG backbone), 4.06 ($\text{O-CH}_2-\text{CH}_2-\text{N-}$) ppm.

$^1\text{H-NMR}$ (D_2O , pH adjusted to 5.5 with NaOD and HCl pH): $\delta = 0.70$ -1.41 ($\text{CH}_2-\text{CH}(\text{CH}_3)-\text{O}$ of PPG chain and $-\text{CH}_2\text{C}(\text{CH}_3)-$ methacrylic CH_3), 2.02 ($-\text{CH}_2\text{C}(\text{CH}_3)-$ of methacrylic backbone), 2.96 ($-\text{N}(\text{CH}_3)_2$), 3.67 ($\text{CH}_2-\text{CH}_2-\text{O}$ PEG backbone), 4.36 ($\text{O-CH}_2-\text{CH}_2-\text{N-}$) ppm.

PLUR-bis-PDEAEMA: $^1\text{H-NMR}$ (Toluene- d_8): $\delta = 1.00$ ($-\text{N}(\text{CH}_2-\text{CH}_3)_2$), 1.15 ($\text{CH}_2-\text{CH}(\text{CH}_3)-\text{O}$ of PPG chain), 1.21-1.53 ($-\text{CH}_2\text{C}(\text{CH}_3)-$ methacrylic CH_3), 1.74 ($-\text{PEG-O-C(O)C}(\text{CH}_3)_2-\text{CH}_2-$), 2.13-2.40 ($-\text{CH}_2\text{C}(\text{CH}_3)-$ of methacrylic backbone), 2.39-2.81 ($\text{O-CH}_2-\text{CH}_2-\text{N-}$ and $-\text{N}(\text{CH}_2-\text{CH}_3)_2$), 3.37, 3.46, 3.52 ($\text{CH}_2-\text{CH}(\text{CH}_3)-\text{O}$ and $\text{CH}_2-\text{CH}(\text{CH}_3)-\text{O}$ in the PPG chain, $\text{CH}_2-\text{CH}_2-\text{O}$ PEG backbone), 4.07 ($\text{O-CH}_2-\text{CH}_2-\text{N-}$) ppm.

$^1\text{H-NMR}$ (D_2O , pH adjusted to 5.5 with NaOD and HCl): $\delta = 0.70$ -1.50 ($-\text{N}(\text{CH}_2-\text{CH}_3)_2$, $\text{CH}_2-\text{CH}(\text{CH}_3)-\text{O}$ of PPG chain and $-\text{CH}_2\text{C}(\text{CH}_3)-$ methacrylic CH_3), 1.81 ($-\text{PEG-O-C(O)C}(\text{CH}_3)_2-\text{CH}_2-$), 3.33 ($-\text{N}(\text{CH}_2-\text{CH}_3)_2$), 3.65 ($\text{CH}_2-\text{CH}_2-\text{O}$ PEG backbone), 4.33 ($\text{O-CH}_2-\text{CH}_2-\text{N-}$) ppm.

PLUR-bis-PDIAEMA: $^1\text{H-NMR}$ (Toluene- d_8): $\delta = 0.99$ ($-\text{N}((\text{CH}-(\text{CH}_3)_2)_2)$), 1.16 ($\text{CH}_2-\text{CH}(\text{CH}_3)-\text{O}$ of PPG chain), 1.36 ($-\text{CH}_2\text{C}(\text{CH}_3)-$ methacrylic CH_3), 2.12-2.43 ($-\text{CH}_2\text{C}(\text{CH}_3)-$ of methacrylic backbone), 2.73 ($\text{O-CH}_2-\text{CH}_2-\text{N-}$), 2.93 ($-\text{N}((\text{CH}-(\text{CH}_3)_2)_2)$), 3.35, 3.47, 3.52 ($\text{CH}_2-\text{CH}(\text{CH}_3)-\text{O}$ and $\text{CH}_2-\text{CH}(\text{CH}_3)-\text{O}$ in the PPG chain, $\text{CH}_2-\text{CH}_2-\text{O}$ PEG backbone), 4.04 ($\text{O-CH}_2-\text{CH}_2-\text{N-}$) ppm.

¹H-NMR (D₂O, pH adjusted to 5.5 with NaOD and HCl); $\delta = 0.70-1.50$ (CH₂-CH(CH₃)-O of PPG chain, -N((CH-(CH₃)₂)₂ and CH₂C(CH₃)- methacrylic CH₃), 1.78 (-PEG-O-C(O)C(CH₃)₂-CH₂-), 2.95 (-N((CH-(CH₃)₂)₂), 3.66 (CH₂-CH₂-O PEG backbone), 4.32 (O-CH₂-CH₂-N-) ppm.

4.5.4 DLS and loading measurements samples

DLS solutions were prepared dissolving the polymers in deionized water (1 mg/ml). The solution was filtered with a 45 μ m filter and left to equilibrate overnight.

Loading measurements were carried out as follows. 1000 μ l of micellar dispersions of polymer (concentrations 1 mg/ml) were mixed with 50 μ l of a 3×10^{-5} M solution of Nile Red in THF. The samples were protected from light and THF was allowed to evaporate overnight. The size of the aggregates was determined by DSL. The Nile Red fluorescence was recorded on a Synergy2 Biotek plate reader with Gen5 software at 25 or 37°C, using an excitation filter at 540 ± 25 nm and an emission filter at 620 ± 40 nm.

4.5.5 Study of glucose oxidase kinetic in presence of PLUR-bis-PDEAEMA-L

1.160 ml of PLUR-bis-PDMAEMA-L (1mg/ml) water solution loaded with Nile Red at pH 8 were introduced in a vial. 30 μ l of a 14 mM stock solution of glucose were added into the vial and the sample was left to equilibrate at 25 or 37°C in a water bath. The pHmeter electrode was introduced into the vial and then 30 μ L of catalase (to quench the H₂O₂ formed) and 30 μ L of glucose oxidase were added into the sample and the pH values were determined as a function of time.

5 References

- 1 Wade A. Braunecker, K. M. Controlled/living radical polymerization: Features, developments, and perspectives. *Progress in Polymer Science* **32**, 93-146 (2007).
- 2 Moad, G. S., D. H. *The Chemistry of Free-Radical Polymerization*. (1995).
- 3 Webster, O. W. LIVING POLYMERIZATION METHODS. *Science* **251**, 887-893, doi:10.1126/science.251.4996.887 (1991).
- 4 Chiefari, J. *et al.* Living free-radical polymerization by reversible addition-fragmentation chain transfer: The RAFT process. *Macromolecules* **31**, 5559-5562, doi:10.1021/ma9804951 (1998).
- 5 Wang, J.-S. & Matyjaszewski, K. Controlled/"Living" Radical Polymerization. Halogen Atom Transfer Radical Polymerization Promoted by a Cu(I)/Cu(II) Redox Process. *Macromolecules* **28**, 7901-7910, doi:10.1021/ma00127a042 (1995).
- 6 Wang, J.-S. & Matyjaszewski, K. Controlled/"living" radical polymerization. atom transfer radical polymerization in the presence of transition-metal complexes. *Journal of the American Chemical Society* **117**, 5614-5615, doi:10.1021/ja00125a035 (1995).
- 7 Patten, T. E., Xia, J. H., Abernathy, T. & Matyjaszewski, K. Polymers with very low polydispersities from atom transfer radical polymerization. *Science* **272**, 866-868, doi:10.1126/science.272.5263.866 (1996).
- 8 Matyjaszewski, K., Gaynor, S., Greszta, D., Mardare, D. & Shigemoto, T. 'Living' and controlled radical polymerization. *Journal of Physical Organic Chemistry* **8**, 306-315, doi:10.1002/poc.610080414 (1995).
- 9 Miwa, Y., Yamamoto, K., Sakaguchi, M. & Shimada, S. Well-defined polystyrene grafted to polypropylene backbone by "living" radical polymerization with TEMPO. *Macromolecules* **34**, 2089-2094, doi:10.1021/ma001449f (2001).
- 10 Moad, G., Rizzardo, E. & Thang, S. H. Living Radical Polymerization by the RAFT Process. *Australian Journal of Chemistry* **58**, 379-410, doi:http://dx.doi.org/10.1071/CH05072 (2005).
- 11 Greszta, D., Mardare, D. & Matyjaszewski, K. "Living" radical polymerization. 1. Possibilities and limitations. *Macromolecules* **27**, 638-644, doi:10.1021/ma00081a002 (1994).
- 12 Hawker, C. J. MOLECULAR-WEIGHT CONTROL BY A LIVING FREE-RADICAL POLYMERIZATION PROCESS. *J. Am. Chem. Soc.* **116**, 11185-11186, doi:10.1021/ja00103a055 (1994).
- 13 Goto, A. & Fukuda, T. Kinetics of living radical polymerization. *Progress in Polymer Science* **29**, 329-385, doi:10.1016/j.progpolymsci.2004.01.002 (2004).
- 14 Matyjaszewski, K. Atom Transfer Radical Polymerization (ATRP): Current Status and Future Perspectives. *Macromolecules* **45**, 4015-4039, doi:10.1021/ma3001719 (2012).
- 15 Wang, J. S. & Matyjaszewski, K. LIVING CONTROLLED RADICAL POLYMERIZATION - TRANSITION-METAL-CATALYZED ATOM-TRANSFER RADICAL POLYMERIZATION IN THE PRESENCE OF A CONVENTIONAL RADICAL INITIATOR. *Macromolecules* **28**, 7572-7573, doi:10.1021/ma00126a041 (1995).
- 16 Wang, J. S. & Matyjaszewski, K. CONTROLLED LIVING RADICAL POLYMERIZATION - ATOM-TRANSFER RADICAL POLYMERIZATION IN THE PRESENCE OF TRANSITION-METAL COMPLEXES. *J. Am. Chem. Soc.* **117**, 5614-5615, doi:10.1021/ja00125a035 (1995).

References

- 17 Wang, J. S. & Matyjaszewski, K. CONTROLLED LIVING RADICAL POLYMERIZATION - HALOGEN ATOM-TRANSFER RADICAL POLYMERIZATION PROMOTED BY A CU(I)CU(II) REDOX PROCESS. *Macromolecules* **28**, 7901-7910, doi:10.1021/ma00127a042 (1995).
- 18 Udding, J. H. T., K. J. M.; van Zanden, M. N. A.; Hiemstra, H.; Speckamp, W. N. . *Journal of Organic Chemistry* **59**, 1993 (1994).
- 19 Pintauer, T., McKenzie, B. & Matyjaszewski, K. in *Advances in Controlled/Living Radical Polymerization* Vol. 854 *Acs Symposium Series* (ed K. Matyjaszewski) 130-147 (2003).
- 20 Szwarc, M., Levy, M. & Milkovich, R. POLYMERIZATION INITIATED BY ELECTRON TRANSFER TO MONOMER. A NEW METHOD OF FORMATION OF BLOCK POLYMERS1. *J. Am. Chem. Soc.* **78**, 2656-2657, doi:10.1021/ja01592a101 (1956).
- 21 Matyjaszewski, K., Patten, T. E. & Xia, J. H. Controlled/"living" radical polymerization. Kinetics of the homogeneous atom transfer radical polymerization of styrene. *J. Am. Chem. Soc.* **119**, 674-680, doi:10.1021/ja963361g (1997).
- 22 Matyjaszewski, K. & Xia, J. H. Atom transfer radical polymerization. *Chemical Reviews* **101**, 2921-2990, doi:10.1021/cr940534g (2001).
- 23 Greszta, D. & Matyjaszewski, K. Mechanism of controlled/"living" radical polymerization of styrene in the presence of nitroxyl radicals. Kinetics and simulations. *Macromolecules* **29**, 7661-7670, doi:10.1021/ma9608840 (1996).
- 24 Shen, Y. Q., Tang, H. D. & Ding, S. J. Catalyst separation in atom transfer radical polymerization. *Progress in Polymer Science* **29**, 1053-1078, doi:10.1016/j.progpolymsci.2004.08.002 (2004).
- 25 Tsarevsky, N. V. & Matyjaszewski, K. Environmentally benign atom transfer radical polymerization: Towards "green" processes and materials. *Journal of Polymer Science Part a-Polymer Chemistry* **44**, 5098-5112, doi:10.1002/pola.21617 (2006).
- 26 Matyjaszewski, K. in *Controlled Radical Polymerization* Vol. 685 *ACS Symposium Series* Ch. 16, 258-283 (American Chemical Society, 1998).
- 27 Kabachii, Y. A., Kochev, S. Y., Bronstein, L. M., Blagodatskikh, I. B. & Valetsky, P. M. Atom Transfer Radical Polymerization with Ti(III) Halides and Alkoxides. *Polymer Bulletin* **50**, 271-278, doi:10.1007/s00289-003-0157-9 (2003).
- 28 Le Grogne, E., Claverie, J. & Poli, R. Radical Polymerization of Styrene Controlled by Half-Sandwich Mo(III)/Mo(IV) Couples: All Basic Mechanisms Are Possible. *J. Am. Chem. Soc.* **123**, 9513-9524, doi:10.1021/ja010998d (2001).
- 29 Kotani, Y., Kamigaito, M. & Sawamoto, M. Re(V)-Mediated Living Radical Polymerization of Styrene:1 ReO2I(PPh3)2/R-I Initiating Systems. *Macromolecules* **32**, 2420-2424, doi:10.1021/ma981614f (1999).
- 30 Ando, T., Kamigaito, M. & Sawamoto, M. Iron(II) Chloride Complex for Living Radical Polymerization of Methyl Methacrylate1. *Macromolecules* **30**, 4507-4510, doi:10.1021/ma961478j (1997).
- 31 Kato, M., Kamigaito, M., Sawamoto, M. & Higashimura, T. Polymerization of Methyl Methacrylate with the Carbon Tetrachloride/Dichlorotris-(triphenylphosphine)ruthenium(II)/Methylaluminum Bis(2,6-di-tert-butylphenoxide) Initiating System: Possibility of Living Radical Polymerization. *Macromolecules* **28**, 1721-1723, doi:10.1021/ma00109a056 (1995).
- 32 Braunecker, W. A., Itami, Y. & Matyjaszewski, K. Osmium-Mediated Radical Polymerization. *Macromolecules* **38**, 9402-9404, doi:10.1021/ma051877r (2005).

References

- 33 Wang, B., Zhuang, Y., Luo, X., Xu, S. & Zhou, X. Controlled/"Living" Radical Polymerization of MMA Catalyzed by Cobaltocene. *Macromolecules* **36**, 9684-9686, doi:10.1021/ma035334y (2003).
- 34 Granel, C., Dubois, P., Jérôme, R. & Teyssié, P. Controlled Radical Polymerization of Methacrylic Monomers in the Presence of a Bis(ortho-chelated) Arylnickel(II) Complex and Different Activated Alkyl Halides. *Macromolecules* **29**, 8576-8582, doi:10.1021/ma9608380 (1996).
- 35 Lecomte, P., Drapier, I., Dubois, P., Teyssié, P. & Jérôme, R. Controlled Radical Polymerization of Methyl Methacrylate in the Presence of Palladium Acetate, Triphenylphosphine, and Carbon Tetrachloride. *Macromolecules* **30**, 7631-7633, doi:10.1021/ma970890b (1997).
- 36 Gillies, M. B. *et al.* A DFT Study of R–X Bond Dissociation Enthalpies of Relevance to the Initiation Process of Atom Transfer Radical Polymerization. *Macromolecules* **36**, 8551-8559, doi:10.1021/ma0351672 (2003).
- 37 Xia, J., Paik, H.-j. & Matyjaszewski, K. Polymerization of Vinyl Acetate Promoted by Iron Complexes. *Macromolecules* **32**, 8310-8314, doi:10.1021/ma991075u (1999).
- 38 Sarbu, T., Pintauer, T., McKenzie, B. & Matyjaszewski, K. Atom transfer radical polymerization of styrene in toluene/water mixtures. *Journal of Polymer Science Part A: Polymer Chemistry* **40**, 3153-3160, doi:10.1002/pola.10404 (2002).
- 39 Brar, A. S. & Kaur, S. Atom transfer radical polymerization of N-vinyl carbazole: Optimization to characterization. *Journal of Polymer Science Part A: Polymer Chemistry* **44**, 1745-1757, doi:10.1002/pola.21296 (2006).
- 40 Wang, Y., Zhang, Y., Parker, B. & Matyjaszewski, K. ATRP of MMA with ppm Levels of Iron Catalyst. *Macromolecules* **44**, 4022-4025, doi:10.1021/ma200771r (2011).
- 41 Lu, X. *et al.* Controllable synthesis of poly(N-vinylpyrrolidone) and its block copolymers by atom transfer radical polymerization. *Polymer* **48**, 2835-2842, doi:http://dx.doi.org/10.1016/j.polymer.2007.03.048 (2007).
- 42 Narrainen, A. P., Pascual, S. & Haddleton, D. M. Amphiphilic diblock, triblock, and star block copolymers by living radical polymerization: Synthesis and aggregation behavior. *Journal of Polymer Science Part A: Polymer Chemistry* **40**, 439-450, doi:10.1002/pola.10122 (2002).
- 43 Shipp, D. A., Wang, J.-L. & Matyjaszewski, K. Synthesis of Acrylate and Methacrylate Block Copolymers Using Atom Transfer Radical Polymerization. *Macromolecules* **31**, 8005-8008, doi:10.1021/ma981033q (1998).
- 44 Beers, K. L., Boo, S., Gaynor, S. G. & Matyjaszewski, K. Atom Transfer Radical Polymerization of 2-Hydroxyethyl Methacrylate. *Macromolecules* **32**, 5772-5776, doi:10.1021/ma990176p (1999).
- 45 Matyjaszewski, K., Nakagawa, Y. & Jasieczek, C. B. Polymerization of n-Butyl Acrylate by Atom Transfer Radical Polymerization. Remarkable Effect of Ethylene Carbonate and Other Solvents. *Macromolecules* **31**, 1535-1541, doi:10.1021/ma971444r (1998).
- 46 Arshadi, M., Yamdagni, R. & Kebarle, P. Hydration of the halide negative ions in the gas phase. II. Comparison of hydration energies for the alkali positive and halide negative ions. *The Journal of Physical Chemistry* **74**, 1475-1482, doi:10.1021/j100702a014 (1970).
- 47 Pintauer, T., McKenzie, B. & Matyjaszewski, K. Determination of the equilibrium constant for bromide dissociation from ATRP active Cu(II) complexes and its

References

- effect on the overall catalyst activity. *Abstracts of Papers of the American Chemical Society* **224**, U441-U441 (2002).
- 48 Tsarevsky, N. V., Pintauer, T. & Matyjaszewski, K. Deactivation efficiency and degree of control over polymerization in ATRP in protic solvents. *Macromolecules* **37**, 9768-9778, doi:10.1021/ma048438x (2004).
- 49 Tang, W. & Matyjaszewski, K. Effect of Ligand Structure on Activation Rate Constants in ATRP. *Macromolecules* **39**, 4953-4959, doi:10.1021/ma0609634 (2006).
- 50 Munakata, M., Kitagawa, S., Asahara, A. & Masuda, H. CRYSTAL-STRUCTURE OF BIS(2,2'-BIPYRIDINE)COPPER(I) PERCHLORATE. *Bulletin of the Chemical Society of Japan* **60**, 1927-1929, doi:10.1246/bcsj.60.1927 (1987).
- 51 Pallenberg, A. J., Koenig, K. S. & Barnhart, D. M. SYNTHESIS AND CHARACTERIZATION OF SOME COPPER(I) PHENANTHROLINE COMPLEXES. *Inorganic Chemistry* **34**, 2833-2840, doi:10.1021/ic00115a009 (1995).
- 52 Rorabacher, D. B. Electron Transfer by Copper Centers. *Chemical Reviews* **104**, 651-698, doi:10.1021/cr020630e (2004).
- 53 Tang, W. & Matyjaszewski, K. Effects of initiator structure on activation rate constants in ATRP. *Macromolecules* **40**, 1858-1863, doi:10.1021/ma062897b (2007).
- 54 Lin, C. Y., Marque, S. R. A., Matyjaszewski, K. & Coote, M. L. Linear-free energy relationships for modeling structure-reactivity trends in controlled radical polymerization. *Macromolecules* **44**, 7568-7583, doi:10.1021/ma2014996 (2011).
- 55 Woodworth, B. E., Metzner, Z. & Matyjaszewski, K. Copper Triflate as a Catalyst in Atom Transfer Radical Polymerization of Styrene and Methyl Acrylate. *Macromolecules* **31**, 7999-8004, doi:10.1021/ma981032y (1998).
- 56 Georges, M. K., Veregin, R. P. N., Kazmaier, P. M. & Hamer, G. K. NARROW MOLECULAR-WEIGHT RESINS BY A FREE-RADICAL POLYMERIZATION PROCESS. *Macromolecules* **26**, 2987-2988, doi:10.1021/ma00063a054 (1993).
- 57 Veregin, R. P. N., Georges, M. K., Kazmaier, P. M. & Hamer, G. K. FREE-RADICAL POLYMERIZATIONS FOR NARROW POLYDISPERSITY RESINS - ELECTRON-SPIN-RESONANCE STUDIES OF THE KINETICS AND MECHANISM. *Macromolecules* **26**, 5316-5320, doi:10.1021/ma00072a007 (1993).
- 58 Goto, A. *et al.* Mechanism-Based Invention of High-Speed Living Radical Polymerization Using Organotellurium Compounds and Azo-Initiators. *J. Am. Chem. Soc.* **125**, 8720-8721, doi:10.1021/ja035464m (2003).
- 59 Gaynor, S. G., Wang, J.-S. & Matyjaszewski, K. Controlled Radical Polymerization by Degenerative Transfer: Effect of the Structure of the Transfer Agent. *Macromolecules* **28**, 8051-8056, doi:10.1021/ma00128a012 (1995).
- 60 Iovu, M. C. & Matyjaszewski, K. Controlled/Living Radical Polymerization of Vinyl Acetate by Degenerative Transfer with Alkyl Iodides. *Macromolecules* **36**, 9346-9354, doi:10.1021/ma034892+ (2003).
- 61 Chiefari, J. *et al.* Thiocarbonylthio Compounds (SC(Z)S-R) in Free Radical Polymerization with Reversible Addition-Fragmentation Chain Transfer (RAFT Polymerization). Effect of the Activating Group Z. *Macromolecules* **36**, 2273-2283, doi:10.1021/ma020883+ (2003).

References

- 62 Ganachaud, F. *et al.* Molecular Weight Characterization of Poly(N-isopropylacrylamide) Prepared by Living Free-Radical Polymerization. *Macromolecules* **33**, 6738-6745, doi:10.1021/ma0003102 (2000).
- 63 Tong, Y.-Y., Dong, Y.-Q., Du, F.-S. & Li, Z.-C. Synthesis of Well-Defined Poly(vinyl acetate)-b-Polystyrene by Combination of ATRP and RAFT Polymerization. *Macromolecules* **41**, 7339-7346, doi:10.1021/ma800799x (2008).
- 64 Wojciech, J. in *Progress in Controlled Radical Polymerization: Mechanisms and Techniques* Vol. 1100 *ACS Symposium Series* Ch. 13, 203-216 (American Chemical Society, 2012).
- 65 Kazmaier, P. M., Daimon, K., Georges, M. K., Hamer, G. K. & Veregin, R. P. N. Nitroxide-mediated "living" free radical polymerization: A rapid polymerization of (chloromethyl)styrene for the preparation of random, block, and segmental arborescent polymers. *Macromolecules* **30**, 2228-2231 (1997).
- 66 Hawker, C. J. *et al.* Well-defined random copolymers by a "living" free-radical polymerization process. *Macromolecules* **29**, 2686-2688 (1996).
- 67 Haddleton, D. M. *et al.* Identifying the nature of the active species in the polymerization of methacrylates: Inhibition of methyl methacrylate homopolymerizations and reactivity ratios for copolymerization of methyl methacrylate/n-butyl methacrylate in classical anionic, alkyllithium/trialkylaluminum-initiated, group transfer polymerization, atom transfer radical polymerization, catalytic chain transfer. *Macromolecules* **30**, 3992-3998 (1997).
- 68 Stockmayer, W. H. Distribution of Chain Lengths and Compositions in Copolymers. *The Journal of Chemical Physics* **13**, 199-207, doi:doi:http://dx.doi.org/10.1063/1.1724022 (1945).
- 69 Pakula, T. & Matyjaszewski, K. Copolymers with controlled distribution of comonomers along the chain, 1: Structure, thermodynamics and dynamic properties of gradient copolymers. Computer simulation. *Macromol. Theory Simul.* **5**, 987-1006 (1996).
- 70 Greszta, D. & Matyjaszewski, K. Gradient copolymers - A new class of materials. *Am Chem Soc Polym Prepr Div Polym Chem* **37**, 569-570 (1996).
- 71 Ziegler, M. J. & Matyjaszewski, K. Atom transfer radical copolymerization of methyl methacrylate and n-butyl acrylate. *Macromolecules* **34**, 415-424, doi:10.1021/ma001182k (2001).
- 72 Mayo, F. R. & Lewis, F. M. Copolymerization. I. A Basis for Comparing the Behavior of Monomers in Copolymerization; The Copolymerization of Styrene and Methyl Methacrylate. *Journal of the American Chemical Society* **66**, 1594-1601, doi:10.1021/ja01237a052 (1944).
- 73 Arehart, S. V. & Matyjaszewski, K. Atom transfer radical copolymerization of styrene and n-butyl acrylate. *Macromolecules* **32**, 2221-2231, doi:10.1021/ma981693v (1999).
- 74 Greszta, D., Matyjaszewski, K. & Pakula, T. Gradient copolymers of styrene and acrylonitrile via atom transfer radical polymerization. *Am Chem Soc Polym Prepr Div Polym Chem* **38**, 709-710 (1997).
- 75 Arehart, S. V., Greszta, D. & Matyjaszewski, K. Gradient copolymers of styrene and n-butyl acrylate through atom transfer radical polymerization. *Am Chem Soc Polym Prepr Div Polym Chem* **38**, 705-706 (1997).
- 76 Fineman, M. & Ross, S. D. Linear method for determining monomer reactivity ratios in copolymerization. *Journal of Polymer Science* **5**, 259-262, doi:10.1002/pol.1950.120050210 (1950).

References

- 77 Kelen, T. & Tüds, F. Analysis of the Linear Methods for Determining Copolymerization Reactivity Ratios. I. A New Improved Linear Graphic Method. *Journal of Macromolecular Science: Part A - Chemistry* **9**, 1-27, doi:10.1080/00222337508068644 (1975).
- 78 Meyer, V. E. & Lowry, G. G. Integral and differential binary copolymerization equations. *Journal of Polymer Science Part A: General Papers* **3**, 2843-2851, doi:10.1002/pol.1965.100030811 (1965).
- 79 Rossignoli, P. J. & Duever, T. A. Estimation of copolymer reactivity ratios: a review and case studies using the error-in-variables model and nonlinear least squares. *Polym React Eng* **3**, 361-395 (1995).
- 80 Polic, A. L., Duever, T. A. & Penlidis, A. Case studies and literature review on the estimation of copolymerization reactivity ratios. *J Polym Sci Part A* **36**, 813-822, doi:10.1002/(sici)1099-0518(19980415)36:5<813::aid-pola14>3.0.co;2-j (1998).
- 81 Hauch, E., Zhou, X., Duever, T. A. & Penlidis, A. Estimating reactivity ratios from triad fraction data. *Macromolecular Symposia* **271**, 48-63, doi:10.1002/masy.200851106 (2008).
- 82 Van Herk, A. M. Least-squares fitting by visualization of the sum of squares space. *Journal of Chemical Education* **72**, 138-140 (1995).
- 83 in *Measurement Error in Nonlinear Models C&H/CRC Monographs on Statistics & Applied Probability* 41-64 (Chapman and Hall/CRC, 2006).
- 84 Kelland, M. A. History of the Development of Low Dosage Hydrate Inhibitors. *Energy & Fuels* **20**, 825-847, doi:10.1021/ef050427x (2006).
- 85 Kuznetsova, T., Sapronova, A., Kvamme, B., Johannsen, K. & Haug, J. Impact of Low-Dosage Inhibitors on Clathrate Hydrate Stability. *Macromolecular Symposia* **287**, 168-176, doi:10.1002/masy.201050124 (2010).
- 86 Semenov, A. P., Gushchin, P. A., Ivanov, E. V., Vinokurov, V. A. & Sapozhnikov, D. A. Homo- and Copolymers of N-Acryloylpyrrolidine and N-Vinylpyrrolidone as Kinetic Inhibitors of Hydrate Formation. *Chem Technol Fuels Oils* **46**, 417-423, doi:10.1007/s10553-011-0243-x (2011).
- 87 Perrin, A., Musa, O. M. & Steed, J. W. The chemistry of low dosage clathrate hydrate inhibitors. *Chemical Society Reviews* **42**, 1996-2015, doi:10.1039/c2cs35340g (2013).
- 88 Reyes, F. T. & Kelland, M. A. First Investigation of the Kinetic Hydrate Inhibitor Performance of Polymers of Alkylated N-Vinyl Pyrrolidones. *Energy & Fuels* **27**, 3730-3735, doi:10.1021/ef400587g (2013).
- 89 Jiang, X., Li, Y., Lu, G. & Huang, X. A novel poly(N-vinylcaprolactam)-based well-defined amphiphilic graft copolymer synthesized by successive RAFT and ATRP. *Polymer Chemistry* **4**, 1402-1411, doi:10.1039/c2py20933k (2013).
- 90 Liu, J., Debuigne, A., Detrembleur, C. & Jérôme, C. Poly(N-vinylcaprolactam): A Thermoresponsive Macromolecule with Promising Future in Biomedical Field. *Advanced Healthcare Materials* **3**, 1941-1968, doi:10.1002/adhm.201400371 (2014).
- 91 Singh, P., Srivastava, A. & Kumar, R. Synthesis of amphiphilic poly(N-vinylcaprolactam) using ATRP protocol and antibacterial study of its silver nanocomposite. *Journal of Polymer Science Part A: Polymer Chemistry* **50**, 1503-1514, doi:10.1002/pola.25911 (2012).
- 92 Xiong, Y. *et al.* Synthesis and Mechanistic Study of Palladium Nanobars and Nanorods. *Journal of the American Chemical Society* **129**, 3665-3675, doi:10.1021/ja0688023 (2007).

References

- 93 Ferrer, D. *et al.* Three-Layer Core/Shell Structure in Au–Pd Bimetallic Nanoparticles. *Nano Letters* **7**, 1701-1705, doi:10.1021/nl070694a (2007).
- 94 Hasan, T. *et al.* Stabilization and “Debundling” of Single-Wall Carbon Nanotube Dispersions in N-Methyl-2-pyrrolidone (NMP) by Polyvinylpyrrolidone (PVP). *The Journal of Physical Chemistry C* **111**, 12594-12602, doi:10.1021/jp0723012 (2007).
- 95 O'Connell, M. J. *et al.* Band Gap Fluorescence from Individual Single-Walled Carbon Nanotubes. *Science* **297**, 593-596, doi:10.1126/science.1072631 (2002).
- 96 Zelikin, A. N., Such, G. K., Postma, A. & Caruso, F. Poly(vinylpyrrolidone) for Bioconjugation and Surface Ligand Immobilization. *Biomacromolecules* **8**, 2950-2953, doi:10.1021/bm700498j (2007).
- 97 Deng, J. *et al.* Facile Synthesis and Thermoresponsive Behaviors of a Well-Defined Pyrrolidone Based Hydrophilic Polymer. *Macromolecules* **41**, 3007-3014, doi:10.1021/ma800145s (2008).
- 98 Ramos, J., Imaz, A. & Forcada, J. Temperature-sensitive nanogels: Poly(N-vinylcaprolactam) versus poly(N-isopropylacrylamide). *Polymer Chemistry* **3**, 852-856, doi:10.1039/c2py00485b (2012).
- 99 Makhaeva, E. E., Tenhu, H. & Khokhlov, A. R. Conformational Changes of Poly(vinylcaprolactam) Macromolecules and Their Complexes with Ionic Surfactants in Aqueous Solution. *Macromolecules* **31**, 6112-6118, doi:10.1021/ma980158s (1998).
- 100 Makhaeva, E. E., Tenhu, H. & Khokhlov, A. R. Behaviour of poly(N-vinylcaprolactam) macromolecules in the presence of organic compounds in aqueous solution. *Polymer* **41**, 9139-9145, doi:http://dx.doi.org/10.1016/S0032-3861(00)00258-5 (2000).
- 101 Lozinsky, V. I. *et al.* Synthesis of N-vinylcaprolactam polymers in water-containing media. *Polymer* **41**, 6507-6518, doi:http://dx.doi.org/10.1016/S0032-3861(99)00844-7 (2000).
- 102 Wan, D., Zhou, Q., Pu, H. & Yang, G. Controlled radical polymerization of N-vinylcaprolactam mediated by xanthate or dithiocarbamate. *Journal of Polymer Science Part A: Polymer Chemistry* **46**, 3756-3765, doi:10.1002/pola.22722 (2008).
- 103 Wan, D., Satoh, K., Kamigaito, M. & Okamoto, Y. Xanthate-Mediated Radical Polymerization of N-Vinylpyrrolidone in Fluoroalcohols for Simultaneous Control of Molecular Weight and Tacticity. *Macromolecules* **38**, 10397-10405, doi:10.1021/ma0515230 (2005).
- 104 Beija, M., Marty, J.-D. & Destarac, M. Thermoresponsive poly(N-vinyl caprolactam)-coated gold nanoparticles: sharp reversible response and easy tunability. *Chemical Communications* **47**, 2826-2828, doi:10.1039/c0cc05184e (2011).
- 105 Hussain, H. *et al.* Synthesis and self-assembly of poly(styrene)-b-poly(N-vinylpyrrolidone) amphiphilic diblock copolymers made via a combined ATRP and MADIX approach. *Journal of Polymer Science Part A: Polymer Chemistry* **46**, 5604-5615, doi:10.1002/pola.22882 (2008).
- 106 Hurtgen, M., Liu, J., Debuigne, A., Jerome, C. & Detrembleur, C. Synthesis of thermo-responsive poly(N-vinylcaprolactam)-containing block copolymers by cobalt-mediated radical polymerization. *Journal of Polymer Science Part A: Polymer Chemistry* **50**, 400-408, doi:10.1002/pola.25045 (2012).
- 107 Kermagoret, A. *et al.* Double thermoresponsive di- and triblock copolymers based on N-vinylcaprolactam and N-vinylpyrrolidone: synthesis and comparative study

References

- of solution behaviour. *Polymer Chemistry* **5**, 6534-6544, doi:10.1039/c4py00852a (2014).
- 108 Kavitha, T., Kang, I.-K. & Park, S.-Y. Poly(N-vinyl caprolactam) grown on nanographene oxide as an effective nanocargo for drug delivery. *Colloids and Surfaces B: Biointerfaces* **115**, 37-45, doi:http://dx.doi.org/10.1016/j.colsurfb.2013.11.022 (2014).
- 109 Patel, R., Ahn, S., Chi, W. & Kim, J. Poly(vinyl chloride)-graft-poly(N-vinyl caprolactam) graft copolymer: synthesis and use as template for porous TiO₂ thin films in dye-sensitized solar cells. *Ionics* **18**, 395-402, doi:10.1007/s11581-011-0641-4 (2012).
- 110 Percec, V. *et al.* Aqueous Room Temperature Metal-Catalyzed Living Radical Polymerization of Vinyl Chloride. *Journal of the American Chemical Society* **124**, 4940-4941, doi:10.1021/ja0256055 (2002).
- 111 Jakubowski, W. & Spanswick, J. (Google Patents, 2011).
- 112 Matyjaszewski, K. & Tsarevsky, N. V. Nanostructured functional materials prepared by atom transfer radical polymerization. *Nat. Chem.* **1**, 276-288, doi:10.1038/nchem.257 (2009).
- 113 Matyjaszewski, K., Patten, T. E. & Xia, J. Controlled/"Living" Radical Polymerization. Kinetics of the Homogeneous Atom Transfer Radical Polymerization of Styrene. *Journal of the American Chemical Society* **119**, 674-680, doi:10.1021/ja963361g (1997).
- 114 Matyjaszewski, K. Radical nature of Cu-catalyzed controlled radical polymerizations (atom transfer radical polymerization). *Macromolecules* **31**, 4710-4717 (1998).
- 115 Rakhmatullina, E., Braun, T., Chami, M., Malinova, V. & Meier, W. Self-Organization Behavior of Methacrylate-Based Amphiphilic Di- and Triblock Copolymers. *Langmuir* **23**, 12371-12379, doi:10.1021/la7023132 (2007).
- 116 Rostami Daronkola, M. & Semsarzadeh, M. Study of macroinitiator efficiency and microstructure-thermal properties in the atom transfer radical polymerization of methyl methacrylate. *J Polym Res* **15**, 403-411, doi:10.1007/s10965-008-9185-3 (2008).
- 117 Huang, J., Pintauer, T. & Matyjaszewski, K. Effect of variation of [PMDETA]₀/[Cu(I)Br]₀ ratio on atom transfer radical polymerization of n-butyl acrylate. *Journal of Polymer Science Part A: Polymer Chemistry* **42**, 3285-3292, doi:10.1002/pola.20175 (2004).
- 118 Xia, J., Gaynor, S. G. & Matyjaszewski, K. Controlled/"Living" Radical Polymerization. Atom Transfer Radical Polymerization of Acrylates at Ambient Temperature. *Macromolecules* **31**, 5958-5959, doi:10.1021/ma980725b (1998).
- 119 Liu, S. & Mishra, M. K. Atom Transfer Radical Polymerization of Menthyl Acrylate. *Macromolecules* **40**, 867-871, doi:10.1021/ma062058p (2007).
- 120 Park, K. C., Idota, N. & Tsukahara, T. Synthesis of NIPAAm-based polymer-grafted silica beads by surface-initiated ATRP using Me₄Cyclam ligands and the thermo-responsive behaviors for lanthanide(III) ions. *Reactive and Functional Polymers* **79**, 36-46, doi:http://dx.doi.org/10.1016/j.reactfunctpolym.2014.03.011 (2014).
- 121 Xia, Y., Yin, X., Burke, N. A. D. & Stöver, H. D. H. Thermal Response of Narrow-Disperse Poly(N-isopropylacrylamide) Prepared by Atom Transfer Radical Polymerization. *Macromolecules* **38**, 5937-5943, doi:10.1021/ma050261z (2005).
- 122 Jennings, K. R. Spectrometric identification of organic compounds (Fifth Edition) R. M. SILVERSTEIN, G. C. BASSLER AND T. C. MORRILL. Wiley, New York,

References

1991. No. of pages: 430. ISBN 0471 63404 2. Price: £50.25, \$76.10. *Organic Mass Spectrometry* **26**, 813-813, doi:10.1002/oms.1210260923 (1991).
- 123 Landis, W. R. & Perrine, T. D. Nuclear Magnetic Resonance and Infrared Spectroscopic Study of N-Vinyl Compounds. *Applied Spectroscopy* **22**, 161-164, doi:10.1366/000370268774383499 (1968).
- 124 Fischer, H. The Persistent Radical Effect: A Principle for Selective Radical Reactions and Living Radical Polymerizations. *Chemical Reviews* **101**, 3581-3610, doi:10.1021/cr990124y (2001).
- 125 Zhang, L., Liang, Y. & Meng, L. Thermo-sensitive amphiphilic poly(N-vinylcaprolactam) copolymers: synthesis and solution properties. *Polymers for Advanced Technologies* **21**, 720-725, doi:10.1002/pat.1495 (2010).
- 126 Cao, Y. & He, W. Functionalized Biocompatible Poly(N-vinyl-2-caprolactam) With pH-Dependent Lower Critical Solution Temperature Behaviors. *Macromolecular Chemistry and Physics* **212**, 2503-2510, doi:10.1002/macp.201100414 (2011).
- 127 Astbury, G. R., Bugand-Bugandet, J., Grollet, E. & Stell, K. M. in *Institution of Chemical Engineers Symposium Series*.150 edn 505-522.
- 128 Van Steenberge, P. H. M. *et al.* Linear Gradient Quality of ATRP Copolymers. *Macromolecules* **45**, 8519-8531, doi:10.1021/ma3017597 (2012).
- 129 Ballistreri, A., Foti, S., Montaudo, G. & Scamporrino, E. Evolution of aromatic compounds in the thermal decomposition of vinyl polymers. *Journal of Polymer Science: Polymer Chemistry Edition* **18**, 1147-1153, doi:10.1002/pol.1980.170180401 (1980).
- 130 Demirelli, K., Coşkun, M. & Kaya, E. A detailed study of thermal degradation of poly(2-hydroxyethyl methacrylate). *Polymer Degradation and Stability* **72**, 75-80, doi:http://dx.doi.org/10.1016/S0141-3910(00)00204-4 (2001).
- 131 Huang, S.-J., Wang, T.-P., Lue, S.-I. & Wang, L.-F. Pentablock copolymers of pluronic F127 and modified poly(2-dimethyl amino)ethyl methacrylate for internalization mechanism and gene transfection studies. *International Journal of Nanomedicine* **8**, 2011-2027, doi:10.2147/ijn.s44222 (2013).
- 132 Özlem, S. & Hacaloglu, J. Thermal degradation of poly(n-butyl methacrylate), poly(n-butyl acrylate) and poly(t-butyl acrylate). *Journal of Analytical and Applied Pyrolysis* **104**, 161-169, doi:http://dx.doi.org/10.1016/j.jaap.2013.08.008 (2013).
- 133 Roy, S. G. *et al.* Synthesis, characterization and thermal degradation of dual temperature- and pH-sensitive RAFT-made copolymers of N,N-(dimethylamino)ethyl methacrylate and methyl methacrylate. *Polymer International* **62**, 463-473, doi:10.1002/pi.4335 (2013).
- 134 Zhang, S., Tao, Q., Wang, Z. & Zhang, Z. Controlled heat release of new thermal storage materials: the case of polyethylene glycol intercalated into graphene oxide paper. *Journal of Materials Chemistry* **22**, 20166-20169, doi:10.1039/c2jm33316c (2012).
- 135 Wiemer, B. D. D. Perrin and W. L. F. Armarego: Purification of Laboratory Chemicals. 3. Aufl., Oxford. Pergamon Press, 1988, 391 S., zahlr. Tab., \$ 37,50, ISBN 0-08-034714-2. *Acta hydrochimica et hydrobiologica* **17**, 632-632, doi:10.1002/aheh.19890170605 (1989).
- 136 Hay, R. W., Lawrance, G. A. & Curtis, N. F. A convenient synthesis of the tetraaza-macrocyclic ligands trans-[14]-diene, tet a, and tet b. *Journal of the Chemical Society, Perkin Transactions 1*, 591-593, doi:10.1039/p19750000591 (1975).

References

- 137 Zaijun, L. U., Huang, X. & Huang, J. Synthesis, characterization, and hydrolysis of PVAc-PSPVAc via charge transfer polymerization. *J Polym Sci Part A* **37**, 2595-2600 (1999).
- 138 Baker, M. I., Walsh, S. P., Schwartz, Z. & Boyan, B. D. A review of polyvinyl alcohol and its uses in cartilage and orthopedic applications. *Journal of Biomedical Materials Research Part B: Applied Biomaterials* **100B**, 1451-1457, doi:10.1002/jbm.b.32694 (2012).
- 139 Friis, N., Goosney, D., Wright, J. D. & Hamielec, A. E. Molecular weight and branching development in vinyl acetate emulsion polymerization. *Journal of Applied Polymer Science* **18**, 1247-1259, doi:10.1002/app.1974.070180424 (1974).
- 140 Langer, R. Polymer-controlled drug delivery systems. *Acc. Chem. Res.* **26**, 537-542, doi:10.1021/ar00034a004 (1993).
- 141 Mardare, D. & Matyjaszewski, K. "Living" radical polymerization of vinyl acetate. *Macromolecules* **27**, 645-649, doi:10.1021/ma00081a003 (1994).
- 142 Wakioka, M., Baek, K.-Y., Ando, T., Kamigaito, M. & Sawamoto, M. Possibility of Living Radical Polymerization of Vinyl Acetate Catalyzed by Iron(I) Complex I. *Macromolecules* **35**, 330-333, doi:10.1021/ma0115444 (2001).
- 143 Tang, H., Radosz, M. & Shen, Y. Atom transfer radical polymerization and copolymerization of vinyl acetate catalyzed by copper halide/terpyridine. *AIChE Journal* **55**, 737-746, doi:10.1002/aic.11706 (2009).
- 144 Xue, Z. & Poli, R. Organometallic mediated radical polymerization of vinyl acetate with Fe(acac)₂. *Journal of Polymer Science Part A: Polymer Chemistry* **51**, 3494-3504, doi:10.1002/pola.26751 (2013).
- 145 Debuigne, A., Caille, J.-R., Willet, N. & Jérôme, R. Synthesis of Poly(vinyl acetate) and Poly(vinyl alcohol) Containing Block Copolymers by Combination of Cobalt-Mediated Radical Polymerization and ATRP. *Macromolecules* **38**, 9488-9496, doi:10.1021/ma051246x (2005).
- 146 Chen, Y.-J. *et al.* Hybridization of CMRP and ATRP: A Direct Living Chain Extension from Poly(vinyl acetate) to Poly(methyl methacrylate) and Polystyrene. *Macromolecules* **48**, 6832-6838, doi:10.1021/acs.macromol.5b01101 (2015).
- 147 Gupta, B., Anjum, S. & Ikram, S. Characterization and physicochemical studies of crosslinked thiolated polyvinyl alcohol hydrogels. *Polym. Bull.* **70**, 2709-2725, doi:10.1007/s00289-013-0982-4 (2013).
- 148 Kabanov, A. V. & Alakhov, V. Y. in *Amphiphilic Block Copolymers* (ed Paschalis Alexandridis/Björn Lindman) 347-376 (Elsevier Science B.V., 2000).
- 149 Euranto, E. K., Noponen, A. & Kujanpaa, T. α -Haloalkyl esters. *Acta Chem. Scand.* **20**, 1273-1280, doi:10.3891/acta.chem.scand.20-1273 (1966).
- 150 Kwak, Y., Yamamura, Y. & Matyjaszewski, K. ATRP of Styrene and Methyl Methacrylate with Less Efficient Catalysts and with Alkyl Pseudohalides as Initiators/Chain Transfer Agents. *Macromolecular Chemistry and Physics* **211**, 493-500, doi:10.1002/macp.200900509 (2010).
- 151 Koumura, K., Satoh, K. & Kamigaito, M. Mn₂(CO)₁₀-Induced Controlled/Living Radical Copolymerization of Methyl Acrylate and 1-Hexene in Fluoroalcohol: High α -Olefin Content Copolymers with Controlled Molecular Weights. *Macromolecules* **42**, 2497-2504, doi:10.1021/ma9001275 (2009).
- 152 Li, G.-H. & Cho, C.-G. Synthesis and micellar behavior of poly(vinyl alcohol-b-styrene) copolymers containing PVA blocks with different syndiotacticity. *Colloid Polym Sci* **283**, 946-953, doi:10.1007/s00396-004-1242-9 (2005).

References

- 153 Liao, L.-F., Lien, C.-F. & Lin, J.-L. FTIR study of adsorption and photoreactions of acetic acid on TiO₂. *Physical Chemistry Chemical Physics* **3**, 3831-3837, doi:10.1039/b103419g (2001).
- 154 Holland, B. J. & Hay, J. N. The thermal degradation of poly(vinyl alcohol). *Polymer* **42**, 6775-6783, doi:http://dx.doi.org/10.1016/S0032-3861(01)00166-5 (2001).
- 155 Martinelli, A., Tighzert, L., D'Ilario, L., Francolini, I. & Piozzi, A. Poly(vinyl acetate)/polyacrylate semi-interpenetrating polymer networks. II. Thermal, mechanical, and morphological characterization. *Journal of Applied Polymer Science* **111**, 2675-2683, doi:10.1002/app.29291 (2009).
- 156 Jones, D. S., Lorimer, C. P., McCoy, C. P. & Gorman, S. P. Characterization of the physicochemical, antimicrobial, and drug release properties of thermoresponsive hydrogel copolymers designed for medical device applications. *Journal of Biomedical Materials Research Part B: Applied Biomaterials* **85B**, 417-426, doi:10.1002/jbm.b.30960 (2008).
- 157 Kawaguchi, Y., Itamura, Y., Onimura, K. & Oishi, T. Effects of the chemical structure on the heat resistance of thermoplastic expandable microspheres. *Journal of Applied Polymer Science* **96**, 1306-1312, doi:10.1002/app.21429 (2005).
- 158 Grohens, Y., Hamon, L., Spěváček, J. & Holl, Y. The gel-like structure of polymer in thin films: an explanation of the thickness dependent glass transition? *Macromolecular Symposia* **203**, 155-164, doi:10.1002/masy.200351314 (2003).
- 159 Jose, J., Shehzad, F. & Al-Harhi, M. A. Preparation method and physical, mechanical, thermal characterization of poly(vinyl alcohol)/poly(acrylic acid) blends. *Polym. Bull.* (2014).
- 160 Alexandridis, P. & Hatton, T. A. POLY(ETHYLENE OXIDE)-POLY(PROPYLENE OXIDE)-POLY(ETHYLENE OXIDE) BLOCK-COPOLYMER SURFACTANTS IN AQUEOUS-SOLUTIONS AND AT INTERFACES - THERMODYNAMICS, STRUCTURE, DYNAMICS, AND MODELING. *Colloids and Surfaces a-Physicochemical and Engineering Aspects* **96**, 1-46, doi:10.1016/0927-7757(94)03028-x (1995).
- 161 Kabanov, A. V., Batrakova, E. V. & Alakhov, V. Y. Pluronic (R) block copolymers as novel polymer therapeutics for drug and gene delivery. *Journal of Controlled Release* **82**, 189-212, doi:Pii s0168-3659(02)00009-3 10.1016/s0168-3659(02)00009-3 (2002).
- 162 Prud'homme, R. K., Wu, G. & Schneider, D. K. Structure and Rheology Studies of Poly(oxyethylene-oxypropylene-oxyethylene) Aqueous Solution. *Langmuir* **12**, 4651-4659, doi:10.1021/la951506b (1996).
- 163 Mortensen, K. Structural studies of aqueous solutions of PEO-PPO-PEO triblock copolymers, their micellar aggregates and mesophases; A small-angle neutron scattering study. *Journal of Physics-Condensed Matter* **8**, A103-A124, doi:10.1088/0953-8984/8/25a/008 (1996).
- 164 Lecommandoux, S. & Borsali, R. On the physics of block copolymers. *Polym. Int.* **55**, 1161-1168, doi:10.1002/pi.1927 (2006).
- 165 Robbins, M. O., Kremer, K. & Grest, G. S. PHASE-DIAGRAM AND DYNAMICS OF YUKAWA SYSTEMS. *Journal of Chemical Physics* **88**, 3286-3312, doi:10.1063/1.453924 (1988).
- 166 Linse, P. in *Amphiphilic Block Copolymers* 13-40 (Elsevier Science B.V., 2000).
- 167 Zhou, Z. & Chu, B. Light-scattering study on the association behavior of triblock polymers of ethylene oxide and propylene oxide in aqueous solution. *Journal of*

References

- Colloid and Interface Science* **126**, 171-180, doi:http://dx.doi.org/10.1016/0021-9797(88)90111-7 (1988).
- 168 Alexandridis, P., Holzwarth, J. F. & Hatton, T. A. Micellization of Poly(ethylene oxide)-Poly(propylene oxide)-Poly(ethylene oxide) Triblock Copolymers in Aqueous Solutions: Thermodynamics of Copolymer Association. *Macromolecules* **27**, 2414-2425, doi:10.1021/ma00087a009 (1994).
- 169 Wanka, G., Hoffmann, H. & Ulbricht, W. The aggregation behavior of poly-(oxyethylene)-poly-(oxypropylene)-poly-(oxyethylene)-block-copolymers in aqueous solution. *Colloid and Polymer Science* **268**, 101-117, doi:10.1007/bf01513189.
- 170 Vadnere, M., Amidon, G., Lindenbaum, S. & Haslam, J. L. Thermodynamic studies on the gel-sol transition of some pluronic polyols. *Int. J. Pharm.* **22**, 207-218, doi:10.1016/0378-5173(84)90022-x (1984).
- 171 Wang, P. & Johnston, T. P. Kinetics of sol-to-gel transition for poloxamer polyols. *Journal of Applied Polymer Science* **43**, 283-292, doi:10.1002/app.1991.070430207 (1991).
- 172 Di Biase, M. *et al.* Photopolymerization of Pluronic F127 diacrylate: a colloid-templated polymerization. *Soft Matter* **7**, 4928-4937 (2011).
- 173 Missirlis, D., Hubbell, J. A. & Tirelli, N. Thermally-induced responses in nanoparticle assemblies: possible formation of a colloidal glass and its perspective applications. *Soft Matter* **2**, 1067-1075 (2006).
- 174 Mortensen, K. & Pedersen, J. S. Structural study on the micelle formation of poly(ethylene oxide)-poly(propylene oxide)-poly(ethylene oxide) triblock copolymer in aqueous solution. *Macromolecules* **26**, 805-812, doi:10.1021/ma00056a035 (1993).
- 175 Brown, W., Schillen, K. & Hvidt, S. Triblock copolymers in aqueous solution studied by static and dynamic light scattering and oscillatory shear measurements: influence of relative block sizes. *The Journal of Physical Chemistry* **96**, 6038-6044, doi:10.1021/j100193a072 (1992).
- 176 Robbins, M. O., Kremer, K. & Grest, G. S. Phase diagram and dynamics of Yukawa systems. *The Journal of Chemical Physics* **88**, 3286-3312, doi:doi:http://dx.doi.org/10.1063/1.453924 (1988).
- 177 Alakhov, V. Y., Moskaleva, E. Y., Batrakova, E. V. & Kabanov, A. V. Hypersensitization of Multidrug Resistant Human Ovarian Carcinoma Cells by Pluronic P85 Block Copolymer. *Bioconjugate Chemistry* **7**, 209-216, doi:10.1021/bc950093n (1996).
- 178 Escobar-Chavez, J. J. *et al.* Applications of thermoreversible pluronic F-127 gels in pharmaceutical formulations. *J. Pharm. Pharm. Sci.* **9**, 339-358 (2006).
- 179 Escobar-Chávez, J. J., Quintanar-Guerrero, D. & Ganem-Quintanar, A. In Vivo Skin Permeation of Sodium Naproxen Formulated in Pluronic F-127 Gels: Effect of Azone® and Transcutol®. *Drug Development and Industrial Pharmacy* **31**, 447-454, doi:doi:10.1080/03639040500214662 (2005).
- 180 Miyazaki, S., Takeuchi, S., Yokouchi, C. & Takada, M. Pluronic F-127 gels as a vehicle for topical administration of anticancer agents. *Chemical & pharmaceutical bulletin* **32**, 4205-4208 (1984).
- 181 Miyazaki, S. *et al.* Pluronic F-127 gels as a novel vehicle for rectal administration of indomethacin. *Chemical & pharmaceutical bulletin* **34**, 1801-1808 (1986).
- 182 Venne, A., Li, S., Mandeville, R., Kabanov, A. & Alakhov, V. *Hypersensitizing effect of pluronic L61 on cytotoxic activity, transport, and subcellular distribution of doxorubicin in multiple drug-resistant cells.* Vol. 56 (1996).

References

- 183 Kazunori, K., Glenn S, K., Masayuki, Y., Teruo, O. & Yasuhisa, S. Block copolymer micelles as vehicles for drug delivery. *Journal of Controlled Release* **24**, 119-132, doi:10.1016/0168-3659(93)90172-2 (1993).
- 184 Mathot, F., van Beijsterveldt, L., Pr eat, V., Brewster, M. & Ari en, A. Intestinal uptake and biodistribution of novel polymeric micelles after oral administration. *Journal of Controlled Release* **111**, 47-55, doi:10.1016/j.jconrel.2005.11.012 (2006).
- 185 Ayman F. El-Kattan, C. S. A., Nanhye Kim, Bozena B. Michniak. Effect of Formulation Variables on the Percutaneous Permeation of Ketoprofen from Gel Formulations. *Drug Delivery* **7**, 147-153, doi:doi:10.1080/10717540050120188 (2000).
- 186 Liaw, J. & Lin, Y. C. Evaluation of poly(ethylene oxide)-poly(propylene oxide)-poly(ethylene oxide) (PEO-PPO-PEO) gels as a release vehicle for percutaneous fentanyl. *Journal of Controlled Release* **68**, 273-282, doi:10.1016/s0168-3659(00)00268-6 (2000).
- 187 Pillai, O. & Panchagnula, R. Transdermal delivery of insulin from poloxamer gel: ex vivo and in vivo skin permeation studies in rat using iontophoresis and chemical enhancers. *Journal of Controlled Release* **89**, 127-140, doi:10.1016/s0168-3659(03)00094-4 (2003).
- 188 Shin, S.-C. & Kim, J.-Y. Enhanced permeation of triamcinolone acetonide through the buccal mucosa. *European Journal of Pharmaceutics and Biopharmaceutics* **50**, 217-220, doi:10.1016/s0939-6411(00)00101-6 (2000).
- 189 Moghimi, S. M. Modulation of lymphatic distribution of subcutaneously injected poloxamer 407-coated nanospheres: the effect of the ethylene oxide chain configuration. *FEBS Letters* **540**, 241-244, doi:10.1016/s0014-5793(03)00273-4 (2003).
- 190 Paavola, A., Kilpel inen, I., Yliruusi, J. & Rosenberg, P. Controlled release injectable liposomal gel of ibuprofen for epidural analgesia. *International Journal of Pharmaceutics* **199**, 85-93, doi:10.1016/s0378-5173(00)00376-8 (2000).
- 191 Kozlov, M. Y., Melik-Nubarov, N. S., Batrakova, E. V. & Kabanov, A. V. Relationship between Pluronic Block Copolymer Structure, Critical Micellization Concentration and Partitioning Coefficients of Low Molecular Mass Solutes. *Macromolecules* **33**, 3305-3313, doi:10.1021/ma991634x (2000).
- 192 Hubbell, J. A. Enhancing Drug Function. *Science* **300**, 595-596, doi:10.1126/science.1083625 (2003).
- 193 Gyulai, G. *et al.* Preparation and characterization of cationic pluronic for surface modification and functionalization of polymeric drug delivery nanoparticles. *Express Polym. Lett.* **10**, 216-226, doi:10.3144/expresspolymlett.2016.20 (2016).
- 194 Chiappetta, D. A. & Sosnik, A. Poly(ethylene oxide)-poly(propylene oxide) block copolymer micelles as drug delivery agents: Improved hydrosolubility, stability and bioavailability of drugs. *European Journal of Pharmaceutics and Biopharmaceutics* **66**, 303-317, doi:http://dx.doi.org/10.1016/j.ejpb.2007.03.022 (2007).
- 195 Schmaljohann, D. Thermo- and pH-responsive polymers in drug delivery. *Advanced Drug Delivery Reviews* **58**, 1655-1670, doi:http://dx.doi.org/10.1016/j.addr.2006.09.020 (2006).
- 196 Koetting, M. C., Peters, J. T., Steichen, S. D. & Peppas, N. A. Stimulus-responsive hydrogels: Theory, modern advances, and applications. *Materials Science and Engineering: R: Reports* **93**, 1-49, doi:http://dx.doi.org/10.1016/j.mser.2015.04.001 (2015).

References

- 197 Schoener, C. A., Hutson, H. N. & Peppas, N. A. pH-responsive hydrogels with dispersed hydrophobic nanoparticles for the oral delivery of chemotherapeutics. *Journal of Biomedical Materials Research Part A* **101A**, 2229-2236, doi:10.1002/jbm.a.34532 (2013).
- 198 Yang, L., Wu, X., Liu, F., Duan, Y. & Li, S. Novel Biodegradable Polylactide/poly(ethylene glycol) Micelles Prepared by Direct Dissolution Method for Controlled Delivery of Anticancer Drugs. *Pharmaceutical Research* **26**, 2332-2342, doi:10.1007/s11095-009-9949-4 (2009).
- 199 Raphael, M. O., Samuel, J. H. & Kinam, P. *Hydrogels and Biodegradable Polymers for Bioapplications*. Vol. 627 (American Chemical Society, 1996).
- 200 Cheng, W., Kumar, J. N., Zhang, Y. & Liu, Y. pH- and Redox-Responsive Poly(ethylene glycol) and Cholesterol-Conjugated Poly(amido amine)s Based Micelles for Controlled Drug Delivery. *Macromolecular Bioscience* **14**, 347-358, doi:10.1002/mabi.201300339 (2014).
- 201 DeConti, R. C., Toftness, B. R., Lange, R. C. & Creasey, W. A. Clinical and Pharmacological Studies with cis-Diamminedichloroplatinum(II). *Cancer Research* **33**, 1310-1315 (1973).
- 202 Wang, W. *et al.* Toxicity and in vivo biological effect of the nanoparticulate self-supported hydrogel of a thermosensitive copolymer for non-invasive drug delivery. *Journal of Biomedical Materials Research Part A* **102**, 17-29, doi:10.1002/jbm.a.34694 (2014).
- 203 Pabla, N. & Dong, Z. Cisplatin nephrotoxicity: Mechanisms and renoprotective strategies. *Kidney International* **73**, 994-1007, doi:http://dx.doi.org/10.1038/sj.ki.5002786 (2008).
- 204 Fan, X., Zhao, X., Qu, X. & Fang, J. pH sensitive polymeric complex of cisplatin with hyaluronic acid exhibits tumor-targeted delivery and improved in vivo antitumor effect. *International Journal of Pharmaceutics* **496**, 644-653, doi:http://dx.doi.org/10.1016/j.ijpharm.2015.10.066 (2015).
- 205 Saisyo, A. *et al.* pH-sensitive polymeric cisplatin-ion complex with styrene-maleic acid copolymer exhibits tumor-selective drug delivery and antitumor activity as a result of the enhanced permeability and retention effect. *Colloids and Surfaces B: Biointerfaces* **138**, 128-137, doi:http://dx.doi.org/10.1016/j.colsurfb.2015.11.032 (2016).
- 206 Gerweck, L. E., Vijayappa, S. & Kozin, S. Tumor pH controls the in vivo efficacy of weak acid and base chemotherapeutics. *Molecular Cancer Therapeutics* **5**, 1275-1279, doi:10.1158/1535-7163.mct-06-0024 (2006).
- 207 Tannock, I. F. & Rotin, D. Acid pH in Tumors and Its Potential for Therapeutic Exploitation. *Cancer Research* **49**, 4373-4384 (1989).
- 208 Chen, Y.-C., Lo, C.-L. & Hsiue, G.-H. Multifunctional nanomicellar systems for delivering anticancer drugs. *Journal of Biomedical Materials Research Part A* **102**, 2024-2038, doi:10.1002/jbm.a.34850 (2014).
- 209 Mortensen, K. Phase Behaviour of Poly(ethylene oxide)-Poly(propylene oxide)-Poly(ethylene oxide) Triblock-Copolymer Dissolved in Water. *EPL (Europhysics Letters)* **19**, 599 (1992).
- 210 Mortensen, K. in *Amphiphilic Block Copolymers* (ed Paschalis Alexandridis/Björn Lindman) 191-220 (Elsevier Science B.V., 2000).
- 211 Braunecker, W. A. & Matyjaszewski, K. Controlled/living radical polymerization: Features, developments, and perspectives. *Progress in Polymer Science* **32**, 93-146, doi:http://dx.doi.org/10.1016/j.progpolymsci.2006.11.002 (2007).

References